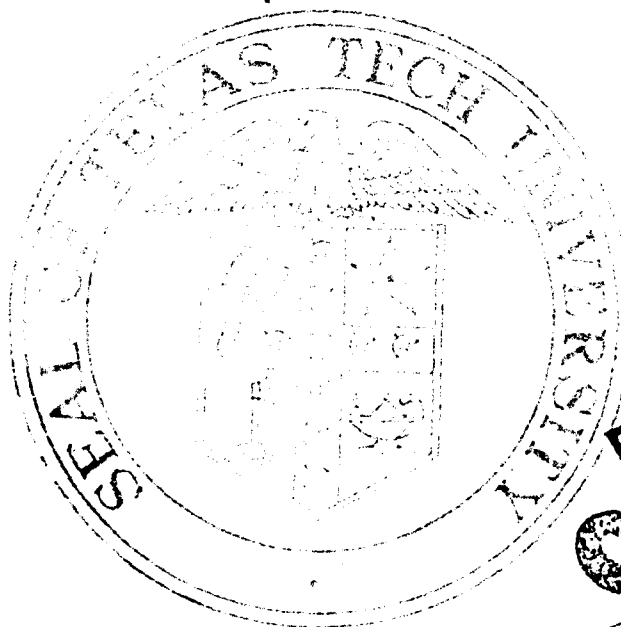


AD A110720

LEVEL WORKSHOP ON REPETITIVE OPENING SWITCHES

(January 28-30, 1981)

M. Kristiansen and K. Schoenbach
Workshop Co-Chairmen



333

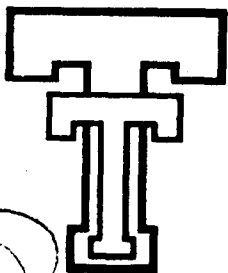
DTIC
ELECTE
FEB 10 1982

Sponsored by
Battelle Columbus Laboratories

April 20, 1981

DISTRIBUTION STATEMENT A
Approved for public release;
Distribution Unlimited

Plasma Laboratory
Department of Electrical Engineering



Texas Tech University

LUBBOCK, TEXAS 79402-0903

UNCLASSIFIED

SECURITY CLASSIFICATION OF THIS PAGE (When Data Entered)

REPORT DOCUMENTATION PAGE		READ INSTRUCTIONS BEFORE COMPLETING FORM
1. REPORT NUMBER NONE	2. GOVT ACCESSION NO A110 770	3. RECIPIENT'S CATALOG NUMBER
4. TITLE (and Subtitle) Workshop on Repetitive Opening Switches		5. TYPE OF REPORT & PERIOD COVERED Final Report
		6. PERFORMING ORG. REPORT NUMBER
7. AUTHOR(s) M. Kristiansen K. H. Schoenbach		8. CONTRACT OR GRANT NUMBER(s) DAAG29 76 D 0100
9. PERFORMING ORGANIZATION NAME AND ADDRESS Texas Tech University Lubbock, TX 79409		10. PROGRAM ELEMENT, PROJECT, TASK AREA & WORK UNIT NUMBERS
11. CONTROLLING OFFICE NAME AND ADDRESS U. S. Army Research Office Post Office Box 12211 Research Triangle Park, NC 27709		12. REPORT DATE Apr 20, 81
		13. NUMBER OF PAGES 329
14. MONITORING AGENCY NAME & ADDRESS (If different from Controlling Office)		15. SECURITY CLASS (of this report) Unclassified
		15a. DECLASSIFICATION/DOWNGRADING SCHEDULE
16. DISTRIBUTION STATEMENT (of this Report) Approved for public release; distribution unlimited.		
17. DISTRIBUTION STATEMENT (of the abstract entered in Block 20, if different from Report) NA		
18. SUPPLEMENTARY NOTES The view, opinions, and/or findings contained in this report are those of the author(s) and should not be construed as an official Department of the Army position, policy, or decision, unless so designated by other documentation.		
19. KEY WORDS (Continue on reverse side if necessary and identify by block number)		
20. ABSTRACT (Continue on reverse side if necessary and identify by block number) A workshop on Repetitive Opening Switches was conducted by Texas Tech University for the US Army Research Office. Several papers on a wide range of innovative opening switch concepts were presented. Discussions about the research needs to advance the state-of-the-art in this important, emerging field are summarized. A consensus on research topics and their importance is summarized and a suggested research priority list given.		

Scientific Services Program

U.S. Army Research Office

P

Final Report on
WORKSHOP ON REPETITIVE OPENING SWITCHES

Sponsored by

Battelle Columbus Laboratories
Contract DAAG29-76-D-0100
Delivery Order No. 1714
200 Park Drive
P.O. Box 12297
Research Triangle Park, NC 27709

Conducted by

Plasma and Switching Laboratory
Department of Electrical Engineering
Texas Tech University, Lubbock, Texas 79409

at

Tamarron, Colorado

on

January 28-30, 1981

Submitted by

M. Kristiansen
P.W. Horn Professor
Workshop Chairman

K.H. Schoenbach
Assistant Professor
Workshop Co-Chairman

April 20, 1981

1106 534

The views, opinions, and/or findings contained in this report are those of the author(s) and should not be construed as an official Department of the Army position, policy, or decision, unless so designated by other documentation.

TABLE OF CONTENTS

I. Workshop Advisory Committee	iii
II. Abstract	1
III. Introduction	2
IV. Workshop Summary	6
V. Contributed Papers	17
1. Introductory Remarks (T.M. Martin)	18
2. Opening Switch Technology (R.J. Harvey and A.J. Palmer)	20
3. Optically Controlled Discharges (A.H. Guenther)	47
4. Exploratory Concepts of Opening Switches (K.H. Schoenbach, M. Kristiansen, E.E. Kunhardt, L.L. Hatfield, and A.H. Guenther)	65
5. Relaxation Processes and LTE in Models of Pulsed Electric Discharges (A.V. Phelps)	106
6. Performance Predictions for E-Beam Controlled On/Off Switches (Laurence E. Kline)	121
7. Switching Experiments with a Small E-Beam (P. Bletzinger)	128
8. Opening Switch Using Spoiled Electrostatic Confinement (Igor Alexeff)	143
9. Magnetoplasma dynamic and Hall Effect Switching for Repetitive Interruption of Inductive Circuits (P.J. Turchi)	149
10. Vacuum Arc Switching (A.S. Gilmour, Jr.)	164
11. A Plasma Focus Interrupting Switch for Use With Inductive Energy Storage (G.M. Molen and H.C. Kirby)	177
12. Problems of Repetitive Opening Switches Demonstrated on Repetitive Operation of a Dense Plasma Focus (Jürgen Salge)	189
13. Opening Switches for Vacuum Inductive Storage (V. Bailey, J. Creedon, L. Demeter, and D. Sloan)	199

14.	Vacuum Interrupters and Thyratrons as Opening Switches - - - - -	233
	(E.M. Honig)	
15.	A Comparison Between an SCR and a Vacuum Interrupter System for Repetitive Opening - - - - -	246
	(W.M. Parsons)	
16.	Fuse Switches for High Current Inductive Pulse Compression Systems - - - - -	259
	(R.E. Reinovsky and D.L. Smith)	
17.	Fuses and Repetitive Current Interruption - - - - -	269
	(Ihor M. Vitkovitsky)	
18.	Experiments with an Explosively Opened Plasma Switch - - -	284
	(B.N. Turman and T.J. Tucker)	
19.	Pulses of Energy from an Inductive Store - - - - -	297
	(Gordon K. Simcox)	

V. Appendices

A.	Fundamentals of Inductive Energy Storage - - - - -	313
	(M. Kristiansen)	
B.	Suggested Sources of Information for Various Opening Switch Concepts - - - - -	325
C.	List of Participants - - - - -	327

Accession For
NTIS Grant
DTIC TAB
Unannounced
Justification
By
Distribution
Avail
DTIC
A

Workshop Advisory Committee

M. Kristiansen	Texas Tech University (Chairman)
K. Schoenbach	Texas Tech University (Co-Chairman)
E. Kunhardt	Texas Tech University
A. Guenther	Air Force Weapons Laboratory
F. Rose	Naval Surface Weapons Laboratory
B. Wright	Electronics Technology and Device Lab, US Army
R. Harvey	Hughes Research Laboratory
P. Turchi	R & D Associates
T. Martin	Sandia National Laboratories

Ex-Officio

B. Guenther	Army Research Office
R. Lontz	Army Research Office
A. Hyder	Air Force Office of Scientific Research

ABSTRACT

A workshop on Repetitive Opening Switches was conducted by Texas Tech University for the U.S. Army Research Office. Several papers on a wide range of innovative opening switch concepts were presented. Discussions about the research needs to advance the state-of-the-art in this important, emerging field are summarized. A consensus on research topics and their importance is summarized and a suggested research priority list given.

INTRODUCTION

A Workshop on "Repetitive Opening Switches" was sponsored by the U.S. Army Research Office and conducted by Texas Tech University at Tamarron, Colorado on January 28-30, 1981. The workshop was attended by 40 participants from universities, industry, national laboratories, and government agencies. Except for an initial, classified briefing (conducted at the Air Force Weapons Laboratory in Albuquerque) the workshop presentations and deliberations were unclassified. The underlying reasons for the interest in repetitive opening switches were summarized by DoD and DoE representatives. Several of the workshop participants then made formal presentations and most of their papers are included in this report.

The goals of the workshop were to examine the state-of-the-art in repetitive opening switches and to establish the most important and fruitful research areas and set priorities for advancing the capability in this important field. Some suggested parameters for discussions at this workshop were:

Switch hold-off voltage	$V_{oc} > 10 \text{ kV}$
Switch conduction current	$I > \text{kA}$
Switch opening time	$\tau_{open} < 1 \mu\text{s}$
Pulse Repetition rate (pulses per second)	$\text{PRR} > 10 \text{ pps}$

Since there have been very few successes to date in repetitive opening switches, it was deemed necessary to include discussions on single shot switches (e.g. fuses) and counterpulsed systems (e.g. vacuum interrupters) to set the background for the discussions about the much more difficult goal set for this workshop.

The interest in repetitive opening switches is, as explained in the Appendix, caused by the potentially high energy storage density that can be achieved through the use of inductive systems (at least one order of magnitude higher than that of capacitive systems). A brief discussion of the fundamentals of inductive energy storage systems together with an example of one of the largest known operating inductive energy systems (single shot and slow, however) are given in the Appendix. As explained in the Appendix, the key technological problem in developing a successful inductive energy storage system is the opening switch. When attempting

to open a conducting switch rapidly in an inductive system the $L \frac{di}{dt}$ effect results in a very high voltage across the switch which tends to maintain a conducting arc between the switch electrodes. How to interrupt the conduction process against a high driving voltage is the essence of the opening switch problem. For repetitive switching it is particularly important that the interruption process is highly efficient so that the losses do not change the basic behavior of the interruption process. For purely inductive loads there are fundamental constraints to this efficiency, as explained in the Appendix. In the case of resistive loads the efficiency can, in principle, be very high and it is important to seek switches with the most efficient control of the discharge interruption mechanism.

Table I shows some sample problem areas of current interest where repetitive opening switches would be very valuable and Table II show some examples of useful pulse length applications. In this research field a wide range of sub-disciplines are needed, as indicated by the simplified chart in Fig. 1.

Table I

SOME TYPICAL SWITCH REQUIREMENTS OF CURRENT INTEREST

	Directed Energy Weapons	Inertial Confinement Fusion	Electric Launchers (Guns)
V_{oc}	.1-1 MV	3 MV	5-20 kV
Pulse Repetition Rate	$5 \times (10^3 - 10^4)$	10 pps	100-500 pps
I_{peak}	10-100 kA	100 kA	1-5 MA
Life	$10^6 - 10^8$ shots	10^9 shots	$10^6 - 10^8$ shots
Turn-on Time	$\sim \mu s$	$< \mu s$	$< ms$

Table II

SOME EXAMPLES OF USEFUL PULSE LENGTHS
FOR VARIOUS APPLICATIONS

- 1) $\tau_p \gtrsim 100$ ns: (replaces water line)
 e.g. $\sim 10^4$ pps, ~ 1 MV (Beam Weapon)
 $\sim 10^2$ pps, ~ 1 MV (Inertial Confinement Fusion Reactor)
 $< .01$ pps, ~ 1 MV (Simulation)

- 2) $\tau_p \sim 1-10$ μ s: (Capacitor or water line charging or direct transfer to resistive load)
 e.g. Beam Weapons, ICF Reactor, Simulator with V and pulse repetition rate as above, or Laser Weapon with 10-100 pps and .1-1 MV.

- 3) $\tau_p \sim 1$ ms: (to resistive load)
 e.g. drive of iron-core betatron (beam weapon) with 100 kV/turn, 10-100 kA, ~ 10 pps or electromagnetic propulsion

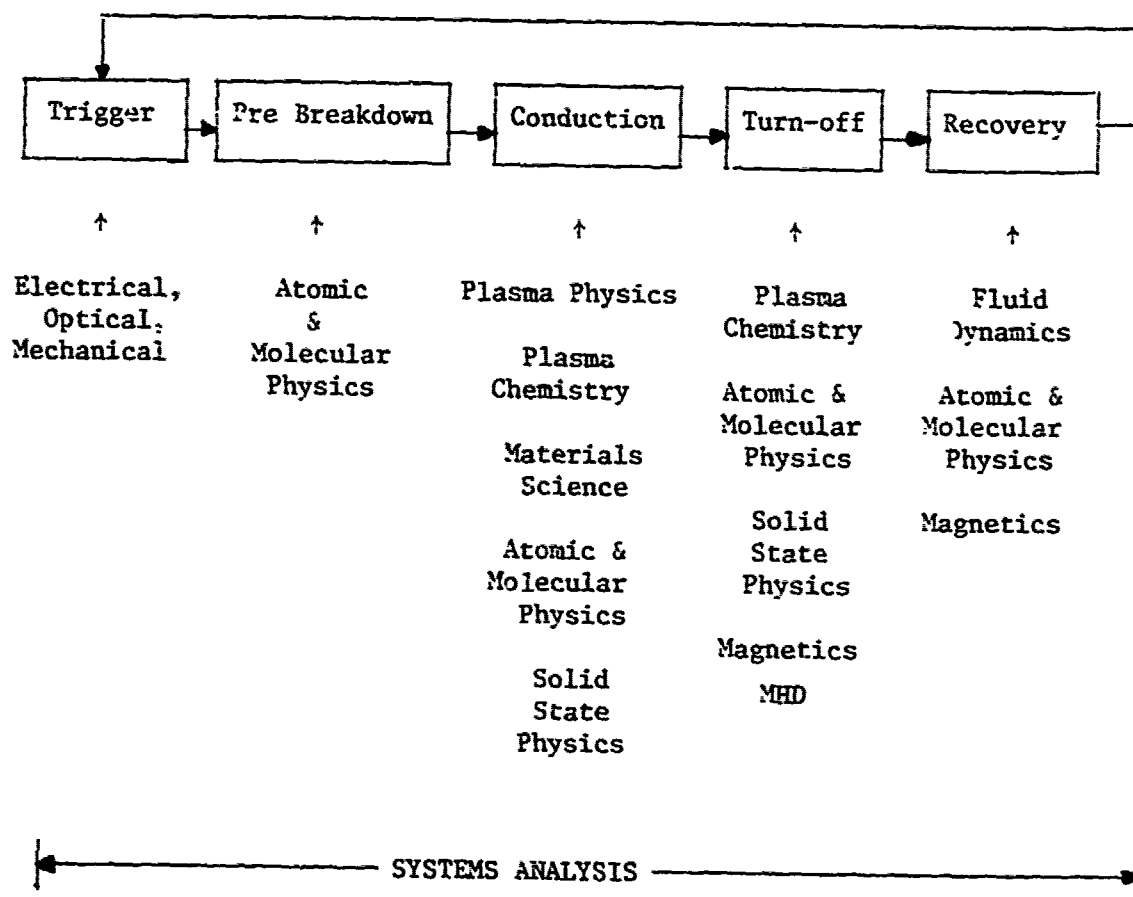


Fig. 1 Schematic Representation of Opening Switch Operations Sequence and Some Related Research Topics.

WORKSHOP SUMMARY

From the presented papers and the discussions that followed, it is clear that the state-of-the-art for single shot and counterpulsed switches is quite impressive. It is, however, difficult to envision an extension of these concepts to high repetition rate, low jitter, long life operation. These concepts may still be of interest for single burst mode operation and as test switches for other components in the development of viable inductive energy storage systems. They are also useful in what one can learn about how opening switches work, and in providing test cases for analytical models. It was argued that the counterpulsed SCR's or vacuum interrupters could achieve respectable repetition rates and lifetimes. This seems especially to be the case for the SCR's but it appears that the combination of the cost of the solid state material and the required counterpulsing circuit will make such a system costly and that it may also be energy inefficient and bulky (large size and weight). Other semiconductor devices, such as the Hall effect switch described in one of the Workshop presentations, do not have the counterpulsing requirement and may hence prove to be lighter, more efficient and less expensive than SCR's.

Much of the interest of the workshop participants was directed towards electron beam and optically controlled discharges. Several laboratories are conducting or planning experiments along these lines. It was clear, however, that much needed basic information is not available and that this makes it impossible to make an adequate analytical assessment of these concepts at the present time. It was felt that code-developments, coupled with experiments, were particularly needed. This work must also pay close attention to the poorly understood plasma chemistry in these switches and develop models for discharges and discharge processes.

For all switches it is important to pay attention to the energy efficiency of the switch in terms of energy switched and the energy consumed. Some switches, such as the e-beam sustained switch and the counterpulsed switches, have unique problems related to their particular interruption techniques (i.e. the e-beam and the counterpulse systems, respectively). Particularly important is the question if a particular

switch concept can be developed to sustain the inductor charging current for a time considerable longer than the output pulse length. In other words, what kind of pulse compression can be expected? A reasonable criterion seems to be that the ratio of inductor charging time to output pulse length should be larger than 10. In principle, this can be overcome by using a staged switch system where a slow, high current switch is used to build up the inductor current. This switch is then opened, transferring the current to a parallel, fast switch with less Coulomb ($\int i dt$) capability which opens when the first switch has recovered, thereby effecting a pulse sharpening (see Fig. 2). This concept has been applied in USSR single shot inductive energy storage systems where as many as 3 successive pulse sharpening switches have been used and in the NRL Trident system. Such a scheme increases the cost, size, and complexity and tends to reduce the reliability of the switch system and is better avoided, if possible. The basic concept of staged opening switches can also be used to provide a limited burst of output pulses from an inductive energy storage system. This scheme may well be a first step in developing fast, repetitive opening switches.

Obviously, several of the participants felt particularly strongly about the switches which they were closely associated with. An effort has been made to summarize and compare some near and far term capabilities of some of the switches in Table III. The numbers in () indicate the long term expected performance parameters. This table should obviously be read with caution since the numbers represent in some cases a very limited opinion sample (ranging from 1-10). These numbers have not been reviewed or verified in any other manner. It was felt, however, that the numbers represent the best "educated guesses" of active researchers in the field and hence are useful.

Efforts were made to outline the basic research issues which would lead to a better understanding and hence better design procedures for repetitive opening switches. These discussions were organized by workshop subgroups under the direction of E. Kunhardt, M. Parsons, P. Turchi, and I. Vitkovitsky. Switches with limited burst mode operation potential were also included for completeness.

The results of these discussions and recommendations are summarized in Table IV. Note that these research issues are not prioritized since

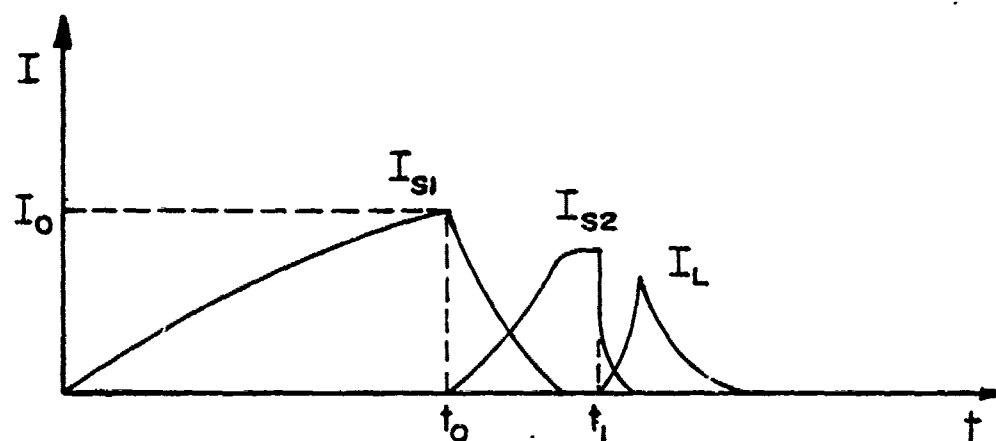
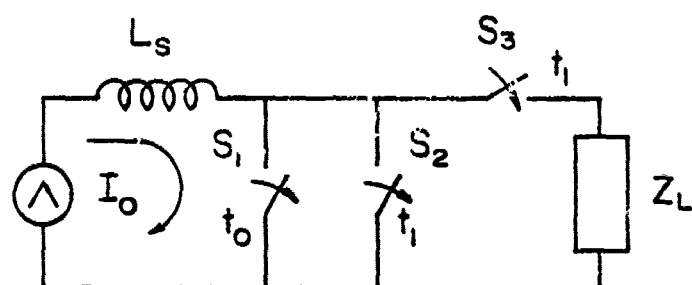


Fig. 2 The Use of Transfer Switches

Table III
SUGGESTED OPERATING PARAMETERS FOR SOME REPETITIVE OPENING SWITCH CANDIDATES

Parameter	V_{oc} (V)	V_{closed} (V)	J (A/cm ²) or I (A)	$\frac{dI}{dt}$ (A/μs)	Max. cw Reprate (pps)	Max. Burst Reprate	Life (Shots)	Needed Research
Switch Concept								
Electron Beam Controlled	$2 \times 10^4 - 5 \times 10^5$ (10^6)	$10^3 - 2 \times 10^4$ ($< 10^3$)	$10 - 10^3$ A/cm ² $10^3 - 10^5$ A (10^6 A)	$10^{11} - 10^{13}$ (10^{14})	$1 - 10^3$ ($10^3 - 10^5$)	$25 - 10^5$ ($10^5 - 10^6$)	$10^3 - 10^5$ ($10^5 - 10^8$)	Plasma chemistry, gas dynamics, electrode materials
Optically Controlled	10^5	10^3	10^4 A	10^{12}	10^4			Molecular Physics
Dense Plasma Focus	$5 \times 10^4 - 3 \times 10^5$	$10^2 - 10^3$	10^5 A/cm ² $4 \times 10^4 - 10^6$ A	5×10^{12}	25	10^5		Effects of B.C. focus formation, R. stability
Plasma Erosion	10^6		10^6 A	10^{14}		$> 10^3$		
Reflex Discharge	$< 10^6$ ($10^5 - 10^7$)	$3 - 4 \times 10^4$ ($1 - 15 \times 10^3$)	5×10^4 A/cm ² ($> 10^5$ A/cm ²)	($> 10^{13}$)	$.5 - 1 \times 10^3$	$2 - 10 \times 10^3$		Proof of concept
Spoiled Electro- static Conf.	10^4 (10^5)	500 (300)	3 A (10^3 A)	10^5 (10^8)	10^3 (10^5)	10^3 (10^5)	10^5	Scaling
Controlled Plasma Instabi- lities	$1 - 3 \times 10^5$	10^3	10^6 A/cm ² 10^5 A	10^{13}	10^4	10^5		Plasma Physics
$\vec{J} \times \vec{B}$ (Thyratron)	5×10^4	10^3	200 A	2×10^8	$> 10^3$			Plasma-Wall- B field interfaces
SCR (Counterpulsed)	5×10^3 (10×10^3)		4.5×10^3 A (10^4 A)	5×10^8 (2×10^9)	$2 - 4 \times 10^4$ (5×10^4)	$2 - 4 \times 10^4$ (5×10^4)	$10^7 - 10^8$ ($10^7 - 10^{15}$)	Pulse rating of SCR's

Table III (cont Inued)

Parameter Switch Concept	V_{oc} (V)	V_{closed} (V)	J (A/cm^2) or I (A)	$\frac{dI}{dt}$ (A/s)	Max. cw Reprate (pps)	Max. Burst Reprate	Life (Shots)	Needed Research
Vacuum Interrupter (counterpulsed)	3.5×10^4 -2×10^5	50	25×10^3 A (10^5 A)	$10^9 - 10^{10}$	25 (50)	25 (50)	$10^3 - 10^5$ ($10^5 - 10^6$)	Electrode Material, Recovery
Fuse	10^6		25×10^7 A/cm ² (10^8 A/cm ²)	3×10^{13} ($> 10^{14}$)		(6 pulses, Multistage)		Discharge media
Explosive (Chemical)	$.4 - 1 \times 10^6$		3×10^5 A	2×10^{13}				
Crossed Field Tube	10^5 (2.5×10^5)	500 (200)	10^4 A (2×10^4 A)	10^9 (10^{10})	10^2 (10^5)	10^5	3×10^7 (10^9)	
Vacuum Arc Interrupter	2.5×10^4 (10^5)	20-30	10^4 A (5×10^4 A)	5×10^9 ($> 10^{10}$)	10^3 ($1 - 5 \times 10^4$)		10^8 Coulomb transfer	Increased current capability-parallelism
Hall Effect	0.8 kV (1.6 kV/cm)	8 V (16 V/cm)	3.4 kA/cm ²	4×10^{10} A/cm ² -s	10^5 pps (10^6 pps)			Research on Hall effect material
Magneto-Plasma Dynalic	10^5 V/cm	$1 - 3 \times 10^3$ V/cm	3×10^5 A/cm ²	10^{12} A/cm ² -s	10^5 pps			Power flow at vacuum-plasma edge

TABLE IV

BASIC RESEARCH ISSUES

BASIC RESEARCH PROBLEMS	RESEARCH APPROACH	SWITCH CONCEPT
1. Discharge modeling and comparative experiments. Code development to produce circuit model. Inclusion of plasma chemistry.	Develop codes and carry out carefully planned experiments to check the code validity. Develop user oriented codes that enables the nonexpert to state problem in electrical circuit terms. Include plasma chemistry effects in the code.	Depending on the code (several will be needed) this applies to essentially all the gas discharge switch concepts. Particularly obvious ones are the electron beam and optically controlled, diffuse discharge switches
2. Compile and measure (when needed) fundamental data such as rate coefficients, cross-sections, etc.	Conduct literature search. Carry out basic measurements for gases and gas mixtures under conditions of interest to 1. & 3.	Essentially all gaseous switches, but especially those in 3..
3. Production of diffuse discharges. Establish conditions for arc development. Develop fundamental understanding to enable choice of gas mixtures with high breakdown field, high conductivity in conducting phase, fast recovery, etc.	Carry out a series of comparable experiments, utilizing input from 2. above, to determine optimum gas mixtures, pressures, and excitation conditions for diffuse discharge switches	Electron beam and optically controlled. Crossed field tube, spoiled electrostatic confinement, reflex discharge, plasma erosion, thyrons
4. Electrode phenomena. Surface physics of arc and diffuse discharges (e.g. sputtering) Photo-electric effect.	Conduct a careful experiment involving several gases, mixtures pressure, discharge conditions, etc., to establish the "best" electrode materials.	Essentially all gas discharge switches (including vacuum interrupter).

TABLE IV (Continued)

BASIC RESEARCH PROBLEMS	RESEARCH APPROACH	SWITCH CONCEPT
5. Motion of conducting plasma due to applied B-field. Effect of nonuniformities (asymmetries) in conduction channel on B field interaction.	Study interaction of high current plasma discharges with the vacuum/plasma/field interfaces manipulated electromagnetically to explain such features as residual plasmas (outside main conduction region), propagation of electromagnetic energy in plasma/vacuum field environment, energy dissipation, low density-high current conduction, etc.	$\frac{dL}{dt}$, Dense plasma focus, Magneto-plasma-dynamic
6. Plasma instabilities. Non-classical transport phenomena (Generated beams, anomalous resistivity, etc.)	Identify conditions for "triggering" plasma instabilities. Utilize information developed in fusion research and adapt to partially ionized, low temperature discharges. Conduct comparative experiments.	Dense plasma focus. Magneto-plasma-dynamic. Macro- and micro-instabilities.
7. Effects of quenching media on inductive and resistive fields and the hydrodynamics of the media and their heating/cooling rates. Investigations of conductivity, diffusion mechanisms, breakdown energy requirements, etc.	Make systematic studies, under comparative conditions, of a wide range of quenching materials (solid, gas, liquid). Instrument for careful, V, I, T measurements. Interpret chemistry involved.	Fuses JxB and magneto-plasma-dynamic devices with quenching medium.
3. Develop superconducting materials with improved stability and higher transition temperatures.	Fundamental materials development.	Superconducting switches

TABLE IV (Continued)

BASIC RESEARCH PROBLEMS	RESEARCH APPROACH	SWITCH CONCEPT
9. Flow dynamics in gas and liquid interrupters. Arc cooling rates. Recovery rate, effect of contamination	Carry out measurements under controlled conditions with varying flow velocities, current densities, and electric fields	Gas and liquid interrupters
10. Magnetic switch material development	Develop materials with high μ_r , B_{sat} , low loss	Magnetic (saturable inductor) switches.

this was not a direct goal of the workshop. An effort has been made, however, by the workshop coordinator and the Advisory Committee to prioritize some of the research issues, as shown in Table V.

It is clear that a cooperative research program between pulsed power technologists, plasma physicists, atomic and molecular physicists, plasma chemists, material scientists, and surface physicists is called for. Such a planned, coordinated program between research groups with the right expertise is expected to offer the best chance for rapid improvements in the understanding of the complex, interrelated problems at hand. No single research group seems to possess all the required expertise but combinations of a few groups should be able to cover all the most important basic phenomena without excessive administrative coordination problems.

Much of the needed research is also of importance to the development of advanced gas discharge lasers (e.g. diffuse discharges at high voltage and high repetition rates). It is, therefore, important to keep close contact with this research community. Much of their past and present code development work may prove to be very valuable to the opening switch problem.

In the areas of materials problems and gas flow dynamics there are also clear common interests with researchers in the area of repetitive closing switches. Appropriate contacts and exchanges should be established. It may, for instance, be valuable to hold discussion sessions at meetings of common interest, such as the IEEE International Pulsed Power Conference.

A switch concept which was not discussed in any depth at the workshop was that of magnetic switching using saturable materials, such as ferrites or metglass. This was primarily due to the lack of attending experts in this field. Brief discussions indicated, however, that this topic deserves more consideration than it received.

Some valuable, clarifying comments about opening switches were made by P. Turchi. He pointed out that:

- Energy required to open the switch can be divided in two parts:
 - 1) Fundamental (flux conservation, internal losses)
 - 2) Technical (energy required to move switch contacts or change conductivity).

TABLE V
SUGGESTED RESEARCH PRIORITIES

- 1a) Discharge Modeling (including plasma chemistry) and Comparative Experiments.
- 1b) Production of Diffuse Discharges with High Hold-off Voltage, High Conductivity, High Current Density, and Fast Recovery.
- 1c) Measurements of Basic Data Needed in a) and b) Above, such as Cross-sections, Rate Coefficients, etc.
- 2a) Motion of Gas Discharges in Magnetic Fields.
- 2b) Plasma Instabilities, Non-classical Transport Phenomena.
- 3) Determine the Limits to Various Solid State Switching Schemes
- 4) Electrode Surface Physics of Arc and Diffuse Discharges
- 5) Effects of Quenching Media on Discharges

- Importance of stray inductances and magnetic energy stored in the switch itself compared to the switching energy
- Importance (especially from an engineering viewpoint) of taking the energy to operate the switch from the inductive store itself and not from another source, such as a separate capacitor bank.

The need for novel ideas in this field is clear. It is, by no means, certain that any of the proposed schemes to date can be extrapolated and engineered in the high power, high repetition rate, long life regimes of primary interest. The research area is one of high risk and of potentially extremely high pay-off.

It is believed that the workshop served a very useful function : it stimulated new ideas and thoughts in this important field. Another workshop is recommended on the same basic topic about 2 years from this first one. This report can then be used as a common background briefing for the participants and a basis for starting the discussions. In the follow up workshop, only participants with clearly new ideas or results beyond what is covered here should make formal presentations. The workshop participants should then split into discussion groups and report back with their results and recommendations at the end of the workshop. A workshop on discharge modeling and accompanying verification experiments is also recommended as soon as possible.

CONTRIBUTED PAPERS

INTRODUCTORY REMARKS

T.H. Martin
Sandia National Laboratories
Albuquerque, N.M. 87117

Inductive energy storage and switching systems have long held promise for small, light, energy dense stores in comparison to capacitor banks. However, their use has never developed in terawatt pulsed power accelerators now being used or proposed for inertial confinement fusion or directed energy weapons. To be competitive, the repetitive opening switches should be able to replace present repetitive closing switches. For comparison, a SNL repetitive gas switch now operates at 1.5 MV, 20 kA at 20 pps with 2 kJ per pulse for 10^7 shots. At one shot per day, SNL closing switches now operate at 2.5 MV, 0.2 MA with 40 kJ per pulse. Repetitive opening switches are only approaching these parameters. Subsequently, the SNL inductive storage research program is concentrating on explosive inductive energy stores and explosive opening switches capable of scaling to at least 100 megajoules. This energy level is beyond the present Marx capacitive energy stores. Other SNL programs that relate to inductive energy storage or repetitive pulse technology are:

PULSAR — a program to obtain repetitive microsecond pulses using flux compression of a super conductor magnetic field.

FAST CLOSING MAGNETIC SWITCHING — a research program to replace the present rapidly charged, pulse line water switching with magnetic core saturable reactors.

MULTI-MEGAVOLT PULSE TRANSFORMER — a program to provide repetitive pulses at several megavolts at rates to 20 pps to water capacitor energy stores. The present transformers operate to 1.5 MV, 2 kJ at 20 pps.

REP RATE MARK GENERATORS — a program to provide 1 MV, 10 kJ at 10 pps from a capacitor energy store.

The requirements for relatively short pulses (~ 40 ns), high powers (~ 100 TW), and reuseable switching make inductive energy stores usage difficult for ICF applications. In an ICF power plant, lifetimes between 10^9 and 10^{10} pulses will be required for reactor operation. If repetitive opening switches are seriously proposed for these applications, considerable development must be initiated to narrow the present relative opening and closing switch capabilities.

OPENING SWITCH TECHNOLOGY*

Robin J. Harvey and A. Jay Palmer

Hughes Research Laboratories
Malibu, California

Abstract

A review of high power opening switch technology is presented. The basic physics of opening switches is described in a unified format by categorizing the opening impedance of a switch as either resistive, capacitive, or inductive. The most important of the known high power opening switch mechanisms are then reviewed according to this classification scheme. Fundamental limits to opening speed and generalized scaling laws for the dependence of opening speed on interrupted current and hold off voltage are identified. Some speculation on new approaches for developing opening switches with advanced performance is presented on the basis of the perspective provided by the review format. Several summary charts are presented which can be used to provide at a glance a broad perspective of this complex field. A comprehensive bibliography is provided for access to more detailed information on specific switch types.

*This work supported by U.S. Army Research Office through Battelle Columbus Laboratories, Contract No. DAAG29-76-D-0100, Delivery Order No. 1744.

SECTION I

INTRODUCTION

Opening switches are key elements in the development of inductive energy storage and high energy systems. This study is directed at finding new current interrupting mechanisms; it is also directed at assessing existing mechanisms, their limitations as switches, and their state of development. This task is open-ended as posed, so we have implicitly assumed that, to be considered, the mechanisms must have a promise of conducting at least tens of kiloamperes at low loss, and interrupting against tens of kilovolts. The ratio of the conduction period to the interruption time is a measure of the power compression and the efficiency of a switch. We assume that this ratio must be at least a factor of ten to begin to be of practical use. Short opening times are needed for many applications. We have included considerations of existing switch mechanisms with millisecond opening times in order to put them into perspective with more interesting possibilities for opening switches in microseconds or less. A similar factor of interest is the repetition rate. Existing single shot mechanisms are included to show what can now be done, but repetitive operation at tens of pulses per second or more is needed.

The first section of this study is an attempt to describe the complex subject in as simple a format as possible. We note that for time scales slower than the transit time of light, only three basic mechanisms exist (resistive, inductive and capacitive) which can be responsible for the development of voltage across a circuit element. We examine a variety of known switch mechanisms and show how they may be categorized and analyzed in terms of these three basic impedance changing mechanisms. This characterization procedure is not always unique, but we have used it to derive general scaling rules and limitations which are qualitatively consistent with the existent data. A detailed analysis of a given switch type is likely to be more complex. The number of parameters that need to be considered are often extensive since many limiting mechanisms may exist simultaneously. Also, a given

switch concept will usually have validity only when it is considered as a system component which is operated in sequence with other switches. Therefore, the scope of this paper is introductory in nature.

In the course of this study we have noted several general areas which may be of speculative interest. For example, the impedance models which we used are invalid if traveling electromagnetic waves are important. Can one use microwaves to cut off conduction? Pulse forming networks using saturable reactors have been demonstrated as pulse compression systems and they eliminate the need for active repetitive closing switches in some cases. Can such magnetic switching be of utility where opening switches are required? None of the known switches use capacitive opening as the main mechanism (other than through an external commutation capacitor). Are there ways to use C to open switches? Ultimately, fuses are the highest power opening switches known, and scaling is not a problem for short single pulses. Since solid or liquid metallic conduction must eventually be used for the charging phase, how can one achieve a reversible conductor to insulator (or semiconductor) transition that does not self destruct?

IMPEDANCE CHARACTERIZATION

Out of the plethora of techniques available for high power current interruption, there are generally only a few classes of devices known to be suitable for any specified application and even less designs that will give optimal performance using available technology. Often, there are no known techniques to suit projected or existing requirements. This is especially true at currents above 10 kA at voltages above 10 kV and switching times under 1 μ sec. Here, there is a need for a unified format for searching out and categorizing processes available for current interruption. In this study we employ such a unified format to survey all known mechanisms for high power current interruption.

An opening switch may be characterized by a generalized time dependent impedance, $Z(t)$. An optimal switch is one in which $Z(t)$ can exhibit a maximum reversible time rate of change. As illustrated in Figure 1, there are only three basic electrodynamic contributions to

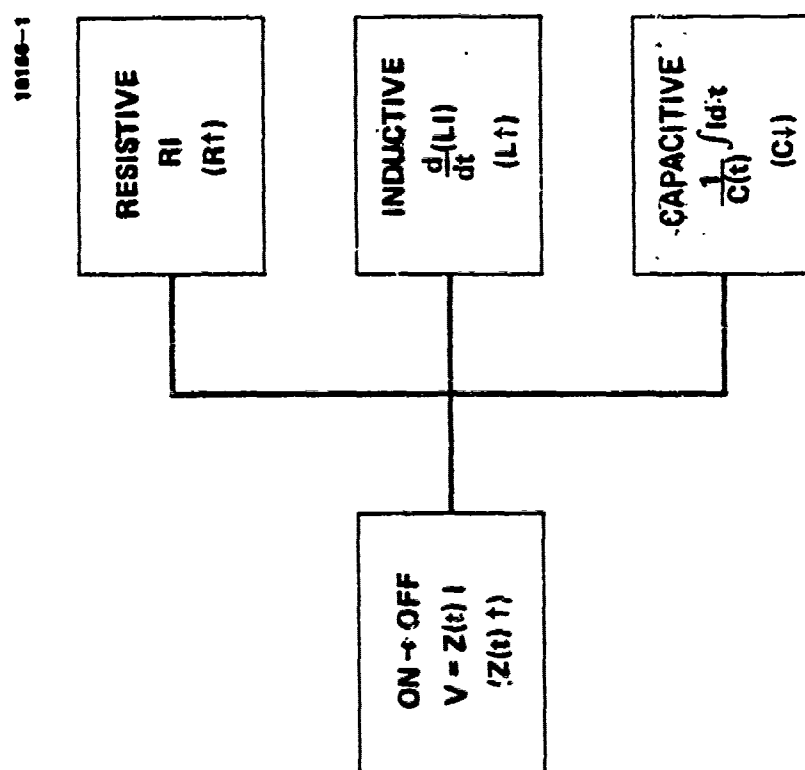


Figure 1. Fundamental opening impedances.

$Z(t)$, the resistive, inductive, and capacitive characteristics of the switch.

A rigorous demonstration of how these time dependent characteristics contribute to the effective impedance of the switch is obtained by writing down the principle of conservation of energy for the total electric and magnetic fields within the switch volume from Maxwell's equation

$$\int dv [\nabla \cdot (\bar{E} \times \bar{H}) + \bar{E} \cdot \bar{J} + \frac{\partial \bar{B}}{\partial t} \cdot \bar{H} + \frac{\partial \bar{D}}{\partial t} \cdot \bar{E}] = 0 \quad (1)$$

where E , D , B , and H are the usual field definitions, J is the current density and the integral is over the volume of the switch. If one neglects the contribution of the self-energy of the charges to the integral (which is not at ones control) and neglects radiative energy transfer and loss (which is valid for typical switch speeds and volumes), then Eq. (1) can be shown to reduce to:

$$\begin{aligned} \text{Power} = \bar{I} \bar{R} \bar{I} + \bar{I} \frac{\dot{\bar{L}}}{2} \bar{I} + \bar{V} \left(\frac{1}{2\dot{\bar{C}}} \right) \bar{V} \\ + \bar{I} \bar{L} \dot{\bar{I}} + \bar{V} \bar{C} \dot{\bar{V}} \end{aligned} \quad (2)$$

where the vectors \bar{V} and \bar{I} represent the loop voltages across the switch and the loop currents through the switch, while the matrices \bar{R} , \bar{L} , and \bar{C} are the generalized time-dependent resistance, inductance, and capacitance of the switch.

It is evident from Eq. (2) that $1/2 dL/dt$ and $2 (dC/dt)^{-1}$ enter into the effective impedance of the switch as resistances. An essential difference, of course, is that the dL/dt and dC/dt terms are due to macroscopic mechanical interactions and are in principle reversible. They do not need to cause heat dissipation in the switch as the resistive contribution to Z does. Motors, generators, flux compressors, and saturable reactors are examples of dL/dt interactions which could be used to perform the function of a repetitive switch. Examples of dC/dt are rare, due to the low value of capacitance across a typical switch. The principal exception is the space charge dominated sheath of a glow

discharge where the spacings are very small and relative motions may be at high speed. (The use of an auxiliary commutation capacitor in combination with a closing switch to produce a step function capacitance could also be put into this category.)

In general, devices cannot be treated as lumped parameters. But most have a dominant characteristic. We have classified the switch opening mechanisms as resistive, capacitive or inductive depending on whether the voltage increase on opening is caused dominately by increased dissipation in the switch, electrostatic effects, or increased self-inductance respectively. Thus, for example, the various arc discharges and solid state conductors which are interrupted by the application of a transverse magnetic field, by forced convection, or by a state change are examples of resistive opening mechanism since in all of these methods the increased switch voltage is due to increased energy dissipation in the switch. The vacuum tube and cross-field discharge interrupters are examples of electrostatic opening mechanisms since the voltage increase which occurs during interruption is due in part to the nondissipative alteration of space charge in the switch caused by the depletion of charge carriers. This characterization of opening switches according to whether the opening mechanism is resistive, capacitive, or inductive is not a precise procedure, but it does assist in determining the fundamental limitations of a given switch type. It also provides a broad perspective of available techniques to better assure that an optimal choice of switching mechanism has been made. For example, processes controlled by resistive impedance will have well-defined repetition rate limits imposed by heat dissipation on opening, while capacitive and inductive impedance mechanisms will tend to have transit time limits to the switching speed.

In Section II below we review many of the known high power opening switch mechanisms according to the above classification scheme. In Section III we discuss the fundamental limits on the opening speed of each of the impedance categories. We present generalized theoretical scaling laws for the dependence of the opening speed on current and voltage and compare the general scaling law with known switch performance

characteristics. In Section IV we identify potential new approaches for developing opening switches with advanced performance. Section V contains an annotated bibliography.

SECTION II

REVIEW OF OPENING SWITCH MECHANISMS

Ultimately only moving charges can carry current; but the medium through which they move may be of any of the known states of matter, mixtures of these states or just a vacuum. The current may be interrupted by changing the state of the medium, altering the source of charge carriers or by applying forces to the medium or to the carriers. Table 1 shows where representative opening switches fall on a chart of conducting media versus typical interruption mechanisms. The size of the chart is a function of our choice of the finiteness of the subdivisions which we have included and it could be reorganized to suit one's point of view. But this form of representation does indicate the extent of coverage of this parameter space by state-of-the-art devices and allows us to consider what combinations, such as liquid metal (jets)/phase change (fuse), might lead to a practical device where none is now known to exist.

The enclosed bibliography may be used to give a detailed knowledge of the behavior of the particular opening switches noted. Some benefit may be gained by first reviewing the interruption mechanisms from the perspective of reducing the complexity of the entries down to the most basic form. In the following analyses we discuss each of the switch types and later note several areas which show up as not covered by existing technology. (These appear as bracketed entries in Table 1.)

A. RESISTIVE (OR THERMAL) OPENING MECHANISMS

1. State Changing (Fuses and Superconducting Transition Switches)^{R1-R11}

The most familiar of the state changing resistive opening switches is the fuse (R1-R6). The fuse opening mechanism is the boiling and vaporization of a metallic conductor caused by Joule heating. Since the explosive boiling of the fuse element is irreversible, repeated operations require repeated installation of a new fuse element. The rate at which this can be done clearly depends on the inertia of the element.

Table I: Summary of Opening Switch Mechanisms

INTERRUPTION MECHANISM		PHASE CHANGE	COMBINATION-RECOMBINATION	CONTROLLED IONIZATION	POTENTIAL BARRIER	INSTABILITY	HIGH SPEED MECHANICAL MOTION	E-M WAVE	HALL EFFECT	NONLINEAR MEDIA CHANGE
CONDUCTING MEDIUM	SUPERCONDUCTOR	SUPERCONDUCTOR								
	METAL	FUSE					(RAIL GUN?)			
SEMICONDUCTOR		METAL TRANSITION	SCR		TRANSISTOR				HALL EFFECT DEVICES	
	LOW PRESSURE		THYRATRON	XFT, SECS, E-BEAM		PLASMA FOCUS		(?)	THYRATRON	
GAS	HIGH PRESSURE		CIRCUIT BREAKERS, SPARK GAPS	LASER, E-BEAM CONTROLLED			ARC FREE INTERRUPTER EXPLOSIVE SWITCHES		ARRESTERS	
	VACUUM		LMPV, VACUUM CONTACTORS	(PHOTO ELECTRIC?)	REFLEX DIODE, VACUUM TUBE	VACUUM ARC		(?)	VACUUM ARC	
SURFACE										
LIQUID		(LM FUSE?)								
FERRITE (HIGH μ)										SATURABLE REACTORS
(?) (HIGH ϵ)										(SATURABLE CAPACITORS)

104B4 5

The highest peak powers attained in opening switches have been achieved using fuses. (Currents of 2×10^6 A and voltages of 200 kV have been reported, separately.) These devices are essentially fuses embedded at high pressure in quartz sand or H_2O to ensure a high voltage holdoff (at least temporarily) following heating of a metal conductor past the boiling point.

Another example of a state change resistive opening switch is the superconducting switch (R7-R11). In the superconducting switch, the superconducting to normal-conducting transition is used to change the resistance from essentially zero to a few ohms. This transition is forced by exceeding the critical magnetic field, the critical current or the critical temperature. Submicrosecond switching times may be obtained in this manner, at currents up to at least 13 kA. In order to make energetically efficient use of the switch, the normal switch resistance must be kept much higher than the load resistance while the internal inductance of the switch must be kept low. Otherwise, the heat loading of the cryogenic (LHe) system will rise to unacceptable levels.

2. High Pressure Arcs (Circuit Breakers, Explosive Switches, Spark Gaps) R12-R14

High pressure arcs require a finite power input to maintain a discharge. By temporarily commutating the current to near zero, the gas temperature (and thereby the conductivity of the gas), decays with time. By combining commutation with a mechanical increase in the arc length and/or by a forced flow of gas the required commutation time can be reduced.

In the high pressure discharges, most of the voltage drop occurs in the positive column of the arc where the input electrical power is balanced by heat dissipation. This dissipation increases at constant current during the lengthening and cooling of the arc. Thus the opening mechanism is classified as resistive. The time period during which voltage rise may occur is the period after current commutation when the volumetric ionization rate is falling. Since the arcs are thermally ionized, the characteristic time scale controlling the opening voltage

rise is the cooling time for the arc. Thus the opening speed will depend on parameters such as thermal conductivities, physical size of the arc, and radiative transfer rates. Since the current through the switch will usually determine the radius of the arc, there will be a rather close relationship between the current carrying capacity of the switch and the opening speed. The holdoff voltage will, of course, depend on the gap length and gas pressure. The repetition rate of these switches is controlled by the inertia of the mechanical or gas flow mechanism which establishes the arc length.

3. Low Pressure Arcs (Vacuum Arcs, LMPV, Crossed Field Closing Switches) (R15-R18)

Vacuum arcs are normally characterized by the appearance of small cathode arc spots which emit partially ionized jets of metal vapor towards the anode. These spots have a finite chopping current and can be interrupted by the use of commutation in tens of microseconds. Increasing the current tends to increase the number of cathode spots and gas vapor. Empirically, the slope of the commutating current must be less than $\sim 185 \text{ A/}\mu\text{s}$ in order to achieve a fast voltage recovery. At currents above about 50 kA larger anode arc spots form and the needed recovery time increases markedly to milliseconds. The processes involved are thermally controlled and we may classify them as resistive.

4. Hall Effect (Magnetically Switched Arcs, Thyratrons, and Semiconductors) (R19-R23)

The opening mechanism in these switches is an induced decrease in the mobility of charge carriers in the switch caused by the application of a magnetic field perpendicular to the current flow. This drives the arc into contact with walls, cooling the discharge or extends the discharge and causes violent instabilities to develop. Crudely, the basic mechanism can be classified as resistive. In the case of magnetically switched arcs and thyratrons, the discharge can be extinguished entirely if the induced voltage rise is high enough, whereas in the case of the semiconductors, the off state resistance remains fairly low ($\sim 0.05\Omega$).

The opening speed depends on the rate of increase of the applied magnetic field and on the current flow. The maximum current in these switches is limited primarily by the average current through heat dissipation. The holdoff voltage of these switches is controlled by the strength of the magnetic field together with the usual dependence on gap size and pressure, and breakdown field thresholds.

Current levels on the order of hundreds of amperes have been magnetically switched off in vacuum arcs and thyratrons against voltages of on the order of 10 kV with opening times ranging from 1-20 μ sec. Analogous Hall effect semiconductor switches are limited to voltage drops of 600 V at 1-2 kA. Lightning arrestors often use magnetic fields to help extinguish ac arcs at atmospheric pressure.

5. Controlled Ionization (Electron Beam Sustained Discharges) R24,25

In an electron beam sustained discharge opening switch, a high energy electron beam enters a high pressure gas volume between the switch electrodes through a thin metal foil. The volumetric ionization produced in the gas by the electron beam is multiplied by the E-field of the switch. The voltage and current are maintained below the level where the discharge is self-sustaining so that when the electron beam is shut off the switch opens. As with most high pressure discharges, most of the voltage drop appears in the space-charge-neutral portion of the discharge gap and most of the voltage rise on opening of the switch also occurs here. This must be accompanied by increased dissipation so the opening process is an example of a resistive impedance increase.

B. ELECTROSTATIC OPENING MECHANISMS

1. Current Commutated Discharge (Thyratrons C1, C2)

Repetitive closing switches can always be used in combination with a commutation capacitor and another closing switch to function as an interrupter. Thyratrons and SCRs are typical high repetitive rate devices that may be used in this mode. These switches develop a charge

density during conduction which must be dispersed during the recovery period. Recovery can often be aided by the proper choice of inverse voltage to sweep out the charge and reset the switch to the off state.

2. Controlled Ionization (Cross Field Interrupter Tubes and Electrostatic Confinement Discharges)(C3, C4)

These devices are true interrupters. They forcibly interrupt the current by quenching the volumetric production of charge carriers through the removal of confining magnetic or electric fields in a low pressure discharge. In the case of cross field tubes (XFTs), the tube conducts only when the gyro radius of electrons emitted from the cathode is less than the separation of the electrodes, thus allowing the electrons to undergo a sufficient number of ionizing collisions to sustain the discharge. Similarly, in the so-called spoiled electrostatic confinement switch (SECS), a low pressure wire anode discharge is made self-sustaining only when the endplates are at cathode potential. Under this condition, electrons emitted from the cathode can make many orbits around the anode wire causing sufficient ionization to sustain the discharge. When the magnetic field is eliminated in the XFTs, or the endplates are brought to anode potential in the SEC device, ionization is reduced drastically and the discharges are extinguished.

In both of these devices most of the discharge voltage appears across the space charge limited cathode fall. Thus the voltage rise on opening is partly accounted for by the reduced capacitance of the sheath as the unreplenished charges are swept out of the discharge gap. The exceptionally short spacing of the sheath and high speed it develops makes these devices the closest capacitive analogue to the resistive controlled ionization opening mechanism (electron beam sustained discharge).

3. Potential Barrier (Vacuum Tubes, Transistors)

Vacuum tubes and transistors are true opening switches. They utilize an applied potential barrier to interrupt or gate the current

flow. The voltage rise on opening is accompanied by a decreasing capacitance of the space charge as the electrons are swept out of the grid-anode gap. The opening speed thus depends on the geometry and dimension of the anode to grid gap, and the space charge limited electron (or hole) velocity which is determined in part by the tube voltage. The peak current is limited in the case of the vacuum tube by the thermionic emission rate of the cathode and by dissipation in the transistor. The average current or repetition rate is usually limited by the heat dissipation. The voltage holdoff of the vacuum tube is determined by the vacuum breakdown voltage which increases with increasing tube dimension and is thus closely correlated with the opening speed.

Average power ratings of vacuum tubes presently go as high as 3.6 MW at radio frequencies. The maximum current is on the order of 1.2 kA while the peak power is limited to about 60 MW. Voltages are typically 60 kV, although higher voltages are possible at reduced current and average power. Conduction voltages are typically 10% of the peak voltage.

4. Saturable Capacitors (G3)

Zucker and Bostick have pointed out that nonlinear dielectric media with ideal saturation properties could be used to reversibly interrupt the flow of current into a capacitor. Such nonlinear capacitors could be used as voltage enhancing pulse forming networks (see magnetic switching). New materials are needed.

C. INDUCTIVE OPENING MECHANISMS

1. Current Constriction (Explosive Liners, Plasma Focus) L1, L2

Explosive liners can be regarded as the inductive analogue of the fuse. Like the fuse, the switch element is a metallic conductor which is explosively destroyed. However, this is done by external explosive forces that drive the liner inward rather than by Joule heating of the conductor. The self inductance of the device, as well as the mutual inductances change with time. But there is no fundamental novelty present which cannot be found in other electro-mechanical generators. In

the plasma focus the time scales are much shorter. Here, a high current arc is compressed rapidly by self-generated magnetic fields. This compression can occur rapidly enough so that the voltage induced by dL/dt during the compression exceeds the resistive drop of the arc and the original current source. If this voltage could be sustained, then we would have the possibility of a high power inductive opening switch.

2. Magnetic Switching (Saturable Reactors) L3, L4

We have discussed the mechanical contributions to \dot{L} above. Since the inductance may also be controlled through the magnetization of a nonlinear medium, there is a solid state analog called magnetic switching. This has been exploited in the case of pulse compression by starting with capacitive energy storage and using a pulse forming network composed of saturable reactors and standard capacitors. Here the long duration, low current input pulse is sequentially increased in amplitude and contracted in time as the inductors saturate.

The saturable capacitor discussed earlier is the analog to magnetic switching. New circuit configurations and materials are needed for inductive energy storage.

3. Electric Rail Guns, L5

Electric Rail Guns are essentially linear motors where a conducting projectile is driven along a pair of rails by high $J \times B$ forces. The energy used for the acceleration can be accounted for by the $d(1/2LI^2)/dt$ of the current loop. Speeds of ~ 1 cm/ μ sec are considered in the literature. These mechanical speeds are consistent with those of ions in plasmas and a variety of novel effects are conceivable. External magnetic fields placed along the rail can conceivably turn the gun into a pulse generator or driven oscillator with a transient life time limit given by thermal destruction of the projectile or rails.

SECTION III

SUMMARY AND GENERAL SCALING LAWS

The division of opening switches into the above three categories allows one to make some rough generalizations of scaling behavior. Of primary interest is the general dependance of opening speed on operating conditions. Below, we identify some rough scaling laws for the dependence of switch opening speed on the interrupted current or on holdoff voltage for the resistive, capacitive, and inductive mechanisms separately and compare these generalizations with demonstrated switch performance.

A. RESISTIVE

Figure 2 shows some representative samples of fuse and superconductor opening times and interrupted currents reported in the literature. It is difficult to generalize a single scaling law for the opening times of these switches for several reasons. For example, fuse and superconductor element geometries can vary from wires to thin foils and due to self inductance the opening time will differ considerably for the different geometries. However, a fundamental limit to the opening time for a wire superconductor can be noted for reference. This time is given by the minimum time for the over-critical magnetic field to penetrate the normal metal through the skin depth. This time is given by

$$\tau \sim \delta^2 \sigma \mu \pi \quad (3)$$

where σ and μ are the conductivity and permittivity of the normal metal and δ is the skin depth. The skin depth is then set equal to the radius of the wire, which in turn is related to the peak current in the switch through

$$r = \delta = \frac{\mu I}{2\pi H_c} \quad (4)$$

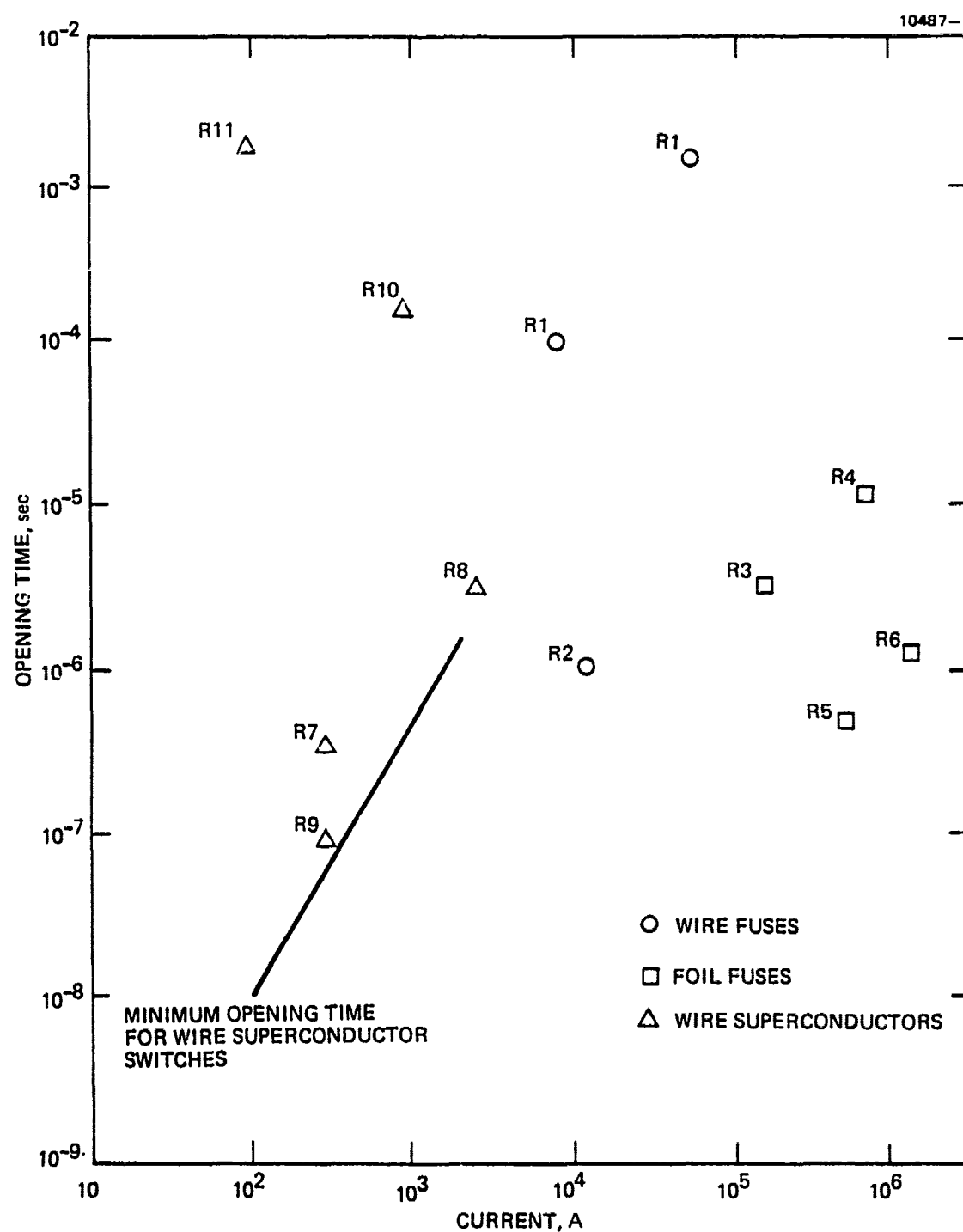


Figure 2. State changing opening switches.

where H_c is the critical field and I is the current. This gives the $\tau \sim I^2$ limit shown in the figure.

In principle, the super conducting switch response time can be reduced by using thin films. High currents would require wide films. Since a high normal resistance is also needed to avoid self heating, this would force long lengths and a large surface area. Devices of this type are likely to be limited by cost and design considerations.

In Figure 3, we show representative performance data for the other major category of resistive opening impedance switches — the commutated arcs and the electron beam sustained discharge switch. In the commutated arcs, the fundamental limit to opening time is a cooling time. In the case of forced gas arcs, it is the cooling time of a plasma column; in the case of vacuum arcs it is the cooling time of the cathode arc spot. This cooling time is controlled by thermal conduction and radiation, and is proportional to the effective cross-section of the arc which in turn goes roughly as the current. This scaling is seen to be approximately borne out by the data in Figure 3. For the vacuum arcs, the data shown is taken in a regime where multiple arc spots occur on the cathode. Above a current level of $\sim 7 \times 10^4$ A, these arcs tend to collapse onto a single anode spot whose cooling time is much longer as illustrated in Figure 3. These devices are well developed.

The electron beam sustained discharge must be regarded separately from the above arc discharges. Recombination times, attachment times, and inductive times can all contribute to the opening time of this switch. A phenomenological scaling law has been presented in Ref. R24 and is illustrated in Figure 3.

There appears to be a practical limit of about 10^5 A where the efficiency of the switch drops. Efficiency and conduction time appear to be the key limits.

B. ELECTROSTATIC

For most of the capacitive opening mechanisms, the characteristic opening time is the time it takes for the major carrier to transit the space charge dominated gap. During the final opening phase, the voltage

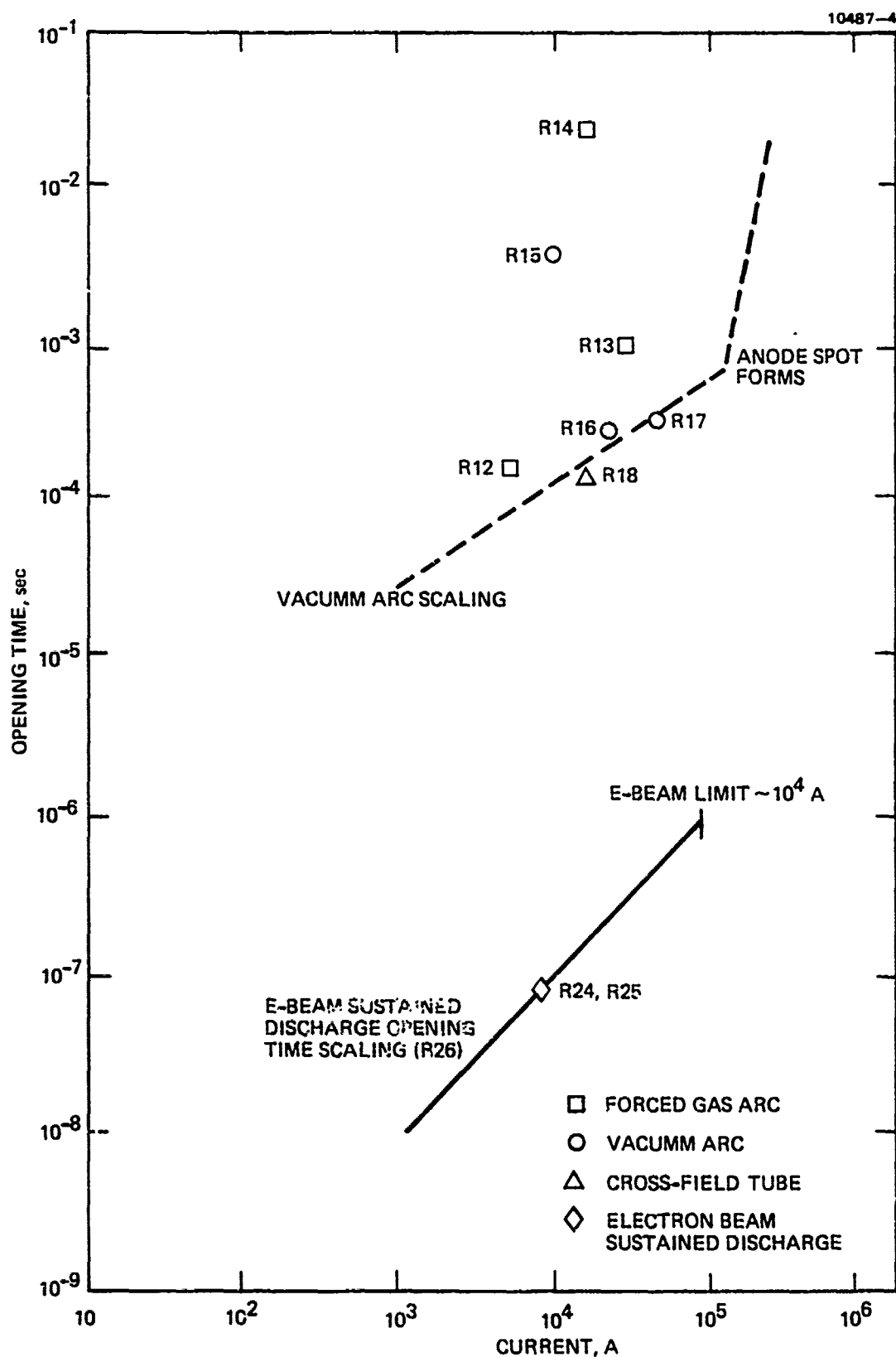


Figure 3. Commutated discharge and electron beam sustained discharge opening switches.

across this gap is comparable to the holdoff voltage of the switch. Also, in the case of a discharge plasma, the space charge dominated gap (cathode sheath) will approach the electrode gap once ionization stops. So we can estimate the characteristic opening time as

$$\tau = \frac{d}{\left[\left(\frac{e}{2m} \right)^{1/2} v^{1/2} \right]} \quad (5)$$

where d is the electrode gap, v is the holdoff voltage and e/m is the charge to mass ratio of the major charge carriers.

The electrode gap, d , must be chosen large enough to maintain the electric field in the gap below a breakdown field E_B . So we can write

$$\tau = \frac{v^{1/2}}{\left(\frac{e}{2m} \right)^{1/2} E_B} \quad (6)$$

Thus, the opening speed of the capacitive opening impedance switches depends on voltage as expected. Figure 4 shows this scaling law for electron charge carriers and for helium ion charge carriers together with some representative performance data points.

Peak currents are limited by plasma instabilities during conduction, and glow to arc transitions during interruption. The use of commutation in parallel with forced interruption may be able to increase the peak current levels above the present 10-15 kA XFT limits. Also better plasma models for the interaction of multiple electrodes may reveal means of enhancing the interruption speed.

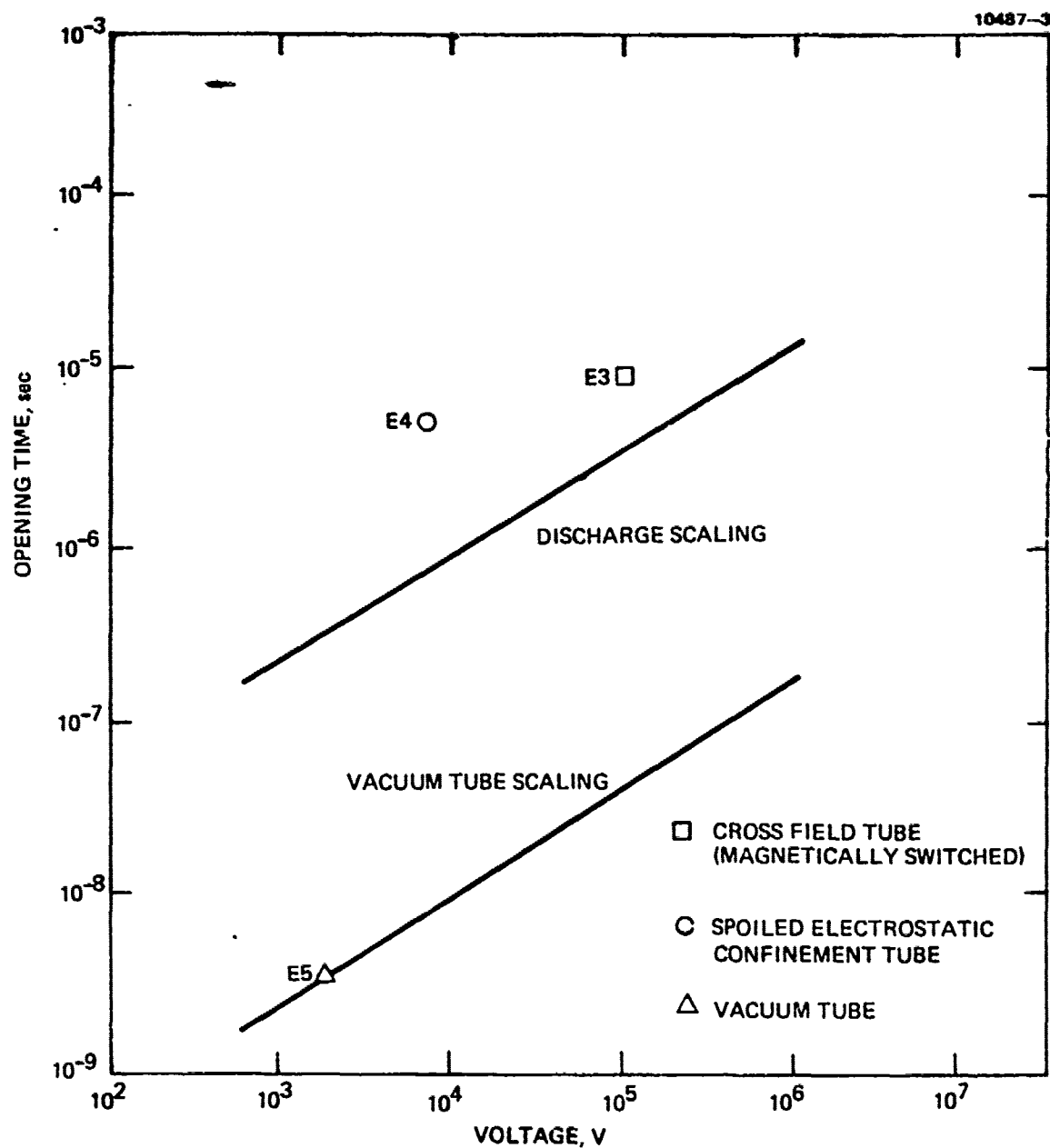


Figure 4. Electrostatic opening switches.

C. INDUCTIVE

In an inductive opening mechanism, the voltage across the switch is driven up due to a forced increase in the self-inductance of the switch. When this induced voltage becomes comparable to the applied Emf, current flow through the switch will stop. The applied Emf will remain across the switch if the switch conductivity is also reduced to zero during this time. As long as this conductivity reduction occurs in a time which is short compared to the inductive voltage rise time, the switch opening impedance can be regarded as inductive and the characteristic opening time can be written

$$\tau = [dL/dt/L_0]^{-1} \quad (7)$$

where L_0 is the mean switch inductance.

A way to develop a model analogous to the electrostatic case would be to replace the electrostatic force by the $J \times B$ force. However, in this case there is no similar limit on the B field (other than the strength of materials), but there are limits imposed by complicated dynamics (instabilities) which cannot be treated in so general a fashion.

SECTION IV

POSSIBLE AREAS OF IMPROVEMENT

The state of the art of opening switches appears to be limited to single pulse devices such as fuses switching very high powers ($\sim 10^{12}$ W) or; to repetitive devices having considerably lower power capability ($\sim 10^9$ W). If cost and complexity were not limiting constraints, brute force means could be used to combine the above features. Several projected alternates have already been noted in the text. The more "far out" ones include: saturable capacitors, ultrahigh speed projectiles, and non-exploding fuses. Plasma instabilities can work (via L or C) to induce the high transient voltages needed to bring currents below the chopping current. These are normally not well controlled. Are there ways to trigger such instabilities at many locations simultaneously? In the free electron laser, the electron beam transfers its energy to an electromagnetic wave. Can one stop the flow of charge carriers by the use of coherent high energy radiation? Are there new nonlinear media which can have their ϵ and/or μ controlled by external means at high speed?

Judging by the open areas we have shown in Table 1, the long term prospects for new higher power opening switches are still open. Statistically, other concepts are likely to be demonstrated in the future. Failing this, the prospect for efficiently combining the best features of the known interrupting mechanisms depends on the overall system characteristics. Figure 5 shows the state of the art of the peak powers as a function of the operating pulse widths of typical switches. The dotted lines are low repetition rate devices. The preferred approach for the near term is to design the system around available opening switches.

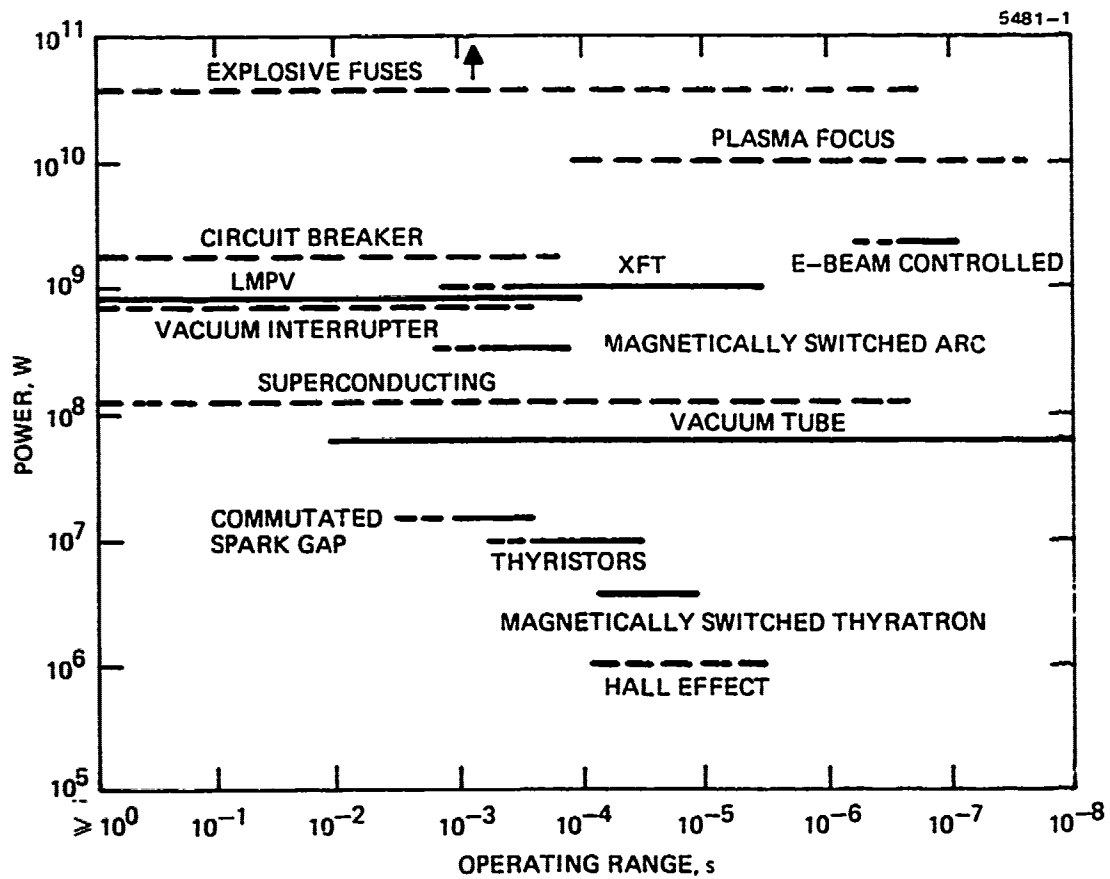


Figure 5. Power versus opening time summary.

A. GENERAL REVIEW PAPERS ON HIGH POWER OPENING SWITCHES

- G1 R.J. Harvey, "Opening Switches," Pulsed Power Workshop Proceedings, 1976, Vol. 1, p. 35.
- G2 T.R. Burkes, J.P. Craig, M.O. Hagler, M. Kristiansen, W.M. Portnoy, "A Review of High Power Switch Technology," IEEE Trans. Elect. Devices, ED-26, #10, 1401, 1979.
- G3 W.H. Bostick, et al., Eds., Proc. Int'l. Conference on Energy Storage, Compression, and Switching, Plenum Press, Tornino, Italy, Nov., 1974.
- G4 IEEE Trans. Elect. Devices, "Special Issue on Pulse Power Modulators," ED-26, #10, 1979.
- G5 Proc. 2nd IEEE Inst. Pulsed Power Conference, Lubbock, Texas, 1979.
- G6 Proc. Particle Beam Research Work Shop, USAF Academy, January 1980.

B. RESISTIVE OPENING IMPEDANCE SWITCHES

- R1 J. Salge, et al., Pg. 477 in Ref. G3.
- R2 F. Damidau, et al., 7th Sym. on Fusion Technology, Grenoble, France, Oct. 1972. EUR-4938, p. 453.
- R3 M. Friedman and M. Urey, Rev. Sci. Inst., 48, 279, 1977.
- R4 C.A. Bleys, et. al.. Pg. 497 in Ref. G3.
- R5 A.B. Andrezen, et al., Apparatury, Leningrad (USSR), Nov. 1973, Transl. of NUEFA-T-161.
- R6 G. Schenk, "Metallic Foil Used as Circuit Breaker for Fast and High Current Commutation from Inductive Storage," Ph.D. Thesis, Technische Universitat Braunschweig, FRG, 1974.
- R7 M. Pillsticker, Proc. 6th Sym. Eng. Prob. Fusion Res., San Diego, 11/18/75, p. 453.
- R8 J.D.G. Lindsay, et al., IEEE Trans. Mag. Vol. MAG-11, No. 2 p. 594, March 1975.
- R9 H. Laquer, P. 279 in Ref. G3.
- R10 K. Menke and Yu. A. Shishov, Joint Inst. Nuclear Res. (-P8-7855), Dubna (USSR), 1974.
- R11 D. Hagedorn and P. Dullenkopf, Cryogenics, 14, No. 8, p. 429, August 1974.

- R12 H.J. King, et al., IEEE Trans. Power App & Systems, PAS-99, 911 (1980).
- R13 A. Falter, et al., Proc. 13th Pulse Power Symp., Buffalo, NY, 1978.
- R14 Reference G4, page 295.
- R15 Reference G2, page 308.
- R16 T. Mukutmoni and H.H. Woodson, Proc. 6th Sym. Eng. Prob. Fusion Res., San Diego, 11/18/75, p. 651.
- R17 W.O. Eckhardt, Proc. 9th Symposium Fusion Technology, Garmisch-Partenkirchen. FRG, June 1976.
- R18 M. Lutz, R. Harvey, IEEE Trans. Plasma Science, PS-4, 118, 1976.
A. Grekhov, et al., Fizika i Tekhnika Poupvodnikov, 5, 1409, 1971.
P.S. Raderecht, Int. J. Electron. 36, 399, 1974.
- R19 E.K. Inall, et al., Proc. 6th Sym. Eng. Prob. Fusion Res., San Diego, 11/18/75, p. 666.
- R20 A.S. Gilmour, Jr., and D.L. Lockwood, IEEE Trans. Elec. Devices, ED-22, No. 4, April 1975.
- R21 M. Weiner, IEEE Conf. Record 1976, 12th Modulator Symposium, Feb. 4, 1976, p. 224.
- R22 R.J. Wheldon, IEEE Conf. Record 1976, 12th Modulator Symposium, Feb. 4, 1976, p. 219.
- R23 C.W. Kimblin, et al., IEEE Conf. Rec. 1976, IEEE Int. Conf. Plasma Sci., Austin, Texas, May 1976.
- R24 R.F. Frenslar, et al., 2nd Int. IEEE Pulsed Power Conf., Lubbock, Texas, 1979, pg 368.
- R25 L.A. Miles, et al., p. 68, IEEE Conf. Record 1980, 14th Pulse Power Modulator Symposium.

C. CAPACITIVE OPENING IMPEDANCE SWITCHES

- E1 W. Knauer, R. Harvey, p. 259, Conf. Record IEEE Int. Conf. in Plasma Science, 78C141357-3NPS.
- E2 R.F. Caristi, et al., Ref. G4, p. 1427.
- E3 M. Lutz and G. Hofmann, IEEE Trans. (Plasma Science), Vol. 2, pp. 11-24, March 1974; R.J. Harvey and M.A. Lutz, IEEE Trans. Plasma Sci. PS-4, No. 4, December 1976.

E4 I. Alexef and R. Dyer, IEEE Trans. Plasma Science PS-8, No. 3, 163, 1980.

E5 M.M. Howland, p. 246, 2nd Int. IEEE Pulsed Power Conf., Lubbock, Texas, 1979.

D. INDUCTIVE OPENING IMPEDANCE SWITCHES

L1 J. Wyatt, et al., IEEE Conf. Rec. 1976, IEEE Int. Conf. Plasma Sci., Austin, Texas, May 1976.

L2 P.J. Turchi, p. 125, Ref. G3.

L3 M. Weiner, p. 91, Ref. G5.

L4 D.L. Binx, et al., LLL report UC1D-18831, Nov. 1980.

L5 W.R. Snow, et al., Princeton/AIAA/DGLR 14th Int. Electric Propulsion Conf., Paper 79-2095, Oct. 1979.

OPTICALLY CONTROLLED DISCHARGES

Arthur H. Guenther
Air Force Weapons Laboratory
Albuquerque, New Mexico 87117

OPTICALLY CONTROLLED DISCHARGES

Arthur H. Guenther
Air Force Weapons Laboratory
Albuquerque, New Mexico 87117

Abstract

Laser triggering of high voltage switches employing various dielectric media is well established as a precision technique for initiating conduction. The use of fiber optics to transport optical energy, alleviating the necessity for critical alignment has as well been demonstrated. However, the optical control of discharges is a subject which should be investigated in a much broader sense for other pulsed power applications such as directed discharges, opening switch possibilities, arc diversion, etc. Knowledge of such processes as optogalvanism, and other resonant interaction mechanisms can significantly reduce the discharge control energy requirements. Furthermore, it could eventually lead to the greater use of solid state elements with a concurrent extended lifetime and high reliability. In addition, efficient use of control energy would reduce presently unacceptable energy requirements for repetitive switch operations. A variety of opportunities and possibilities will be discussed for both initiating, terminating or diverting discharges in various types of switches.

A. INTRODUCTION

In other papers at this meeting we have heard about the growing interest and weight and size advantages offered by inductive energy storage systems. This interest is not new-born, it has always been with us in the pulse power community. However, as we know, the effective use of inductive stores requires a rapidly opening switch. This requirement has been most successfully met to date by fuses of one type or another. To make inductive energy storage systems a viable alternative in many of the DoD and DoE applications a long life, reliable repetitive opening switch is necessary.

R. Harvey has afforded us a fairly comprehensive summary of the opening switch concepts that come to ones mind, from primarily classical or commercial considerations. In this paper, I wish to approach the problem from a slightly different vantage point.

At the outset let me set the stage for what is to follow as it applies to the principal subject of this workshop. Let's look at Figure 1. To me there are two avenues to opening switches, one is the brute force approach characterized by mechanical devices, staging, fuses or all of them in various combinations. Generally these approaches have met with some success in single shot situations or slow opening, modest rep-rate scenarios in which the opening time has not been rapid, certainly not as rapid as required for our interests. When one adds the opening speed and repetitive frequency characteristics, together with the energy and voltage levels of interests that are necessary for our applications, this approach, I believe, is dead ended and should only be pursued for what we can learn about opening switch behavior.

On the other hand those approaches which do not have inherent limitations on repetitive operation such as those employing external discharge control techniques, e.g. e-beam or lasers should be pursued and pursued vigorously, particularly if they are capable of operating with diffuse discharges.

To embark on this approach in a sound technical manner requires something which has been needed from time immemorial and that is!

A FULL, TIME-DEPENDENT, ANALYTICAL DESCRIPTION OF SWITCHING DISCHARGES WHICH TREATS ALL SPECIES, THEIR DENSITIES AND TEMPERATURES, REACTION AND RADIATION RATES, FLOW OR FLUID MECHANICS, CHEMISTRY, SPATIALLY RESOLVED, WITH ALLOWANCES FOR GEOMETRY AND ELECTRODE/INSULATOR INFLUENCES.

Such a full treatment will be a long time in coming. It is a non-trivial problem. However, such a time dependent

OPENING SWITCH PROBLEM

BRUTE FORCE

CLEVER

STAGED

MECHANICAL

FUSING

ADD

REP-RATE

REQUIREMENT

A POSSIBILITY

E-BEAM - OPTICAL CONTROL - - -

DIFFUSE

DISCHARGES

Fig. 1

description of switching discharges would allow its employment in circuit analysis codes such as Circus, Sceptre, NET II, etc. One could then:

1. Assess the effect of the switch and its discharge on the circuit operation.
2. Assess the influence that the driver and load portion of the circuit has on the discharge.

And finally and most important:

3. Determine what effect modification of the discharge by external means (e.g., e-beam injection, resonant optical interaction, etc.) would have on circuit operation.

A not too obvious but simple example would be to optimize the gain uniformity characteristics of a discharge in a conducting state, as in an electrically excited laser cavity, as opposed to designing the cavity geometry to hold off the most voltage in the open state. We should not forget that for some of us the discharge itself is the load.

Historically one modifies the circuit to account for the discharge portion of a circuit whether it be in the switch or the load itself. Imagine how advantageous it would be if we could control the discharge to make it perform in an optimum manner in a given circuit.

We must investigate the physics and chemistry of all the species in a switch or discharge; assess the important processes, obtain the requisite data base, and model the Dynamics of Dielectric Discharges. (D^3) This will require a knowledge of excited state behavior, particularly metastables, and the appropriate energy transfer or channeling routes during various time domains of a switch's operating cycle, all as a function of control energy introduction characteristics over meaningful operating regimes (i.e. pressure, field, etc.)

B. OPTICAL CONTROL OF DISCHARGES

Let me concentrate on optically controlled switches, past, present and future. I will not go back so far in

nistory as to revisit photoconductivity, nor even ultraviolet irradiation, although this latter approach certainly led to great reduction in switch jitter, but only in closing gaps. I want to start my comments since the advent of the laser, for this is the key element in what is to follow as applied to a possible route to a repetitive opening switch.

We could spend considerable time reviewing the subject of laser triggered switching (LTS) and describing all its demonstrated achievements in low jitter closing switches to 4 MV, at rep rates ~ 50 Hz, in multiple switches, for multiple channels, operations in all classes of materials from vacuum to gas to liquids to solids, and even semiconductors, as well as on the surfaces of dielectrics. In the semiconductor case jitter well below 10 picoseconds has been observed, with concurrent short delay times. Triggering in many cases can be done with microjoules, at any wavelength with, a variety of pulse lengths. For a comprehensive review of this area see Ref. 1.

Applications of this type of triggering has continued to grow as lasers themselves have matured. Some of the reasons for its increased acceptance are concerned with the fact that lasers have become more reliable, secondly it has been shown that sufficient triggering energy can be piped, through a generally less than optimum environment, characteristic of many pulse power systems, by fiber optics⁽²⁾ eliminating the necessity for the maintenance of a critical optical alignment of super-cleanliness. The trigger is also electrically uncoupled from the high voltage. Finally and perhaps most importantly, newer short wavelength lasers such as KrF and other excimers are in fact principally pulse power systems themselves, requiring pulsed electron beam excitation. This later point has aided acceptance by the pulse power community which frequently considers such strange topics as optics, etc. as alien or at least arcane.

Inspection of Table 1 shows some of the wide range of actual discharge interactions using lasers. This Table in

TABLE 1
MODERN OPTICAL CONTROL OF DISCHARGES USING LASERS

1. Laser Triggered Switching electrode initiation volume breakdown LIBORSA inverse bremsstrahlung	8. Double Frequency Operation breakdown/recovery
2. Fiber Optic Triggering multichannel	9. Enhanced Arc Cooling
3. Laser Directed Discharges	10. Plasma Chemistry arc steering surface discharges
4. Laser Sustained Discharges	11. Solid State Switches closing, opening, surface discharges
5. Multiphoton Ionization	12. Superionic Conductors (inverse photoelectric effect)
6. Gas Seeding for Resonant Initiation	13. - - - - -
7. Optogalvanism	

a - R.H. Measures, N. Drewell, and P. Cardenal, J. Appl. Opts., 18 (1979)
pp 1824-1827

fact points the way to some obvious advantages for discharge control as relates to repetitive opening switches. How far one can go, what range of control could one exert, and the requirements on control energy are not known. But what has been demonstrated to date is enough to wet one's appetite.

Going through the Table: Laser triggered switching already discussed in the introduction usually concerns initiation of a discharge at an electrode surface, by the introduction of ionization due to gas breakdown (usually by inverse bremsstrahlung) or the emission of charged particles from the electrode surface. Slower breakdown mechanisms like shock waves or faster mechanisms like volume breakdown and U.V. photon assisted streamer formation is also known.⁽¹⁾ We have already pointed out the demonstrated feasibility of fiber optics for controlling delay and its facility in initiating multiple switches or multiple channels.

Lasers have been used for directed discharges. In fact they have been used to select a discharge path which is not necessarily in the highest field region or to the electrode in closest proximity.⁽³⁾ This opens up the possibility of a laser driven diverter switch, one possible form of a repetitive opening switch.^(1, following paper) Ample evidence exists for laser sustained discharges as well, that is, discharges which are maintained by the introduction of external optical energy.⁽⁴⁾ This is a direct analogy to the e-beam sustained discharge. However, generally all of the above laser techniques, while successful and reasonably efficient in initiating, directing or sustaining discharges, they are not as efficient or potentially as useful for our intended purpose. What we have been doing so far is using the laser as a convenient source of easily introduced or transportable power or energy, we have used its coherence and beam divergence properties and to some extent its monochromaticity. What we haven't done is use its frequency tunability or wavelength selectivity to more efficiently and effectively interact with the dielectric medium of the switch. The development and

general availability of tunable lasers of increasing power, efficiency, spectral range and improved reliability should now encourage us to investigate the potential of this feature (tunability) of the laser for the purpose of efficiently controlling discharges.

We are getting closer to a more optimum optical interaction with a discharge. Moving down the list of interactions in Table 1 we see multiphoton ionization - that simply means with an intense laser we do not need a photon energy greater than the ionization potential or band gap of a dielectric. Because of the high photon flux there is a distinct and measurable probability of ionization by the simultaneous absorption of two or more photons. This process which can be resonant or non resonant with energy states will become important in later discussion.

We all know that the most efficient way to couple energy into a system is at resonance. Item 6 in our Table points out that by gas seeding your dielectric, i.e. placing some small quantity of a material which is resonant in wavelength with the laser you have in your laboratory, can lead to a most efficient production of ionization for a given amount of laser energy, greatly reducing the laser power requirements, further improving its reliability and lifetime. Seeding on the scale suggested will not modify the hold-off characteristics of your switch to any measurable extent (e.g., use a little trimethyl amine in SF_6 when using a KrF laser.⁽⁵⁾ Such seeding would not have a comparable effect on e-beam controlled discharges. Seeding allows the use of very low laser fluxes, it allows for spreading out the available energy in a laser beam to enhance diffuse or large volume breakdown, of obvious desirability. We should however concern ourselves with determining the effects of these impurities on the overall dielectric properties of the main insulating component in the switch. Finally one must address the chemistry issues since many of the most attractive seeding materials are organic and their breakdown, modified by any plasma chemistry, may have deleterious effects

on subsequent switching operations e.g. depositing carbon on insulator surfaces.

One word on KrF lasers or others of its type, while we appreciate the advantage of a high photon energy, particularly at resonance, I wonder if this type of laser will ever be employed for long life ($N \sim 10^8 - 10^{10}$ shots) applications for the following reasons. They are at the present time relatively expensive, complex, have reliability problems of their own as regards low jitter command firing and, most seriously, there is a major concern of optical component reliability at these short wavelengths, particularly dielectric coatings and the reduced transmission of fiber optics if they are employed. I make these observations since this is a repetitive opening switch meeting.

C. OPTOGALVANISM

We have been creeping up on the principal thrust of this paper which concerns, in point of fact, the optical control of discharges by lasers under resonant interaction with species present in the switch. By control I mean closing, opening, diverting, sustaining switch discharges and modification of their geometric form. By form I'm referring to the desirability of diffuse or volume discharges. I imagine it would be more difficult to obtain a diffuse discharge in SF_6 initiated by an e-beam than in a seeded SF_6 mixture resonantly excited by a laser. Diffuse discharges are usually formed in ultrafast overvolted gaps, they are advantageous because they are generally of lower impedance, lower inductance, exhibit reduced electrode erosion rates, are easier to extinguish because of reduced arc root temperatures (therefore easier to blow out with reduced magnetic field strengths or gas flow, etc). Gas flow, besides aiding recovery of hold off voltages, can as well be used to guide or direct the laser beam without recourse to optical elements. ⁽⁶⁾

Number 7 on our list in Table 1 is optogalvanism. The optogalvanic effect is a change in the electrical properties of a discharge with radiation at a wavelength corresponding

to an atomic or molecular transition in the discharge i.e., an interaction at resonance. The effect has been known for over 50 years,⁽⁷⁾ but its re-emergence, particularly in optogalvanic spectroscopy⁽⁸⁾ or for the stabilizing of laser cavity discharges (note "control") etc., had been due to the development and accessibility of tunable dye lasers. The technique is as well adaptable to plasma diagnostics.⁽⁹⁾

In the optogalvanic effect both positive and negative impedance changes have been observed. In fact, discharges have been initiated and TERMINATED by the optogalvanic effect.⁽¹⁰⁾

The resonant nature of the interaction not only means a selectivity but an efficiency in the use of the incident optical energy, resulting in less demands for control energy. It is this resonant interaction that allows one to modify the distribution of species, change reaction kinetics, radiation rates, etc. in discharges. For example consider a double frequency operation - one laser at a given wavelength to initiate a discharge by producing ionization while at a later time a second laser operating at a different wavelength would excite a discharge species into a state which is more attaching, thus leading to improved recovery. Knowledge of the D^3 would allow one to effectively employ the different attaching rates for different excited states as a function of electron energy distribution in the discharge, assess the utility of the temperature dependence of attachment coefficients, perhaps have a high attachment rate when a laser is on or off depending upon the control desired. Obviously one would like certain properties during conduction, such as low attachment, high electron velocity, etc. while having high attachment and cooling when opening the switch. These plus other factors, like gas chemistry, and a knowledge of the salient atomic and molecular properties and their variations with field would allow one to more adequately assess the suitability of optogalvanic control.

Martin Gundersen at the University of Southern California

is investigating the possibility of resonant interaction for enhancing radiation losses in a discharge, thus cooling it down more rapidly. This would lead to enhanced recovery rates as well.⁽¹¹⁾ Additionally, high photon fluxes on low current Hg discharges have produced a considerable reduction in the electron temperature and concurrent increase in plasma density.⁽¹²⁾ This observation together with the strong optogalvanic effect observed in Hg⁽⁸⁾ immediately suggests to me the strong possibility of optical control of ignitrons.

Of course there are plenty of options for plasma chemistry as well, through the interaction of lasers with arc plasmas. We can also control arc motion by steering and initiate large area surface discharges. Besides the opportunities concerning plasma chemistry in a positive vein, we should be concerned about plasma chemistry effects for what they might do over extended periods of switch operation.

One final control area that deserves mention before revisiting optogalvanic capabilities relates to condensed and in particular semiconductor switching by laser irradiation. The LASS or light activated silicon switch⁽¹³⁾ has been known for some time. Recent Soviet work in this area by Aleksandrov, et al⁽¹⁴⁾ have employed light activated thyristors at 50,000 amps and 5 kV with nanosecond turn-on and jitter or simultaneity between multiple switches of <0.01 nsec. Westinghouse has even gone further by coupling a laser diode light source to a fiber optic cable coupled to a high power silicon solid state element in a protective circuit. The implication for long life, low maintenance, low cost and high reliability switching is obvious.

Auston⁽¹⁵⁾ has extended laser activated silicon switching to ultrathin stripline geometry where 1.06 μm laser light (which is closely matched to the band gap of silicon) is used to initiate conduction over a large area (avoiding a slow turn-on, or low di/dt due to poor lateral carrier diffusion). He then initiates a surface discharge by irradiation at the frequency doubled wavelength of 0.53 μm in demonstrating

on/off switching operation in less than 10 picoseconds. This is essentially a diverter operation in a semiconductor. Recently Portnoy and Schoenbach⁽¹⁶⁾ have suggested the possibility that one could further enhance opening or recovery in a solid state element by irradiation with an appropriate frequency laser, much as had been proposed earlier in this paper. Their approach is to control recombination by exciting valence electrons into traps acting as recombination centers. Thus there would be a heavy current flow from conduction bands in this resonant interaction.

Finally I would call your attention to recent work on a new opto-electronic process, namely superionic conductors, which demonstrate reversible, orders of magnitude, change in conductivity upon illumination with very modest (1 W/cm^2) fluxes of visible laser light. Scott⁽¹⁷⁾ has dubbed this the inverse photoelectric effect. Materials such as $\text{Ag}_{26}\text{I}_{18}\text{W}_4\text{O}_{16}$, BaMnF_4 and VO_2 are the most frequently studied solid state electrolytes. For this latter compound changes in resistivity of eight orders of magnitude have been observed for phase changes at 65°C upon illumination at low levels with CO_2 radiation at 10.6 m . The speed of the resistivity change has as yet not been measured to my knowledge.

D. CONCLUSION

Now that we have very briefly touched upon several ways that optical radiation can be used to control discharges, what are its advantages and prognosis for the future applications. Table II summarizes some of the issues and characteristics of optogalvanic interactions. Lasers are available, reliable and tunable and therefore selectable in λ . Furthermore they can be made to operate over a wide range of frequencies. For the modest control powers required at resonance, lasers can only become even more reliable. Their efficiency will obviously improve as well. The optogalvanic effect has been seen over a wide range of pressures, again requiring only modest laser powers for large changes in impedance. They have initiated as well as terminated discharges.

The use of lasers allows large area illumination or initiation, therefore there is a good probability of producing diffuse discharges with low impedance, low inductance, fast turn-on, rapid extinction or recovery, and reduced erosion. I know of no other process where the input or control energy is so efficiently used ($\eta \rightarrow 1$) since all interactions take place at resonance either by tuning the laser or seeding the gas to match an available laser. Compare this to an e-beam controlled discharge in efficiency of control energy!

Just one example should be sufficient to demonstrate the power of this process. Optogalvanism is measured in $\Delta Z/P$ or (Ω/mW), i.e. ohms per milliwatt of light absorbed. In the case of a neon plasma, for transitions originating in levels other than $1s$, $\Delta Z/P$ varies between -0.004 and -0.76 ohms/mW while for transitions originating in the $1s$ state $\Delta Z/P$ varies between -4.75 and $+9.12$ Ω/mW .⁽¹⁸⁾

There is no question that there will be continued improvements in component reliability such that some day we may be able to use an all solid-state optogalvanic device, from light source through a fiber optic cable to a semiconductor switch. Other resonant interaction opportunities have been mentioned which should be pursued to assess the potential for solving difficult switching functions in pulse power not solely for repetitive opening switches. There is no question, however, that in this latter area, optimal modification of discharge characteristics is an intriguing possibility.

There are many questions: how large is the effect? at what current densities is it operable?, e.g. will it only operate effectively in a glow discharge?, what is required in terms of input energy?, do we have a sufficient fundamental data base on reaction rates?, what role will gas chemistry play, particularly in repetitive switching operations?, is there a role for optical augmentation of other opening concepts such as instabilities?

One thing is certain, you must first understand the

TABLE II
OPTO-GALVANIC SWITCHING ISSUES AND CHARACTERISTICS

- | | |
|--|--|
| 1. Laser
Tunable, reliable,
repetitive | 6. Suitable for diffuse discharge
→ low erosion |
| 2. Demonstrated operations
in various pressure regimes | 7. Use of fiber optics
demonstrated |
| 3. Can be used to turn on
or turn off | 8. Continual improvements in
reliability and life time
by essentially going to
solid state sources and/or
switches |
| 4. Suitable for large
area initiation | 9. Other resonant effects
possible - cooling |
| 5. Most efficient use of input
control energy is at
resonance:
seeding, selectivity | 10. Other optical control
possible - steering, etc. |

discharge before you can effectively control it. So I end this discourse with the plea that opened this paper.

The use of modern day computers together with the necessary basis data such as multiphoton ionization cross-sections, attachment rates etc., along with all the other factors earlier mentioned should allow one to model discharges from those known reaction or radiation rates under a variety of electrical driving conditions with spatially and temporally resolved dielectric or plasma properties such as density, temperature, etc., in various geometries. A start along these lines would allow one to assess opto-galvanic processes such as impedance changes as a function of distribution variation (disturbance) as caused by the resonant interaction with laser radiation. It could even help us appreciate the effect of pre-ionized gases on successive switching operations.

I know what I have just proposed sounds like an impossible undertaking but there are many pieces of the puzzle available, which can be assembled and put together to approximate behavior. Until then we'll just have to be clever experimentalists and try out our ideas, such as the laser diverter described in the next paper by Karl Schoenbach.

Thank you.

E. REFERENCES

1. A.H. Guenther and J.R. Bettis, J. Phys. D: Appl. Phys., 11, 1577 (1978).
2. H.C. Harjes, et.al., IEEE Trans. Plasma Science, PS-8, 170 (1980).
3. A.G. Akmanov, L.A. Rivlin and V.S. Shil'ayaev, JETP LETT. 8, 258 (1968).
4. M.V. Gerasimenko, G.L. Kozlov, V.A. Kuznetsov and V.A. Masyukov Sov. Tech. Phys. Lett. 5, 8 (1979).
5. Long C. Lee and W.K. Bischel, Molecular Physics Laboratory, SRI International, Menlo Park, CA 94025.
6. David Bogdanoff, Appl. Optics 19, 3326 (1980).
7. G. Erez, S. Lavi and E. Miron, IEEE J. Quant. Elec. QE-15, 1328 (1979).
8. W. J. Van den Hoek and J.A. Visser, J. Appl. Phys. 51, 5292 (1980).
9. D.M. Pepper IEEE J. Quant. Elec., QE-14, (1978).
10. J. Lawler, Dept. of Physics, Univ. of Wisconsin, Madison, Wis., Private Communication.
11. Martin Gundersen, University of Southern California, Private Communication.
12. P.C. Stangeby, E. Allen, and D.A. Frazer, Proc. Xth Int'l. Conf. Phenomena Ionized Gases (Oxford), 30 (1971).
13. L.R. Lowry and D.J. Page, Westinghouse Research and Development Laboratory Scientific Paper 77 - IF5 SWI TS - PI, May 1977; O.S. Zucker, J.R. Long, V.L. Smith, D.J. Page and J.S. Roberts, Int. Top. Conf. on Elec. Beams Research Tech., Albuquerque, N.M. Nov., 1975.
14. V.M. Aleksandrov et.al., Kvant. Elekt. 8, 1 (1981)
15. D.H. Auston, Appl. Phys. Lett 26, 101 (1975).

16. W. Portnoy and K.H. Schoenbach, Texas Tech University, Lubbock, Texas, Private Communication.
17. J.F. Scott, Dept. of Physics and Astrophysics, University of Colorado, Boulder, Colorado, 80309.
18. E.F. Zalewski, R.A. Keller, and R. Engleman, Jr., J. Chem, Phys. 70, 1075 (1979).

EXPLORATORY CONCEPTS OF OPENING SWITCHES

K.H. Schoenbach, M. Kristiansen, E.E. Kunhardt
L.L. Hatfield, and A.H. Guenther

Texas Tech University
Department of Electrical Engineering
Lubbock, Texas 79409

EXPLORATORY CONCEPTS OF OPENING SWITCHES*

K.H. Schoenbach, M. Kristiansen, E. E. Kunhardt,
L.L. Hatfield, and A.H. Guenther ⁺

Texas Tech University
Department of Electrical Engineering
Lubbock, Texas 79409

ABSTRACT

Several concepts for repetitively operating opening switches in the submicrosecond region are analyzed to determine the feasibility and potential for further development.

These concepts include:

- I. The use of atomic and molecular features of electro-negative gases in a laser controlled discharge.
- II. The use of MHD-instabilities.
- III. The use of strong inductive and resistive changes in the dense plasma focus (DPF).

* Supported by the Air Force Office of Scientific Research

⁺ Air Force Weapons Laboratory, Kirtland Air Force Base,
New Mexico 87117

I. Laser Controlled Discharges as Opening Switches

Optically controlled discharges in gas mixtures with a small percentage of electronegative gas offer some very attractive features for their use as opening switches, such as ns-opening time and high repetition rate. The possibility of developing such an optically controlled switch as part of the divertor-circuit shown in Fig. 1 was studied [1]. The idea is to maintain, using a laser, a diffuse discharge in switch α , to transfer energy from the source to the inductor. At a desired time, this discharge is "quenched" and coincidentally another discharge is initiated in gap β by switching the laser over to this gap.

The theoretical investigation of this system was performed in three steps:

1. identification of techniques for producing laser controlled discharges (on-state) in gap α , suitable for opening switch applications.
2. conception of techniques for achieving high recovery rates in the opening switch α (on-to-off transition)
3. simulation, using a computer, of the opening switch performance as part of the divertor circuit (Fig. 1). Discharge characteristics and dynamic behavior affect the performance of the circuit and, in turn, the circuit defines the "boundary conditions" which will place a bound on the desired discharge properties. Since switch closure has been shown to be effected in satisfactory time scales (i.e. nanoseconds) [2], this aspect was not considered in the study.

1. The On-State

A number of factors are used to describe the "on" char-

acteristics of a switch. These factors are, in general, common to all switches (for example, low forward drop and low inductance; see Ref [2] for a listing of these properties). The most important property, in this case, is that the "on" state discharge must be "controlled" by a laser. The term "controlled" is interpreted to be either of the following two conditions: first, the discharge is non-self sustaining and the laser serves to sustain it (i.e. turning of the laser will shut off the discharge); and second, the discharge is also non-self sustaining but the laser serves only as a means for changing the conductivity from a highly resistive state ("off") to a low resistance state ("on"). In this last case, the discharge is sustained by other means. In either one of the above two conditions, the discharge must be a volumetric discharge (i.e. a broad, glow-like discharge) if laser control is to be effected. Two options are described (one for each of the above interpretations of "controlled") which, after analysis using "reasonable values" for the components, proved to be theoretically feasible.

Option 1: A volume discharge of relatively high resistance is first established in the gap. Transition to the "on" state is effected via a laser induced change in the discharge conductivity, i.e. the optogalvanic effect. [3]. From the work of Koppitz [4] and Long [5], a circuit was developed, shown in Fig. 2, for producing a high resistance volume discharge. Referring to Fig. 2, the discharge is produced by closing switch γ and at the same time irradiating the cathode surface of switch α with U-V radiation. The values for the discharge voltage and current at the discharge operating point are determined from the interception of the V-I characteristics of the discharge, and the external circuit load line. The external load line is determined by the impedance of the transmission line supplying the energy to the discharge (See Fig. 2). V-I characteristics for this

type of discharge were computed by Long [5] who found that the slope of the characteristic may be positive or negative depending on the composition of the gas used for the discharge.

Once the broad discharge has stabilized at the operating point, switch β (see Fig. 2) is closed and concurrently the optogalvanic effect produced by the injection of laser radiation will be used to change the conductivity of the discharge. A schematic representation of the physics of this phenomenon is shown in Fig. 3. Basically, the laser radiation of energy $h\nu$ enhances the rate of ionization of the discharge, thus increasing its conductivity. As long as the laser is on, the discharge will be in a state of high conductance, the "on" state. A time evolution of the resistance of the gap showing the various states described is shown in Fig. 4. The change in discharge resistance due to the optogalvanic effect has been demonstrated at low pressures (a few Torr). It is yet to be demonstrated at the pressures necessary for switch applications (a few hundred Torr).

Option 2: A second possibility for creating a laser controlled discharge is to use a two step photoionization. One example is the photoionization of tri-n-methylamine by a U-V flashlamp. Javan and Levine [6] demonstrated a two step process using a flash lamp to produce about 5×10^{12} electrons per cm^3 .

The use of laser radiation in these processes is feasible only if the laser power requirements are reasonable. In a gas mixture, containing a gas with high electric strength and a small percentage of a strongly attaching gas the dominant processes of electron generation and destruction are shown in Fig. 5. Neglecting, furthermore, detachment processes a simple power balance yields the following expression for the laser power required to maintain a discharge:

$$P = \frac{h\nu}{e} \frac{Ik[N_A]}{\kappa_i \mu E},$$

where P is the laser power necessary to sustain a volume discharge, $h\nu$ is the quantum energy of the laser, κ_i is the absorption coefficient of the laser light resulting in photoionization or excitation, μ is the mobility of the electrons in the gas mixture, I is the current in the discharge, E is the electric field across the discharge, k is the attachment coefficient of gas A which is one constituent of the mixture, and $[N_A]$ is the concentration of gas A.

Some typical numbers tried in this expression yield the following:

$$I = 10^3 \text{ A}$$

$$E = 5 \times 10^2 \text{ V/cm}$$

$$k = 10^{-8} \text{ cm}^3/\text{s}$$

$$[N_A] = 5 \times 10^{15} \text{ cm}^{-3}$$

$$\mu = 10^3 \text{ cm}^2/\text{V-s}$$

$$\frac{h\nu}{e} = 3\nu$$

$$\kappa_i = 0.01$$

$$P = 3 \times 10^7 \text{ Watt}$$

These numbers correspond to N_2 used as a buffer gas at 1 atm, a gas such as I_2 as gas A, and tri-n-methylamine as gas E. From this, we conclude that the power requirements on the laser can be met using commercially available lasers.

2. The On-Off-Transition

After the laser is turned off, the transition to the "off" state is governed by the kinetic processes in the discharge, coupled to the dynamic behavior of the external circuit. Using mixtures with electronegative gases, the primary kinetic process that governs the rate of transition to the "off" state is electron attachment. Since this process is dissipative, it should not be operative during the "on" state, but only in the transition phase, otherwise the

losses would be too great for the switch to be of practical use. Two techniques for increasing (by orders of magnitude) the value of the electron attachment rate during the transition phase, above its "on" state value are proposed:

During the transition or opening phase, the voltage across the switch is rapidly increasing, i.e. E/p increases. Thus, it is proposed to use a gas whose attachment rate increases with E/p . As the switch opens, E/p increases, this in turn leads to higher attachment rates and a feedback effect sets in which will lead to rather short transition times (see Sec. 3). Attachment rate coefficients for a number of gases [7] considered are shown in Fig. 6. Analysis of their effect on switch recovery rate will be given in the next section.

Another technique for increasing the attachment rate (i.e. shorter recovery times) during the opening phase is to irradiate the gas mixture with a laser whose photon energy produces a transition from the ground state of the attaching gas component to a vibrational level with larger attachment coefficient. A number of possible molecular gases have been identified. The two most promising are I_2 and HCl. Nygaard et. al. [7] have shown that for I_2 in a buffer gas of N_2 the electron attachment rate increases with temperature. They propose that this is due to a level crossing of the system I_2^* with the system $I + I^-$. The molecule HCl has a reasonably high electron attachment cross section. Allan and Wong [8] have measured the dissociative attachment rates for HCl as a function of temperature and find a strong dependence [6]. A calculation by W. Morgan [9] shows that this requires a change in the cross section from 10^{-17} cm^2 for the $v=0$ vibrational level to 10^{-14} cm^2 for $v=2$ (Fig. 7). The attractive feature of HCl is that an IR laser may be used to populate the $v=2$ level starting from the $v=0$ level, because the molecule is not homonuclear.

3. Circuit Performance; Representative Examples:

In order to determine the requirements and performance of the switch operated as described in the previous sections, the behavior of the switch in a circuit has to be considered. To determine specific requirements such as gas constituents, pressure, gap dimension, etc., the two operating phases described in Sections 2 and 3 can no longer be viewed separately but a self consistent treatment must be done. The main point is that due to the fact that gas mixtures must be used in order to have high hold-off voltage in the "off" state; low resistivity in the "on" state, and high recovery rate (short "on-off" transition time), the specific values for the operating parameters in each of the phases are dependent on each other. This "coupling" between the operating phases is depicted in the diagram in Fig. 5. Note that the attachment rate, which determines the recovery rate, influences the power requirement on the laser used to control the discharge since electron production during the "on" state must be increased to overcome the attachment losses. A computer code (SCEPTRE) capable of treating time dependent circuit elements was used to simulate the behavior of the circuit shown in Fig. 8. The operation of the circuit is as follows: the energy stored in the capacitor C is transferred to the inductor L upon closure of switch α . Subsequently, switch α is opened and switch β is closed, thus affecting the transfer of the energy stored in the inductor to the load R_L .

The component values shown in Fig. 8 are reasonable for a laboratory experiment. Switch α is the opening switch and switch β is assumed to be one which closes in a short time with small jitter. The buffer gas, the major constituent of the gas mixture in the opening switch, was assumed to be N_2 for which the electron mobility is known. The operating point of switch α was set by taking the electric field to gas density ratio (E/N) to be 2 Townsend when the switch was on. For a switch with an area of 25 cm^2 , elect-

rode spacing 1 cm, and a gas pressure of 1 atmosphere this corresponds to about 0.5 kV between the electrodes. Under these conditions the current in the gap is about 1 kA.

Calculations of the current in the opening switch and the power dissipated in the load resistor were done for gas mixtures containing F_2 , NF_3 , and I_2 . (See Fig. 6 for their attachment rate as a function of E/N .) In each case the product of the electron attachment rate and the attaching gas density ($k[N_A]$) was assumed to be $5 \cdot 10^7 \text{ s}^{-1}$. This requires a pressure of only a few Torr of the attaching gas. Also, the electron density in the discharge during the on time was taken to be constant. If a laser was used to maintain the discharge the laser intensity might be constant but the electron density would vary. The results for the current are shown in Fig. 9. Note that the use of I_2 results in a rapid current decrease in the switch compared with the other attaching gases. This agrees with the intuitive arguments given above, stressing the importance of the variation of the attaching rate with E/N . Figure 10 shows the power dissipated in the load resistor for the three gases. Clearly, the short opening time associated with the use of I_2 results in a large power amplification. The use of the gas F_2 is obviously not as effective.

No calculations were made using SF_6 . The attachment coefficient at very low values of E/N for SF_6 is well known and the coefficient is known to drop rapidly as E/N increases. However, not enough quantitative data for a large range of E/N is available for the calculation described above. Results with SF_6 should be similar to those obtained with F_2 .

4. Conclusion

Using the gas mixture proposed above (an ionizing gas, an electronegative gas, and a buffer gas with high dielectric strength) and using the method of Koppitz to produce a volume discharge, it is possible to produce an opening

switch. Computer calculations for a typical circuit assuming a given discharge behavior, and using gases whose attachment rate increases during the opening phase indicate that this switch has very attractive features. Because of the complexity of the discharge system and the lack of knowledge of certain cross sections, an exact calculation of the behavior of such a discharge was not feasible at this time.

II. MHD-Instabilities ($m=0$ and $m=1$) for Opening Switches

Commonly observed MHD-instabilities in current carrying plasma columns are the sausage ($m=0$) and the kink ($m=1$) instability. Figure 11 shows the condition for stability and the growth rate for both instabilities in case of an applied axial magnetic field. At a certain ratio of B_θ/B_z slight changes of this ratio can trigger the instabilities. The onset of the instability and the following change of the plasma geometry is correlated with an increase in inductance and hence in plasma impedance.

1. $m=0$ Instability [10]

To prevent the onset of the $m=0$ instability at low currents an axial magnetic field is applied by means of a flux compression device (Fig. 12). Assuming that the "sharp" pinch stability condition is applicable on a plasma with skin depth on the order of the plasma radius (finite conductivity), the field strength B_z determines the amplitude of the critical current I_{cr} according to:

$$I_{cr} = \sqrt{2} \ 2\pi r_0 \ \frac{B_z}{\mu_0}$$

In order to achieve strong compression and correspondingly high plasma impedance the diffusion of the longitudinal magnetic field across the plasma column should be faster than the compression ($\tau_d \leq \tau_i$). This condition and a minimum temperature condition for the plasma is extremely limiting on the possible range of plasma density and current (Fig. 13). They furthermore allow only the usage of rather heavy gases, like Argon, because of their low sound velocity.

In order to get reasonably large values for the impedance a sequence of flux-compressing systems is proposed, each of them triggering an instability at the same time (Fig. 14). The B_z field is pulsed to get the necessary high field strengths in the plasma. The circuit with the

load resistance is linked to the main circuit by means of switch 2 at the time when the instability is triggered.

Figure 15 shows the circuit calculated by means of the SCEPTRE program. Figures 16 and 17 show the voltage and current in the load for a) a closing switch and b) a capacitance in the load branch of the circuit. The axial magnetic field was chosen to trigger the instability at the time of the maximum current in the main circuit ($t = \tau$). The maximum compression ratio of the $m=0$ instability was assumed to be 10.

In spite of the rather sophisticated experimental set-up and some optimistic assumptions, the opening effect turns out to be rather weak. However, modeling of sequences of voltage spikes seems to be possible with such an experimental set-up, as demonstrated in Fig. 18. Dependent on the current shape, different controllable repetition rates seem to be achievable.

2. $m=1$ Instability [11]

According to the stability condition

$$\frac{kr_0 B_z(r_0)}{B_\theta(r_0)} > 1$$

$m=1$ instabilities can be stabilized by permeating the plasma column with a longitudinal magnetic field. However, in the case of a thin, highly conductive plasma column, a moderate longitudinal magnetic field acts destabilizing [12]. If there is a slight helical perturbation the $\vec{j}_\theta \times \vec{B}_z$ forces drive the plasma to the walls (Fig. 19). When the plasma touches the wall its temperature is lowered considerably and thus the plasma resistance increases - that means the instability will act as an opening switch. An analytical expression for the growth rate of this induced instability can be derived only for $kr \gg 1$ and r small, that means for the initial phase of the instability

and for large initial perturbations.

Helically perturbed plasma columns may be produced by means of high energy electron beam injection into a discharge chamber with an applied axial magnetic field (Fig. 20). The helical shape of the plasma column can be controlled by changing the magnetic field strength. For electron energies of a few 100 keV field strengths of approximately 0.1 T are necessary to force the electrons to spirals with diameters in the order of cm. If such plasma spirals can be produced in high pressure gases (atmospheric pressure), opening switches with opening times in the order of a few 100 ns should be possible.

Some typical data for an $m=1$ instability opening switch yield the following approximate result for the time necessary to reach the wall of the discharge chamber (opening time):

gas: H_2

$$n_e = n_1 = 3 \cdot 10^{19} \text{ cm}^{-3}$$

$$\text{Area of the plasma column: } A = 0.1 \text{ cm}^2$$

$$\lambda = 2 \text{ cm}$$

$$r_o = 1 \text{ cm}$$

$$\text{wall-radius: } R = 3 \text{ cm}$$

$$I = 10^5 \text{ A}$$

$$B_z = 0.16 \text{ T (according to } r_o \approx 1 \text{ cm at an electron energy of 200 keV)}$$

$$\text{Growth rate: } \gamma = 3 \cdot 10^6 \text{ s}^{-1}$$

$$\text{approximate opening time: } \tau = \gamma^{-1} \ln \frac{R}{r_o} = 3.6 \times 10^{-7} \text{ s}$$

III. Dense Plasma Focus as Opening Switch

The dense plasma focus (DPF), which is similar to a z-pinch, shows a strong inductance rise during its compression phase. Additionally, induced axial electric fields in the plasma favor the onset of microinstabilities, such as the two stream instability [13]. Due to this secondary instability anomalous resistive changes up to 0.35Ω were reported in the DPF [14]. These effects, which are correlated with the axial emission of high energy electrons and ions from the focus plasma, occurs repetitively in inductively driven devices [15] (Fig. 21). They offer the possibility to use the DPF as a repetitively working opening switch.

The experimental setup is shown in Fig. 22. The coaxial line is charged by an inductive current source L_c . Charging current flow through the load is avoided by using a small coupling capacitor. During the rundown-phase of the plasma layer a considerable amount of magnetic energy is stored in the line. Part of this energy can be transferred to the load resistance during the compression and focus phase. The coupling capacitor represents a small impedance at the time of the sharply rising plasma resistance in the focus.

The disadvantage of such a plasma focus device is its poor reproducibility and the fact that the repetition rate is hard to control. Higher reproducibility and controllable repetition rate may be achieved by means of cylindrical gas puff injection at the end of the coaxial line [16] (Fig. 23a). Further improvement is possible by choosing a proper electrode shape as shown in Fig. 23b. Due to such an electrode shape the radially inward moving plasma layer is forced to a spheroidal shape with decreasing mass/length ratios and thus higher radial velocities.

Calculations, using a simple snowplough model, show

the influence of electrode shaping on the final plasma impedance (Fig. 24). Assumed is a radius ratio of 100, that means starting with $r_0 = 10$ cm the final radius will be 0.1 cm, a radius which seems reasonable for plasma focus devices. An increase of the impedance/length by a factor of 4 can be expected if the electrode is shaped as shown for $\alpha=2$ instead of being plane.

Assuming $m_0 = 1.57 \cdot 10^9$ kg/cm (1 atmosphere H_2 in a cylinder of 1 mm radius and 1 cm length) injected at $r_0 = 10$ cm and a current rise of 10^{11} A/s, $T_0 = 1.12 \times 10^{-6}$ s and $Z'_0 = 1.8 \times 10^{-3}$ Ω /cm. Hence the maximum impedance for $\alpha = 2$ turns out to be 3.5 Ω /cm. Calculations are performed for a linearly increasing current. For constant current shorter compression times and higher impedances can be expected.

References

1. A. H. Guenther and J. R. Bettis, "The Laser Triggering of High-Voltage Switches," J. Phys. D., 11, 1577 (1978).
2. T. R. Burkes, et. al., "A Critical Analysis and Assessment of High Power Switches," NSWC Report NP 30/78.
3. D. M. Pepper, "Analysis of the Optogalvanic Effect in Discharge Plasmas Using Rate Equations in a Modified Schottky Formalism," IEEE J. Quant. Elect. QE-14, 971 (1978).
4. J. Koppitz, "Nitrogen Discharges of Large Cross Section at High Overvoltage in a Homogeneous Field," J. Phys. D., 6, 1454 (1973).
5. W. H. Long, Jr., "Pulse Forming Networks for High Pressure Discharges," 33rd Gaseous Electronics Conf., Univ. of Oklahoma, Oct. 1980, Abstract EB-5.
6. J. S. Levine and A. Javan, "Observation of Laser Oscillation in a 1-atm CO₂-N₂-He Laser Pumped by an Electrically Heated Plasma Generated via Photoionization," Appl. Phys. Lett. 22, 55 (1973).
7. K. J. Nygaard, H. L. Brooks, and J. R. Hunter, "Negative Ion Production Rates in Rare Gas-Halide Lasers," IEEE J. Quant. Elect. QE-15, 1216 (1979).
8. M. Allan and S. F. Wong, "Dissociative Attachment from Vibrationally and Rotationally Excited CH₁ and HF*," Submitted to J. C. P., June 1980.
9. W. L. Morgan and M. J. Pound, "Kinetics of E-Beam Excited XeCL," 33rd Gaseous Electronics Conf., Univ. of Oklahoma, Oct. 1980, Abstract FB-3.
10. M. Kruskal, M. Schwarzschild, Proc. Roy. Soc. A, 223, 348 (1954).
11. V. D. Shavranov, Sov. Phys. Tech Phys. 15, 175 (1970).
12. G. Bateman, MHD Instabilities, MIT Press, Cambridge 1972, p. 105.

13. K. Schönbach, et. al. Phys. Lett. 62A, 430 (1977).
14. A. Bernard, et. al., 6th Intern. Conf. on Plasma Phys. and Contr. Nuclear Fusion Res., Berchtesgaden, FRG., Oct. 1976 (IAEA-CN-35/E18-4).
15. J. Salge et. al., 2nd Intern. Conf. on Energy Storage, Compression and Switching, Venice, 1978.
16. Fisher, UC Irvine, private communication.

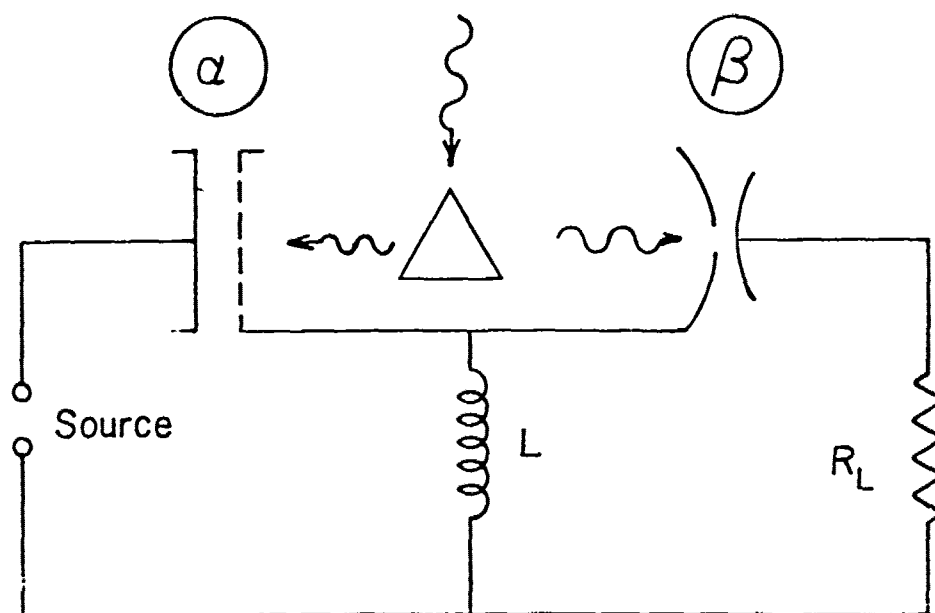
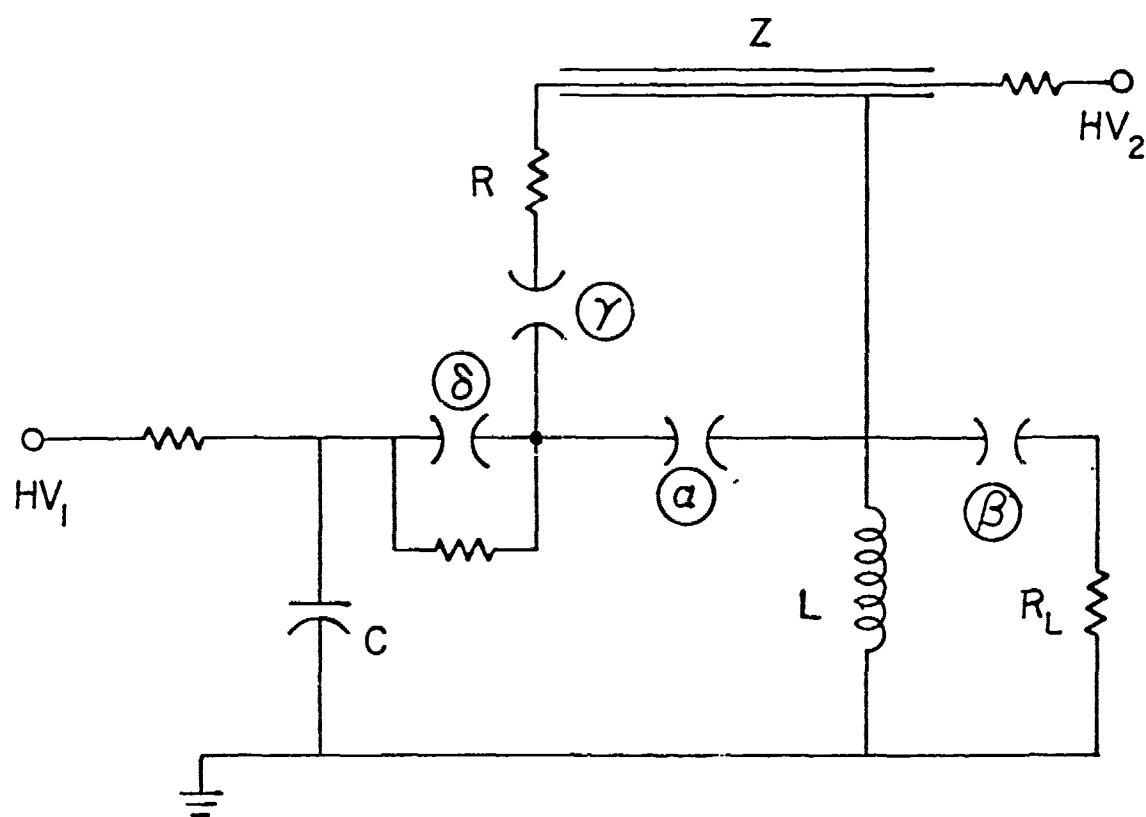


FIG. 1 SCHEMATIC REPRESENTATION OF A SYSTEM
(DIVERTOR CIRCUIT) USING AN OPENING SWITCH



α : opening switch

β γ δ : closing switches

FIG. 2 MODIFIED DIVERTOR CIRCUIT

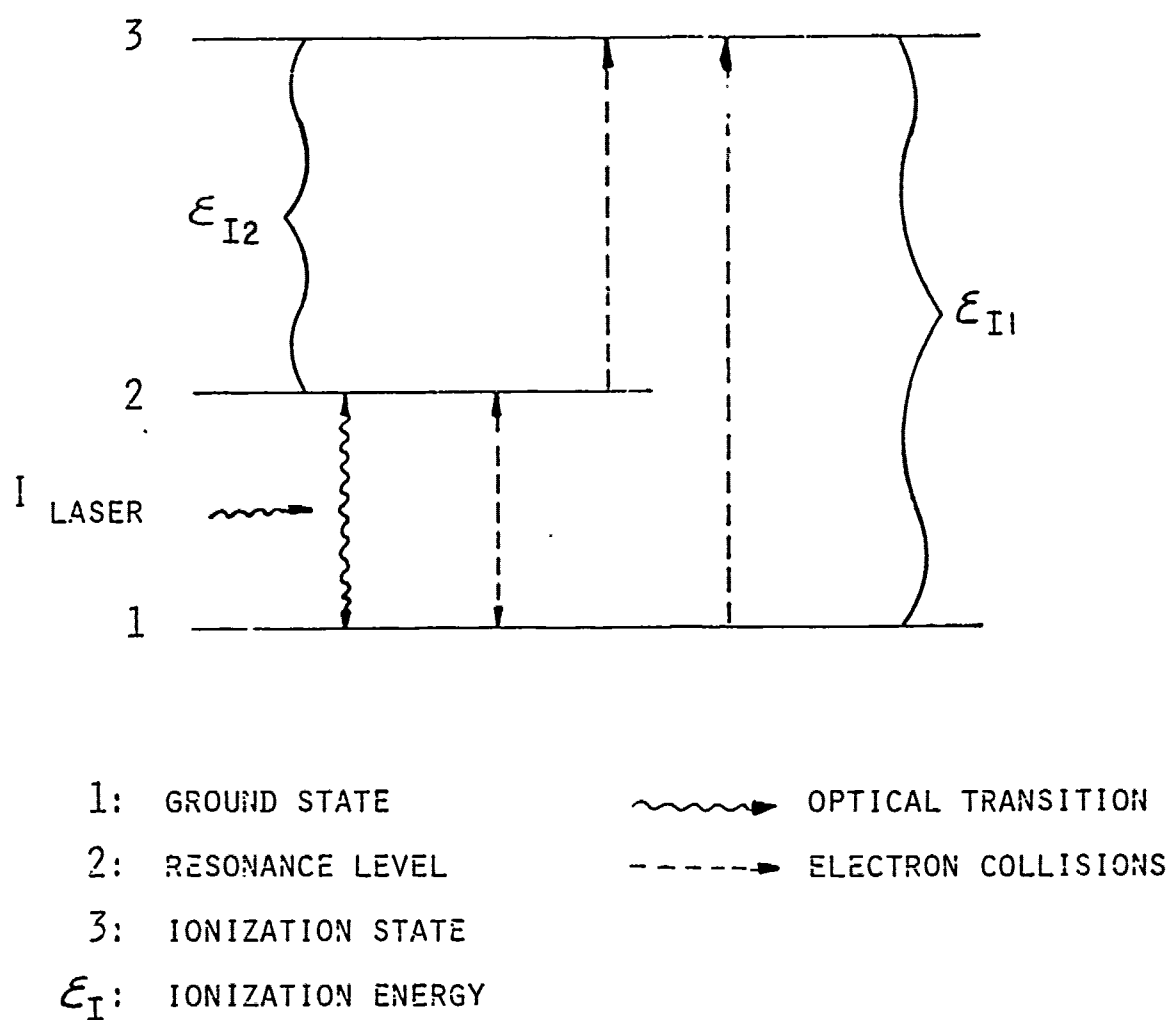


FIG. 3 ENERGY LEVEL DIAGRAM WITH TRANSITION MECHANISM
(OPTOGALVANIC EFFECT)

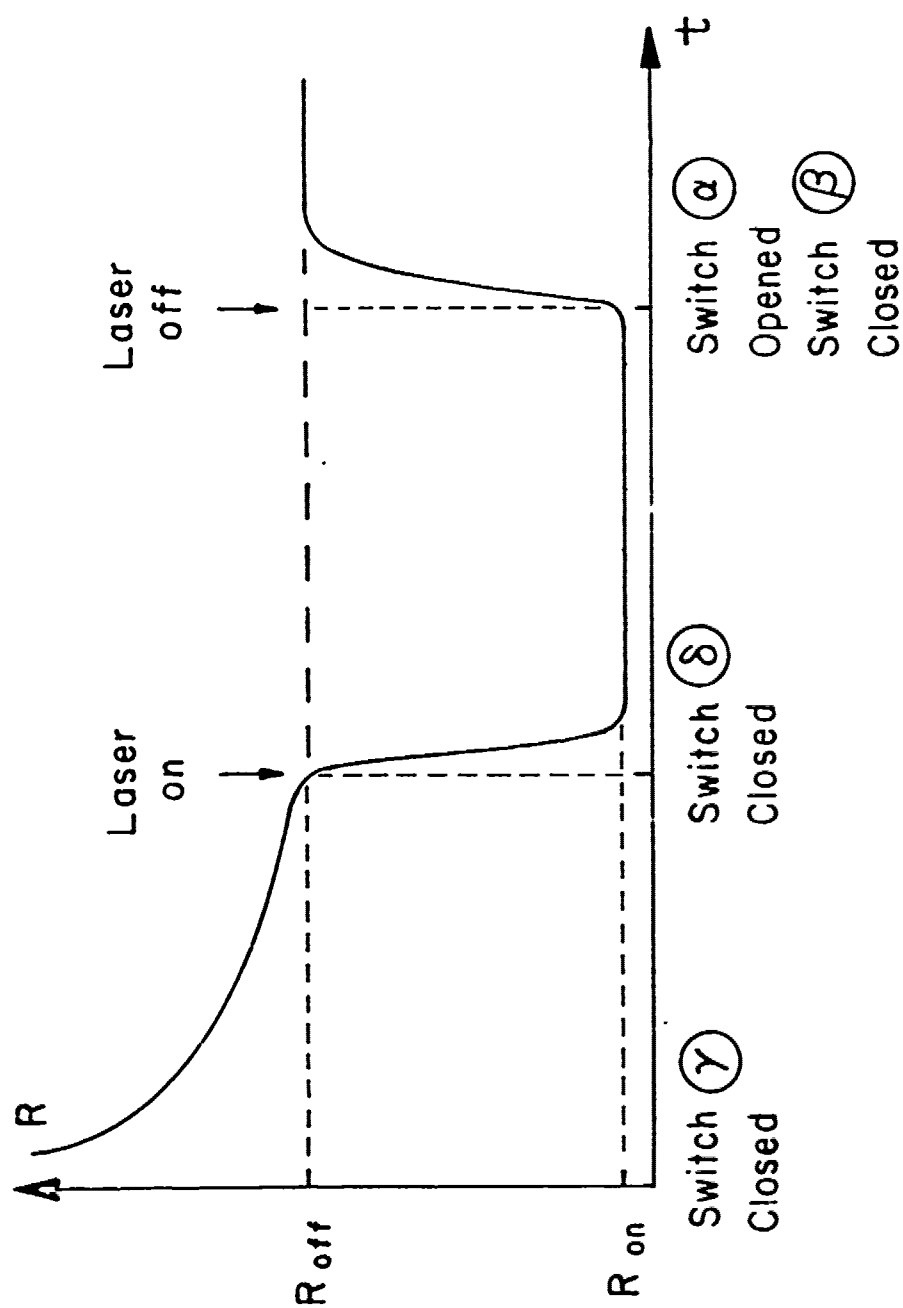
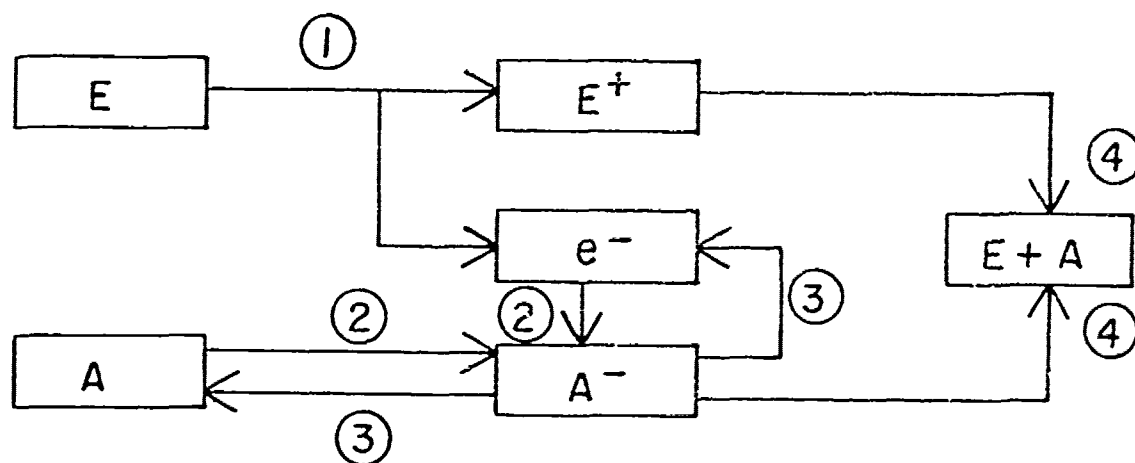


FIG. 4 TIME DEVELOPMENT OF THE OPENING SWITCH RESISTANCE



E : IONIZED GAS

A : ATTACHING GAS

① : IONIZATION

② : ATTACHMENT

③ : DETACHMENT

④ : RECOMBINATION

FIG. 5 SIMPLIFIED REACTION DIAGRAM

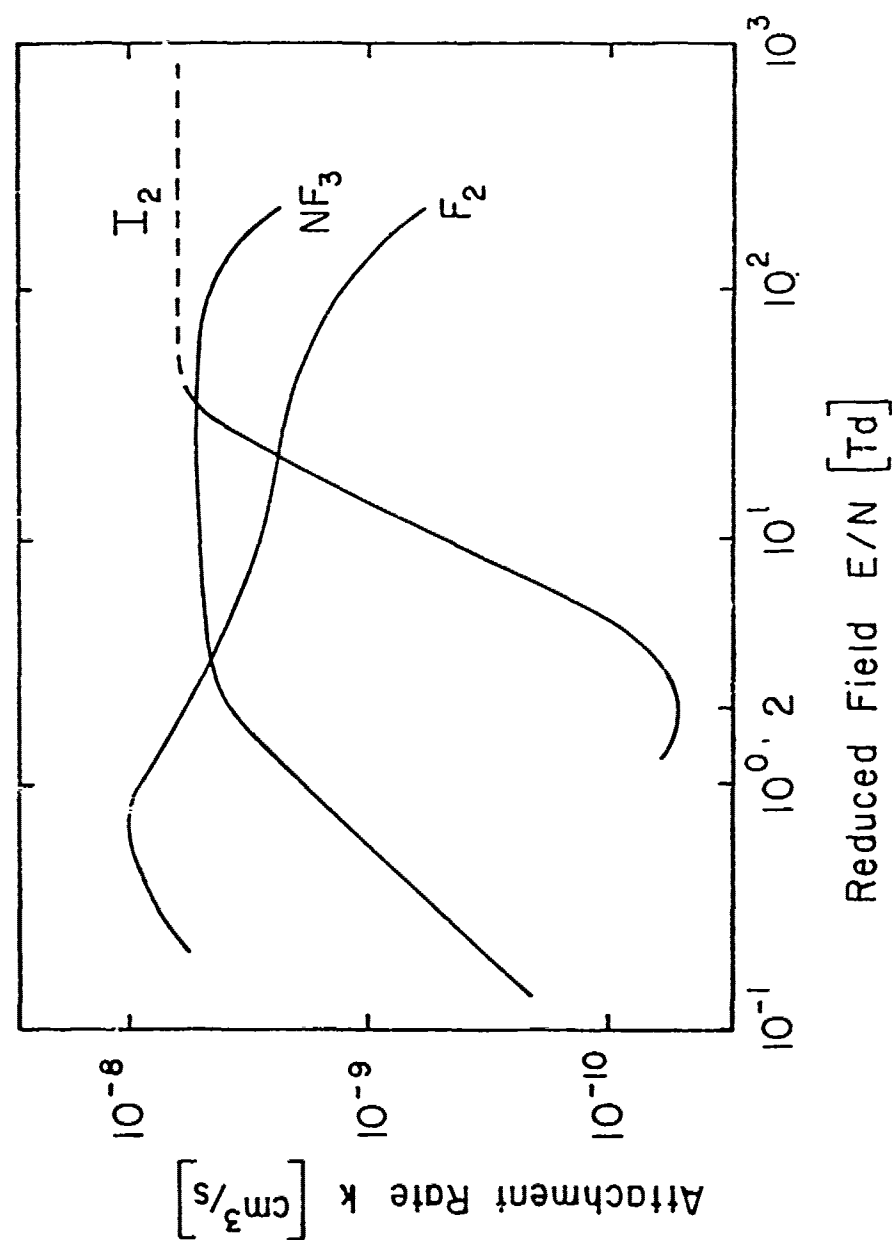
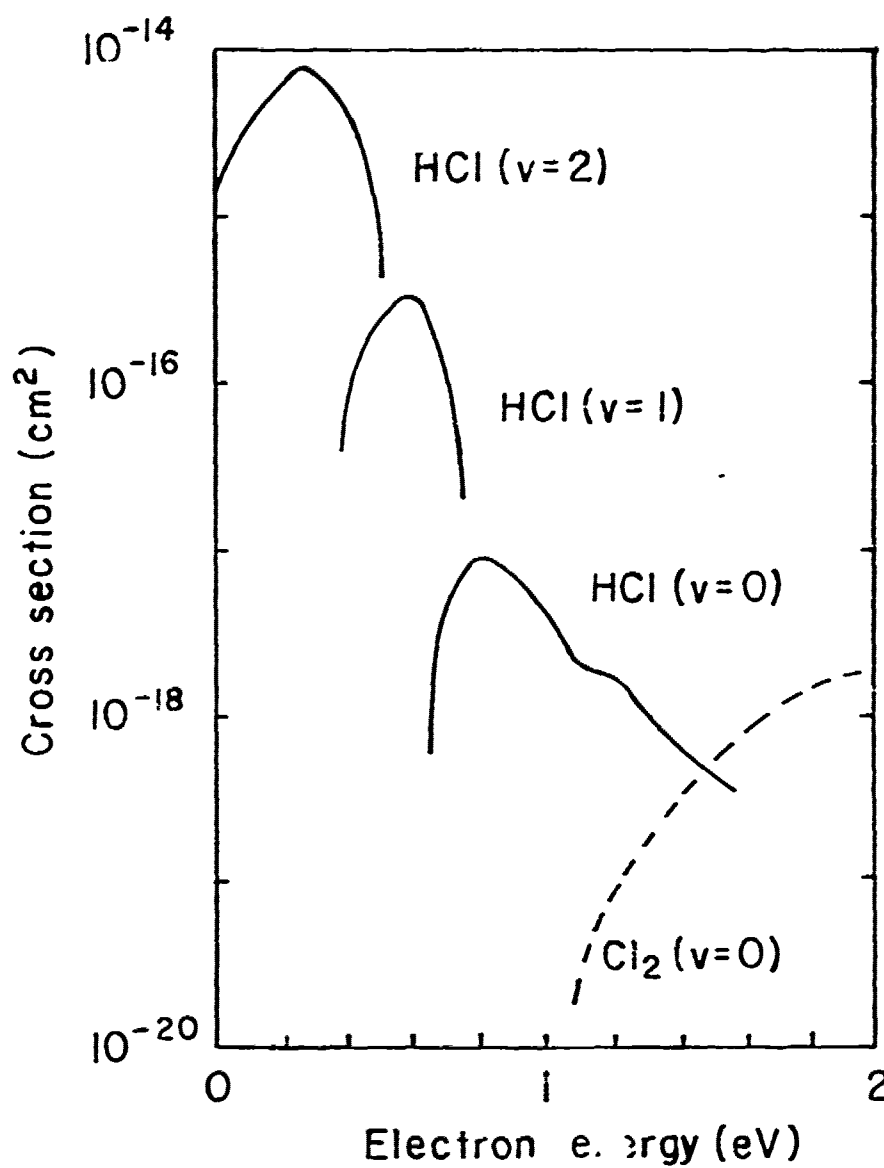
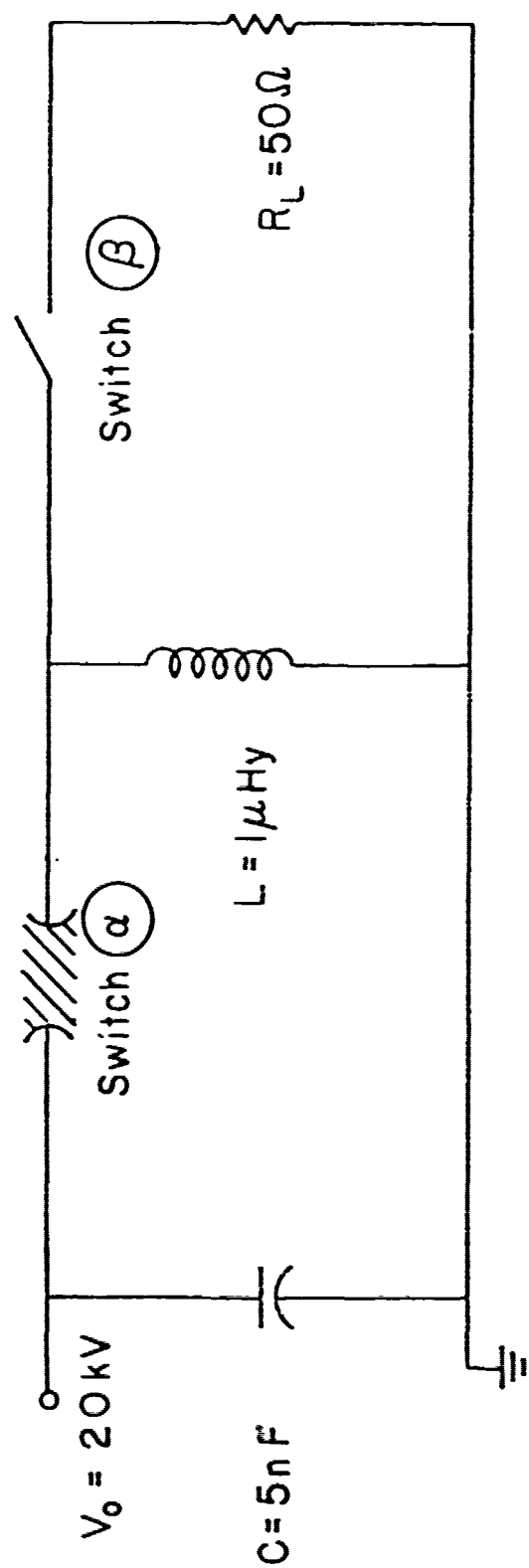


FIG. 6 ATTACHMENT RATE FOR I_2 , NF_3 AND F_2



(HCl cross sections derived from data of Allan and Wong)

FIG. 7 HCl AND Cl₂ DISSOCIATIVE ATTACHMENT
CROSS SECTIONS (REF. 9)



$$t \approx \tau: \quad \frac{E}{N} = 2 \text{ Td}$$

$$\frac{1}{k[N_A]} = 2.10^{-8} \text{ s}$$

FIG. 8 CIRCUIT USED FOR COMPUTER CALCULATIONS

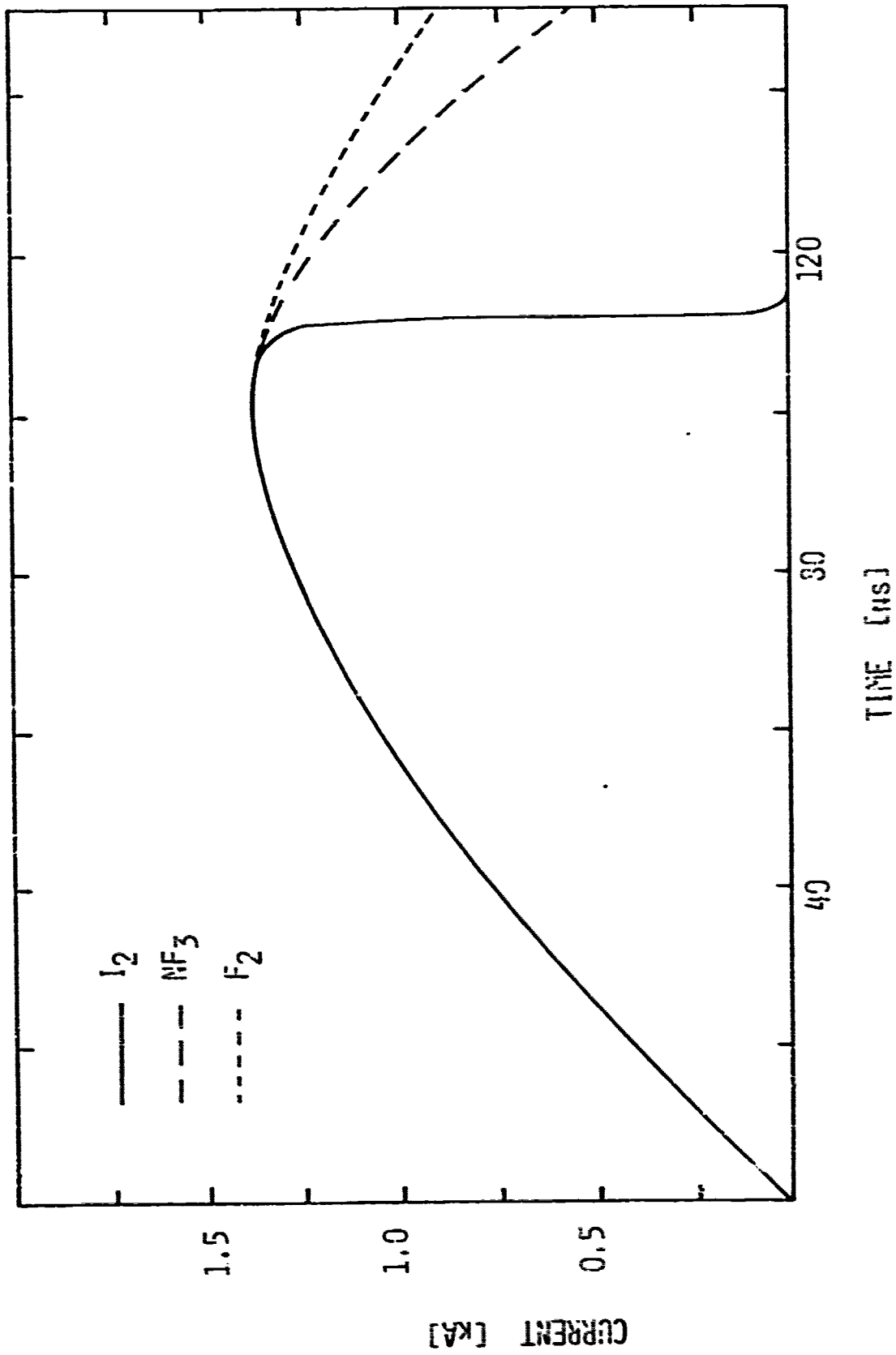


FIG. 9 EVOLUTION IN TIME OF THE CURRENT THROUGH THE OPENING SWITCH

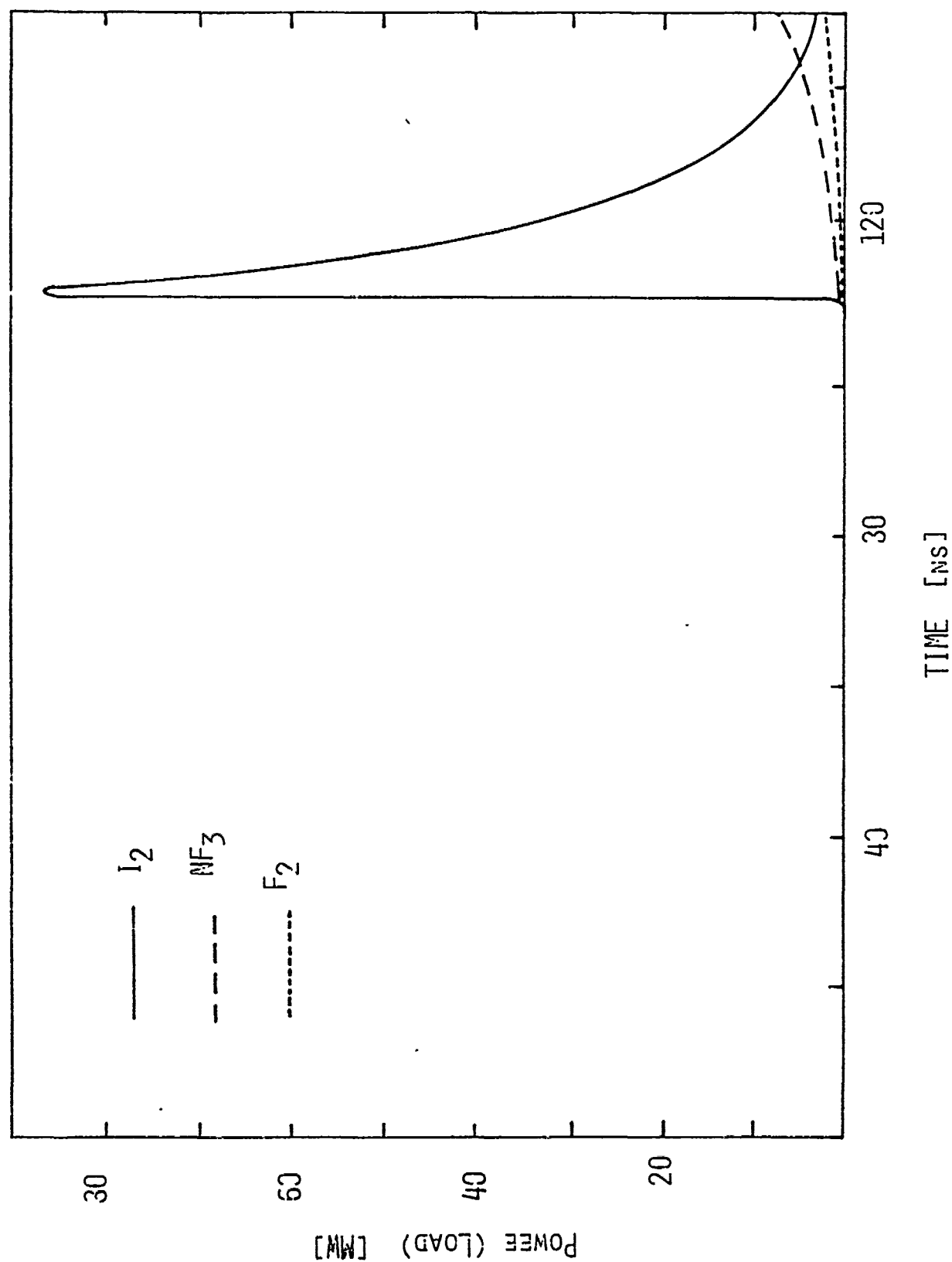
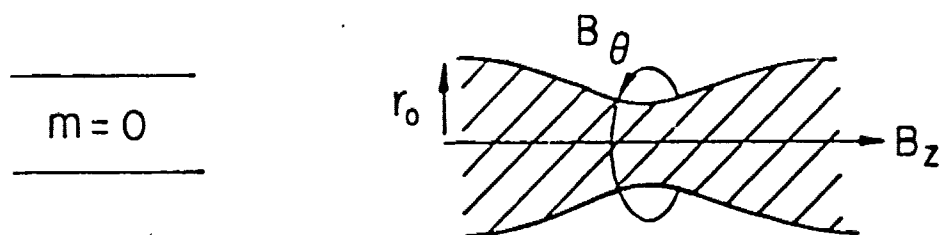


FIG. 10 POWER PULSE DELIVERED TO LOAD

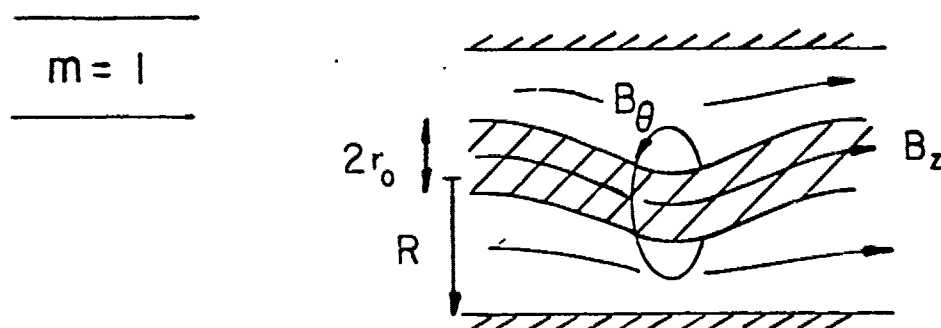


$B_z = 0$ outside the plasma:

stability criterion: $B_z^2 \geq B_\theta^2 / 2$

growth rate: $\gamma \approx a / r_0$

$a = \sqrt{kT_e / M}$ sonic speed



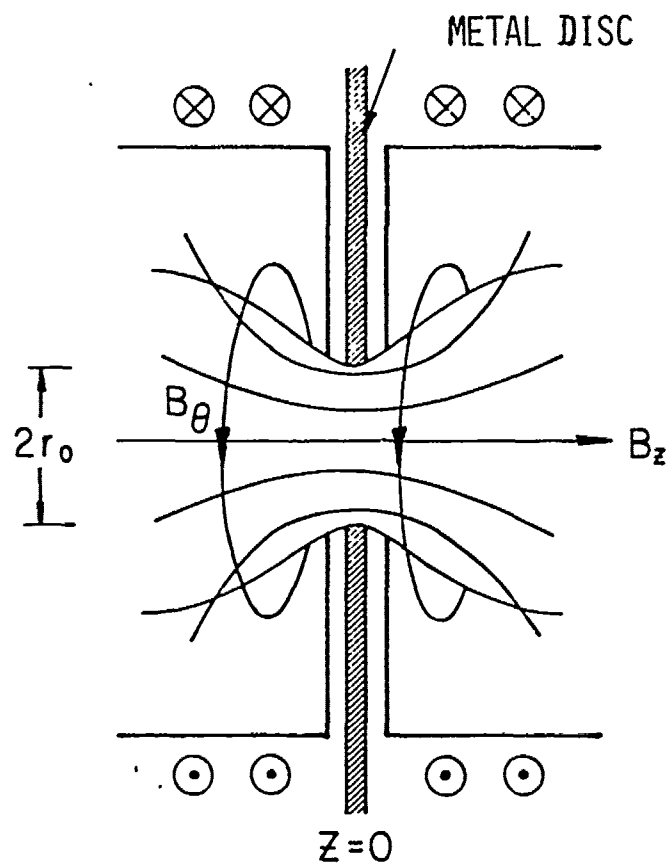
stability criterion: $q(r_0) = \frac{kr_0 B_z(r_0)}{B_\theta(r_0)} > 0$
(Kruskal-Shavranov)

max. growth rate: $\gamma \approx \frac{v_a}{2r_0} \sqrt{1 - \frac{r_0}{R}}$

$v_a = \frac{B_\theta}{\sqrt{\mu_0 \rho}}$ Alfven speed

FIG. 11 PINCH INSTABILITIES WITH AXIAL MAGNETIC FIELD
"SHARP" PINCH (INFINITE CONDUCTIVITY)

$$\underline{m=0}$$



1) PRESSURE BALANCE at $Z=0$

$$nkT = \frac{1}{2\mu_0} (B_z^2 + B_\theta^2) \quad \text{with } B_\theta = \mu_0 \frac{I}{2\pi r_0}$$

2) RESISTIVITY (SPITZER)

$$\eta = 3.04 \times 10^{-3} \frac{Z \ln \Lambda}{T_{ev}^{3/2}} \Omega \text{ cm}$$

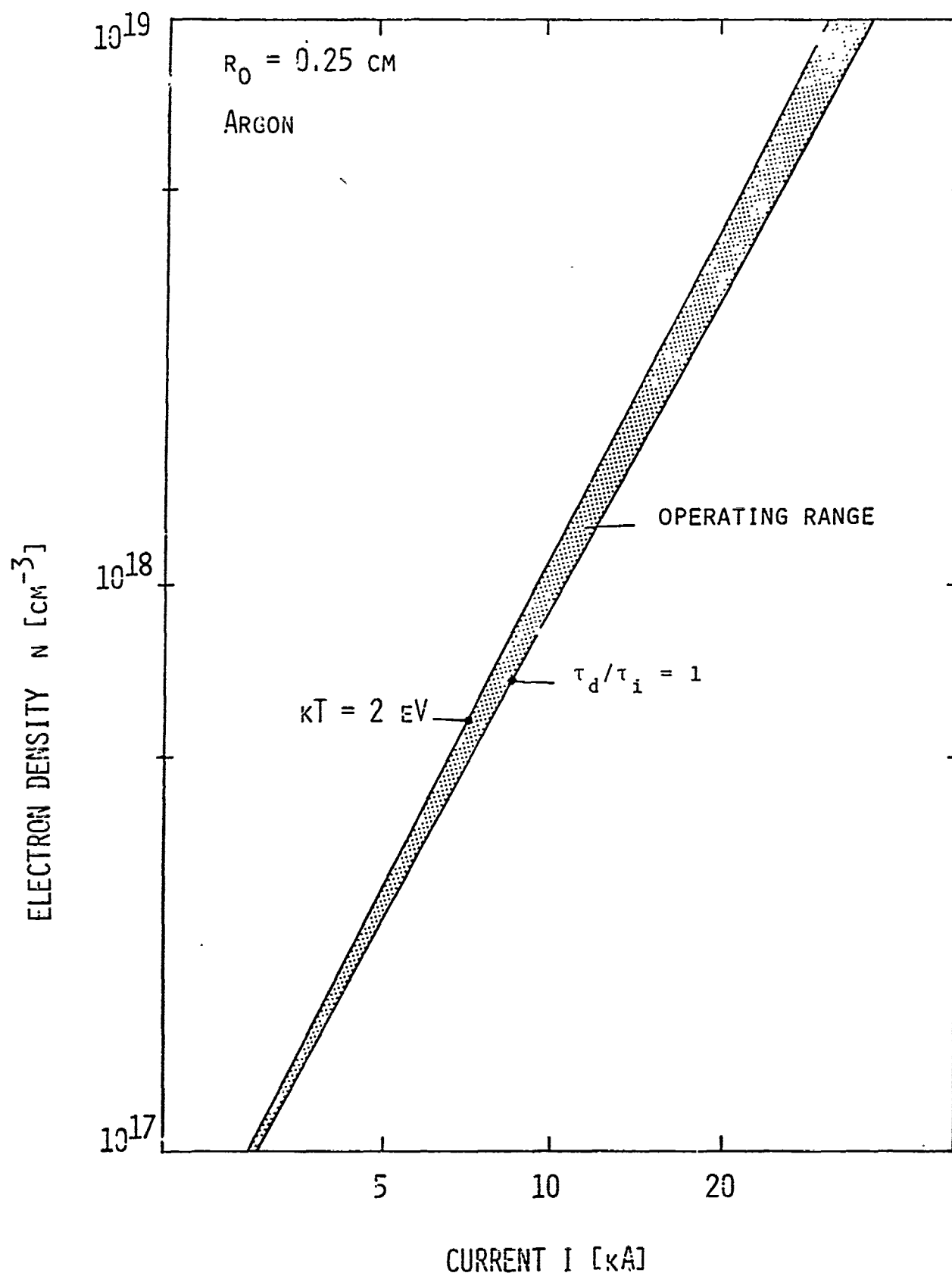
3) DIFFUSION TIME CONSTANT

$$\tau_d = \mu_0 r_0^2 / \eta$$

4) INSTABILITY TIME CONSTANT ($m=0$)

$$\tau_i = r_0 / a \quad a = \text{sonic speed}$$

FIG. 12 FLUX COMPRESSION

FIG. 13 OPERATING RANGE FOR $m = 0$ SWITCH

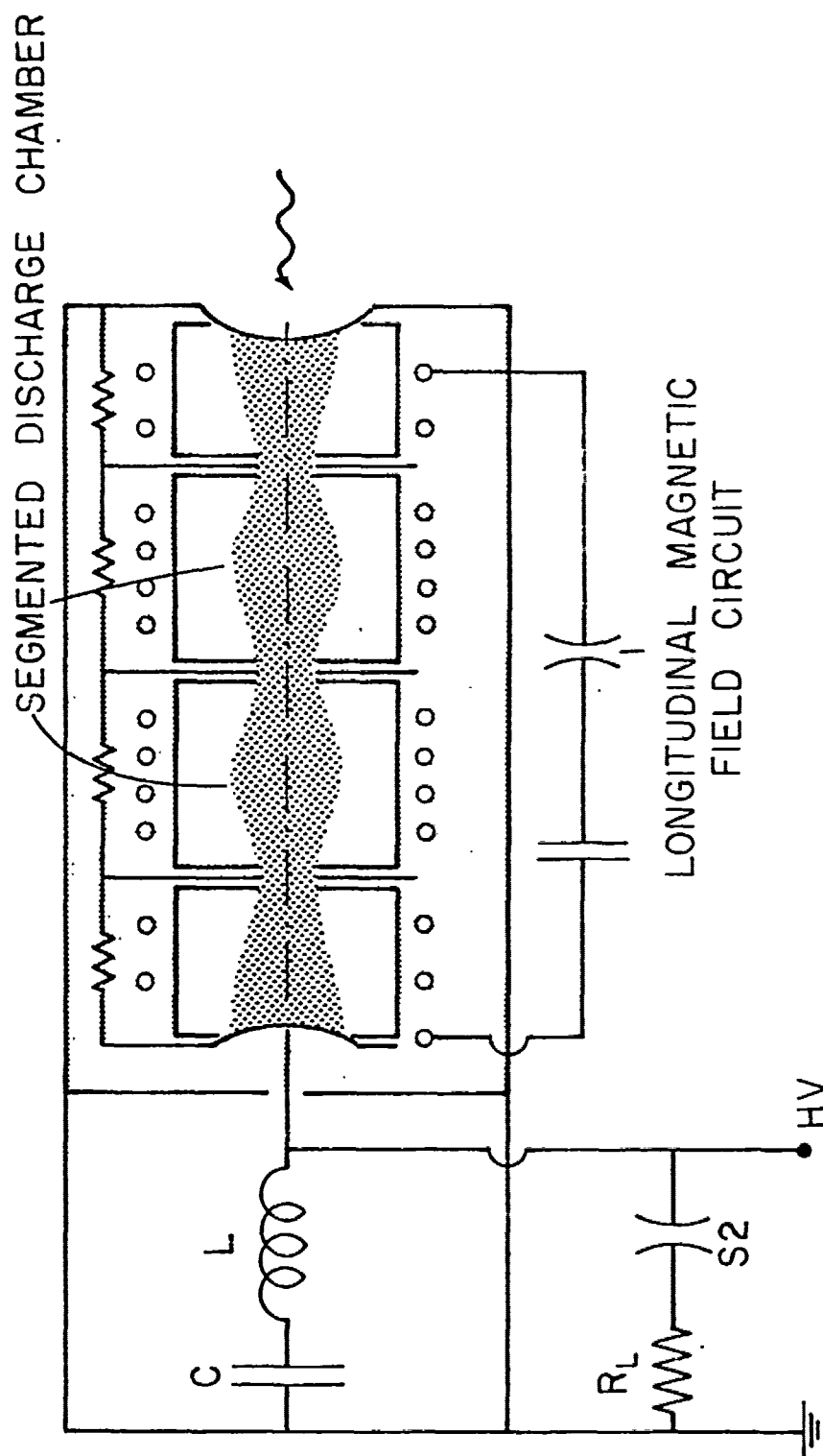


FIG. 14 PHYSICAL ARRANGEMENT FOR $M = 0$ SWITCH

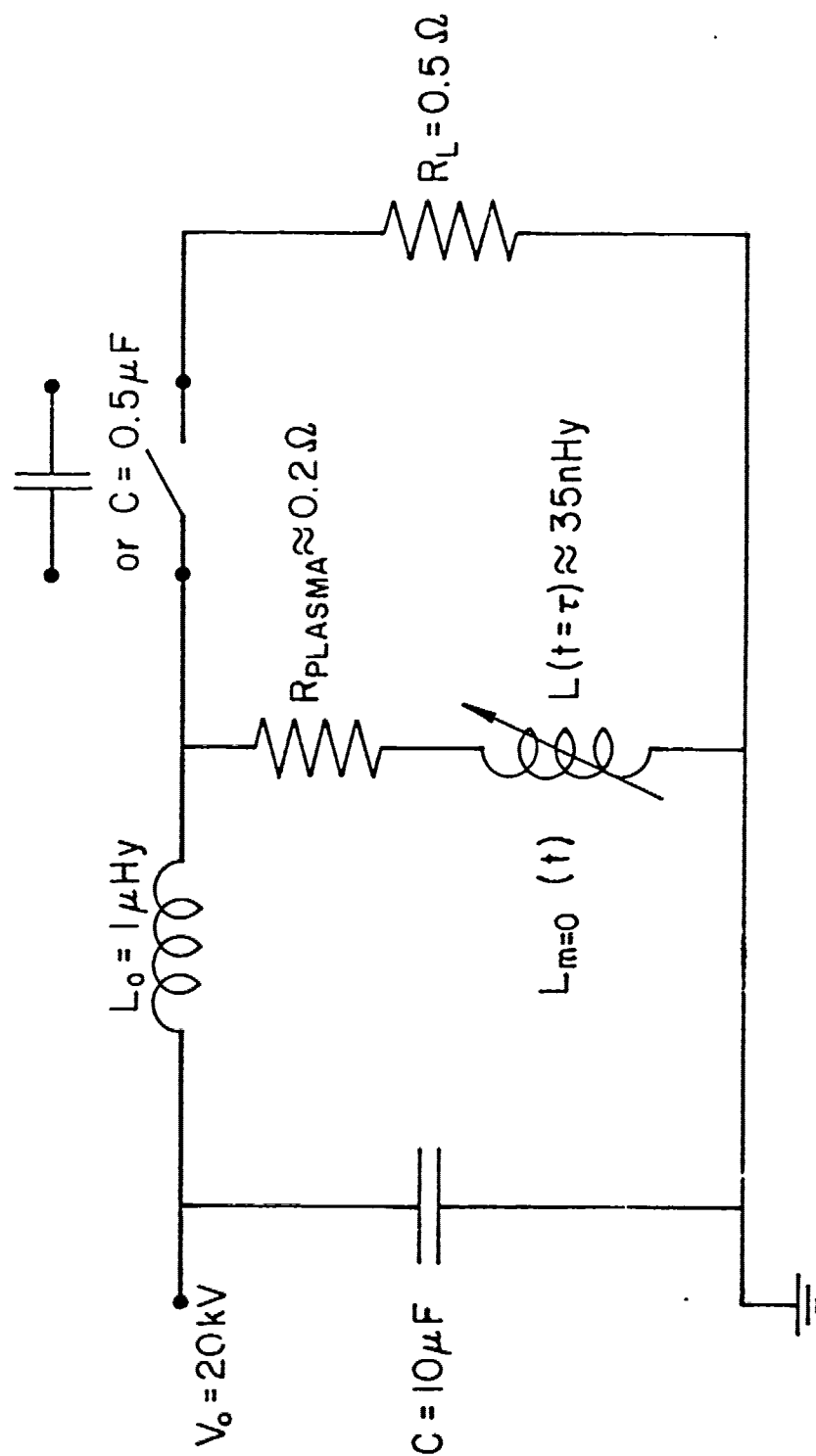


FIG. 15 CIRCUIT, CALCULATED BY MEANS OF SCEPTRE - PROGRAM

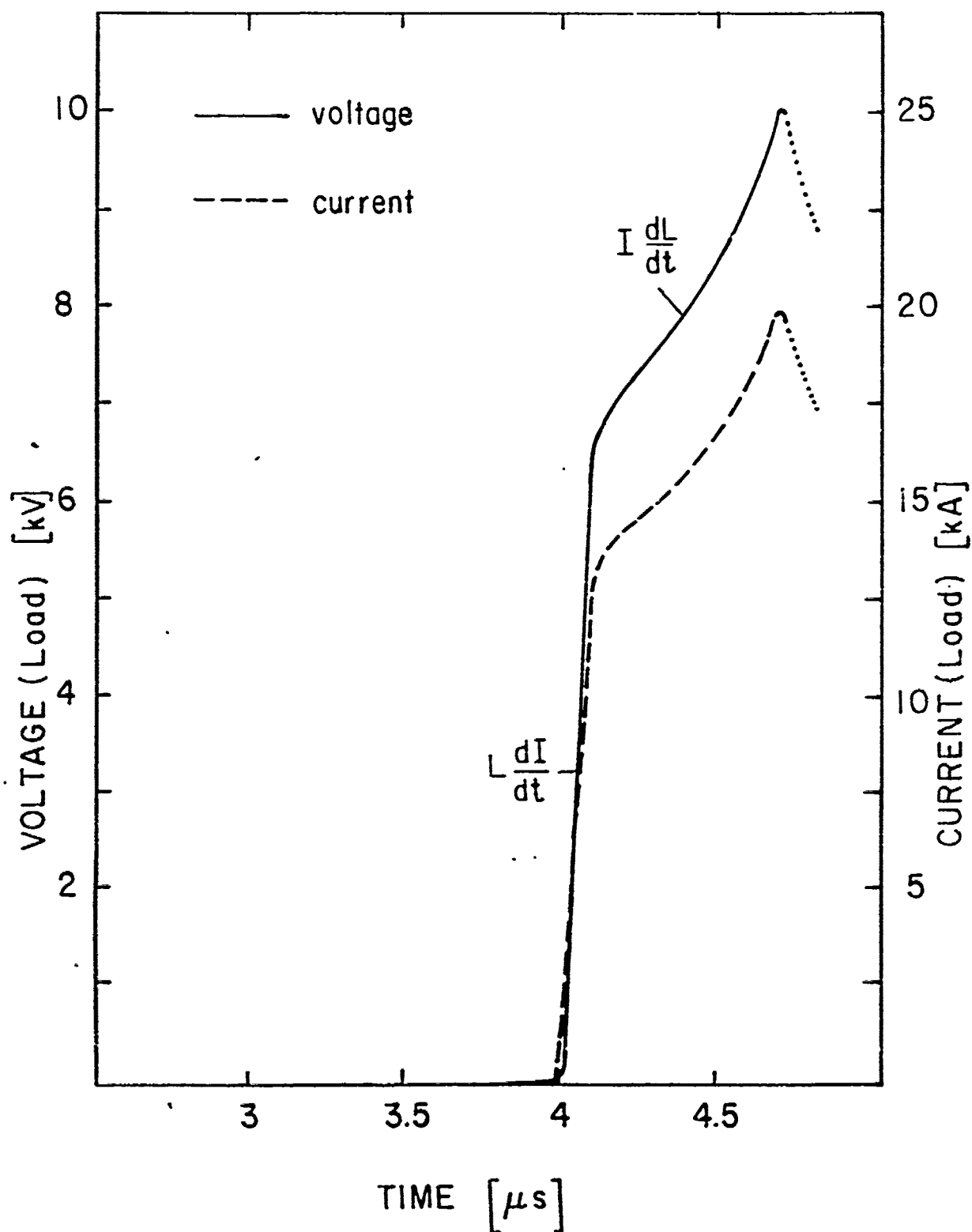


FIG. 16 LOAD VOLTAGE AND CURRENT WITH CLOSING SWITCH

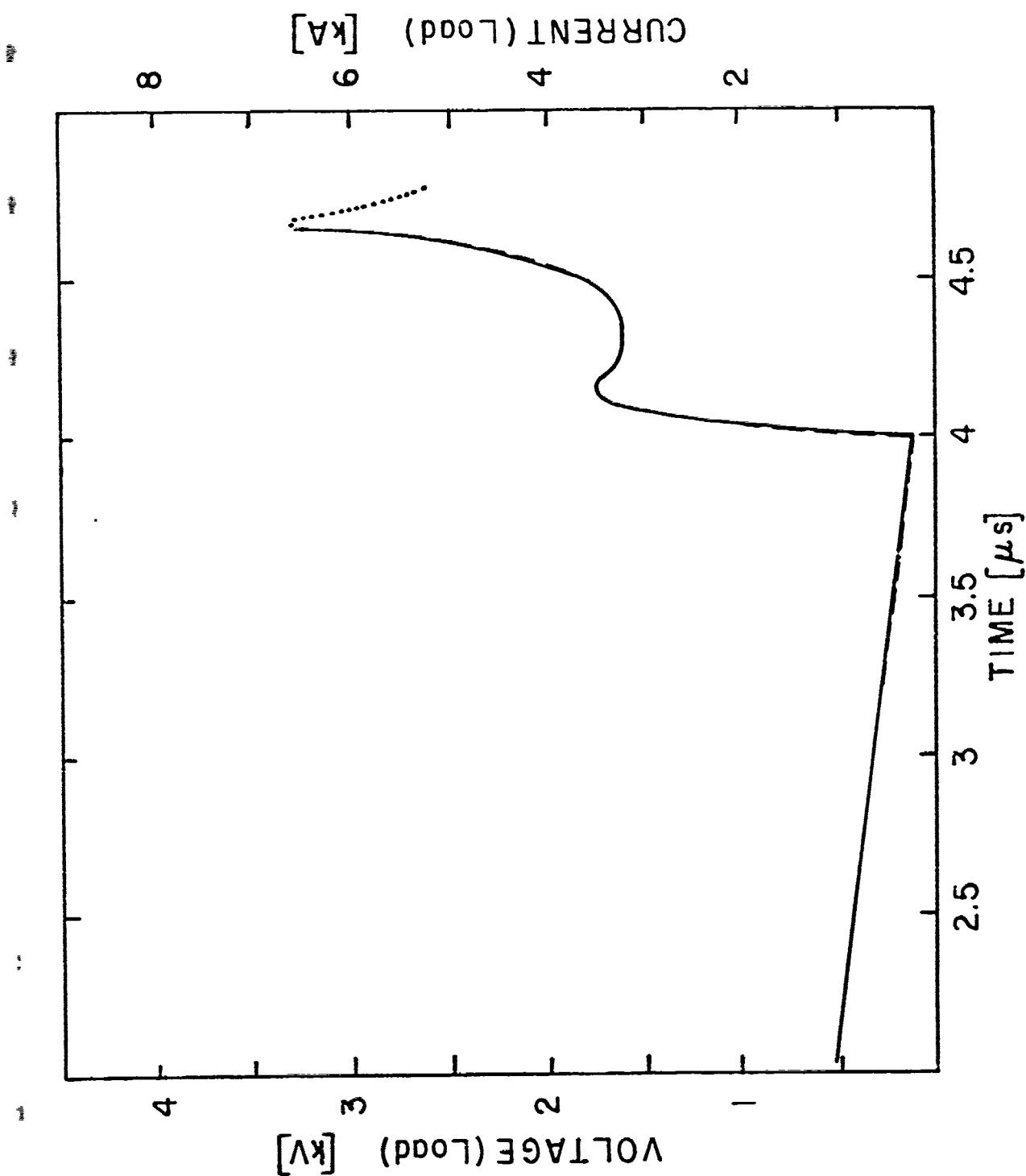


FIG. 17 LOAD VOLTAGE AND CURRENT WITH COUPLING CAPACITOR

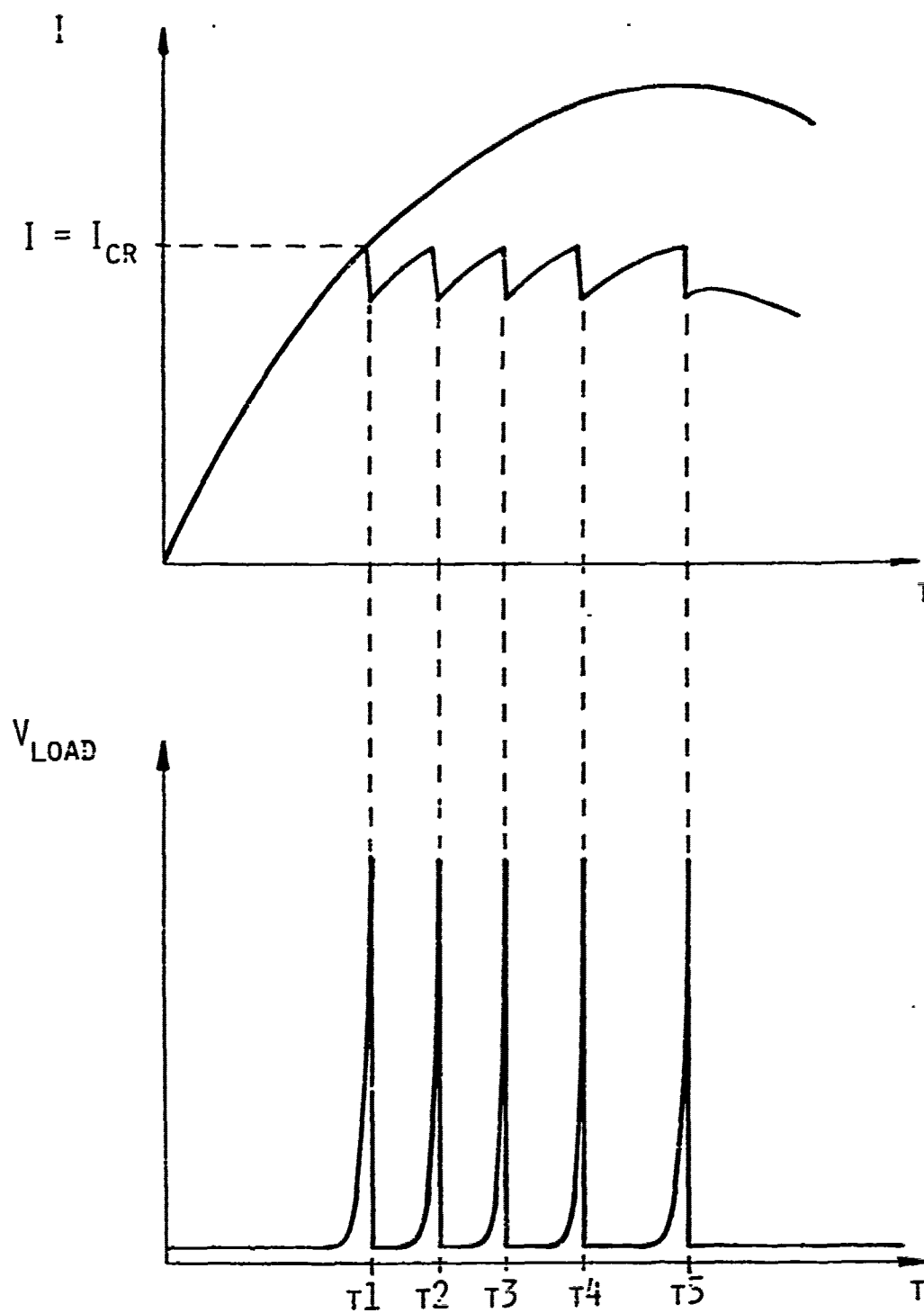
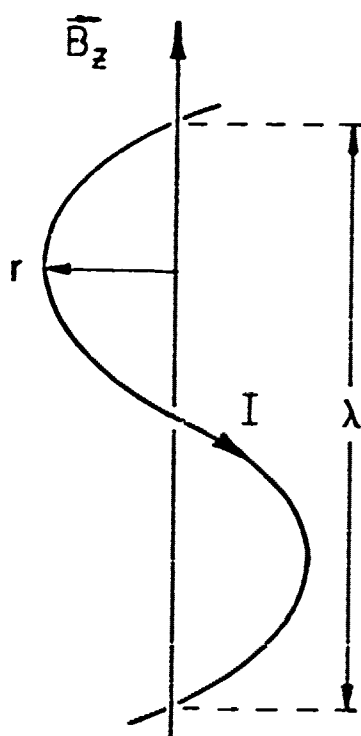


FIG. 18 PRODUCTION OF REPETITIVE VOLTAGE SPIKES



$$\ddot{r} - \frac{k^2 r}{1 + (kr)^2} \dot{r}^2 - \frac{\pi r}{m_0} I B_z = 0$$

$$\text{with } k = \frac{2\pi}{\lambda}$$

m_0 : mass of plasma channel
over the distance $\frac{\lambda}{2}$

for $kr \gg 1$ and \dot{r} small (initial phase)

$$\ddot{r} \approx r_0 e^{\gamma t}$$

$$\text{growth rate: } \gamma = \left[\frac{2\pi I B_z}{m_0} \right]^{1/2}$$

FIG. 19 THIN PLASMA CHANNEL WITH HELICAL PERTURBATION
IN A LONGITUDINAL MAGNETIC FIELD

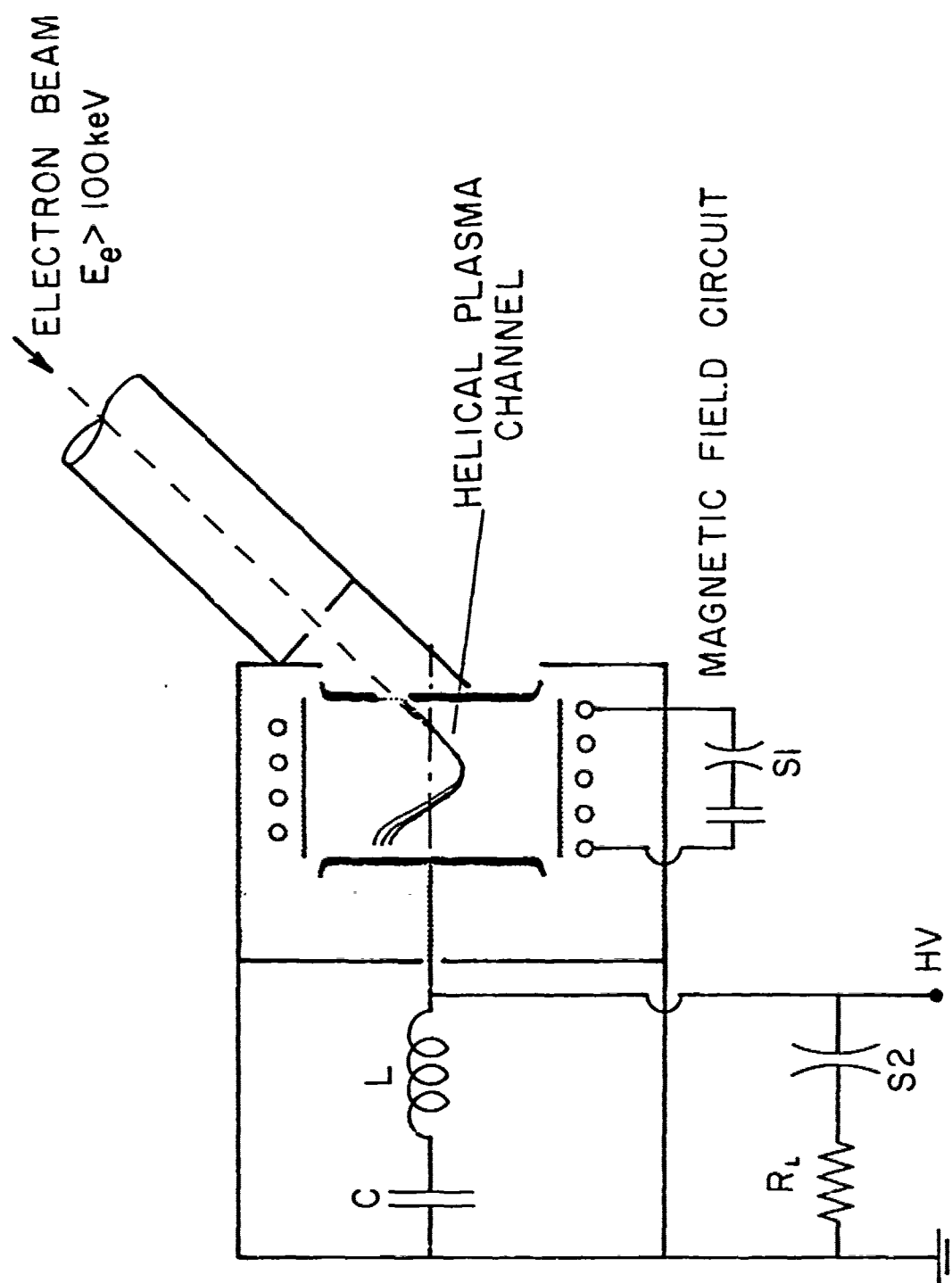


FIG. 20 PHYSICAL ARRANGEMENT FOR $M = 1$ SWITCH

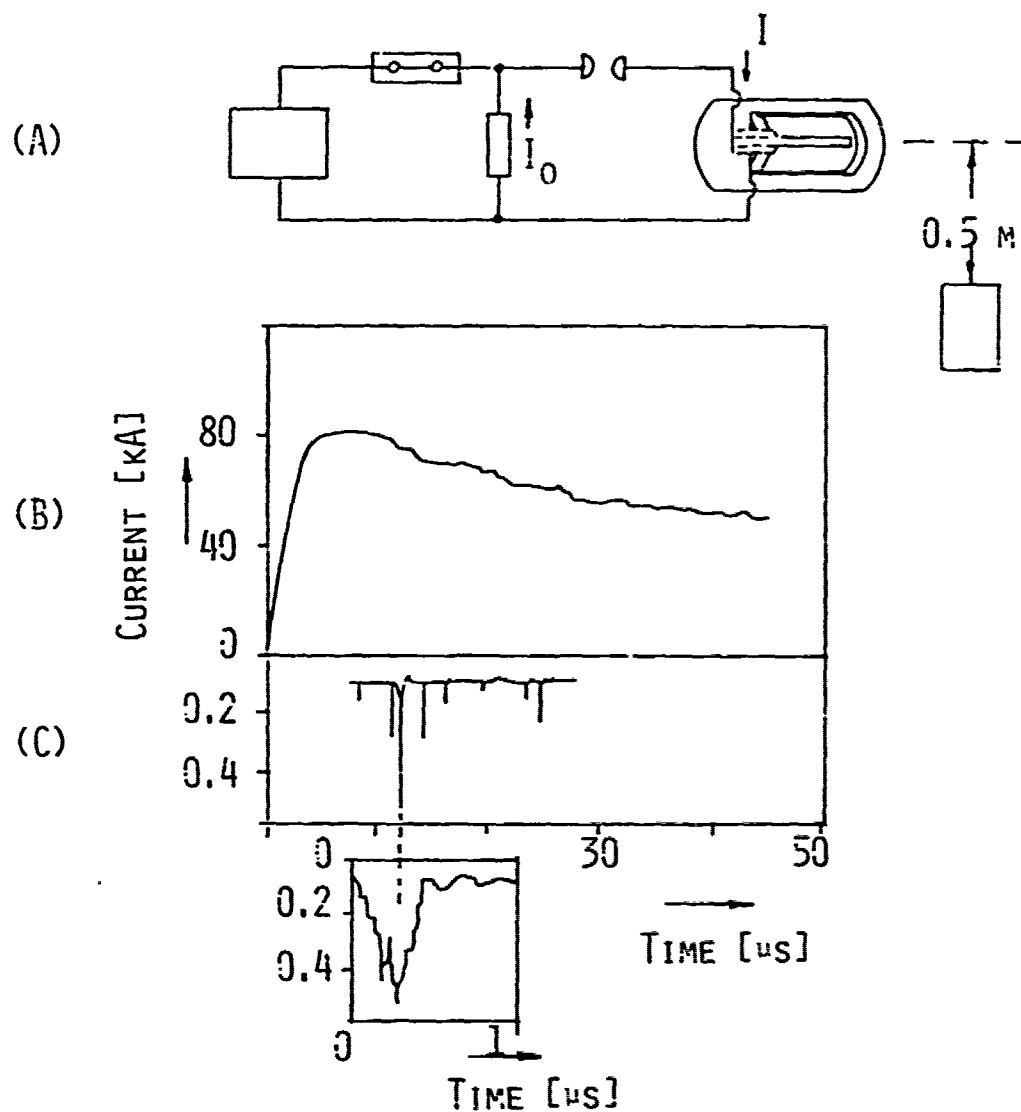


FIG. 21 EXPERIMENTAL ARRANGEMENT AND RESULTS OF A DENSE PLASMA FOCUS POWERED BY A DISCHARGE OF A STORAGE INDUCTOR

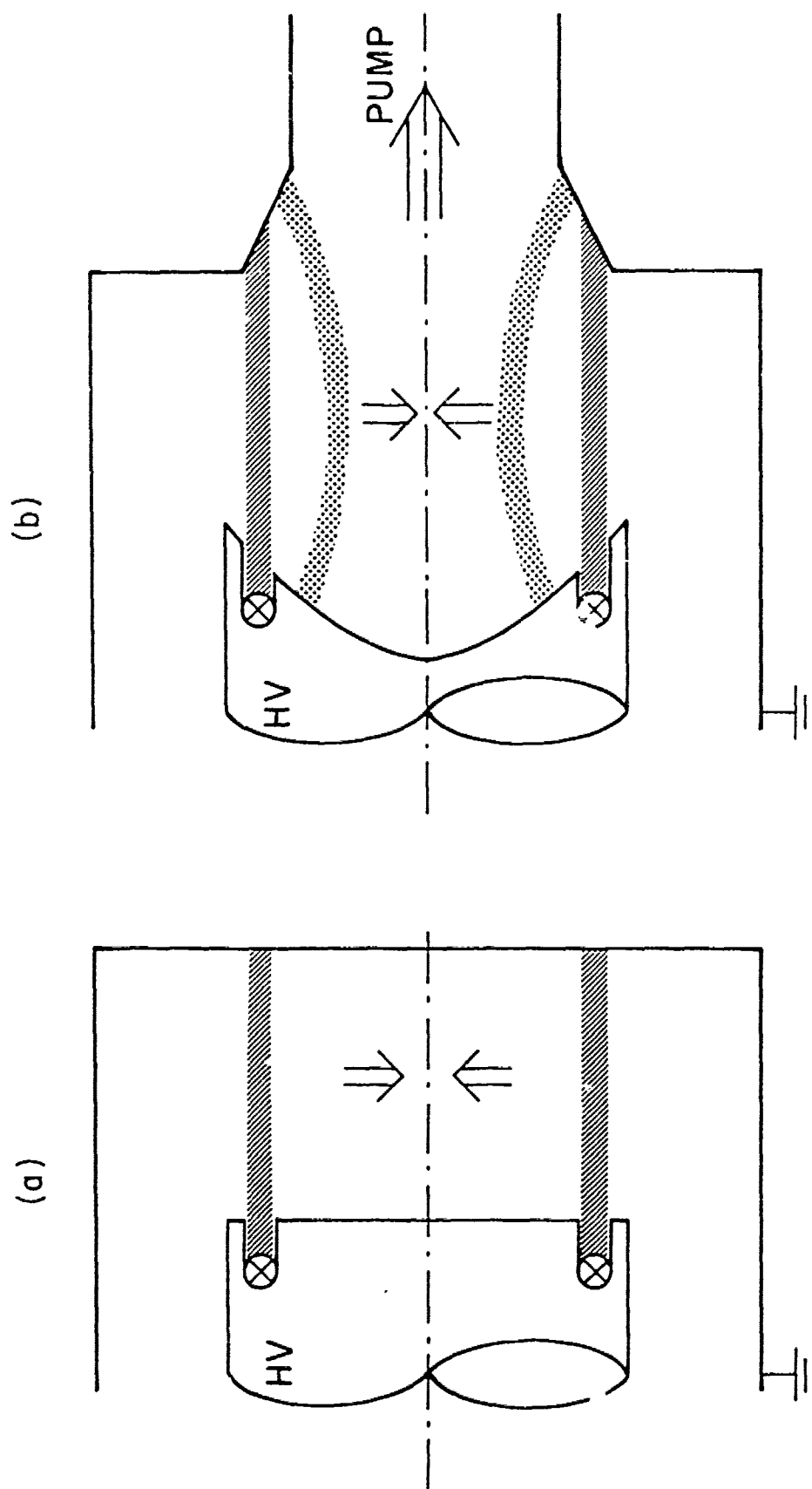
(A) CIRCUIT DIAGRAM

(B) CURRENT IN THE ACCELERATOR

(C) SIGNAL OF THE NEUTRON DETECTOR

(ARBITRARY UNITS)

FROM REF. [7]



(REF. 8)

FIG. 23 GAS PUFF INJECTION

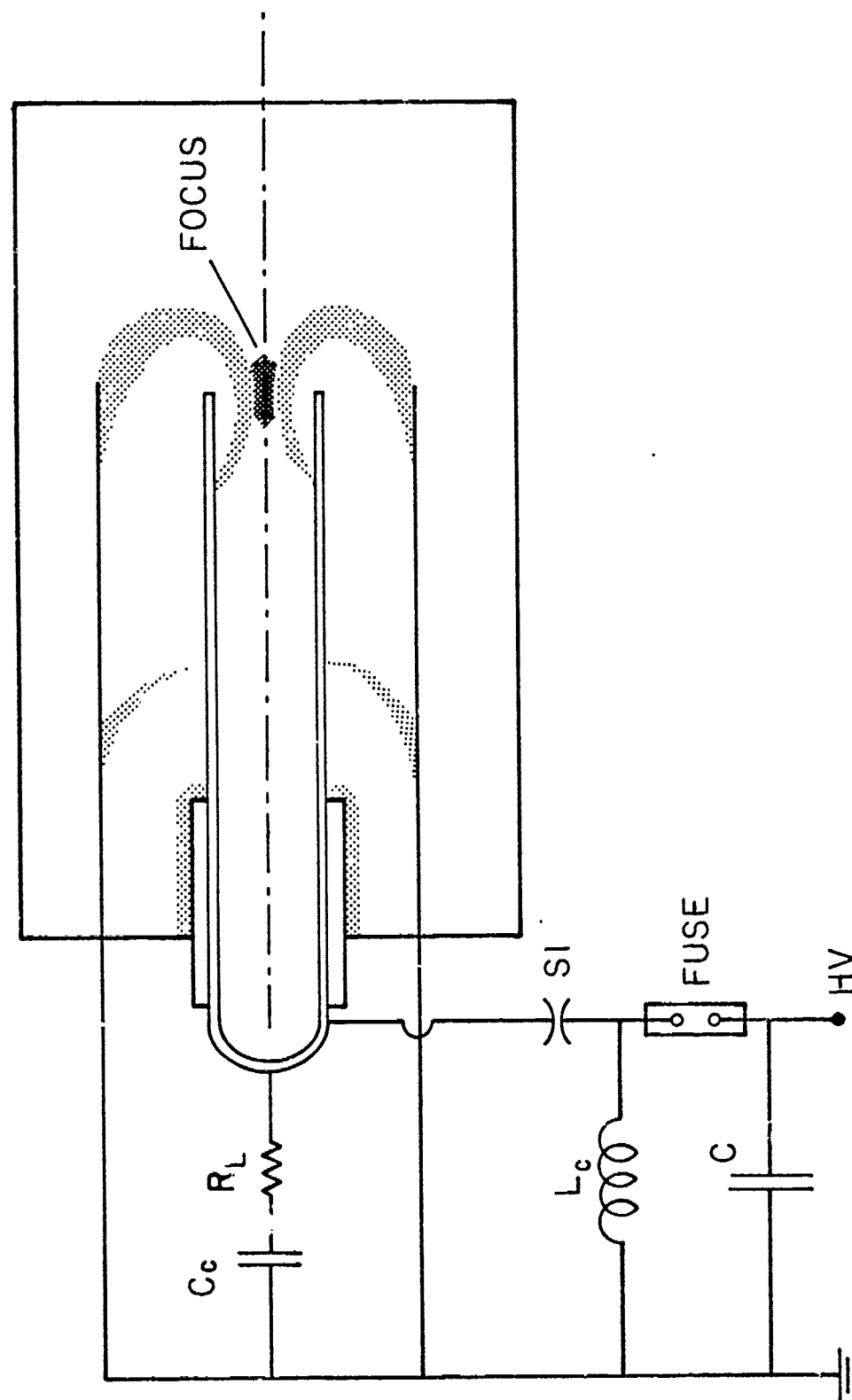


FIG. 22 DENSE PLASMA FOCUS SWITCH ARRANGEMENT

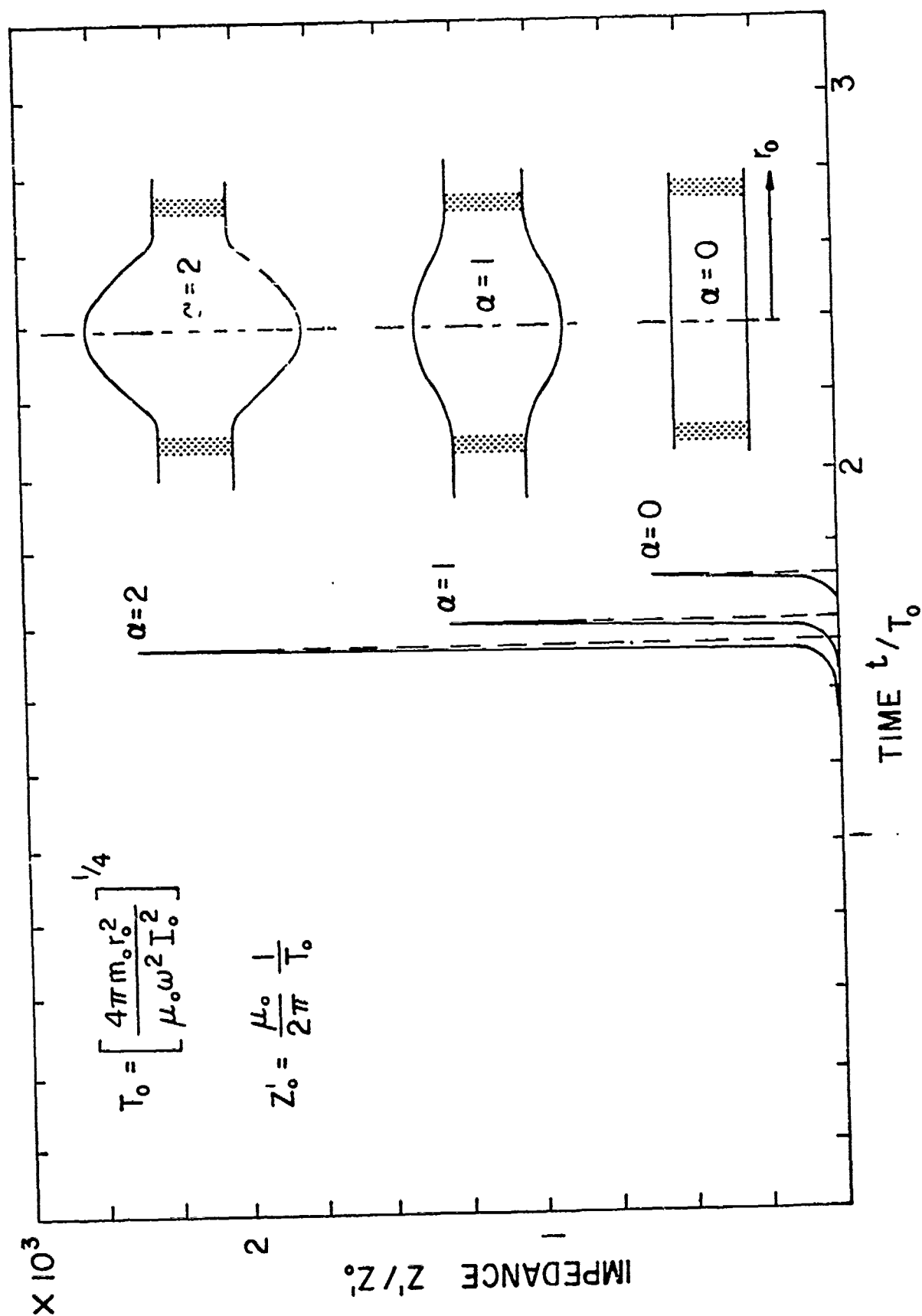


FIG. 24 INFLUENCE OF ELECTRODE SHAPE ON PLASMA IMPEDANCE

Relaxation Processes and LTE in Models of Pulsed
Electric Discharges*

A. V. Phelps⁺

Joint Institute for Laboratory Astrophysics
National Bureau of Standards and University of Colorado
Boulder, Colorado 80309

Abstract

This paper is a review of some of the processes controlling the transition between a weakly ionized gas and local thermodynamic equilibrium (LTE) in pulsed electric discharges, in molecules and gases, such as used in switching devices. The relaxation of the electron energy distribution and number density to their steady-state conditions is governed by processes such as elastic scattering, vibrational and electronic excitation, ionization and recombination. Electron collisions with excited atoms can greatly increase the ionization rates and so influence the approach to LTE. Dissociation of molecules results in large changes in the rates of electron energy loss, ionization, etc. Recent surprising results on gas heating are discussed.

*This work was supported in part by the U. S. Army Research Office.

⁺Staff Member, Quantum Physics Division, National Bureau of Standards.

I. INTRODUCTION

This review discusses some of the important collision process which determine the electric characteristics of pulsed discharges in molecular gases during the breakdown and recovery phases. It is hoped that this discussion will provide an introduction and an updating to some of the data and modeling techniques which are currently available for use in understanding and predicting the behavior of electric discharge switches. Because of the large number of collision and transport process which must be considered when modeling such systems we have arbitrarily limited our discussion to those directly involving the collisions of electrons with atoms and molecules. Thus, we will not consider the relatively familiar radiative energy loss processes, thermal conductivity or gas flow phenomena or circuit and discharge interactions. Because of our recent work with N_2 , most of our examples will be concerned with this gas. This does not mean that we consider N_2 as the gas most suitable for repetitive pulsed switching applications.

During breakdown the electrons initially move in a cold molecular gas with relatively well known properties, e.g., electron-gas collision rates (Sec. II). As the input energy to the discharges increases less familiar processes, such as electron-electron (Sec. II), electron-atom and electron excited atoms processes (Sec. III) become important and cause the densities and distributions in energy of the charged and neutral particles to approach more closely those of local thermodynamic equilibrium (Sec. III). Results of recent modeling studies of the dissociation of diatomic gases show the contribution vibrational excitation followed by dissociation in collisions with neutral molecules or atoms (Sec. IV). Finally, we discuss briefly recent measurements which show surprisingly large rates of molecular gas heating in electrical discharges (Sec. V).

II. ELECTRON ENERGY AND DENSITY RELAXATION

The availability of high speed computers is making possible increasingly accurate models of the behavior of electrons in gases under the influence of applied and space charge generated electric fields [1, 2]. Since we are primarily concerned with the microscopic collision processes and their role in models of electron behavior in gases, we will limit our discussion to models appropriate to uniform electric fields, e.g., spatially independent solutions of the electron Boltzmann equation [3-5] and of the continuity equations for the number density electrons, ions and excited atoms and molecules. In order to simplify and (hopefully) make more real the presentation, the quantitative description of the collision processes will be given in terms of the relaxation time constants for various processes. These time constants are calculated from previously defined rate coefficients [1, 3, 6] assuming a gas density corresponding to one standard atmosphere, i.e., 2.69×10^{25} molecules/m³, and an electron density of 10^{23} electrons/m³. We consider first the electron momentum and energy relaxation processes and then the relaxation of the electron density toward the steady state.

A. Electron Momentum and Energy Relaxation

It is convenient to discuss the relaxation of the electron energy distribution to its steady-state form [3], in terms of time constants for momentum relaxation τ_m and energy relaxation τ_u [6]. The data necessary for evaluation of these parameters are available for a number of gases, e.g., H₂, N₂, O₂, CO, NO, CO₂, NO₂ and air [7]. The lower two curves of Fig. 1 show τ_m and τ_u for N₂ as a function of the characteristic energy ϵ_k of the electrons [6], where the characteristic energy is defined as equal to the ratio of the measurable electron diffusion and mobility coefficients and becomes identically equal to the electron temperature when

the electron distribution function becomes Maxwellian (see Sec. IIB). The data of Fig. 1 show that the momentum relaxation times τ_m are completely negligible on the time scale of pulsed discharge experiments. The same is true for the energy relaxation times τ_u provided the characteristic energy is larger than about 1 eV, i.e., electric field E to gas density N ratios of $E/N > 1 \times 10^{-20} \text{ V m}^2$. An indication that the characteristic energies of interest are greater than about 3 eV ($E/N > 1.5 \times 10^{-19} \text{ V m}^2$) is obtained from a consideration of the ionization growth times τ_i shown in the uppermost curve of Fig. 1. Thus, in order for the electron density to grow by say 10 orders of magnitude in 3 nsec one needs a τ_i value of about 10^{-10} sec or an ϵ_k of about 4 eV.

Recent improvements in techniques for solving the electron Boltzmann equation [5] have been used [8] to show that the conventional solutions to the Boltzmann equation for electrons in N_2 are significantly in error (10 to 30%) for $1.5 < \epsilon_k < 3$ eV. This work is currently being extended [9] to higher E/N values, where ionization becomes the dominant energy loss process. Evidence of the effect of ionization on the relaxation in energy of the higher energy electrons is shown in Fig. 1, where we have plotted a curve of the time required for the ionization rate to reach one half its steady-state value $\tau_{1/2}$ (a kind of induction time), versus ϵ_k . These data were calculated from measurements [10] of the growth of ionization with distance at high E/N and show that very soon after an electron gains enough energy to ionize it undergoes an ionizing collision.

From considerations such as presented here for N_2 , we conclude that techniques are at hand for the accurate calculation of electron energy relaxation, ionization, etc. in weakly ionized molecular gases. However, these techniques have thus far only been applied to N_2 and to H_2 [11].

As the degree of ionization increases, collisions among charged particles become important. Of particular interest

in the present discussion are collisions of pairs of electrons resulting in a redistribution of energy and forcing the electron energy distribution toward a Maxwellian characterized by a true electron temperature as in LTE. A number of calculations have been made of this effect, although only a few apply to molecular gases [12]. The dashed curves of Fig. 1 show approximate values for the time constants for this energy sharing, where the upper line is for an electron density of 10^{20} m^{-3} and the lower line is for 10^{23} m^{-3} . Comparison with the τ_u curve shows that electron-electron collisions dominate the electron energy relaxation process and are expected to result in an approach to Maxwellian electron energy distribution for characteristic electron energies below about 0.8 and 3 eV, respectively. See reference [12] for details. Note that this discussion neglects the possible contribution of collisions of the second kind between electrons and excited molecules to the Maxwellianization of the electron energy distribution [12]. The dashed curve labeled τ_i shows the relatively small changes in the ionization coefficient that occur when the electron energy distribution is changed from that for weakly ionized N_2 to a Maxwellian, while keeping the characteristic energy (not necessarily E/N) constant.

B. Electron Density Relaxation

In this section we consider two extremes of electron production (ionization) and loss (recombination) processes encountered during the build-up or decay of ionization in a pulsed discharge. The solid curves show the time constants characterizing the dominant ionization and electron-ion recombination processes in weakly ionized N_2 . The curve marked τ_i is that for electron impact ionization of N_2 from Fig. 1, while the upper and lower lines marked $\tau_d(\text{N}_2^+)$ and $\tau_d(\text{N}_4^+)$ show approximate values for the time constant for dissociative recombination of electrons to N_2^+ and N_4^+ , respectively [13, 14] at an electron-positive ion density of

10^{23} m^{-3} . According to these curves an electron characteristic energy of about 3 eV ($E/N = 1.5 \times 10^{-19} \text{ V m}^2$), would be required in order to obtain a balance between ionization and recombination at this rather high electron density. Note that since these ionization and recombination processes are not inverse processes such a steady-state discharge may be far from LTE. At such electron densities one would expect a rapid dissociation of the N_2 (see Sec. IV) so that electron collisions with atomic nitrogen would soon dominate the ionization and recombination, as discussed in the next section.

III. EXCITED ATOM EFFECTS AND LTE

The dashed curves of Fig. 2 show ionization τ_{ci} and recombination τ_{cr} time constants for atomic nitrogen calculated from theory [15, 16]. Note that the ionization time constants are much shorter than typical values for the ionization of ground state atoms or molecules. These results are representative of the large amount of modeling of the effects of electron collisions with highly excited atoms on the rates of ionization and recombination in plasmas [17]. These models are often categorized as collisional-radiative models although radiation is predicted to be relatively unimportant at the high gas densities of many switching devices. An extrapolation of the dashed curves of Fig. 2 to their intersection at an electron temperature of about 0.9 eV ($\sim 10400 \text{ K}$) suggests that rather long times ($\sim 3 \times 10^{-7} \text{ sec}$) may be required to reach the steady-state and thermal equilibrium condition. The predicted time constants for the approach to LTE increase rapidly with decreasing electron density.

Rather extensive theoretical investigations of the approach of the steady-state collisional-radiative ionization and recombination process to thermal equilibrium have been carried out [18, 19]. These studies have resulted in detail-

ed criteria for the existence of local thermodynamic equilibrium as a function of plasma density and temperatures.

IV. DISSOCIATION OF MOLECULES

In this section we are concerned with processes leading to dissociation of the molecular gases in an electric discharge. Several modeling studies [20-22] have shown that when a gas, such as N_2 , dissociates at constant particle density N so that E/N remains constant, there are very large increases in the rates of ionization. On the other hand if the dissociation occurs sufficiently rapidly so that expansion does not take place, the E/N value will decrease and there may well be a decrease in the rate of gas ionization. We show in Fig. 3 time constants associated with the dissociation-association process in N_2 (solid curves) and in O_2 (dashed curves).

The solid curve in Fig. 3 marked $e + N_2 \rightarrow 2N + e$ is makes use of our calculation [9] of rate coefficients for the dissociation of N_2 based on a recent analysis of cross sections for the electron impact dissociation of N_2 [23]. Similarly, the dashed curves marked $e + O_2 \rightarrow 2O + e$ show the range of our calculations [24]. Since the differences among various estimates of the rate coefficients for these processes vary by an order of magnitude, there is a serious need for direct measurement of the rate coefficients. Note that these time constants are those for the depletion of the molecular gas and so are proportional to the assumed electron density, i.e., $2.69 \times 10^{20} \text{ m}^{-3}$ corresponding to a fractional ionization of the gas of 10^{-5} . Also, note that in order to obtain a dissociation time constant of 10^{-6} sec at 1 atmosphere density due to thermal dissociation one would require gas temperatures of about 12,000 K and 6000 K for N_2 and O_2 , respectively [25].

The horizontal solid and dashed lines in Fig. 3 show approximate values for the time constants for the recombination of N atoms and of O atoms [25]. The nitrogen calculation is for an atom density half the original gas density while that for oxygen is for an air-like mixture. These rough estimates give time constants for the approach to the steady-state of microseconds as compared to the much shorter times of most of the processes considered in Figs. 2 and 3.

Figure 3 also shows a curve, marked dissociation via V-V transfer, giving the time constant for the dissociation of N_2 as the result of the following sequence of processes: (a) vibrational excitation of N_2 by electrons, (b) transfer of vibrational excitation quanta up the vibration "ladder" due to anharmonic pumping, and (c) dissociation of the very high vibrational levels in collisions with other N_2 molecules [21, 22]. The time constant for this process has been scaled from calculations at lower gas and electron densities, but we do not have the results appropriate to higher degrees of ionization. Note that this process dominates electron impact dissociation at low E/N values in N_2 . This process is relatively much more important in N_2 than in O_2 because of the large cross sections for vibrational excitation of N_2 by electrons relative to those for O_2 .

V. GAS HEATING BY ELECTRONS

A number of investigators have calculated the fraction of the input electrical energy transferred from the electrons to various modes of excitation of gas molecules [26]. Until recently, it has been believed [27] that the energy transferred from the electrons to the vibrational modes of the N_2 molecule is only slowly transferred to translational energy, i.e., heat, because of the very low rate coefficients for vibrational relaxation of the N_2 molecule [28]. However, a growing body of Soviet experimental data [29-31] has shown

that the rate of heating of N_2 by electrons in discharges operating at moderate E/N is much larger than predicted using the low-vibrational relaxation rate coefficients. This has led to the proposal [31] that when the vibrational "temperature" is sufficiently high, a rapid vibrational relaxation occurs via the more closely spaced higher vibrational levels, i.e., the same anharmonic pumping effect responsible for dissociation in Sec. IV.

REFERENCES

- [1] A. J. Davies, C. J. Evans, P. Townsend and P. Woodison, "Computation of Axial and Radial Development of Discharges between Parallel Plane Electrodes," *Proc. Inst. Elec. Eng.* 124, 179 (1977).
- [2] E. E. Kunhardt, "Electrical Breakdown of Gases: the Prebreakdown stage," *IEEE Trans. Plasma Sci.* PS-130, 130 (1980).
- [3] L. G. H. Huxley and R. W. Crompton, The Diffusion and Drift of Electrons in Gases (Wiley, New York, 1974), Chap. 2.
- [4] K. Kitamori, H. Tagashira and Y. Sakai, "Development of Electron Avalanches in Argon -- An Exact Boltzmann Equation Analysis," *J. Phys. D* 13, 535 (1980).
- [5] L. C. Pitchford, S. V. O'Neil and J. R. Rumble, Jr., "Extended Boltzmann Analysis of Electron Swarm Experiments," *Phys. Rev. A* 23, 294 (1980).
- [6] L. S. Frost and A. V. Phelps, "Rotational Excitation and Momentum Transfer Cross Sections for Electrons in H_2 and N_2 from Transport Coefficients," *Phys. Rev.* 127, 162 (1962).
- [7] J. Dutton, "A Survey of Electron Swarm Data," *J. Phys. Chem. Ref. Data* 4, 577 (1975).

- [8] L. C. Pitchford and A. V. Phelps, "Extended Boltzmann Analysis Applied to Electron Swarm Experiments in N_2 ," Paper JA-1, 33rd Gases Electronics Conference, Norman, Oklahoma, 7-10 October 1980.
- [9] L. C. Pitchford and A. V. Phelps (unpublished).
- [10] S. C. Haydon and O. M. Williams, "Combined Spatial and Temporal Studies of Ionization Growth in Nitrogen," J. Phys. D 9, 523 (1976).
- [11] H. A. Blevin, J. Fletcher and S. R. Hunter, "A Monte-Carlo Simulation of the Behavior of Electron Swarms in Hydrogen Using an Anisotropic Scattering Model," Aust. J. Phys. 31, 299 (1978).
- [12] A. Kh. Mnatsakanyan and G. V. Naidis, "Dependence of Electron Energy Distribution in Molecular Nitrogen on the Vibrational Temperature and the Degree of Ionization," Sov. J. Plasma Phys. 2, 84 (1976).
- [13] W. H. Kasner and M. A. Biondi, "Electron-Ion Recombination in Nitrogen," Phys. Rev. 137, A317 (1965).
- [14] D. H. Douglas-Hamilton, "Recombination Rate Measurements in Nitrogen," J. Chem. Phys. 58, 4820 (1973).
- [15] L. M. Biberman, V. S. Vorob'ev and I. T. Yakubov, "Kinetics of Impact-Radiation Ionization and Recombination," Soviet. Phys. - Usp. 15, 375 (1973).
- [16] A. V. Potapov, L. E. Tsvetkova, V. I. Antropov, and G. N. Volkova, "Ionization and Radiation Characteristics of a Nonequilibrium Atomic Nitrogen Plasma," Opt. Spectrosc. 43, 243 (1977).
- [17] L. M. Biberman, V. S. Vorob'ev and I. T. Yakulov, "Low-Temperature Plasma with Nonequilibrium Ionization," Sov. Phys. -- Usp. 22, 411 (1979).
- [18] T. Fujimoto, "Validity Criteria for Local Thermodynamic Equilibrium and Coronal Equilibrium," J. Phys. Soc. Japan 34, 216 (1973).

- [19] T. Fujimoto, "Kinetics of Ionization-recombination of a Plasma Population Density of Excited Ions. II. Ionizing Plasma," J. Phys. Soc. Japan 47, 273 (1979).
- [20] P. Michael, S. Pfau, A. Rutscher and R. Winkler, "Diffionstheoretische Beschreibung der Dissoziation und des Ionenhaushaltes im schwachionisierten Säulenplasma der Wasserstoffentladung," Beitr. Plasmaphysik 20, 97 (1980).
- [21] M. Capitelli, M. Dilonardo and C. Grose, "Selfconsistent Electron Energy Distribution Functions in Nonequilibrium Nitrogen," Chem. Phys. (in press) (1981).
- [22] M. Capitelli and E. Molinari, "Kinetics of Dissociation Processes in Plasmas in the Low and Intermediate Pressure Range," Topics Curr. Chem. 90, 59 (1980).
- [23] E. C. Zipf and R. W. McLaughlin, "On the Dissociation of Nitrogen by Electron Impact and by EUV Photo-Absorption," Planet. Space Sci. 26, 449 (1978).
- [24] S. A. Lawton and A. V. Phelps, "Excitation of the $b^1\Sigma_g^+$ State of O_2 by Low Energy Electrons," J. Chem. Phys. 69, 1055 (1978).
- [25] M. H. Bortner and T. Baurer, DNA Reaction Rate Handbook (General Electric, 1979), p. 24-44.
- [26] A. G. Englehardt, A. V. Phelps, and C. G. Risk, "Determination of Momentum Transfer and Inelastic Collision Cross Sections for Electrons in Nitrogen Using Transport Coefficients," Phys. Rev. 135, A 1566 (1964).
- [27] E. Marode, F. Bastion and M. Bakker, "A Model of the Streamer-Induced Spark Formation Based on Neutral Dynamics," J. Appl. Phys. 50, 140 (1979).
- [28] R. L. Taylor and S. Bitterman, "Survey of Vibrational Relaxation Data for Processes Important in the CO_2-N_2 Laser System, Rev. Mod. Phys. 41, 26 (1969).
- [29] A. D. Kosoruchkina, "Gas Heting in a Nitrogen Glow Discharge," Sov. Phys. Tech. Phys. 20, 576 (1976).

- [30] A. P. Napartovich, V. G. Naumov and V. M. Shashov,
"Heating of a Gas in a Combined Discharge in a Flow of
Nitrogen," Sov. Phys. Dokl. 22, 35 (1977).
- [31] V. Yu. Baranov, F. I. Vysikailo, A. P. Napartovich, V.
G. Niz'ev, S. V. Piqui'skii, and A. N. Starostin,
"Contraction of the Decaying Plasma in a Nitrogen
Discharge," Sov. J. Plasma Phys. 4, 201 (1978).

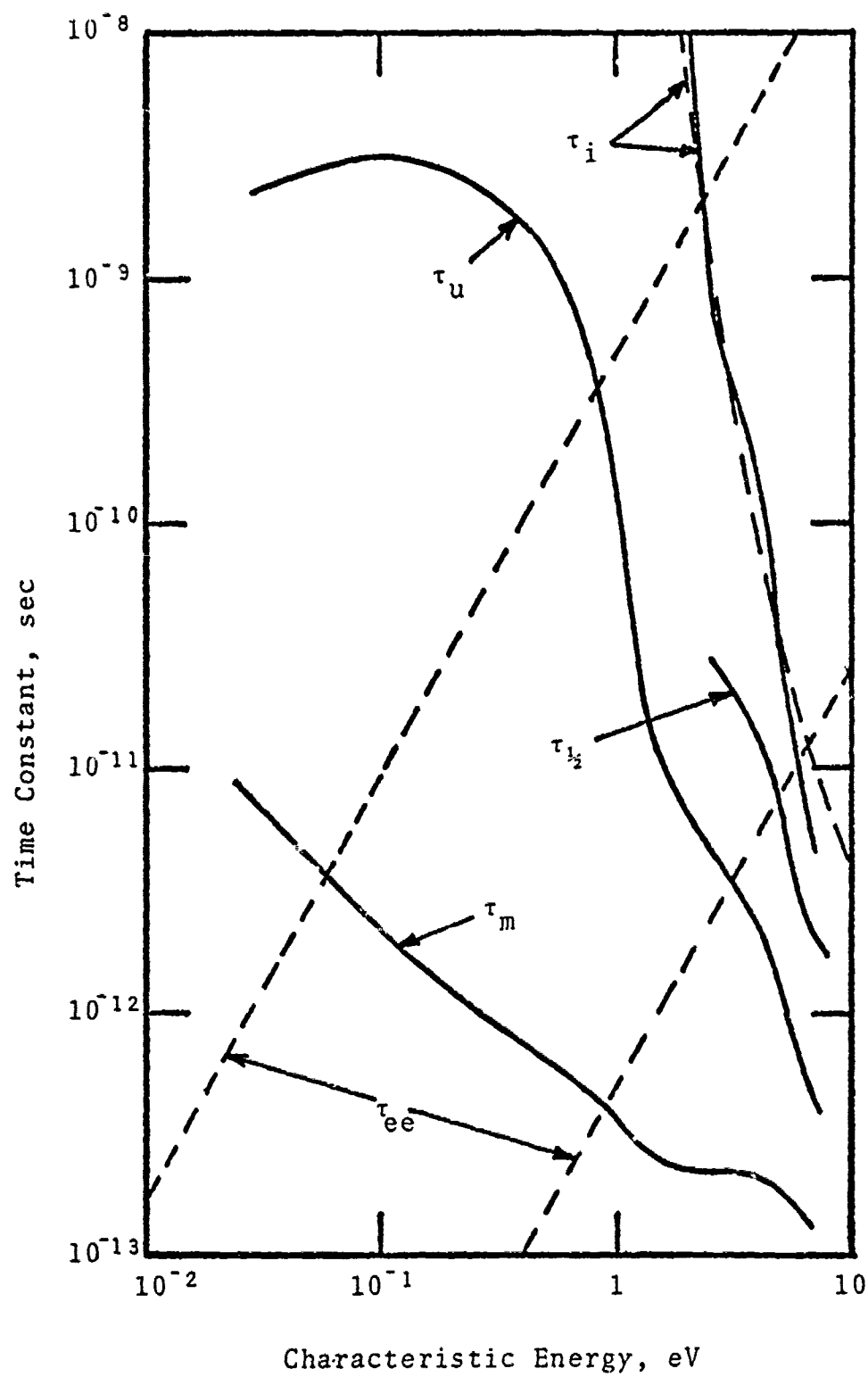


Figure 1. Electron momentum and energy relaxation in N_2 .

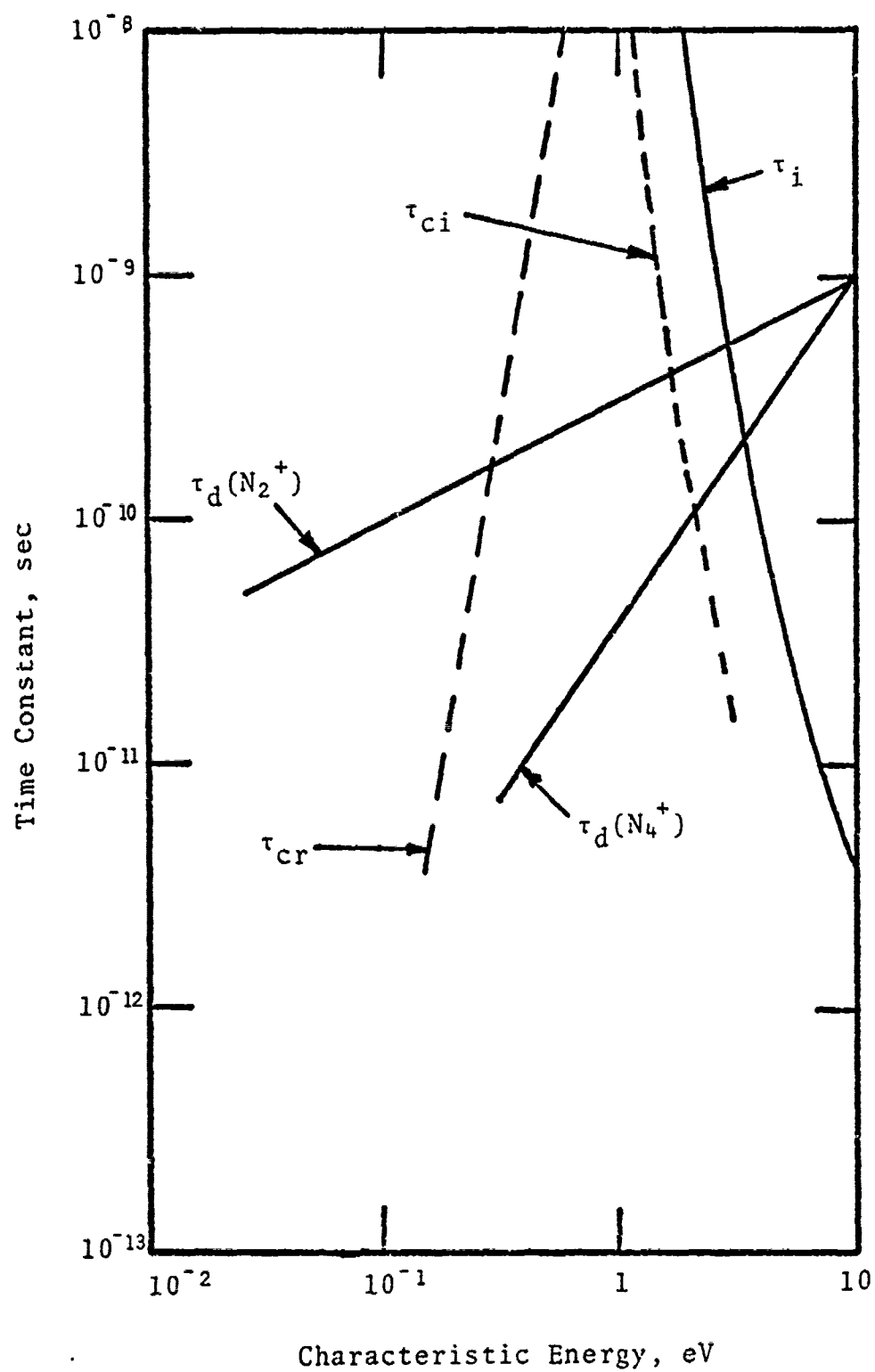


Figure 2. Electron density relaxation in N_2 and N .

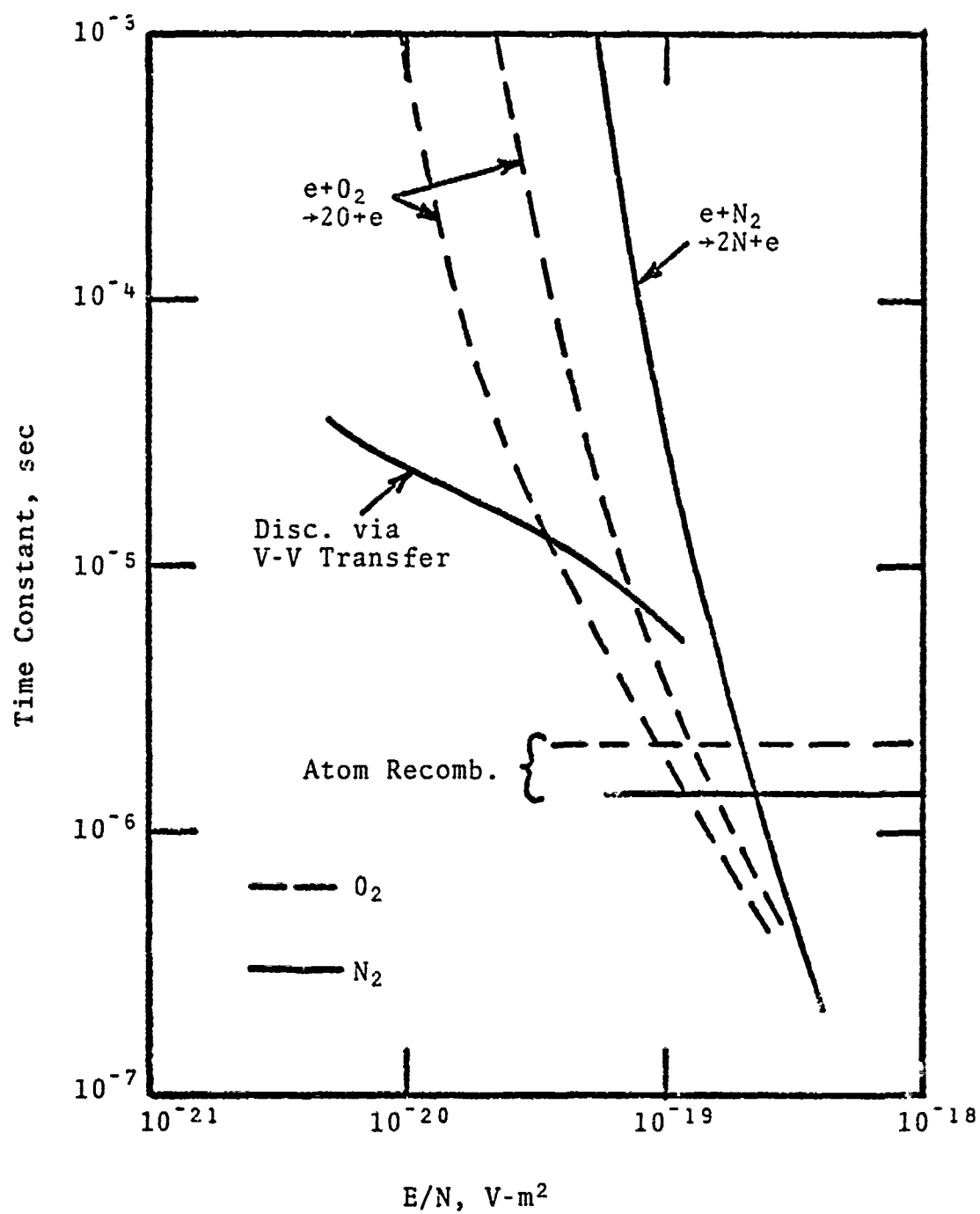


Figure 3. Dissociation and recombination times in N_2 and O_2 for $n_e/N = 10^{-5}$.

PERFORMANCE PREDICTIONS FOR E-BEAM CONTROLLED ON/OFF SWITCHES *

Laurence E. Kline

Westinghouse R&D Center
Pittsburgh, PA 15235

A. Introduction

The high voltage on/off switches discussed in this paper use the low energy secondary electrons in an electron beam sustained discharge as the conducting medium. The operation of the switch and the application of the switch to an inductive energy storage system are shown schematically in Fig. 1. The space between the switch electrodes is filled with a gas at high pressure. The switch conductivity is negligible before the e-beam is turned on because the power supply voltage is below the self-breakdown voltage of the gas in the switch. When the e-beam is turned on, the conductivity increases by many orders of magnitude due to ionization of the gas by the e-beam. While the switch is turned on energy is stored in the inductor. When the energy storage cycle is completed the closing switch is closed and the e-beam switch is opened by turning off the e-beam. The conductivity of the e-beam switch decays at a rate determined by the attachment and recombination properties of the gas in the switch. As the voltage builds up across the e-beam switch, energy is transferred from the storage inductor to the load.

The feasibility of e-beam switches has been demonstrated experimentally using capacitive energy stores

* Supported by U. S. Air Force Contract F33615-78-C-2010.

[1-7]. In most cases both the e-beam and switch current densities were high. Typically the e-beam current was 1-100 A/cm² and the current gain was less than 100. In this regime the e-beam energy is comparable to the energy delivered to the load because the current gain is low and the e-beam voltage is higher than the load voltage in most of the experiments reported in [1-7].

The performance of e-beam switches has also been studied in a regime where the e-beam current density is 0.1-100 mA/cm². Since the current gain varies inversely as the square root of the e-beam current density the energy delivered to the load in this regime is typically much greater than the e-beam energy. The switch efficiency, defined as the load energy divided by the sum of the load, e-beam and switch energies, is limited by the power dissipated in the switch discharge. The feasibility of this regime has also been studied experimentally [2,6].

B. Switch Discharge Model

The model used to predict switch performance assumes that the switch discharge voltage is equal to the positive column voltage. The voltage drops in the electrode sheath regions are neglected. The effect of ionization in the cathode sheath is also neglected. Ionization in the sheath appears to lower the discharge voltage, compared with the predictions of the model used in this study [6].

Electron transport data and static breakdown voltages are required to predict switch performance. These quantities were calculated for nitrogen, argon a nitrogen:argon=1:9 mixture, and methane by numerically solving the Boltzmann equation to find the electron energy distribution. Both the nitrogen-argon mixture and methane have the desirable property that the electron drift velocity is high at low values of the electric field-to-gas density

ratio, E/N . The predicted breakdown voltages are in good agreement with experiment.

C. Application to Inductive Energy Storage Systems

The experimentally controllable variables in an e-beam switch are the e-beam current density, the electrode gap length and cross sectional area, and the gas pressure and composition. The maximum open circuit voltage that the switch must develop determines the required value of the gas density-gap length product, Nd .

In typical experiments [1-7] the e-beam voltage is comparable to the open circuit voltage. Also, the time required to store the energy in the inductor is 10-100 times as long as the time during which energy is delivered to the load. Therefore the current gain (i. e. the ratio of the switch current density to the e-beam current density) must be high so that the energy required to drive the e-beam is much less than the energy delivered to the load. Calculated values of the switch current gain in methane are shown in Fig. 2.

Once the value of Nd has been determined the efficiency of the switch during the on period can be determined. This efficiency increases 1) as the switch resistance decreases and 2) as the e-beam power decreases. For a fixed value of the open circuit voltage V_L and total switch current I the switch resistance decreases as the switch area increases and as the e-beam current density increases. The area required to obtain a specified value of the switch resistance

$$R = V_S/I = (V_S/V_L)V_L/I$$

can be obtained from calculated results of the type shown in Fig. 3. These results were calculated for methane and two pairs of V_L, I values: 1) $V_L=100$ kV and $I=1$ kA and 2) $V_L=33$ kV and $I=20$ kA.

When the e-beam switch opens the voltage that develops is determined by the rate at which the switch can turn off. The turn-off time is determined, in turn, by the electron loss rate in the switch. Calculations for methane show that a small admixture of an attaching gas can dramatically decrease the turn-off time. Predictions for the experimental conditions of Hunter [3-5] give turn-off times as short as 500 nsec in agreement with his experimental results. Shorter turn-off times are possible at the expense of reduced conductivity while the switch is turned on. The energy transfer efficiency from the storage inductor to the load resistor in the circuit of Fig. 1 is limited by the stray inductance of the two loops and the finite opening of the switch. In the limit of small stray inductances and short opening time the energy transfer efficiency approaches 100%.

D. Acknowledgment

Helpful discussions with Paul H. Haley are gratefully acknowledged.

E. References

- [1] B. M. Koval'chuk, V. V. Kremnev, and G. A. Mesyats, "Avalanche Discharge in a Gas and the Generation of Nanosecond and Subnanosecond Large-Current Pulses". Soviet Physics-Doklady 15, 267 (1970).
- [2] B. M. Koval'chuk, Yu. D. Korolev, V. V. Kremnev, and G. A. Mesyats, "The Injection Thyatron - A Completely Controlled Ion Device". Soviet Radio Engr. and Electron Physics 21, 112 (1976).
- [3] R. O. Hunter, "Electron Beam Controlled Low Impedance Discharges". Bull. Am. Phys. Soc. 20, 255 (1975).

- [4] R. O. Hunter, "Electron Beam Controlled Switching",
Proc. 1st Int'l. Pulsed Power Conf., Lubbock, TX,
1975. IEEE Cat. No. 76 CH 1147-8, Paper IC8.

- [5] R. O. Hunter, "Low Impedance Electron Beam
Controlled Discharge Switching System", U. S.
Patent 4,063,130, Dec. 13, 1977.

- [6] P. Bletzinger, "I-V Characteristics of
Externally Ionized Plasmas in Pure Gases",
Proc. 33rd Gaseous Electronics Conf., Norman, OK
Oct. 1980, Paper BB-5.

- [7] K. McDonald, M. Newton, E. E. Kunhardt,
M. Kristiansen and A. H. Guenther, "An Electron-
Beam Triggered Spark Gap", IEEE Trans. on Plasma
Science, PS-8, 181 (1980).

- [8] J. W. Dzimianski and L. E. Kline, "High Voltage
Switch Using Externally Ionized Plasmas", Rpt. No.
AFWAL-TR-80-2041, Air Force Wright Aeronautical Labs.
(1980).

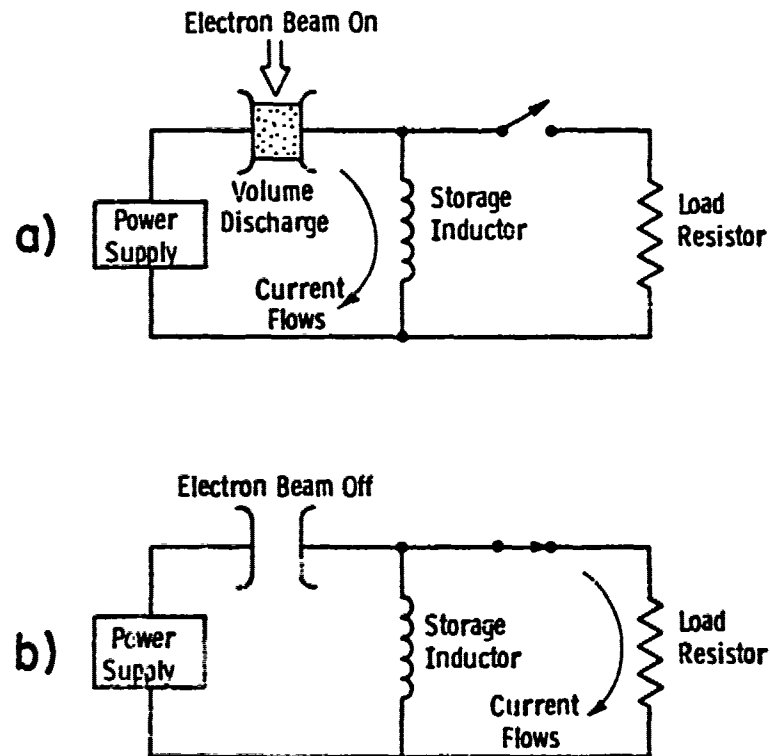


Fig. 1. Schematic Diagram of Electron Beam Switch Operation.

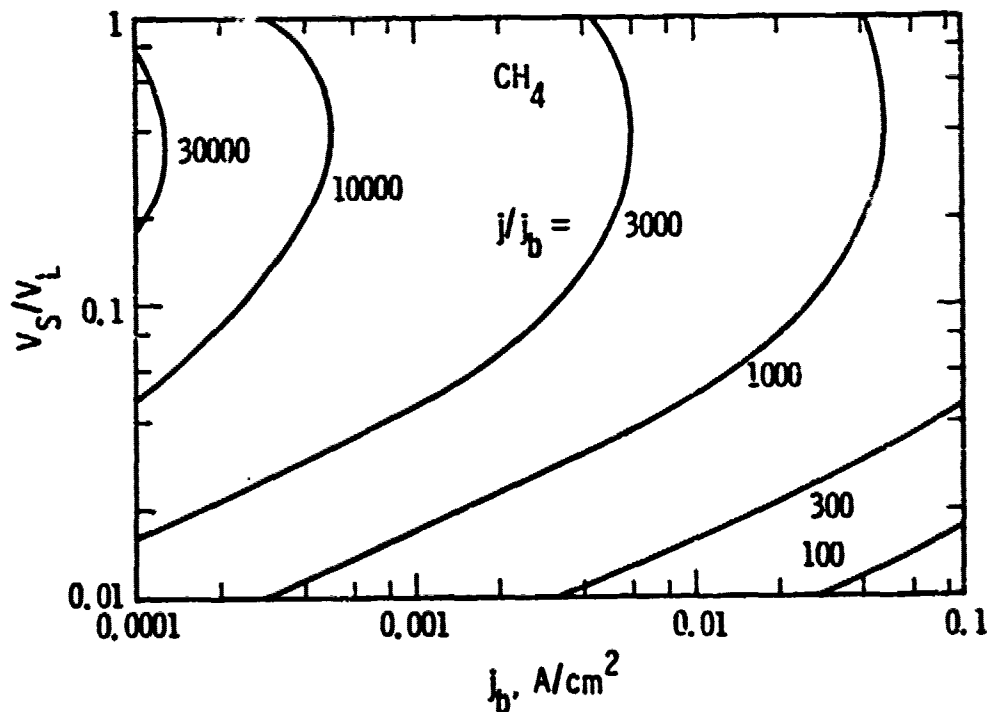


Fig. 2. Switch Current Gain in Methane.

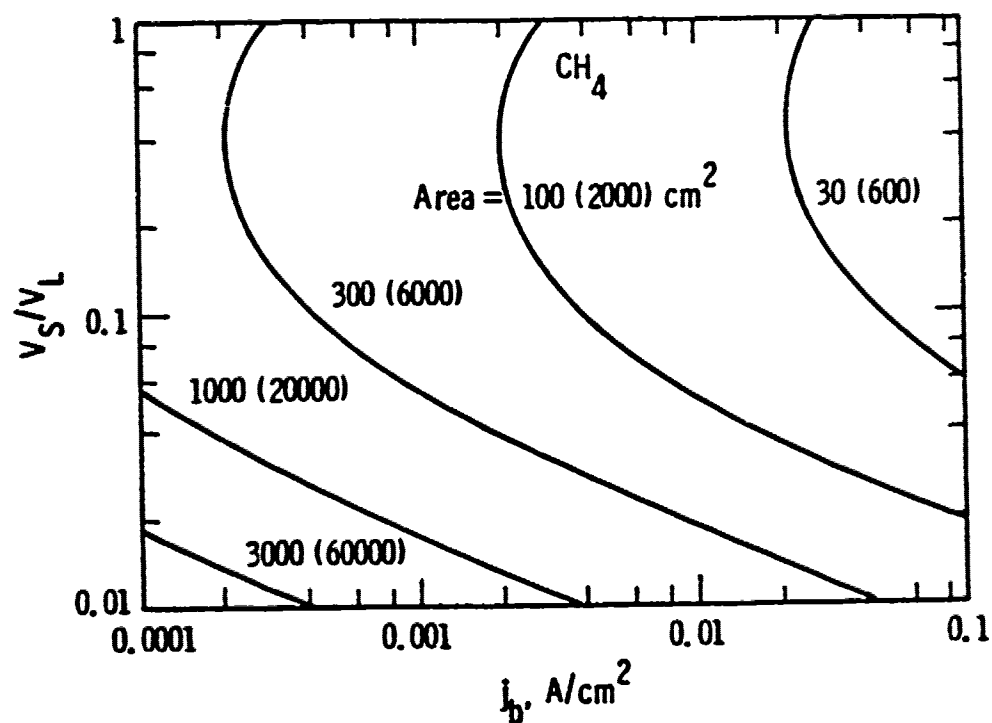


Fig. 3. Switch Areas in Methane. Areas for 1 kA are Given Next to the Curves. Areas in Parenthesis are for 20 kA.

SWITCHING EXPERIMENTS WITH A SMALL E-BEAM

P. Bletzinger

Aero Propulsion Laboratory, WPAFB, OH

ABSTRACT

Experiments with a small E-beam system verified theoretical predictions of the influence of E-beam current density, recombination and attachment coefficients on switch current gain, rise and fall-times. With argon as a switch gas, a new high-conductance regime was discovered, which may be the result of cathode sheath effects.

A. INTRODUCTION

Since the first application of E-beam ionized discharges as controlled on-off switches [1], [2], some further theoretical modelling has delineated more practical parameter ranges which would allow switch currents to be controlled by E-beam currents a factor of at least 1000 smaller [3]. This high current gain would make the application of such devices much more attractive. While the model by L. Kline [3] describes switch performance accurately in terms of the continuity equation for electrons and ions, using computed E/N (Electric Field/Neutral Density) dependent materials coefficients, a good insight into switch behavior can already be obtained using the simpler equations derived by Douglas-Hamilton [4]. From his approximations for recombination dominated or attaching discharges the influence of electron-beam current densities and attachment and recombination coefficients on discharge current density as well as discharge rise and fall times can be estimated. In particular, while for a recombination dominated discharge the current gain $j_{\text{switch}}/j_{\text{beam}}$ is proportional to $\sqrt{1/j_{\text{beam}}}$ [1], an increase in j_{beam} will shorten switch current risetime. The selection of a gas with higher recombination coefficient will shorten both rise and fall time and the addition of an attaching gas has the same effect, while also considerably decreasing the switch conductivity and current gain. This is demonstrated in Fig. 1 where the electron densities cal-

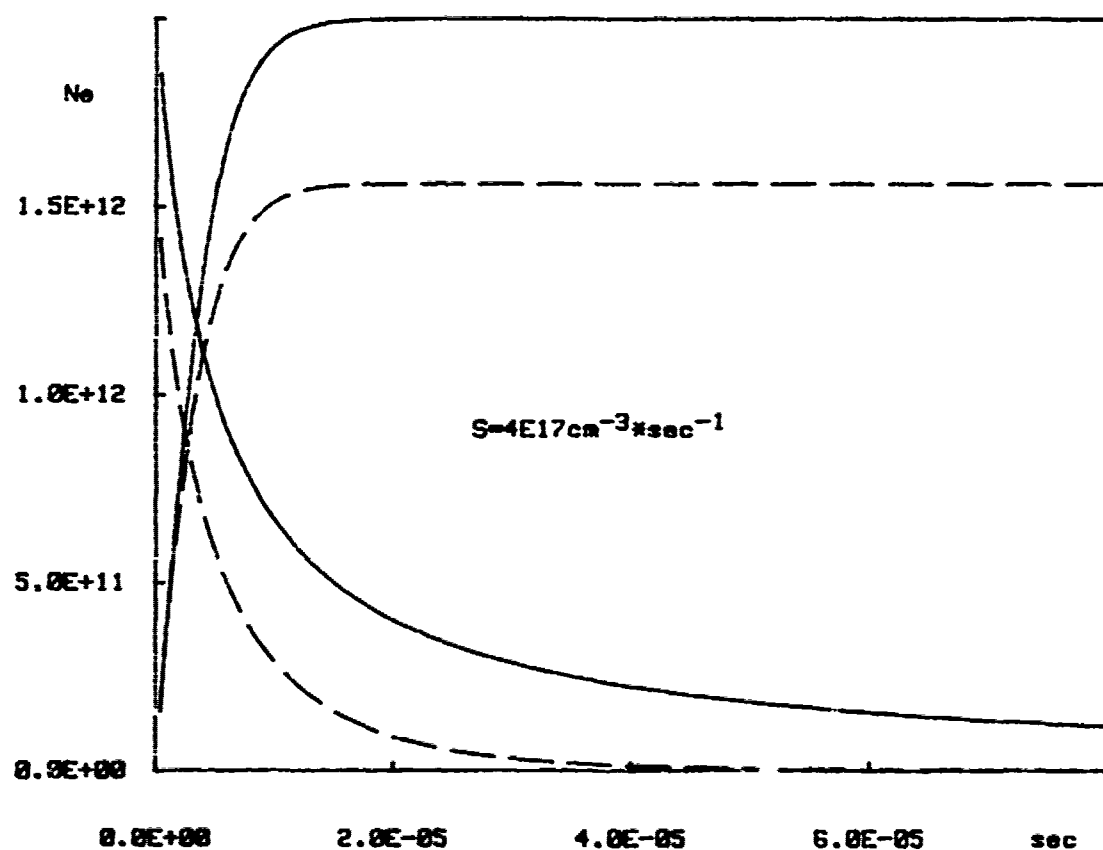
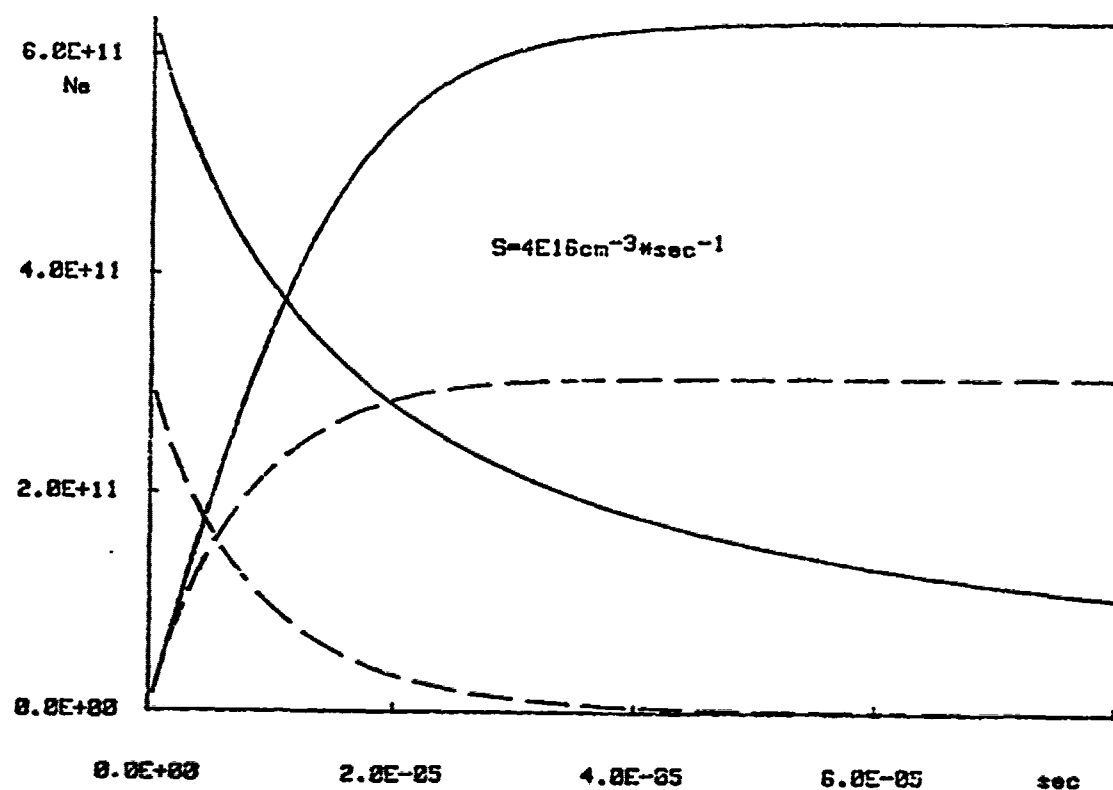


Fig 1: Rise and fall times of electron densities (cm^{-3}) with different electron-beam current densities.

culated using these equations are shown for a gas with recombination only (solid lines) and recombination and attachment (dashed lines) both for switch-on and switch-off and for two source (E-beam current) terms. The recombination coefficient for these curves was assumed to be $1.10^{-7} \text{ cm}^3 \text{ sec}^{-1}$, the attachment frequency 1.10^5 sec^{-1} . Under actual switch conditions, both coefficients can vary over a wide range during the switch-on and switch-off phase.

These relations have been tested using a small, low current density E-beam system connected to a closed-cycle flowing gas loop.

B. EXPERIMENTAL

The E-beam, a commercial unit [5], had a CW total current up to 10mA and pulsed currents up to 400mA at a wide range of pulse widths with rise and fall times of approximately 1 μs . These currents were measured before the foil and currents into the discharge were less than 50% of the input current, over an area of 75cm^2 and at energies of 175KeV. The discharge section had 2 electrodes, the grounded electrode close to the foil having a grid structure collinear with the foil-support structure, the insulated electrode was moveable such that the electrode spacing could be adjusted from 0 to more than 3cm spacing. The discharge section formed part of a stainless steel high vacuum flow-loop, its insulation consisted of machineable glass ceramic and the chamber walls were insulated with a quartz lining. All materials used conformed to ultra-high vacuum standards allowing a base pressure in the system as low as 10^{-9} Torr after prolonged baking. The gas was pumped through the loop with a vane-axial fan with external motor, allowing variable gas flow speeds to more than 10m/sec. A heat exchanger allowed prolonged switch or discharge operation. The switch circuit consisted of a 1 $\mu\text{F}/30\text{KV}$ storage capacitor connected to the solid (cathode) electrode via a 40 ohm copper-sulfate load resistor and being charged by 5 to 30KV power supplies. The pulse repetition rate was limited primarily by the thermal

characteristics of the load resistor.

C. RESULTS

The influence of E-beam current on rise-time is shown in Fig. 2. As the E-beam current (i.e. current into the foil) is raised from 20mA to 400mA, the risetime decreases from more than 20 μ s to about 1 μ s. The peak current for the 20mA E-beam current is more than 15A (limited by the risetime of the switch current) and if we assume a 50% E-beam transmission then the current gain I_{sw}/I_B is well over 1500. As the E-beam current is increased, the current gain decreases, however in this case the maximum current is limited by the I \cdot R drop on the load resistor. Since nitrogen is a non-attaching gas, the fall time is strictly controlled by the recombination rate of nitrogen, is independent of E-beam current, and is in the range of the fall times measured by Douglas-Hamilton [4]. Note that in our case the applied field and therefore the E/N of the discharge varies over a wide range, therefore also the recombination rate can vary during the fall of the switch current. In Fig. 3 the pulse-width was increased to 100 μ s, at an E-beam current of 400mA. The voltage waveform (inverted, 0 volts at the first division from the top) shows that at such large E-beam currents the voltage drop even in nitrogen can be as low as 1000 volts. During this long pulse the capacitor voltage drops, resulting in a decrease of switch current and voltage drop. Using argon as switch gas (Fig. 4), the decay is again dominated by the recombination rate. The rising portion of the switch pulse at large E-beam currents shows some over-shoot, which may be caused by boundary effects, to be discussed later. An example of the effect of an added gas with attachment is shown in Fig. 5. Rise and fall times (at E-beam currents of 200mA) are now in the order of 1-2 μ s. The current during conduction, at the same E-beam current, was reduced from 14A to 9A. Another well known attaching gas, with a considerably larger attachment cross-section, is SF₆. Fig. 6 shows that .02 Torr of SF₆ has about the same effect as 1 Torr of O₂, the current in this case being reduced to

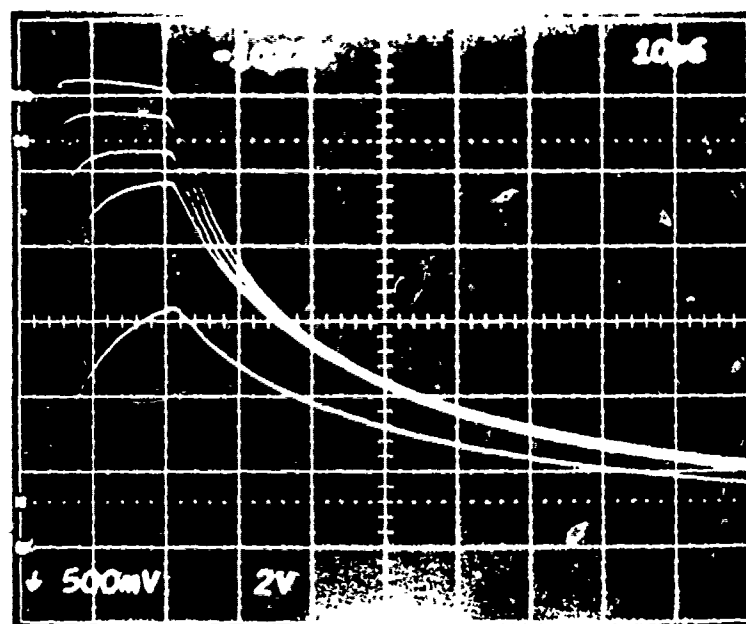


Fig 2: Measured sustainer (switch) currents in 760 Torr N_2 at different E-beam currents. (5 A/vertical division).

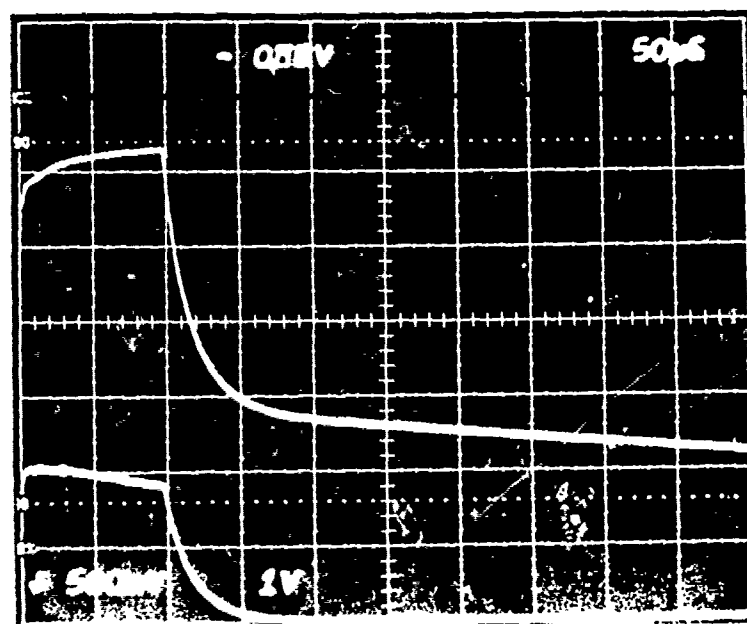


Fig. 3: Sustainer (switch) current and voltage in 760 Torr N_2 . (Upper trace: 1kV/div. Lower trace: 5A/div.)

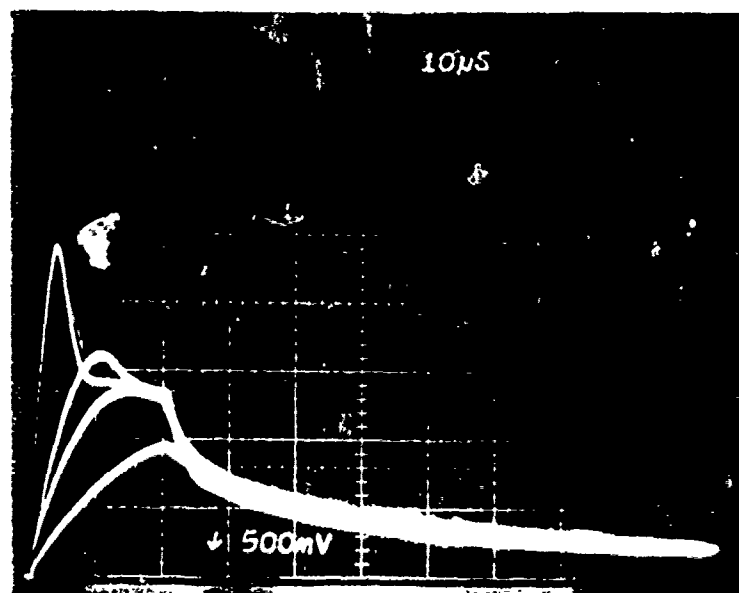


Fig. 4: Sustainer (switch) current in 760 Torr Argon with various E-beam currents. (5A/vertical division).

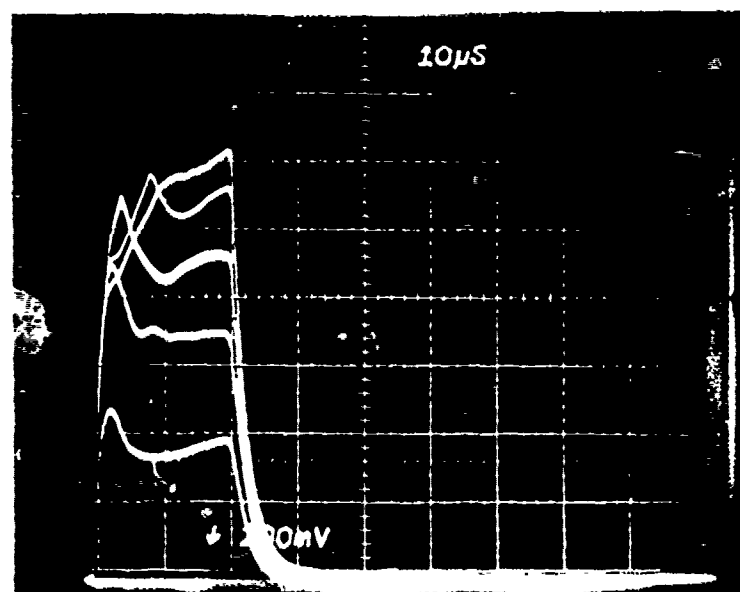


Fig. 5: Sustainer (switch) current in 760 Torr Argon with 1 Torr of oxygen added at various switch voltages. (2A/div).

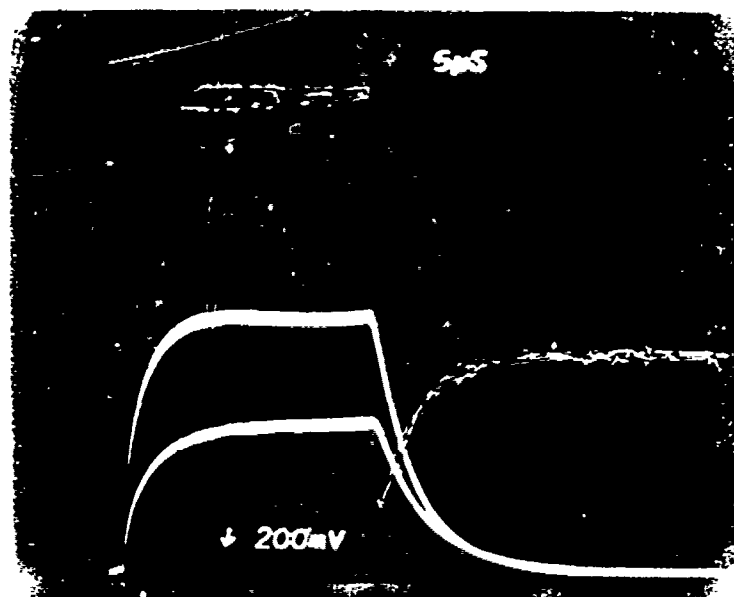


Fig. 6: Sustainer (switch) current in 760 Torr Argon with 0.02 Torr SF_6 added. (2A/div.)

7.5A. Unfortunately, this small amount of SF_6 disappeared after a few discharges, presumably by dissociation and subsequent absorption to the walls. Use of SF_6 therefore would probably require preconditioning of the discharge vessel, similar to the procedures used for sealed-off rare gas halide lasers.

Theoretical analysis of E-beam ionized discharges usually proceeds using a one-dimensional continuity equation with the E-beam generated electrons and ions as source terms and the loss terms taking account of recombination and attachment. Diffusion losses can be neglected at the high pressures and large discharge dimensions used. Since conduction by electrons predominates, one then can use the electron densities obtained and compute the switch current from the product of electron density with the electron drift velocity. The I-V characteristic of such a discharge would be a slowly rising current at increasing discharge voltage,

since for a gas like Ar, for example, recombination losses decrease and the drift velocity increases as a function of the applied electric field. As shown in Fig. 7, for the case of a CW low current discharge, such a characteristic is indeed observed for voltages below approximately 600V (for the electrode distance selected). As the voltage is increased beyond 600V however, the discharge switches over to a different regime with much lower resistance of about 10-20 Ohm. While this characteristic is very similar to a breakdown into a self-ionized discharge, this discharge is both still diffuse and also still completely under the control of the external ionization of the E-beam. Characteristics at higher currents have to be measured under pulsed conditions, shown in Fig. 8. The uppermost values of the currents are also the limits of the current for the corresponding E-beam current. At higher voltages, the I-V curves rapidly decrease their slope to an essentially current limiting characteristic. If an attaching gas is added, this decrease in slope occurs at much lower currents, as indicated in Fig. 8 for the addition of 1 Torr of O_2 . An explanation for this high conductivity regime may be provided by the theoretical analysis of Lowke and Davies [6] who have included the effects of additional ionization in the cathode sheath. As shown in Fig. 9, this additional source of charge carriers will result in a region of increased conductivity. The experimental results, plotted on the same scale, can be compared with the theoretical curve, specifically the slopes of the low-voltage portions of the experimental curves correspond to the slope of the theoretical curve without ionization. The magnitudes of this portion of the I-V characteristic are different because the electric field assumed by Lowke and Davies is much larger (smaller spacing between anode and cathode) than in our experiment. This results in a correspondingly higher drift velocity and conductivity, even though the source functions (E-beam current

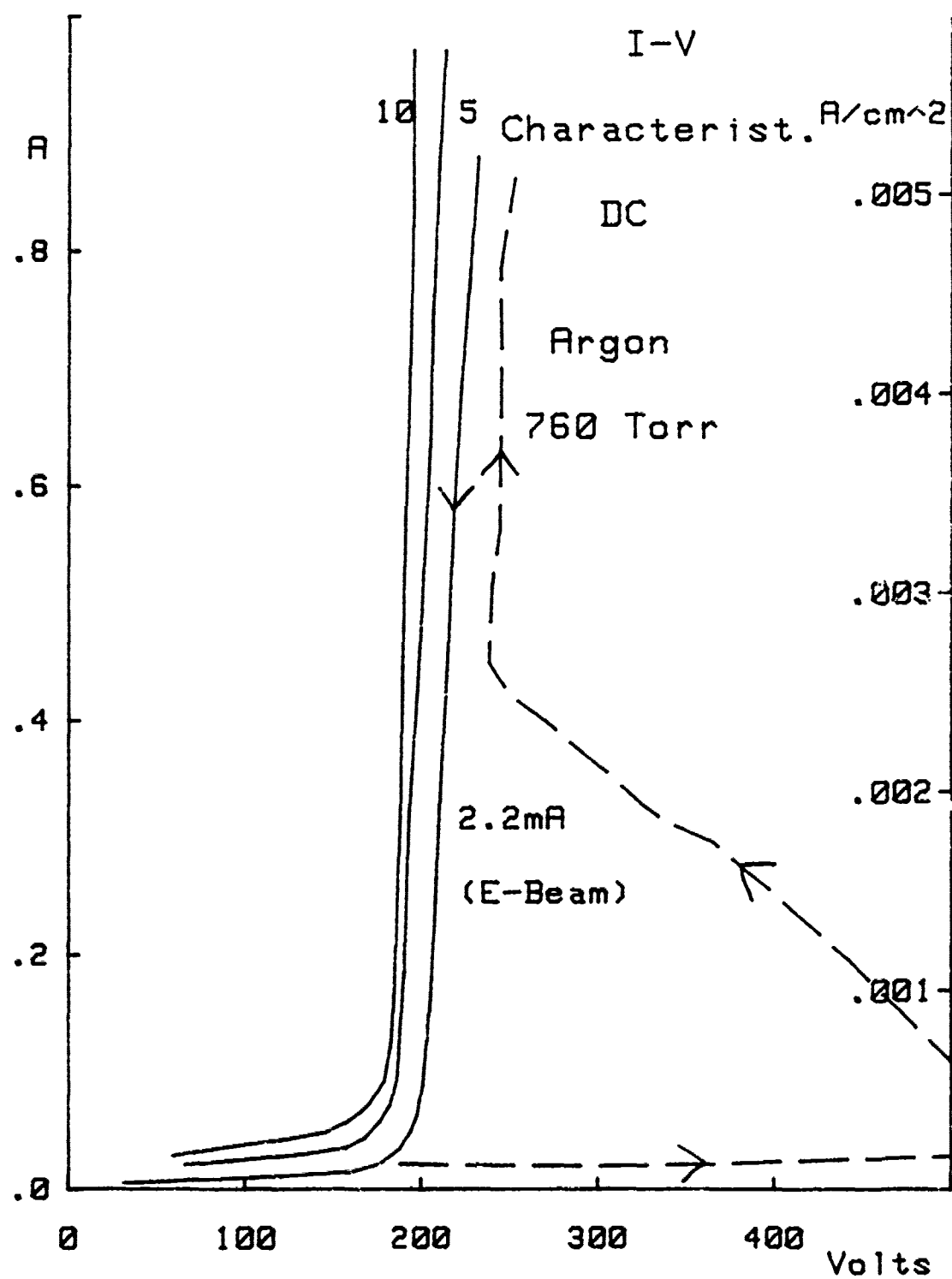


Fig. 7: I-V curves of E-beam ionized switch in 760 Torr Argon (CW).

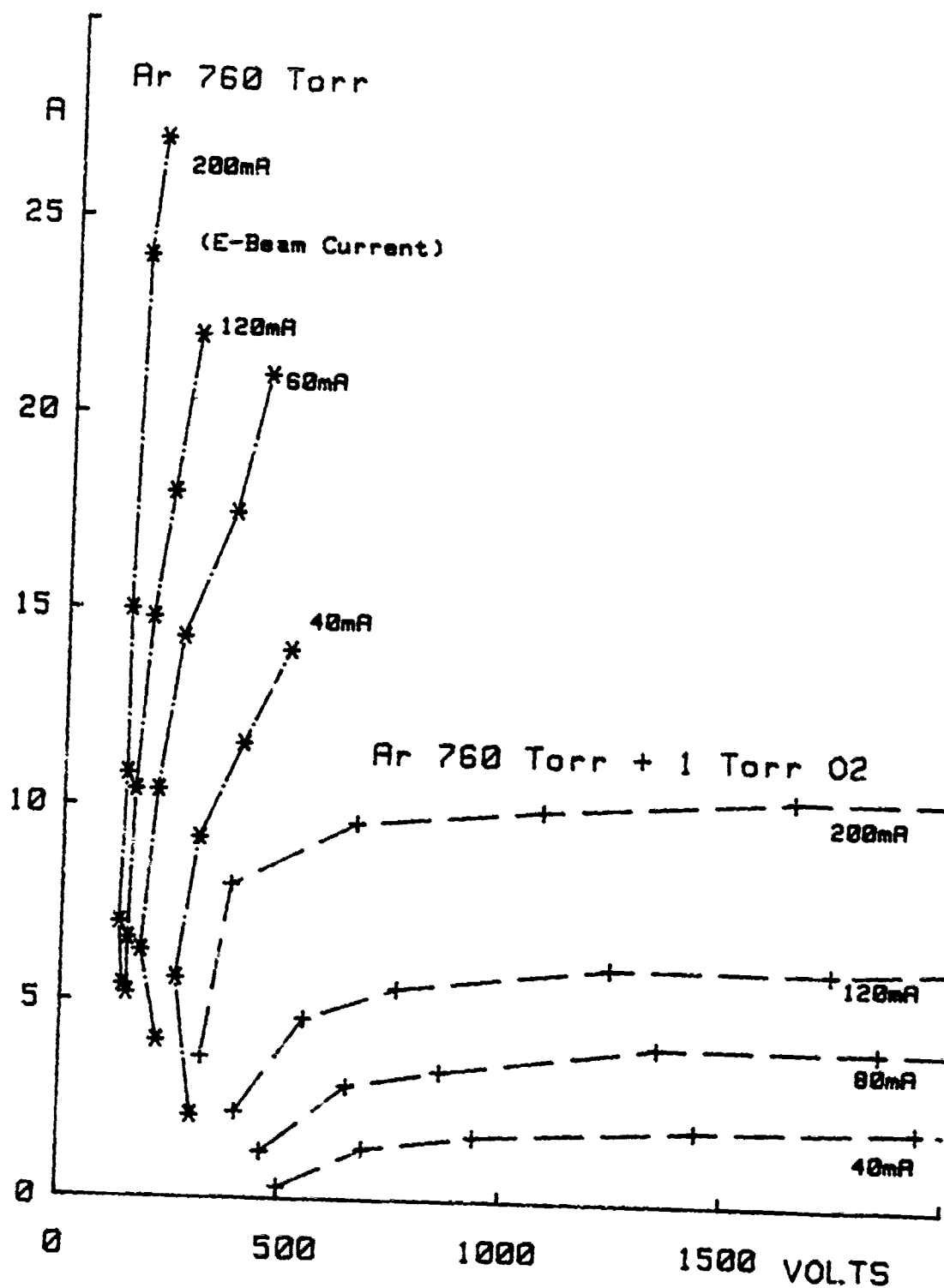


Fig. 8: I-V curves of E-beam ionized switch in 760 Torr Argon and Argon plus 1 Torr of oxygen (pulsed).

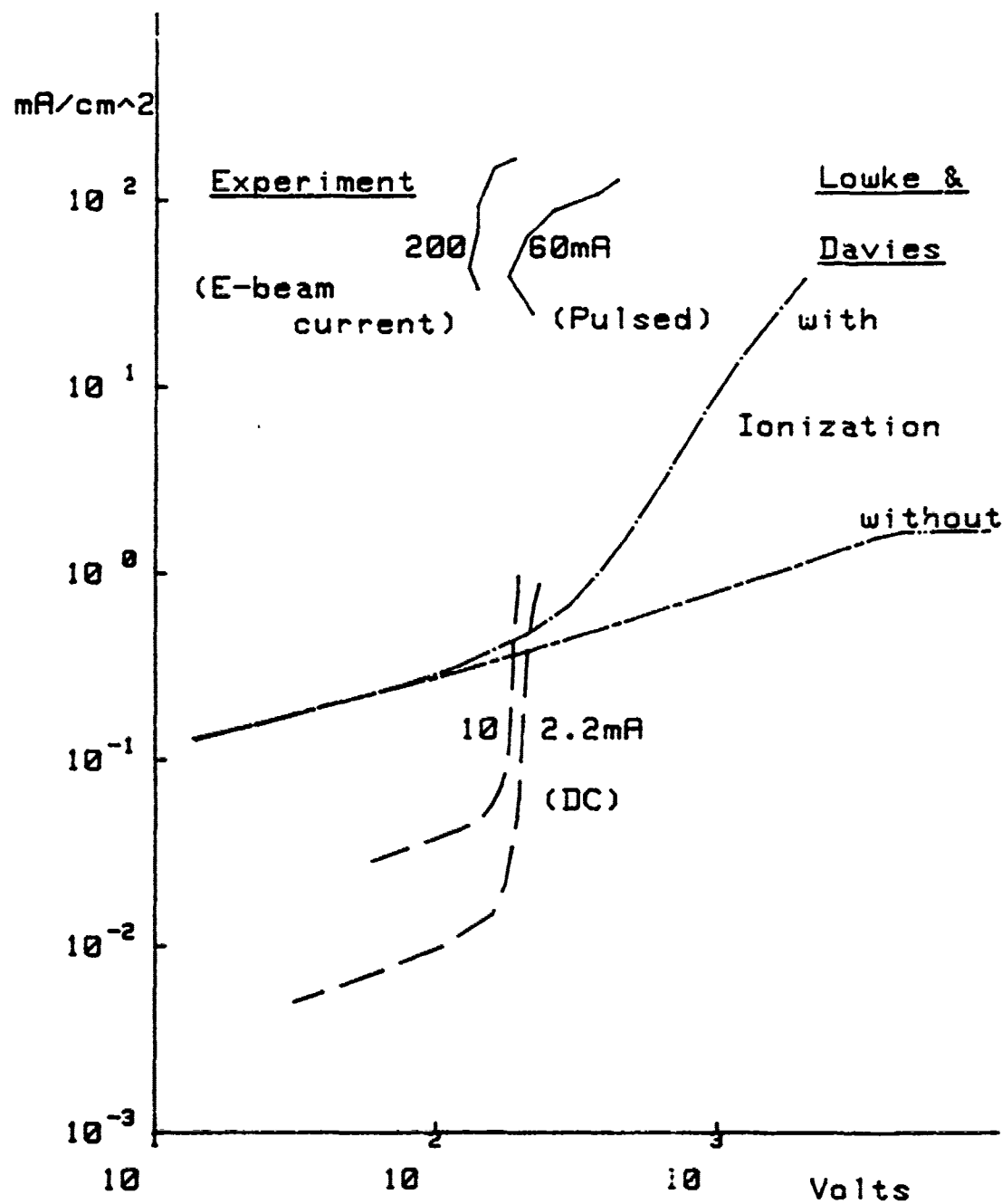


Fig. 9: Comparison of experimental I-V curves with theoretical curves of Lowke and Davies.

densities) are similar for both cases. In the portion of the characteristics where conductivity is enhanced by ionization in the cathode sheath, the experimental results have a much higher conductivity. This may be caused by additional 2-step ionization processes in argon and also secondary cathode emission, both not considered in the theoretical analysis. As mentioned above, the electric fields used in the theoretical analysis are higher, therefore also the onset of the theoretical high conductivity region is shifted towards the lower voltages. The effect of additional ionization in Argon is quite dramatic. This is illustrated in Fig. 10, where the discharge voltage at variable cathode-anode spacings is shown to have a very low slope. As is to be expected, the voltage gradient is a function of both the E-beam and the switch current. The intercept at 0 distance, which indicates the voltage drop across the cathode sheath, is much less than 200 volts. The voltage gradient in the discharge volume is as low as a few volts/cm, which means that the cathode-anode spacing can be extended with little increase of the voltage across the discharge. A limit to such an increase in spacing would be the range of the primary electron beam.

D. SUMMARY AND CONCLUSION

It has been shown that in the limit of low electron-beam current densities current gains of well over 10^3 can be achieved even in gases with non-optimum drift velocities, such as nitrogen and argon. Both investigated gases have low recombination rates, even at the low E/N ranges used in the experiment. This results in rise and fall times which may be too slow for some applications. Addition of small amounts of attaching gases has been shown to decrease the transition times to 1-2 microseconds, at the expense of switch gain and conductivity. Risetime and conductivity also can be improved by increasing the E-beam current, at the expense of current gain. For Argon as a switch gas, a higher

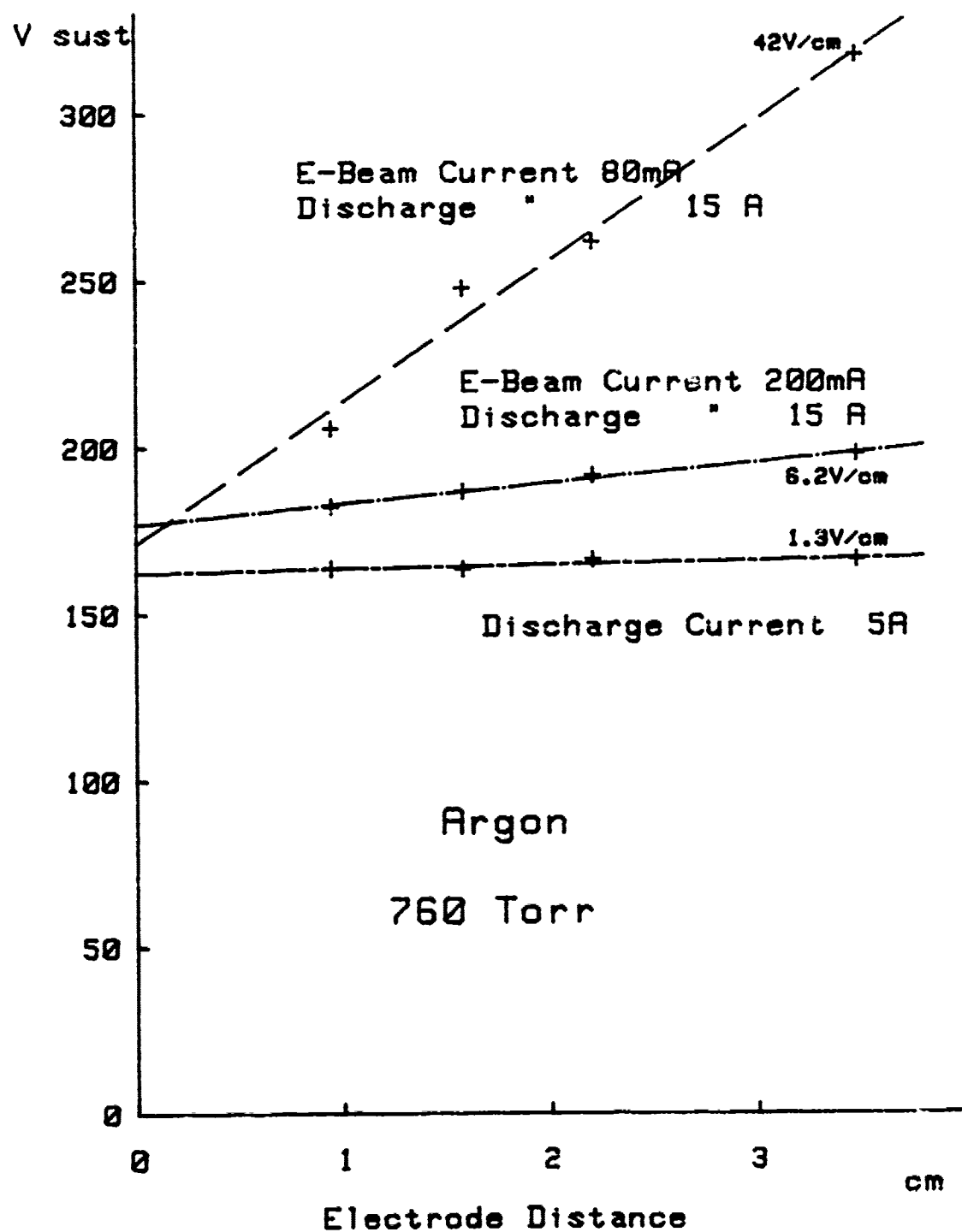


Fig. 10: Discharge voltage versus electrode spacing.

conductance regime has been found which is probably generated by additional ionization in a cathode sheath. The E-beam controlled switch has been shown to operate over a wide parameter range, from DC to $1\mu\text{s}$ rise/fall time pulses and under repetitive conditions. The high conductive regime established for Argon may be extended to other gases or gas mixtures with better dielectric and drift velocity characteristics. This would result in a considerable reduction of the power dissipated in the switch, leading to much increased power-handling capabilities. Among the problem areas still to be investigated are plasma instabilities at high currents and post-discharge breakdowns, which may limit the power-and or voltage handling capabilities.

E. REFERENCES

- [1]. B.M. Koval'chuk, Yu.D. Korolev, V.V. Kremnev and G.A. Mesyats "The Injection Thyatron-a Completely Controlled Ion Device," Sov. Radio Eng. & Electron Phys. 21, 1513 (1976).
- [2]. R.O. Hunter "Electron Beam Controlled Switching," Proc. IEEE Int. Pulse Power Conf., paper IC8-1 (1976); U.S. Patent 4, 063, 130.
- [3]. J.W. Dzimianski and L.R. Kline "High Voltage Switch Using Externally Ionized Plasmas," AFWAL-TR-80-2041, April 1980.
- [4]. D.H. Douglas-Hamilton "Recombination Rate Measurements in Nitrogen," J. Chem. Phys. 58, 4820 (1973).
- [5]. Energy Sciences, Bedford, Massachusetts.
- [6]. J.J. Lowke and D.K. Davies " Properties of Electric Discharges Sustained by a Uniform Source of Ionization," J. Appl. Phys. 48, 4991 (1977).

Opening Switch using Spoiled Electrostatic Confinement

Igor Alexeff, Professor of
Electrical Engineering
University of Tennessee

Abstract

The opening switch using spoiled electrostatic confinement can both close and open a high voltage, current-carrying circuit. In addition, these operations can be done repetitively at a frequency exceeding a kilohertz. The device appears to be both simple to construct and rugged in design.

Introduction

The basic principle of operation of this device is most easily understood in terms of the Paschen minimum.¹ As shown in Fig. 1, the breakdown voltage of a gas-filled diode exhibits a minimum as gas pressure is increased from low values. At low pressure, the voltage is high because an average electron crosses the anode-cathode gap without colliding with a gas atom, and establishing a conducting plasma is difficult.

At high gas pressure, the average electron suffers so many collisions in crossing the anode-cathode gap, that it never gets enough energy to ionize a gas atom, and producing a conducting plasma is difficult.

Only at some intermediate pressure, at which the average electron

¹James D. Cobine, Gaseous Conductors, (Dover, New York, 1958) p. 164.

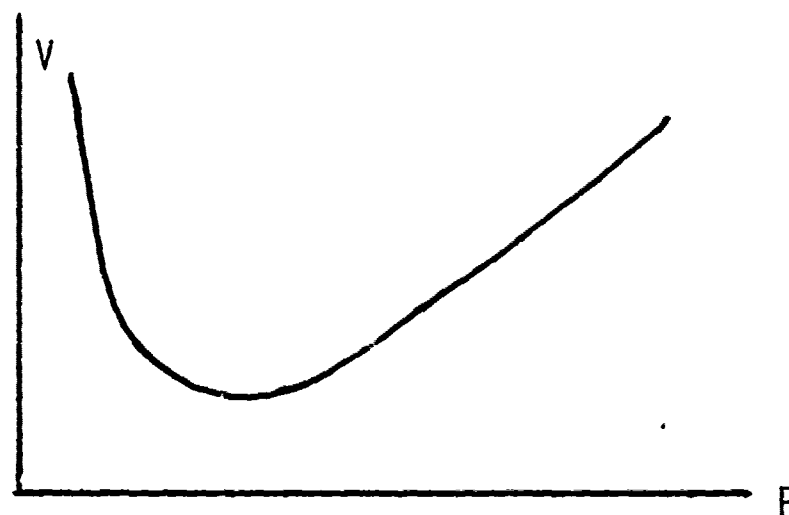


Fig. 1 Paschen Curve

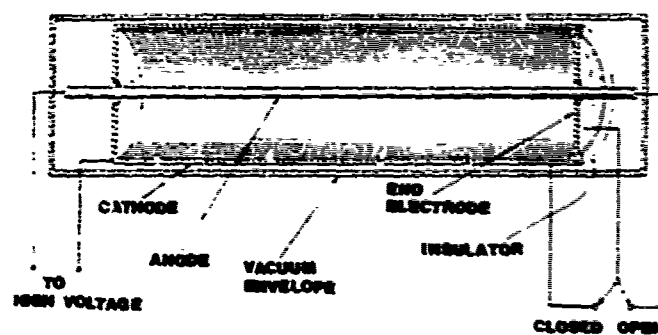


Fig. 2 Schematic of opening switch

both has many collisions with gas atoms, and yet also reaches ionization energy, is the ignition and sustaining discharge voltage at a minimum. This minimum in voltage is the Paschen minimum.

To operate this gas diode as a switch, the gas pressure is reduced far below that of the Paschen minimum. Thus, the diode requires an abnormally high voltage to initiate a discharge, and at its regular operating voltage, is nonconducting-that is, open.

To close the switch, some method of increasing the mean free path of the electron is used to increase the probability of ionization. In effect, the operating point of the diode is moved to the Paschen minimum, and the tube ignites. In the Hughes switch², for example, electrons moving radially in a cylindrical geometry are trapped by an externally applied axial magnetic field to ignite the discharge. The initial electrons are provided either by natural radioactivity and cosmic rays, or by a supplementary discharge. The device characteristically ignites when a plasma forms. This time corresponds to about 10 e-folds in the formation of an electron avalanche, which generally is about 10 microseconds.

The remarkable opening property of these diodes appears when the supplementary electron confinement is removed. The discharge now is occurring in the high vacuum region where it cannot sustain itself. The discharge now extinguishes itself in a time characteristic of the plasma ion loss time from the system. This is characteristically about 5 times the flight time of an average plasma ion to the wall-about 10 microseconds. In the Hughes diode, removing the applied axial magnetic field opens the switch.

²H. Gallagher, C. Hoffmann and M. Lutz, IEEE Trans. Power App. Sys., vol. PAS P. 702, Mar/Apr. 1973.

In the opening switch using spoiled electrostatic confinement, no magnetic field is required. The basic principle of operation is shown in Fig. 2. The basic operating principle was discovered by McClure³. If a wire is charged positively, a random electron will be attracted to it. However, a random electron generally possesses some initial kinetic energy, so this electron will miss the wire, and go into orbit around it. Hence, the electron is trapped radially.

If negatively-biased end plates are added to the system, a radially-trapped electron approaching an end plate will be repelled. The confinement principle resembles the charged particle confinement in a magnetic-mirror machine. McClure demonstrated that such a geometry sustained a discharge at a pressure far below the Paschen minimum³.

If one of the end plates is switched from negative (wall potential) to positive (anode potential), the orbiting electrons escape to this plate.⁴ Experience shows that the discharge then cannot be maintained, and it spontaneously extinguishes. The time constant of the extinguishing process is expected to be on the order of ion escape time to the wall, but this has not yet been measured.

If the end electrode is again made negative, the discharge commences with a random electron entering the system. An avalanche of gas-produced electrons orbiting the wire is then formed. We would expect on the order of 10 e-folds to result in an orbiting electron cloud and switch breakdown, and this time is approximately observed experimentally. Also the time grows shorter as the gas pressure is increased.

³G. W. McClure, Appl. Phys. Lett. 2, p. 233, 1963.

⁴Igor Alexeff and Fred Dyer, IEEE Trans Plasma Sci. PS-8, P. 163, 1980

In our prototype switch, breakdown results in a "closed" voltage of about 500 volts. The open voltage is limited by external arc-over of the insulators in air, and is greater than 10^4 volts. The repetition rate has been as high as 1000 Hz. The escape of plasma ions and the influx of returning gas atoms are the time-determining factors, and the upper-frequency limit has not yet been explored. At present, only a few amperes have been interrupted, but we do not at present see any basic upper limitation to the current-carrying capability. The current to the switched end plate was about 5% of the main discharge current.

The orbits of electrons around the central electrode have been computed for the two-dimensional (infinite wire) case⁵, and the result is that only a little residual kinetic energy results in a narrow but closed orbit. Thus, theoretically, the discharge should be easy to establish. A three-dimensional study, including collective effects, is yet to be done.

One unusual experimental result is that this switch also acts as a free-electron maser if the positive central wire is surrounded by a high-Q cavity resonator.⁶ We have produced intense microwave radiation from $\lambda = 3$ cm to $\lambda = 4$ mm, with the limits being given by the diagnostics available, as we apparently can control microwave radiation by changing the cavity resonator Q, the gas pressure, or the wire diameter. However, one should be aware of the possibility of microwave emission with resulting hazards to nearby electronic circuits.

Concerning further progress on the switch, we feel that at present,

⁵R. H. Hooverman, Journal of Applied Physics. 14, 3505 (1963).

⁶Igor Alexeff and Fred Dyer, Phys. Rev. Letters 45, 351 (1980).

larger models should be constructed, and be operated at higher voltages and currents. A capacitor should provide the high current, and a series capacitor-inductor, the high voltage and current. In this manner, the physical limitations of the switch, and related scientific problems connected with it, should become obvious.

Future prospects for such a switch appear good, as the basic operating principle is simple and well-known, nondestructive, and rapid (no inductors or physically moving mechanical elements are involved). However, further development is needed to explore the limits of the device.

MAGNETOPLASMADYNAMIC AND HALL EFFECT SWITCHING FOR REPETITIVE INTERRUPTION OF INDUCTIVE CIRCUITS

P. J. Turchi
R & D Associates
Arlington, VA.

A. INTRODUCTION

Generally speaking, there are three types of closing/opening switches available: 1) Moving conductor switches - in which contacts are brought together and separated by mechanical and/or kinematic means (for example SF_6 gas-blast circuit breakers, vacuum interrupters, liquid metal plasma valves); 2) Variable conductivity switches - in which various physical processes such as heating, ionization/recombination, or Hall effects alter the conductivity of a region of the circuit (for example, foil or wire fuses, cross-field tubes); 3) Solid-state devices - in which production or depletion of charge carriers in material, and associated electrical potentials are used to control current conduction in a circuit (for example, SCR's thyristors).

The problems and limitations of the various methods indicated above are: 1) Moving conductor switches - slow speed for actuation and rise of hold-off voltage due to mechanical limitations on speed of conductors; 2) Variable conductivity switches - Non-repetitive action because of irreversible destruction of conductor (exploding foil or wire fuses) and large amounts of energy dissipation required to effect conductivity change; 3) Solid-state switches - Low power density, requiring large and expensive systems for many applications of interest.

The Magnetoplasma dynamic Switch

The purpose of the magnetoplasma dynamic switch is to provide a combination closing and opening switch for inductive energy storage systems. The need is for a switch that a) will close on command, providing a low impedance current

conduction path parallel to a relatively slow current interrupter, such as a mechanical circuit breaker; and b) then will be able to open, diverting current into a parallel circuit involving either a useful load or further switching. Typical values of interest are:

Closing Times		Tens of μsec
Closing Voltages	~	Tens of kilovolts
Conduction Times		
After Closure	>	100 μsec
Currents	~	Hundreds of kiloamps
Opening Times	<	10 μsec
Opening Voltages	>	Hundreds of kilovolts

Description and Operation

The basic ingredient of the magnetoplasdynamic switch is the novel use of a controlled high speed plasma flow to create a current conduction path which can then be opened quickly by interruption of the plasma flow. With plasma flow speeds of several cm/ μsec created by a magnetoplasdynamic arcjet, the timescales for closing and opening gaps of several tens of centimeters will be a few microseconds which is orders of magnitude faster than mechanical switches (limited to speeds of less than several mm/ μsec).

The basic system is shown schematically in Fig. 1. An inductive store (1) carries current by means of conduction through an initially closed switch (2). In parallel with switch (2) is the magnetoplasdynamic switch (3), consisting of a magnetoplasdynamic arcjet-type plasma source (3a), triggered by a capacitor bank (3b), and a pair of electrodes (3c) and (3d). The capacitor bank (3b) is connected to the plasma source (3a) by a closing switch (4) (of standard design) so that a plasma stream is created between electrodes (3c) and (3d). The capacitor bank parameters are chosen so that the plasma source current will equal the current in the inductive store at the time when switch (2) is opened (switch (2) could be a mechanical breaker or explosive switch). Switch (2) is opened after the plasma flow is established

MAGNETOPLASMADYNAMIC SWITCH

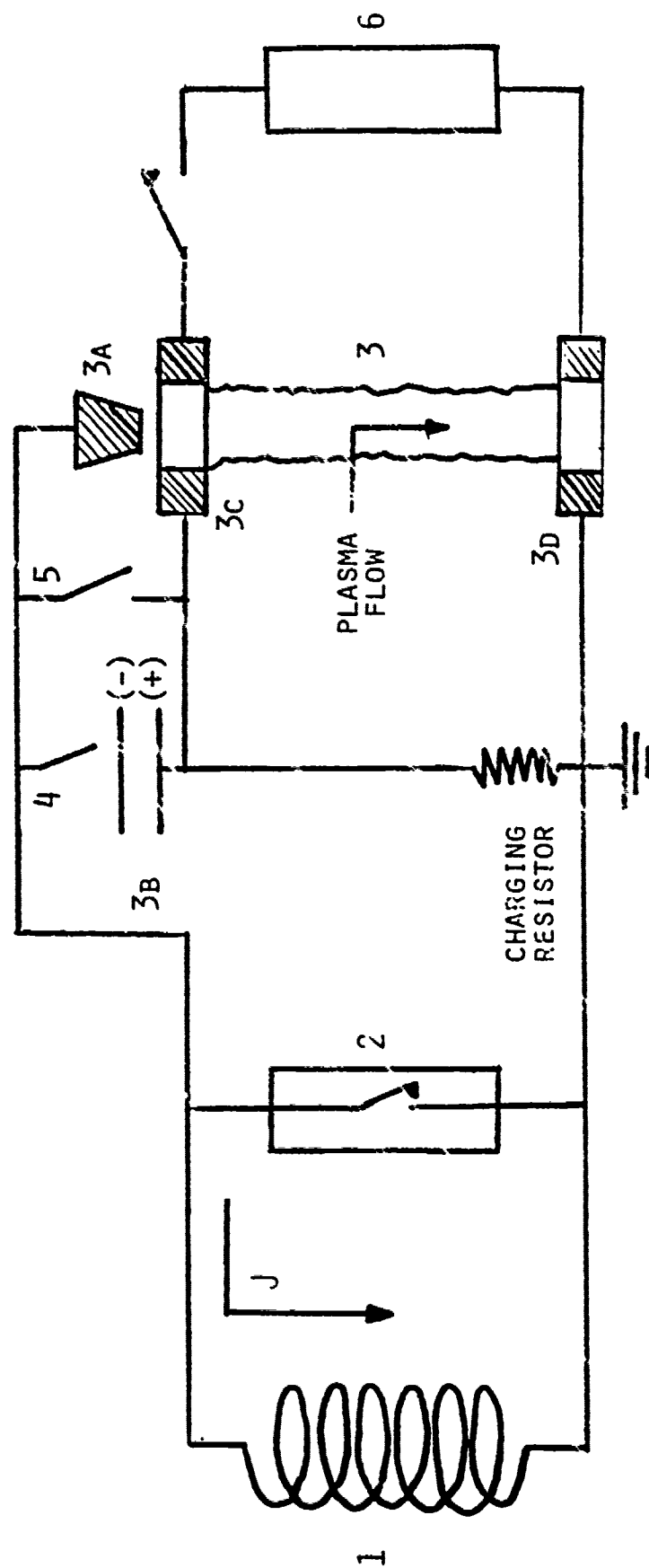


Fig. 1

between electrodes (3c) and (3d). The voltage generated across switch (2) by its opening commutates the inductive store circuit current into the magnetoplasma dynamic switch which will then conduct current sufficiently long for the voltage holdoff strength of switch (2) to reach a satisfactory level. Another switch (5) in close electrical proximity to the plasma source is then closed providing a low impedance conduction path in parallel to the plasma source current. The current in the plasma source will then decay on a time approximately equal to the plasma source inductance divided by its resistance (typically several microseconds).

In order for the plasma flow to be maintained, the thrust of the plasma source must exceed the peak equilibrium centerline-pressure force in the flow due to current conduction between electrodes (3c) and (3d). The thrust of the plasma source is given by $F_s = (\mu/4\pi)J_s^2 K_s$, where J is the current in the plasma source and K_s is a constant (approximately equal to $\ln r_2/r_1 + 3/4$ for many systems, with r_2/r_1 the ratio of outer to inner conductor radii in the plasma source). The peak centerline-pressure force in the flow due to conduction of current J is $F_c = (\mu/8\pi)J^2$. Thus to maintain the plasma flow

$$J_s > J/(2K_s)^{1/2}$$

By the circuit in Fig. 1, initially $J_s = J$ so that the above condition is readily met. After closure of switch (5), however, J_s decays so that, not only does the plasma flow diminish because of diminishing input power, but the pressure of the current conduction in the interelectrode gap further impedes the entrance of flow to the gap. Plasma already in the gap, however, continues to leave at high speed reducing the density of conducting material below that needed for high conductivity, thereby opening the magnetoplasma dynamic switch on the timescale of the gap distance divided by the flow speed. Current is diverted into a parallel

circuit (6), involving either an electrical load or further switching. Reclosing switch (2), opening switches (4) and (5), which are no longer carrying current, and recharging the inductive store (1) and capacitor bank (3b) allows the process described above to be repeated.

Various other techniques are described in the literature for obtaining a quasi-steady plasma flow by magnetic forces. Since these techniques will all tend to behave according to the same thrust density relation with respect to current, substitutions can be made in the design of the plasma source depending on particular applications.

Furthermore, it is not essential to combine electrode (3c) with the plasma source as shown in Fig. 1. Other arrangements may in certain applications be more useful without altering the basic operation of the magnetoplasma-dynamic switch.

The advantages of the magnetoplasma-dynamic switch over other methods are:

- 1) High speed operation due to higher speed conductor motion.
- 2) Higher power density due to convection of dissipated energy.
- 3) Repetitive operation.
- 4) Rugged inexpensive construction.

New features include:

- 1) Use of controlled plasma flow and hydrodynamic cut-off of plasma flow by self-consistent magnetoplasma-dynamic forces.
- 2) Arrangement of circuitry to eliminate high energy auxiliary power sources to drive the magnetoplasma-dynamic switch.
- 3) Combined closing and opening actions in a single unit.

Development of the magnetoplasmadynamic switch requires considerable attention to the quality of the plasma flow, in terms of directionality, and uniformity in time and space. Hurling blobs of plasma in the general direction of two electrodes should not be expected to work in the manner prescribed above. In fact, auxiliary magnetic fields near the electrode surfaces would probably be useful to divert low speed boundary layer plasmas. Relevant research has been conducted on magnetoplasmadynamic flows in repetitively-pulsed arcjets for spacecraft propulsion. The next section discusses repetitive inductive switching to power such arcjets.

Hall Effect Switching For Repetitively Pulsed Arcjets

The use of plasma flows for spacecraft propulsion and satellite maneuvering has been discussed and demonstrated for some time. A basic limitation on the use of electrically-created plasma flows for such thruster applications is the need for electric power suitable for driving plasma thrusters. Steady operation of plasma thrusters at high efficiency requires steady power levels in the megawatt range, which is usually beyond spacecraft capabilities. Repetitive pulsed operation, on the other hand, requires power conditioning to provide high power pulses from low power steady sources. In earth-based laboratory environments, various techniques, such as oil-filled or electrolytic capacitor banks in pulse-forming networks, including triggered spark-gaps, have been used for electric thruster research and development. For spacecraft applications at high power levels and long mission-durations, such laboratory techniques are not satisfactory because of weight limitations and reliability. That is, the principal limitations and/or disadvantages of older methods may be summarized as:

1. High weight and volume for capacitive energy storage.

2. Complexity (therefore low reliability) for repetitive, high voltage spark-gaps and related circuitry for producing a train of high power pulses.

Description and Operation

In the Hall Effect Power Circuit for quasi-steady plasma thrusters, the necessary power pulse to the thruster is created by using Hall-active resistive elements to interrupt the current flow in an inductive energy storage system. Interruption of current flow results in a high voltage pulse which drives the current flow into a circuit leg parallel to the interrupting elements; this new circuit leg contains the thruster so energy is thereby delivered to the plasma thruster flow. The operation of the Hall-active elements as resistive circuit-interrupters depends on the application of high magnetic fields perpendicular to the current flow in the Hall element. The basic Hall element and its current flow are shown in Fig. 2 in a configuration called a Corbino disc. The current flows radially, and a magnetic field is applied axially to increase the effective resistance to radial current flow.

The basic Hall Effect (HE) Power Circuit for plasma thruster ("arcjet") applications is shown in Fig. 3. The Hall element is labelled H , carrying current J from an inductive source (not shown). An important feature of the HE power circuit is the use of the voltage developed across the Hall element to power the excitation field magnet, labelled as inductor L_E , carrying current J_E . In this way, additional cost, weight, and complexity for a separate magnet power supply is avoided. The use of such a "self-excited" circuit also provides an automatic spacing between pulses to the plasma thruster, thereby providing the pulsetrain timing for quasi-steady operation. That is, most of the voltage pulse occurs in the last several per cent of the Hall element switching action, with little voltage developed earlier.

By including a resistor, R_E (not shown) in series with

HALL EFFECT TO CHANGE RESISTANCE

OHM'S LAW:

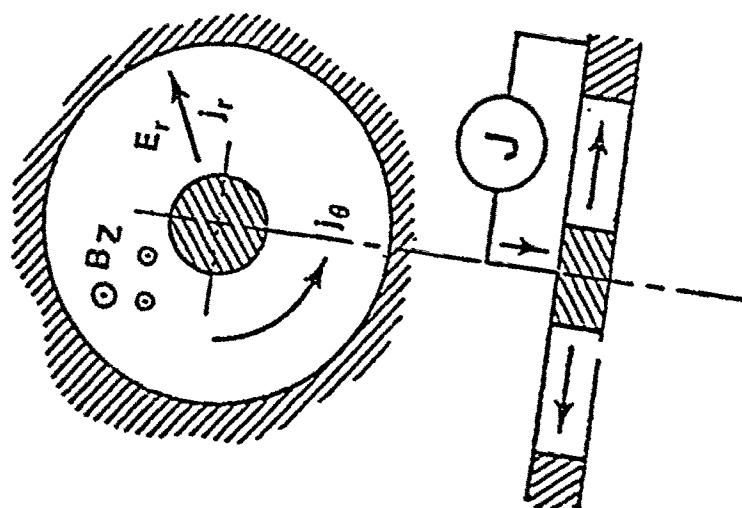
$$\vec{E} = \eta \vec{j} - \vec{u}_e \times \vec{B}$$

IF ONLY N-TYPE CARRIERS,
SO

$$\vec{u}_e = -\vec{j}/ne$$

$$\vec{E} = \eta \vec{j} + \vec{j} \times \vec{B}/ne$$

CORBINO DISC:



$$E_\theta = 0 \quad \vec{B} \approx B \hat{k}$$

$$\eta j_\theta = j_r B/ne$$

$$E_r = \eta j_r + j_\theta B/ne$$

$$= \eta j_r + j_r B^2 / \eta n^2 e^2$$

$$= \eta j_r (1 + K^2 B^2)$$

RESISTANCE:

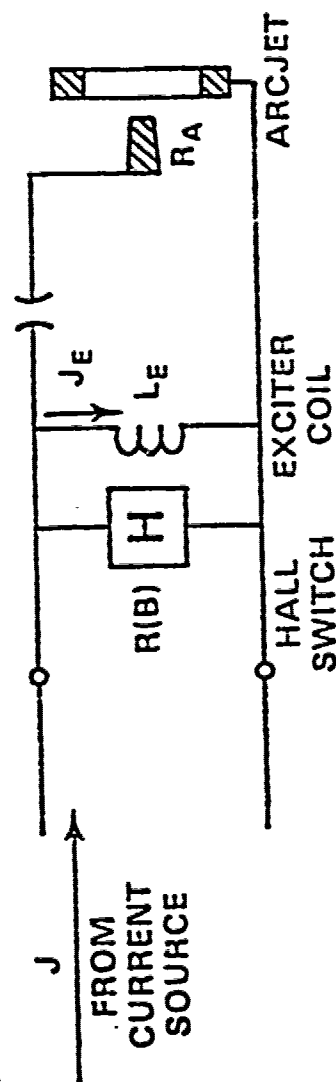
$$R = R_0 (1 + K^2 B^2)$$

Fig. 2

SELF-EXCITED HALL SWITCHING

APPROACH: USE VOLTAGE ACROSS HALL SWITCH TO GENERATE EXCITER FIELD

CIRCUIT (WITHOUT RESISTANCE):



CIRCUIT EQUATION:

$$L_E \frac{dj_E}{dt} = R_0 (1 + C^2 j_E^2) j$$

NORMALIZED:

$$\frac{dj}{d\tau} = (1 + C^2 j^2) \quad \text{WITH } j = j_E/J$$

$$\tau = R_0 t / L_E$$

SOLUTION:

$$j = (Cj)^{-1} \tan Cj\tau$$

$$\tau_f = \frac{j_f}{(\alpha - 1)^{1/2}} \tan^{-1} (\alpha - 1)^{1/2} \quad \text{WHERE } \alpha = R_f / R_0$$

$$= 5.3 \times 10^{-3} \quad \text{FOR } j_f = 0.05 \text{ AND } \alpha = 200$$

10% TO FULL VOLTAGE IN $\Delta\tau = 5.3 \times 10^{-4}$

Fig. 3

the inductor L_E , it is possible to match the peak resistance of the Hall element to the impedance of the arcjet so the output current pulse during quasi-steady arcjet operation will be nearly constant (as required for quasi-steady operation). Some of this series resistance is provided automatically by the magnet winding associated with inductance L_E . An example of circuit values for quasi-steady plasma thruster applications is given in Table I. A sketch of a self-excited Hall switch which corresponds to the circuit operation for Table I is provided in Fig. 4. (Actual geometries for the Hall element and excitation magnet will depend on specific application requirements; in particular, heat transfer and rejection in space environments will probably require an array of Hall elements rather than a single unit as sketched.)

To provide for rapid cut-off of current to the arcjet at the end of the prescribed current pulse, it is useful to reduce the excitation field on the Hall element quickly. This can be done using additional Hall elements in series with the excitation magnet (L_E) as shown in Fig. 5. Such auxiliary Hall switching would be externally excited (using either mechanically-displaced permanent magnets or small capacitor-driven coils). Also shown in Fig. 5 is a low voltage, high current contactor in parallel with the main Hall element, which can be used to extend the time separation between power pulses and/or reduce the dissipation in the Hall element between power pulses.

The operation of the circuit shown in Fig. 5 is the following. With $J_E = 0$, the contactor is opened while shunted by the magnetic field-free Hall switch, H, hereby avoiding significant arcing at the contacts. The resistance of the Hall switch begins to drive currents J_E through the excitation coil L_E , thereby increasing the resistance of the Hall switch and the rate of increase of J_E . In the last several per cent of this self-excited

EXAMPLE OF SELF-EXCITED HALL SWITCH

CIRCUIT
PARAMETERS: $\zeta = 500$ $j_f = 0.05$ $\alpha = 200$ $Q = 21.9$

ARCJET
PARAMETER: $I_A = 8 \text{ mA}$ $J_A = 25 \text{ kA}$ $V_A = 200 \text{ V}$

DERIVED
CIRCUIT
VALUES:

$R_o = 0.28 \text{ m}\Omega$	$J = 28.6 \text{ kA}$	$V_o = 8.0 \text{ V}$	SWITCH CLOSED
$\alpha R_o = 56 \text{ m}\Omega$	$J = 28.6 \text{ kA}$	$V = 1,600 \text{ V}$	SWITCH OPENED
$R_{Eo} = 140 \text{ m}\Omega$	$J_{Ef} = 1.43 \text{ kA}$		

NORMALIZED
TIMES:

$\tau_f = 0.02$	10% TO FULL VOLTAGE $\Delta\tau = 6.7 \times 10^{-4}$
	$\Delta\tau/\tau_f \approx 3\%$

Table I

SKETCH OF SELF-EXCITED HALL SWITCH TWO CORBINO DISCS IN COMMON EXCITER COIL

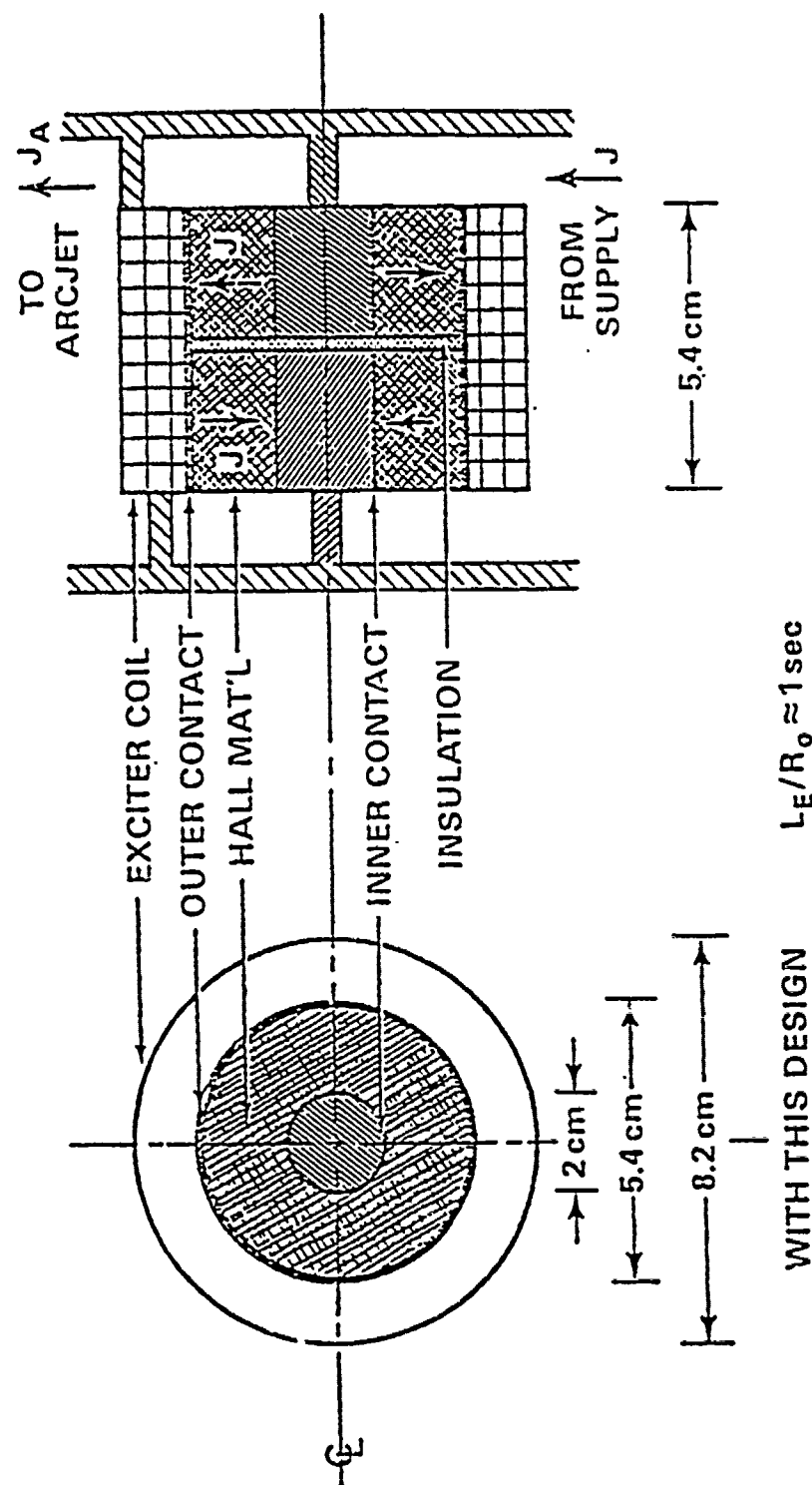
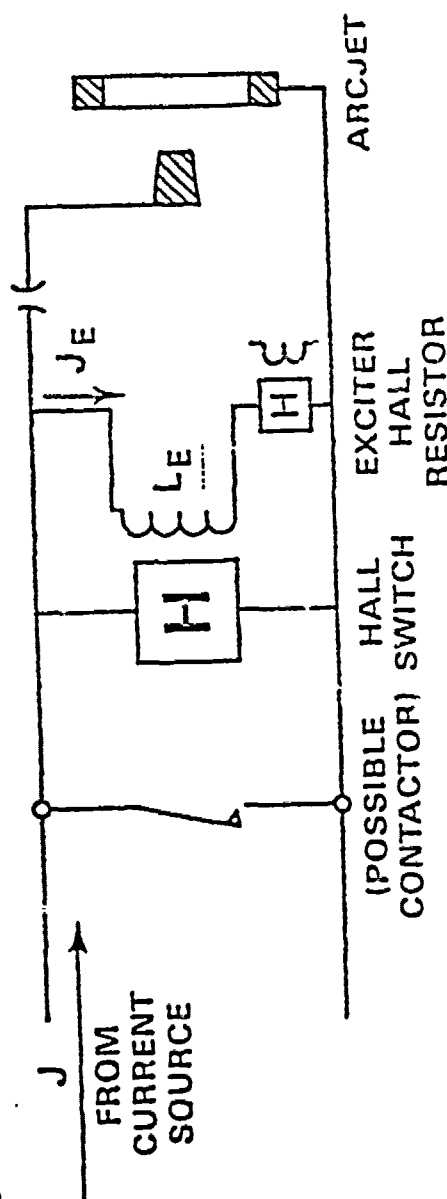


Fig. 4

AUXILIARY SWITCHING

NEEDED: ABILITY TO SHUT-DOWN ARCJET QUICKLY AT
END OF PULSE TO MINIMIZE LOW
PERFORMANCE AT LOW CURRENT

POSSIBLE APPROACH WITH HALL RESISTOR IN EXCITER CIRCUIT:



FOR PREVIOUS NUMERICAL EXAMPLE:

IF MAGNETIC FIELD OF 1.5T APPLIED TO EXCITER HALL RESISTOR
ARCJET CURRENT WILL DROP BY FACTOR OF 4 IN 200 μsec .
VOLTAGE ACROSS THE MAIN HALL SWITCH IS WITHIN 1% OF
FIELD-FREE VALUE AFTER ADDITIONAL 450 μsec

Fig. 5

action, a voltage spike is developed of sufficient magnitude (2 kV) to break down the sparkgap and the input-gas flow in the arcjet. Quasi-steady conditions are quite quickly attained in the arcjet at an impedance such that nearly constant current is diverted from the Hall switch to the arcjet. After a prescribed power pulsetime, the auxiliary Hall resistor is excited, quickly forcing the exciter current J_E to low values, thereby allowing the Hall switch to shunt the arcjet at low resistance values, cutting off the arcjet current. With low voltage across the Hall switch, the contactor can be reclosed and circuit operation can then be repeated after the desired interval of time.

The advantages and new features of the Hall effect power circuit for driving quasi-steady plasma thrusters are:

1. Low weight, volume, and reduced complexity compared to capacitively-driven circuits and externally-powered (vs self-excited) inductively-switched systems.
2. Use of self-excitation in conjunction with the arcjet impedance variation to provide automatically a long interval between high power pulses, nearly steady current during the power pulse and rapid cut-off of power at the end of the power pulse.
3. Use of self-excitation (and de-excitation) to allow a parallel high current contactor to operate without significant arcing on opening and closing.

Various particular arrangement of Hall elements (series/parallel arrays, for example) can be employed in the same circuit arrangement to satisfy specific requirements (such as spacecraft heat transfer constraints). Various Hall active materials can be employed with appropriate changes in the values of excitation field, current, pulse-times, etc. Additional switches, resistors and other e-

lectrical circuit elements can be incorporated with the Hall effect power circuit to adjust current distributions, rise and fall times, heat dissipation, etc. without changing the basic operation of the circuit.

Summary:

Two different techniques have been described for obtaining repetitive circuit interruption. Both techniques, as discussed, are associated with magnetoplasma-dynamic flows. In the case of the magnetoplasma-dynamic switch, a controlled force balance in such a flow is upset to provide the opening switch action. A pulsed magnetoplasma-dynamic flow served as the electrical load in the example given for Hall effect inductive switching. Other loads are, of course, possible. Both switch techniques are amenable to development with rather modest facility requirements and should prove to be useful in various regimes of interest as determined by such development.

Bibliography

1. K. E. Clark and R. G. Hahn, AIAAJ. 8, 216 (1970).
2. O. M. Corbino, Nuovo Cimento 1, 397 (1911).
3. D. A. Kleinman and A. L. Schawlow, J. Appl. Phys. 31, 2176 (1960).
4. P. J. Turchi, NRL Memo Report 3007 (1975).
5. E. K. Inall, A. E. Robson, P. J. Turchi, Rev. Sci., Instrum 48, 462 (1977).
6. P. J. Turchi, 14th Electric Propulsion Conf., Princeton, (Oct. 1979). AIAA Pre-print No. 79-2085.

Vacuum Arc Switching*

A. S. Gilmour, Jr.
State University of New York at Buffalo
4232 Ridge Lea Rd.
Amherst, N.Y. 14226

ABSTRACT

Vacuum arc opening switches are under development at the State University of New York at Buffalo (SUNYAB). The configuration of these devices is such that electron current is forced to flow, primarily, radially outward from the end of a relatively small rod shaped cathode to a ring shaped anode. The source of current is a vacuum arc that is initiated on the surface of the cathode by a pulse to an igniter electrode. This vacuum arc also generates a metallic plasma in the cathode to anode region resulting in a low switch drop during conduction. Current control is achieved through the application of an axial magnetic field.

Operating characteristics that have been achieved (not necessarily in the same device) are circuit interruption at dc voltages up to 25 kV, control of currents up to 10 kA, and operation at repetition frequencies up to 10 kHz. The turn-on and turn-off times are, respectively, as short as one and two microseconds. The pulse width is continuously variable.

BASIC DESCRIPTION OF THE VACUUM ARC OPENING SWITCH

The operating principles of the vacuum arc opening switch are based primarily on the dc vacuum arc interrupter which has been described in the literature.^{1,2} The following brief description is given to orient the reader.

*Partially supported by the Air Force Aeropropulsion Laboratory through The Southeastern Center for Electrical Engineering Education, Contract F 33615-77-C-2059.

The operation of a vacuum arc opening switch depends, of course, to a large extent, on the characteristics of the vacuum arcs. A vacuum arc is a plasma discharge established between two electrodes in a vacuum. The constituent material of the negative electrode is vaporized and ionized by the arc spots to provide the conducting medium. A vacuum arc discharge is an almost ideal medium for use in switching³ because it makes possible a high-vacuum device having excellent insulation properties when nonconducting and it becomes a plasma discharge device with a very low voltage drop during conduction.

Shown in Figure 1 are two configurations of a vacuum arc device capable of interrupting the flow of current.

Vacuum arc ignition can be accomplished by any one of several techniques. For example, several millijoules of energy from a pulsed laser can be used to vaporize and ionize material from either the negative or the positive electrode.⁴ When this plasma bridges the gap between the electrodes, a vacuum arc will occur if sufficient voltage is applied to the electrodes.

A second technique for igniting vacuum arcs is to bring an igniter electrode into contact with the cathode. By passing sufficient current through the contact points, and then withdrawing the igniter electrode, an arc can be initiated. This technique is commonly used in switchgear and is useful when repeated arc ignition is not required.

High-voltage (several thousand volts) breakdown between two electrodes across the surface of an insulator can be used to vaporize one or both electrodes and thus lead to arc ignition. Attempts to use a high voltage pulse to "break down" a vacuum gap (rather than the surface of an insulator) have not produced satisfactory results. This technique has been found to lead to unreliable ignition and there is a strong tendency for arcs to occur where they are not wanted. Finally, substantial energy is dissipated in

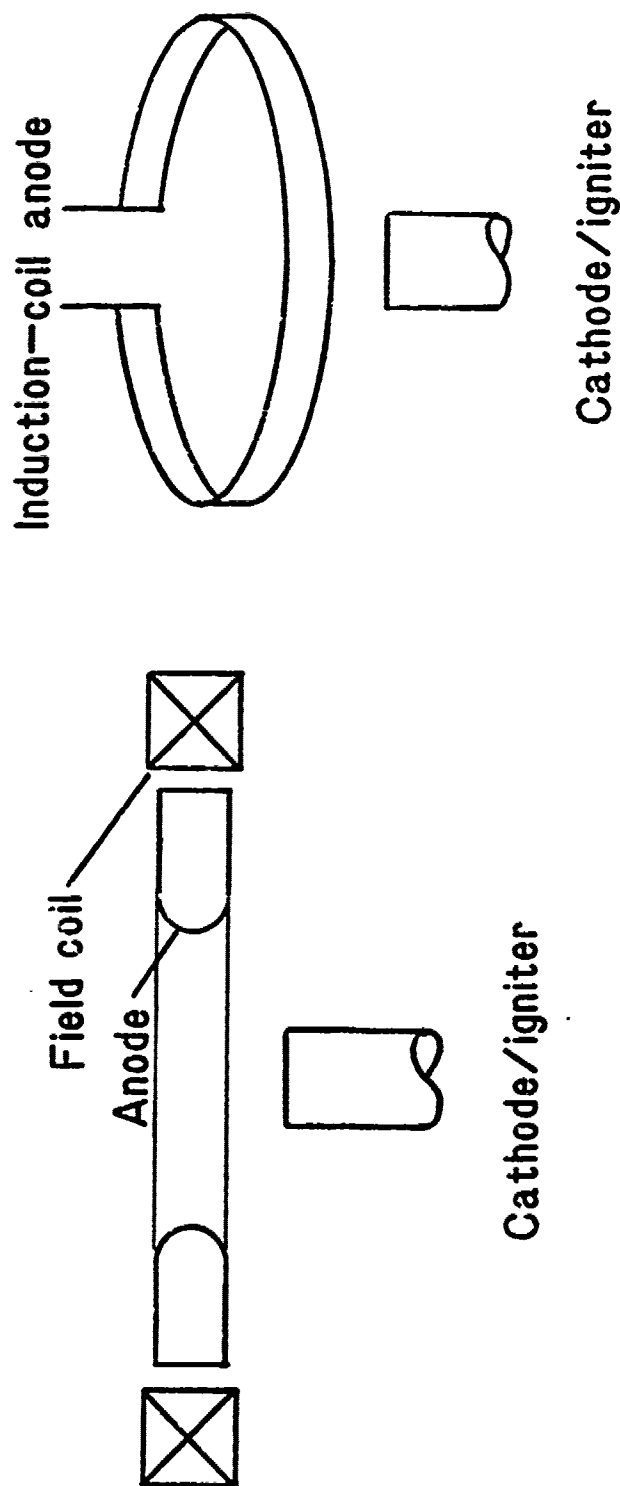


Figure 1. Electrode configurations with interruption capability.

the ignition circuit.

An arc ignition technique reported ⁵ to be extremely successful employs a titanium hydride igniter. A small current pulse is passed through the igniter causing the release of a small amount of hydrogen. The hydrogen ionizes, leading to an arc.

In the arc ignition technique used with a high degree of success at the State University of New York at Buffalo (SUNYAB)^{1,2} a current pulse is used to vaporize a portion of a conductive film on the surface of an insulator located between the cathode and an igniter electrode. Possible configurations of the igniter/cathode assembly are shown in Figure 2. The plasma burst resulting from the ignition current pulse fills the interelectrode space. During the ensuing vacuum arc discharge, the conducting film on the insulator is regenerated by the deposition of material from the metallic plasma. The system is thereby prepared for a subsequent ignition pulse.

The primary advantages of the SUNYAB film vaporization ignition technique over other techniques are:

1. No moving electrodes are required.
2. Insulation problems are minimized because a few relatively low voltage (few hundred volts at most) is required for ignition.
3. Energy supplied by the ignition circuit is used primarily to produce the ignition plasma burst. Thus, ignition energy is minimized. This is particularly important at high repetition frequencies where ignition power is substantial.
4. Automatic cathode positioning is possible.

For efficient arc ignition, the ignition plasma must be permitted to bridge the cathode-anode gap in the most effective manner possible. For example, as is shown

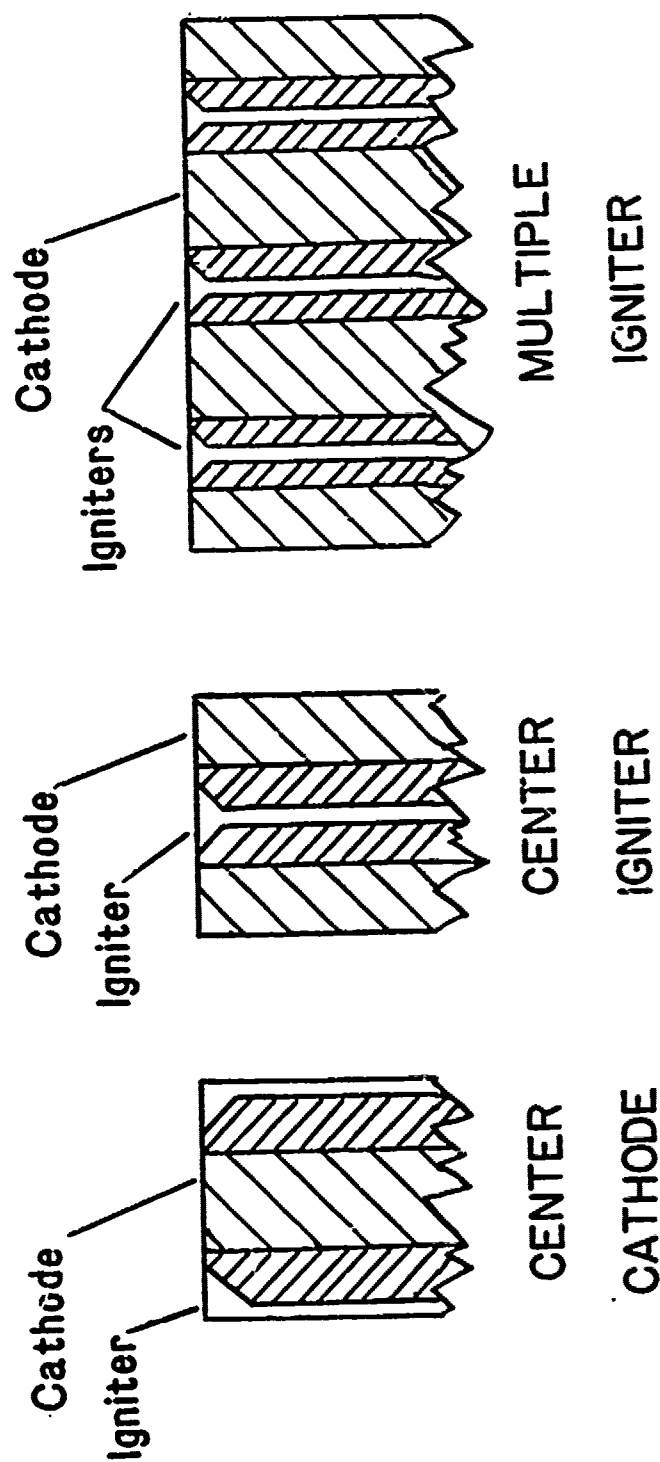


Figure 2. Cathode / igniter configurations.

in Figure 3, an ignition plume that is ejected so that a considerable portion of it is intercepted by the anode (anode in position A) readily leads to the establishment of a vacuum arc. If the anode is located at position B, only a small portion of the ignition plume is intercepted and arc ignition requires a much larger ignition plasma burst and a correspondingly larger ignition energy pulse.

For current limiting or interruption to occur, the electrodes must be of a coaxial geometry.^{1,2} The cathode is a relatively small electrode placed on the axis and the anode is an annulus surrounding the cathode. The arc current may be limited or extinguished by applying a coaxial magnetic field to the device in such a way that the field lines are essentially perpendicular to the paths of the electron current from the cathode to the anode. The effect of the field is to increase the voltage drop across the arc and thereby decrease the discharge current. This is shown for a switch operating at 5 kilovolts in Figure 4. The form of the curve in Figure 4 is very nearly

$$\frac{I_r}{I_o} = \frac{1}{1 + KB_z^2}$$

where

B_z = magnetic flux density

I_o = arc current for $B_z = 0$

I_r = arc current for $B_z > 0$

K = constant

The arc is extinguished when the current is reduced to a value where the average lifetime of the arc becomes very short compared to the duration of the magnetic field pulse. Average arc lifetimes as a function of current are shown for several metals in Figure 5. Notice, for example, that if the current through a copper arc is reduced to a

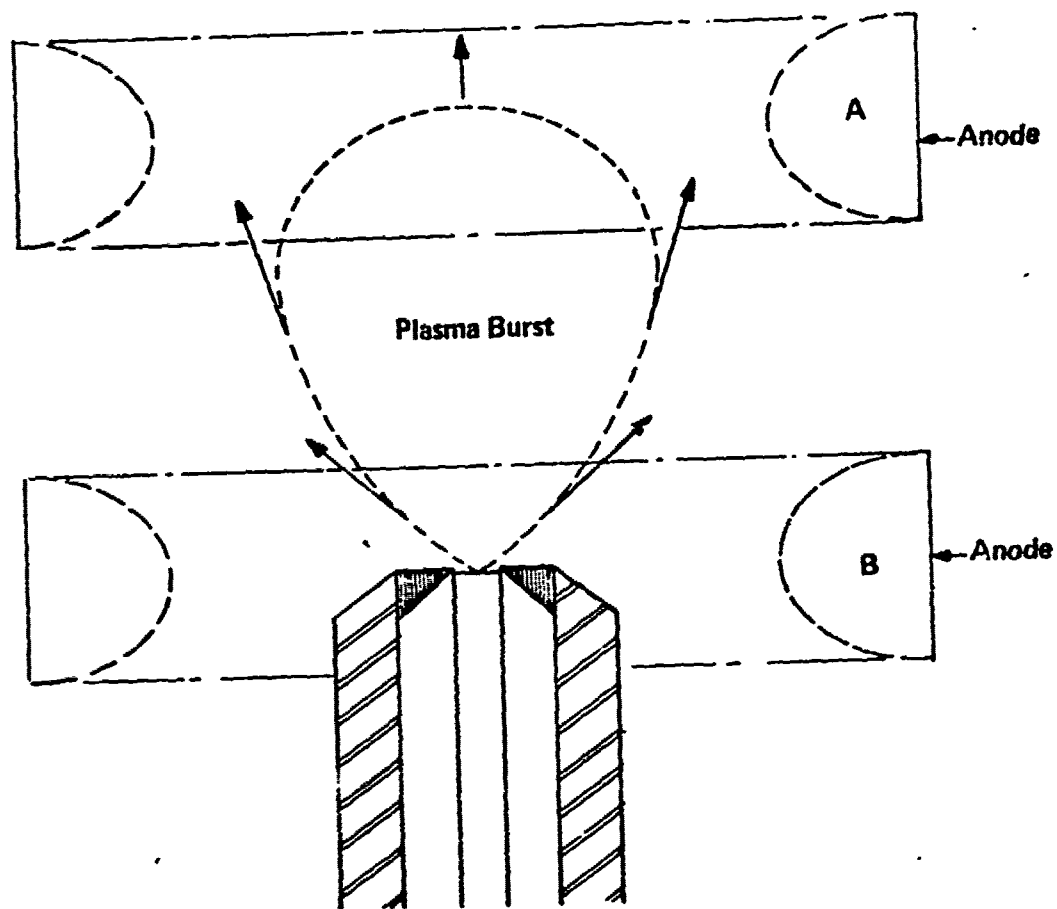


Figure 3. Ignition plasma burst in relation to anode position.

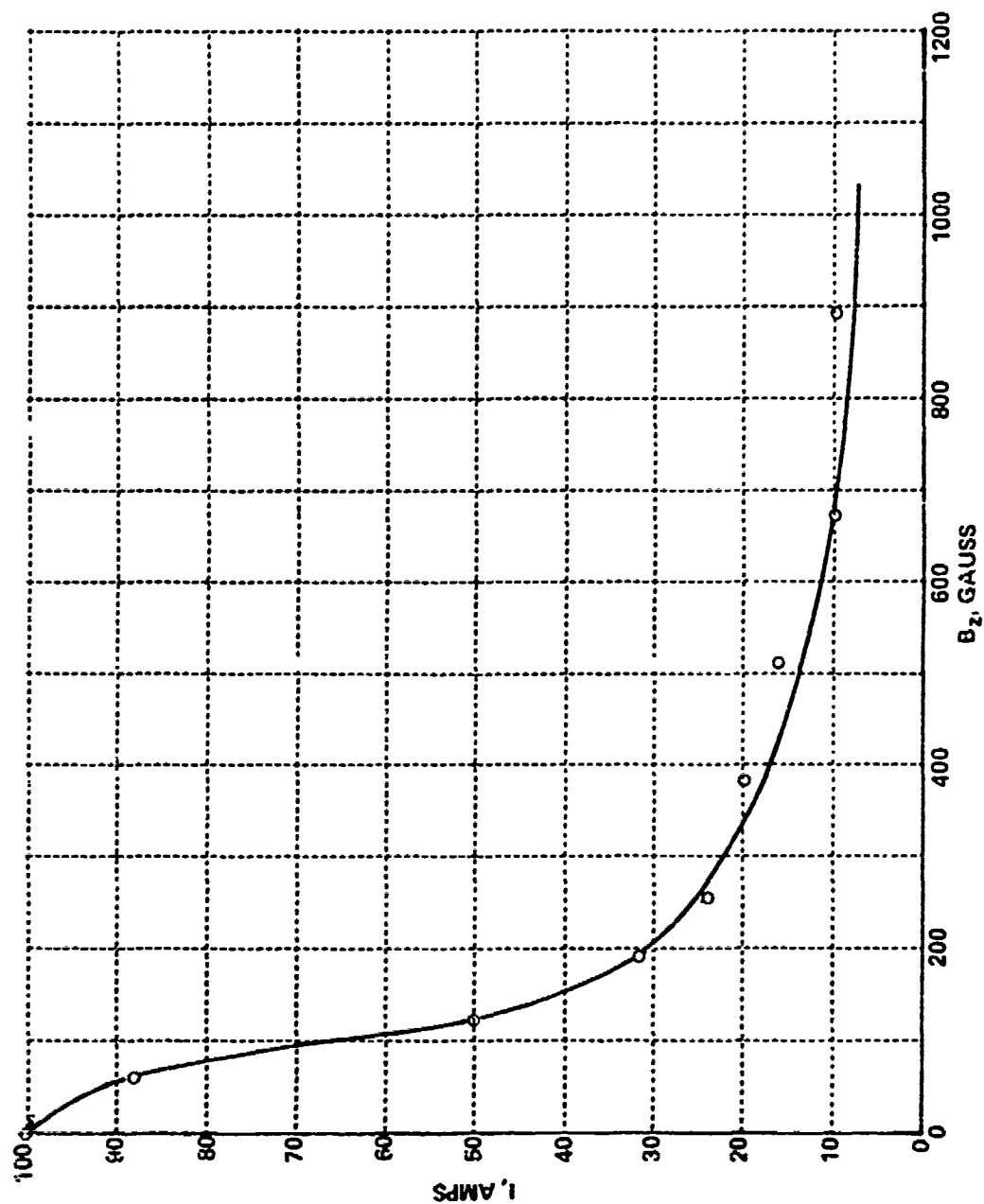


Figure 4. Arc current vs. axial flux density for switch at 5 kV.

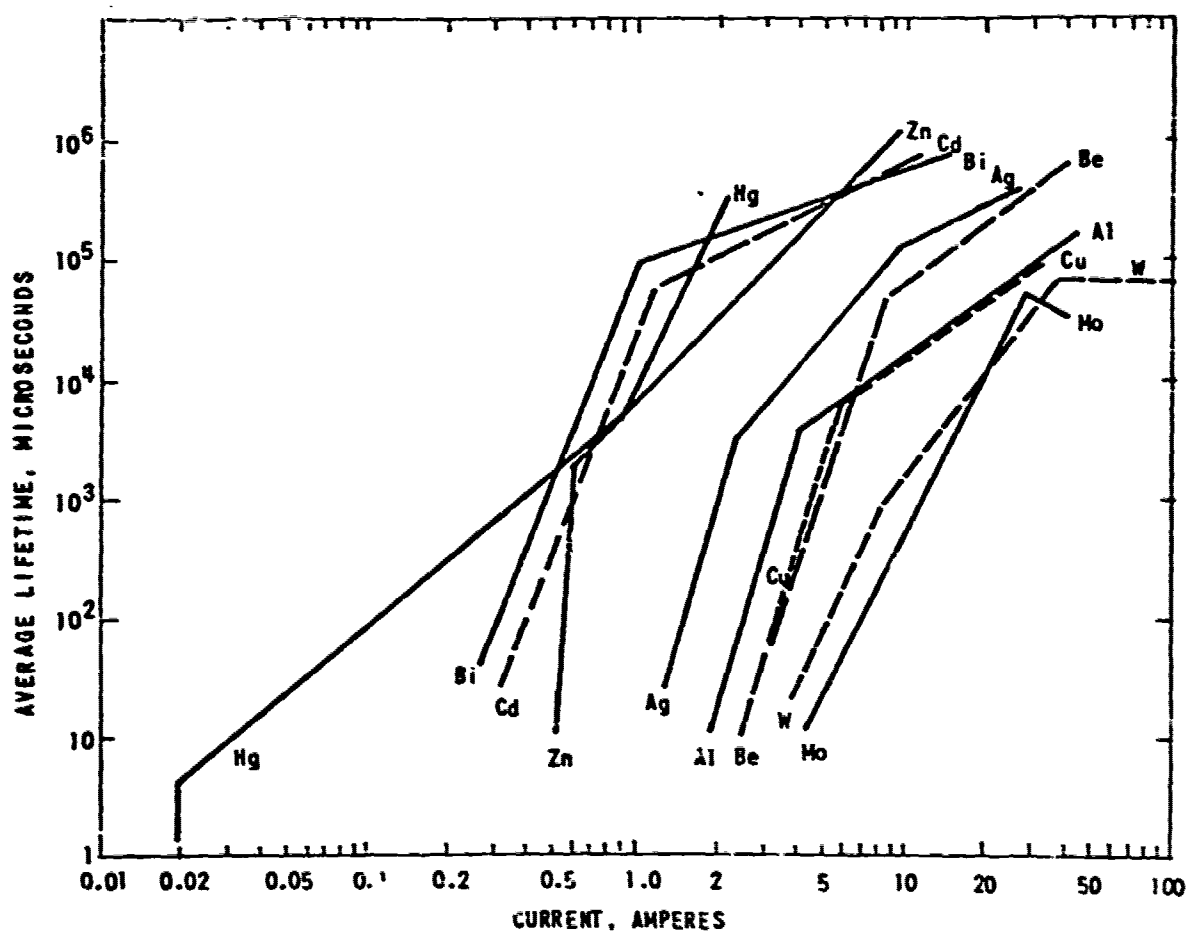


Figure 5. Average arc lifetime as a function of current for pure electrode materials. (from 6.)

value below 2 amperes, that the average lifetime of the arc will be below 10 microseconds. Therefore, if a magnetic field pulse with a length of 10 microseconds is used and if the arc current is reduced to 0.5 amperes, on the average, the arc should be extinguished 50 percent of the time. In practice, to insure current interruption, the duration and amplitude of the magnetic field are increased sufficiently to insure arc extinction. When conduction ceases, metallic vapor is no longer emitted by the cathode. The vapor in the interelectrode space rapidly condenses and the interrupter returns to the high-vacuum state and remains off when the magnetic field is removed.

PRESENT STATUS OF DEVELOPMENT

The present status of development of vacuum arc switches is shown in Figure 6. It must be emphasized that the characteristics listed have not all been achieved at the same time or in the same device. It must also be emphasized that vacuum arc switches are, at the present time, strictly laboratory devices.

FUTURE

With continued research and development, it should be possible to build a device capable of interrupting several tens of kiloamperes at a voltage level on the order of 100 kV at a reasonable repetition frequency. Because of the positive resistance characteristic of vacuum arc switches, it should be possible to parallel them to achieve a much higher current interruption capability.

It should be noted here that a recent informal report of Russian progress on devices nearly identical to the device described in this paper indicates that substantial progress has been made in increasing voltage interruption capability.

CURRENT INTERRUPTED	10 kA
LOAD VOLTAGE INTERRUPTED	25 kV
T on (LASER TRIGGERED)	0.1 μ S
T off	2 μ S
T cond	10 μ S — DC
REPETITION RATE	10 kHz
LIFE	$10^7 - 10^8$ C

Figure 6. Present status of development (not all at the same time or in the same device).

It has apparently been demonstrated in the laboratory that several vacuum arc switches can be used in series to interrupt voltages in excess of 1,000 kV dc at a current of about 10 kA. This work is being performed to develop an interrupter for high voltage dc transmission systems.

Finally, it should be noted that the principle of magnetic interruption of vacuum arcs was first demonstrated over a decade ago. Since then funding has been erratic at best. A substantial, coherent program continuously funded for an extended period with emphasis on basic research as well as development will be required to determine and demonstrate the full capabilities of vacuum arc switches.

SUMMARY AND CONCLUSIONS

Vacuum arc switches hold the promise of being able to satisfy many repetitive opening switch requirements. In separate tests and devices the interruption of dc voltages up to 25 kV and dc currents to 10 kA has been demonstrated. Arc ignition at repetition rates in excess of 10 kHz and interruption at 1 kHz has been demonstrated. Determination and demonstration of the full capabilities of vacuum arc switches depends on the establishment of a substantial, coherent program continuously funded for an extended period with emphasis on basic research as well as development.

REFERENCES

1. A. S. Gilmour, Jr. and D. L. Lockwood, "The interruption of vacuum arcs at high dc voltages", IEEE Trans. on Electron Devices, vol. ED-22, no. 4, pp. 173-180, April 1975.
2. A. S. Gilmour, Jr. and D. L. Lockwood, "Pulsed metallic-plasma generators," Proc. IEEE, vol. 60, pp. 977-991, August 1972.
3. G. A. Farrall, "Vacuum arcs and switching," IEEE Proc. vol. 61, no. 8, pp 1113, August 1973.
4. A. S. Gilmour, Jr. and R. J. Clark, Jr., "Studies on a laser-triggered, high voltage, high vacuum switch tube," Proc. IIIrd International Symposium on Discharges and Electrical Insulation in Vacuum, pp. 367-372, September 1968.
5. J. M. Lafferty, "Triggered vacuum gaps," Proc. IEEE, vol. 54, pp. 23-32, Jan. 1966.
6. J. B. Cobine and G. A. Farrall, "Experimental study of arc stability - I", J. Appl. Phys., vol. 31 pp. 2296-2304, Dec. 1960.

A PLASMA FOCUS INTERRUPTING SWITCH FOR USE
WITH INDUCTIVE ENERGY STORAGE*

G. M. Molen and H. C. Kirbie
Department of Electrical Engineering
Old Dominion University
Norfolk, VA 23508

and

J. L. Cox, Jr.
Department of Physics
Old Dominion University
Norfolk, VA 23508

ABSTRACT

A rather novel geometry is described for using a plasma focus device as an interrupting switch for inductive energy storage circuits. The concept employs a third electrode which is inserted on axis with the anode of the plasma focus device. An arc discharge between these two electrodes completes the circuit to an external, energy-storage inductor. It is anticipated that the current in the arc discharge will be interrupted by the collapse of the plasma focus current sheet toward the system axis.

The switch concept should interrupt currents as large as several hundred kiloamperes in times on the order of tens of

*The investigation of this concept is sponsored by the Naval Surface Weapons Center, Dahlgren, VA under contract no. N60921-80-C-A341 and the National Science Foundation under grant no. CPE-7925563.

nanoseconds. During the time in which the switch is open, restrike voltages as large as several hundred kilovolts may be withstood. Furthermore, it should be possible to operate the switch repetitively by continually firing the plasma focus after the energy storage inductor has recharged.

A. INTRODUCTION

The development of an improved opening switch has recently received considerable interest because of the key role of the switch in the development of inductive energy storage for pulsed, high-energy systems. Inductive storage is attractive since it represents a relatively compact energy storage method as compared with capacitive energy storage. A circuit diagram of a typical pulsed system employing inductive energy storage is shown in Fig. 1. The storage inductor L is charged by the power source with a time constant L/R_s once switch S_1 is closed where R_s is the resistance of the primary circuit. Energy is transferred from the inductor to the load by simultaneously opening switch S_2 and closing switch S_3 . If S_2 is opened in a time much less than L/R_L , where R_L is the resistance of a non-reactive load, the energy stored in the inductor will be transferred efficiently to the load [1].

The closing switches S_1 and S_3 in the circuit do not represent significant difficulties; opening switch S_2 , however, is a major technological obstacle which has limited implementation of such systems. To be useful for present applications, the switch must be able to conduct quasi-dc currents of at least tens of kiloamperes with minimal power dissipated in the switch and be able to interrupt these currents against voltages of tens or hundreds of kilovolts. Furthermore, the opening time must be short in order to minimize power dissipation and transfer energy efficiently. It is also imperative that the switch be able to conduct current for times that are long compared with the times during which that current is interrupted in order for such systems to be

of practical use. The need for repetitive operation in certain applications, however, is perhaps the most difficult problem to solve in the development of a useful opening switch.

B. PLASMA FOCUS DEVICES FOR CURRENT INTERRUPTION

The impedance of the plasma column at the termination of the pinch phase of the plasma focus discharge is known to increase several orders of magnitude [2]. This effect, which is often called an anomalous resistance, is responsible for the intense electric fields produced in the discharge volume which are known to accelerate both ions and electrons to energies exceeding 1 MeV [3]. As a result of this rapid increase in resistance, the discharge current is simultaneously reduced by as much as 30 to 50% in tens of nanoseconds as illustrated in Fig. 2. There has understandably been considerable interest in using this rather natural current interruption as the basis of an opening switch for inductive energy storage circuits.

One possible configuration for using the plasma focus as an opening switch is shown in Fig. 3. Electrical energy is initially stored in the plasma focus capacitor bank. When switch S_1 is closed, a charging current flows through the plasma focus and a series inductor until the current is partially interrupted in the pinch phase of the discharge. A fraction of the energy initially stored in the inductor is then delivered to the load by closing switch S_2 . There are, however, obvious disadvantages in this system. Limitations imposed by the dynamics of the plasma focus limit the series inductance that can be used in the circuit. Furthermore, the relatively short time (several microseconds) available for charging the inductor limits the energy compression ratio that can be obtained.

The switch described in this paper, however, uses a plasma focus in a novel geometry that avoids the disadvantages of the circuit shown in Fig. 3. In the new geometry, the

primary charging circuit is separated from the energy storage bank of the plasma focus. This decoupling of circuits should permit large energy compression ratios to be obtained since there is no longer a limitation on the time required to charge the storage inductor.

C. A PLASMA FOCUS SWITCH USING AN AUXILIARY ELECTRODE

The proposed opening switch uses a conventional dense plasma focus (DPF) in combination with a third or auxiliary electrode as shown in Fig. 4.* The auxiliary electrode is located several centimeters above the center electrode (anode) and concentric with the axis of the plasma focus. Ambient pressure in the discharge vessel is 1 to 3 Torr of hydrogen.

An external magnetic field oriented along the axis of the focus is produced by a coil located outside the cathode of the plasma focus. This dc field initially has a flux density of approximately .05 T which is compressed by the collapsing plasma sheath to a flux density of approximately 75 T. Such an external field has previously been used by other researchers to stabilize the plasma focus pinch so as to increase the duration of the high density channel [4]. Although this axial field is not believed to be an intrinsic part of the switch concept, it is used to provide collimation to ensure that the arc between the auxiliary electrode and the anode remains on axis and is axially symmetric.

The operation of the switch proceeds as follows: The switch is effectively closed by establishing an arc discharge between the auxiliary electrode and the anode of the plasma focus. After the current in the charging circuit reaches a maximum, the plasma focus device is fired causing an annular plasma sheet to form and then finally collapse onto the arc

*The source of energy for the inductive circuit is shown in the figure as a capacitor bank, however, in a practical system a current source such as a homopolar generator would be used.

current as illustrated in Fig. 5. For reasons that are explained below, the leading edge of the collapsing current sheet is expected to penetrate into the arc plasma so that the DPF current and the collinear arc current become thoroughly intermixed. Subsequently, this current system should continue to collapse until the anomalous resistance of the plasma channel and the induced axial electric fields interrupt the current flow.

Penetration of the leading edge of the DPF plasma into the auxiliary discharge plasma is expected to be possible because of induced currents that are produced during the DPF collapse. As the DPF plasma sheet collapses onto the magnetic field B_0 produced by the axial current of the auxiliary discharge, B_0 attempts to penetrate into the leading edge of the current sheet. However, that part of B_0 within the DPF plasma is annihilated within a distance c/ω_p of the leading edge by reverse currents [5] in the DPF plasma where c is the speed of light and ω_p is the plasma frequency of the DPF plasma. For the DPF plasma, $\omega_p^{-1} \approx 10^{-14}$ sec, while the magnetic diffusion time is approximately 10^{-5} sec; the time required for the collapse to take place is approximately 10^{-7} sec. Thus reverse currents are quickly established which persist throughout the DPF collapse. Annihilation of B_0 within the collapsing plasma has the overall effect, therefore, of decreasing the flux associated with the axial auxiliary discharge current. This gives rise to additional induced emf's that tend to increase the axial current flow in the auxiliary discharge circuit. If this current increase were to occur, it would increase B_0 at radii smaller than the radius of the collapsing current sheet and an apparent compression of the original B_0 would be observed. Such flux compression will not occur, however, if the increase in axial current is prevented. In the system described here, such an increase in axial current cannot be produced by current loops in the plasma system because B_0 in advance of the current sheet restricts the axial current flow that would be required; it

would also be inhibited by the external axial magnetic fields discussed above. The only other way in which the axial current can increase is for the current to increase in the total circuit loop that contains the external storage inductor. The inductance is far too large, however, to allow this to occur on the time scale of the DPF collapse. Consequently, B_0 should not be compressed by the DPF collapse. The DPF plasma and the auxiliary discharge plasma, therefore, should be able to mix thoroughly.

An additional mechanism that is expected to be important when the arc current is established along an axial magnetic field was recently reported [6]. According to that work, a high-energy electron beam can be expected to propagate through a dense plasma parallel to a very strong magnetic field only if its length is less than a critical length

$$L_c = \pi V / \omega_p,$$

where V is the beam velocity and ω_p is the plasma frequency of the background plasma. The existence of such a critical length is related directly to the manner in which currents are induced in the plasma by passage of the beam electrons. As the electron beam propagates through the plasma, reverse currents are induced which backstream along the beam channel and provide current neutralization for the beam. In addition, induced currents in the plasma flow radially out of the beam channel to provide charge neutralization for the beam, the extent of which is intrinsically coupled to the degree of current neutralization. If a strong magnetic field is placed parallel to the beam velocity, however, the radial motion of plasma electrons is strongly inhibited. The combination of their backstreaming motion plus this constraint on radial motion causes the plasma electrons to pile up on the beam axis and ultimately halt further beam propagation. The length over which this process takes place, measured relative to the front of the beam, is the critical length, L_c . In the switch

arrangement the arc current can be treated as a beam of electrons that may be subject to critical length limitations. For a typical plasma focus density of 10^{19} cm^{-3} , the critical length for such a beam is approximately $5 \times 10^{-6} \text{ m}$, a distance much smaller than the dimensions of the focus volume.

D. ANTICIPATED CHARACTERISTICS OF THE SWITCH

The voltage required to break down the gap between the auxiliary electrode and the anode of the plasma focus is given by the Paschen curve and the appropriate pd product, where p is the pressure in the vessel and d is the electrode separation. As a representative example, the spark potential at 1 Torr of hydrogen and a separation distance of 1 cm is approximately 300 V. Once the gap breaks down, the discharge will enter the arc regime if sufficiently large currents are available. The voltage drop across the electrode will be approximately 50 V and almost independent of the current.

The switch is opened by triggering the plasma focus device once maximum energy is stored in the magnetic field of the external inductor. It is believed that the actual current interruption will last for tens of nanoseconds. If the current is interrupted in a time interval much shorter than L/R_L , the voltage between the auxiliary electrode and the anode will rise almost instantaneously to a voltage approaching $I_0 R_L$, where I_0 is the charging current [1]. As shown in Fig. 6, the output voltage will then exponentially decay with the time constant L/R_L ; however, at a time Δt later, the switch will again close as the density of the plasma column diminishes. Once the inductor has been recharged, the plasma focus can again be fired as shown in the figure. It is anticipated that the open time, Δt , will be approximately 100 to 200 nsec.

Estimates of the current interrupt capability of such a switch are difficult; however, a peak plasma focus current that is four times the inductive charging current is considered realistic. If this approximation is found valid, the interruption of currents in the hundreds of kiloamperes will

be possible. Since the inductance of the plasma focus is much less than the storage inductance, the energy of the plasma focus can be realistically approximated as 10 percent of the total energy of the system.

E. REFERENCES

- [1] T. F. Trost, et al, "Pulse Power Systems Employing Inductive Energy Storage", Proc. First Intl. Pulsed Power Conf., IEEE Pub. no. 76CH1147-8REG-5, (1976).
- [2] J. W. Mather, in Methods of Experimental Physics. New York: Academic Press, 9, Pt. B, 187 (1971).
- [3] G. M. Molen, "Electron Burst Measurements Produced by a Plasma Focus", Proc. Second Intl. Conf. on Energy Storage, Plenum Press (1978).
- [4] H. L. van Paassen, et al, "X-Ray Spectra from Dense Plasma Focus Devices", Phys. Fluids 13, 2606 (1970).
- [5] J. L. Cox, Jr., et al, "The Reverse Current Induced by Injection of a Relativistic Electron Beam into a Pinched Plasma", Phys. Fluids 13, 182 (1970).
- [6] J. L. Cox, Jr., et al, "Coherent Radiation from Pulsars", Astrophys. J. 229, 734 (1979).

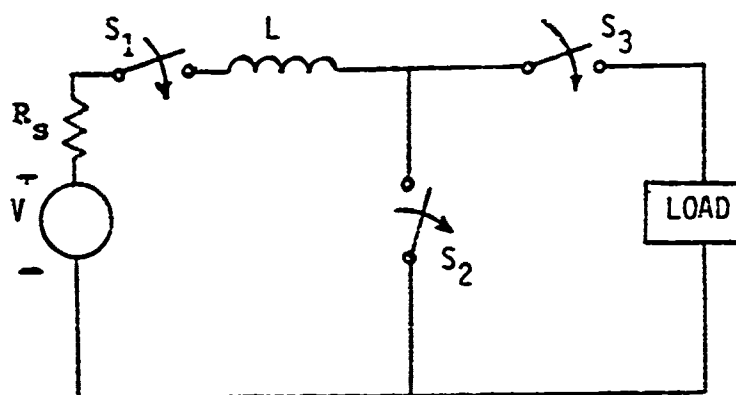


Fig. 1. Basic Inductive Energy Storage Circuit

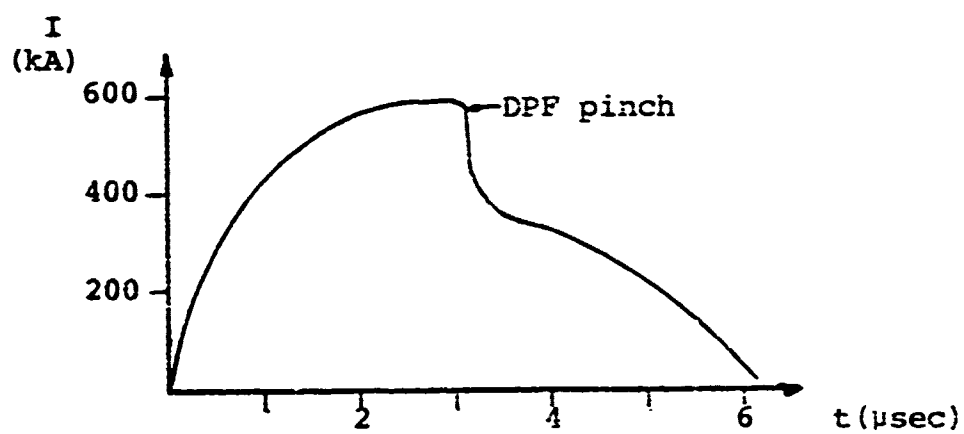


Fig. 2. Plasma Focus Discharge Current

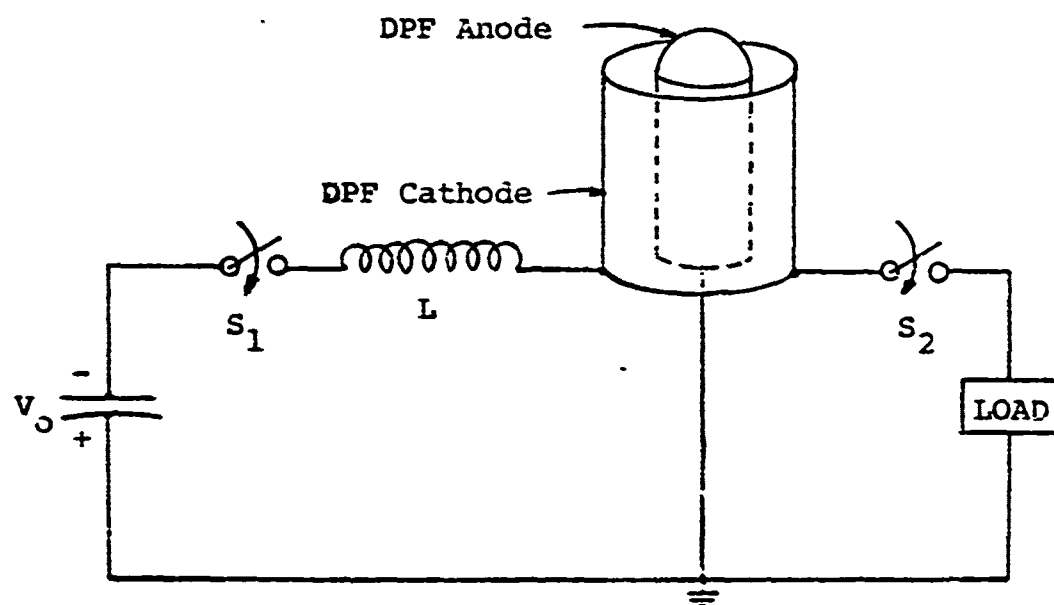


Fig. 3. Inductive Energy Storage Circuit with a Plasma Focus Interrupting Switch

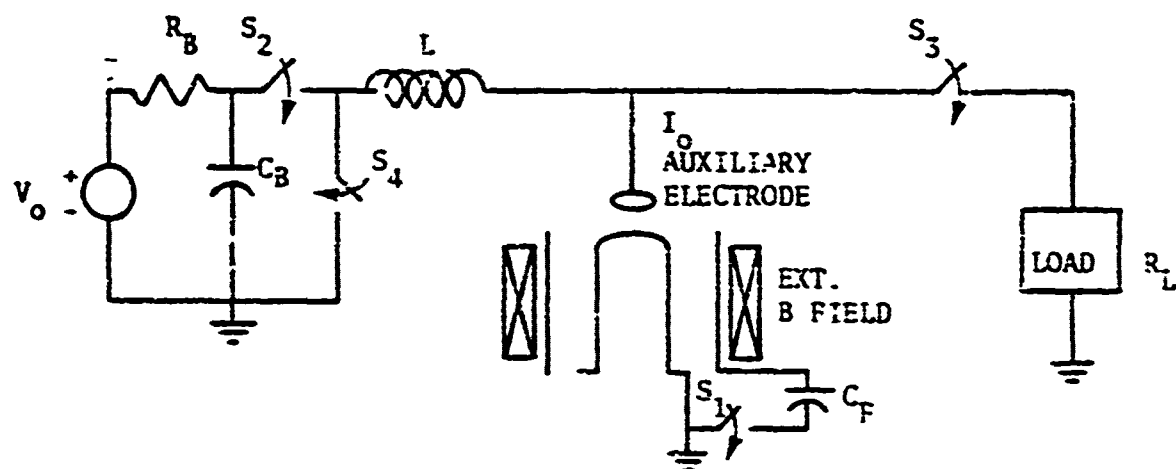


Fig. 4. Inductive Energy Storage Circuit with the Novel Plasma Focus Switch

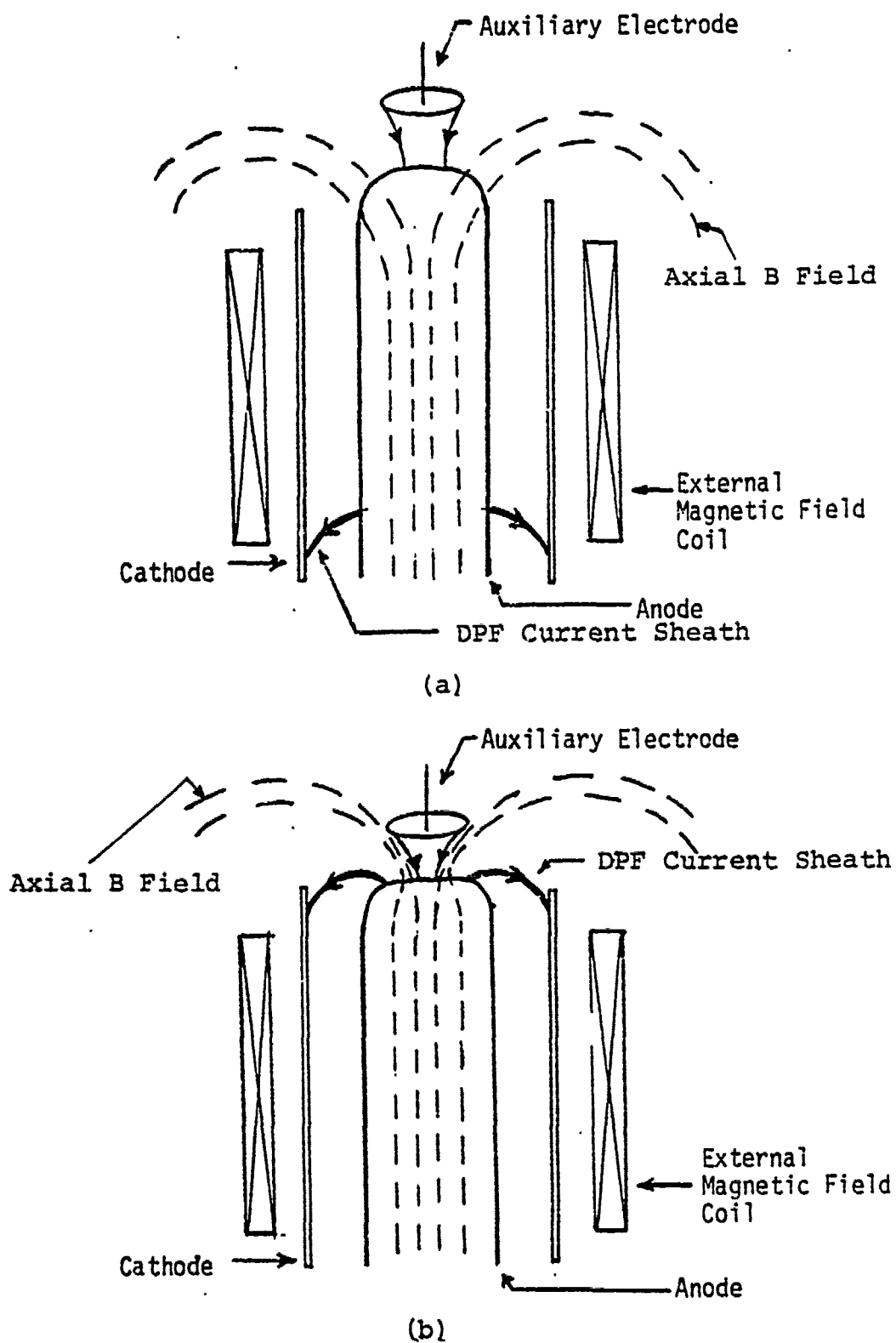


Fig. 5. Description of the Auxiliary and Plasma Focus Discharge Currents at (a) Initial Breakdown of the Plasma Focus and (b) Collapse Phase of the Plasma Focus

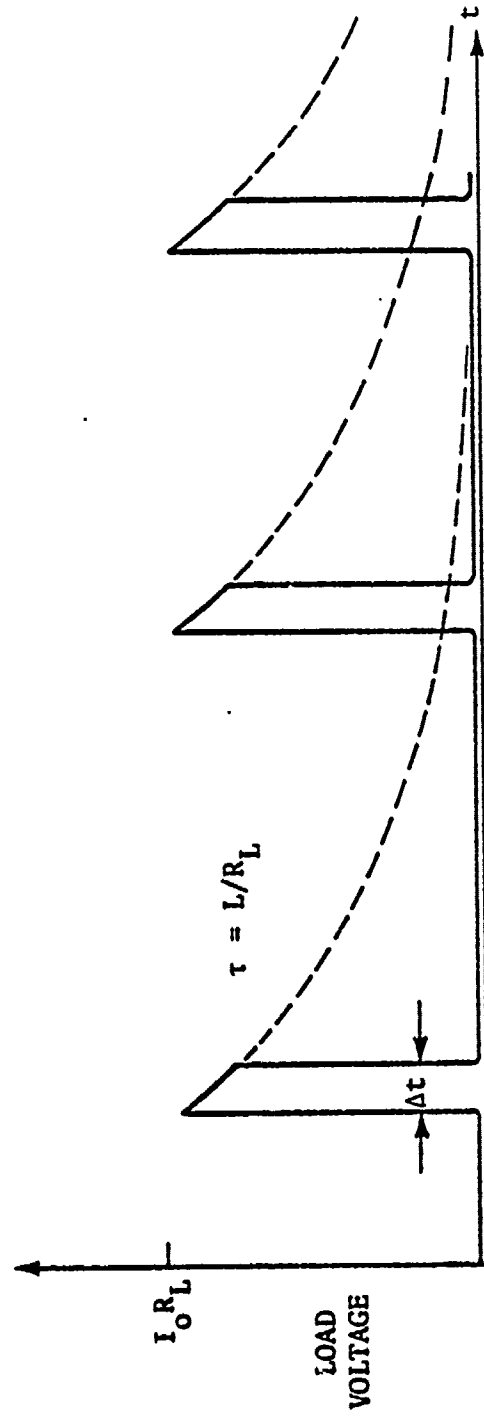


Fig. 6. Anticipated Output Characteristics of Repetitively Pulsed System

PROBLEMS OF REPETITIVE OPENING SWITCHES DEMONSTRATED ON
REPETITIVE OPERATION OF A DENSE PLASMA FOCUS*

Jürgen Salge

Technische Universität Braunschweig
Institut für Hochspannungstechnik
Postfach 3320
D-3300 Braunschweig, FRG

ABSTRACT

A dense plasma focus device powered by an inductive energy storage system is able to produce high voltage pulses of some 10 kV at currents of more than 40 kA. Intervals between two voltage pulses of a few μ s were obtained. The operation mode of a repetitive plasma focus and problems of its application for repetitive opening switches are discussed.

INTRODUCTION

Each application of an inductive energy storage system should result in supplying a given load with power pulses. For a repetitive operation the basic scheme is given in fig. 1. In order to achieve, at a given constant current i , a power P_L the impedance of the load circuit has to change periodically from zero to a corresponding value. It would be the best, if this impedance variation is done by the load itself. In this case additional switching devices can be avoided, the required switching operations are performed by the load itself.

A load without these properties needs several additional switching elements in order to achieve this behaviour. Number and properties of the switching devices are again dependent on the load. Fig. 2 shows such a system for an ohmic load with constant resistance. For S_4 the realistic assumption is made, that its voltage steepness is limited. In comparison to fig. 1

* This work is supported by the Deutsche Forschungsgemeinschaft, Bonn, FRG. The experiments were carried out by Dipl.-Ing. B. Fell.

only one additional repetitive switch is needed, which is able to open and to close periodically. Its losses have to be provided by the store.

In fig. 3 a system with an inductive load is given. To meet the requirements two repetitive opening and closing switches are necessary. The switching losses are remarkably increased.

This paper starts with an interpretation of the repetitive mode of a dense plasma focus device, basing on experimental results [1, 2, 3]. The automatic generation of voltage- and power-pulses is demonstrated for a focus-device supplied by an external magnetic energy store. Furthermore the utilization of such devices for repetitive opening switch-operation is discussed.

1. Repetitive operation of a dense plasmafocus

Fig. 4 shows schematically 6 stages of a discharge. After breakdown on the insulator surface (1) a coaxially high current plasma sheath is formed and driven to the end by Lorentz forces rapidly (2, 3). Above the inner electrode - the anode - a small high resistive area is caused by a first focus event (4). The current through this area produces a voltage- and a corresponding power-pulse. The maximum amplitude of this voltage is limited by the electric strength of the surroundings of the discharge zone. A reignition in the direct vicinity of the discharge (4) occurs and the current is transferred to this area. In the sequence a new radial collapse of the plasma appears (5), resulting in a second focus event (6). The complete process is repeated for many times.

The ideal operation of such a device is shown in fig. 5. Each focus event is accompanied by a voltage- and a power-pulse. The optimum would be achieved by keeping the voltage between the pulse close to zero (1). In any case this voltage has to be small compared to that during the focus event (2).

Undoubtedly such ideal focus device meets all requirements of a repetitive opening switch: It produces a sequence of high voltage pulses at current-levels of some 10 kA. Let us now have a look on the results obtained from realistic

device, shown in fig. 6.

2. Experimental results

The current differs considerably from its ideal trace due to the limited energy content of the store. Voltage- and corresponding power-pulses could be recognized definitely, but its shape and level as well as the intervals between the single pulses are far apart from an ideal behaviour. The maximum voltage peak of 25 kV was obtained at a current of 90 kA, which results in a characteristic ohmic resistance of the discharge at a focus event of $0,3 \Omega$. The pulse width is in the order of $1,5 \mu\text{s}$. Unfortunately the mean voltage between the pulses diminishes only to some kV. Thus the dissipated energy in this period is of the same order of magnitude as the energy consumed during the voltage pulses. This means high energy losses and strong electrode-erosion. From our experiments it can be concluded, that this phenomenon is mainly caused by an unsymmetrical behaviour of the discharge. The reignition takes place at some points of its vicinity only and the current is switched over from the focus area to these points. This results in asymmetrical spokes. After some fruitless attempts the symmetry of the discharge is recovered and efficient focus events are observed again. Nevertheless we have obtained focus-events up to $150 \mu\text{s}$. In our experiments the duration was limited only by the energy content of our storage system. At currents less than 40 kA the focussing process was interrupted.

3. Discussion

It can be concluded from the experimental results, that a repetitive plasma focus device in principal meets the requirements of a repetitive opening and closing switch, but in reality it differs remarkably from its ideal operation mode. On the one hand improvements have to be achieved, in particular concerning a considerable reduction of losses between the focus events. On the other hand it is necessary to improve the uniformity of the focussing process. Up to now we did not realize experiments to investigate these problems. We hope

there will be some chances by changing the electrode geometry of the accelerator and by triggering the reignition symmetrically. Both can equalize also the repetition frequency and the voltage pulshape.

A main advantage of the repetitive mode of the dense plasma focus is the self-preservation of this process. Starting from worse conditions the discharge itself recovers its symmetry resulting in efficient focus-events with high voltage pulses.

References:

- [1] J. Salge, et al., "Sequences of Neutron and X-Ray Flashes during a long-lasting Current in a Plasma Focus Device", Nuclear Fusion 187 (1978)
- [2] J. Salge, et al., "Neutron Pulse-Train Generation in a Plasma Focus Device powered by a long-lasting Current", 2nd Int. Conf. on Energy Storage, Compression and Switching, Venice, 1978
- [3] B. Fell, "Über den repetierenden Betrieb von Plasmafokus-
kusanordnungen bei Speisung mit eingeprägten Stromimpulsen langer Dauer", Thesis, TU Braunschweig, 1981, to be published.

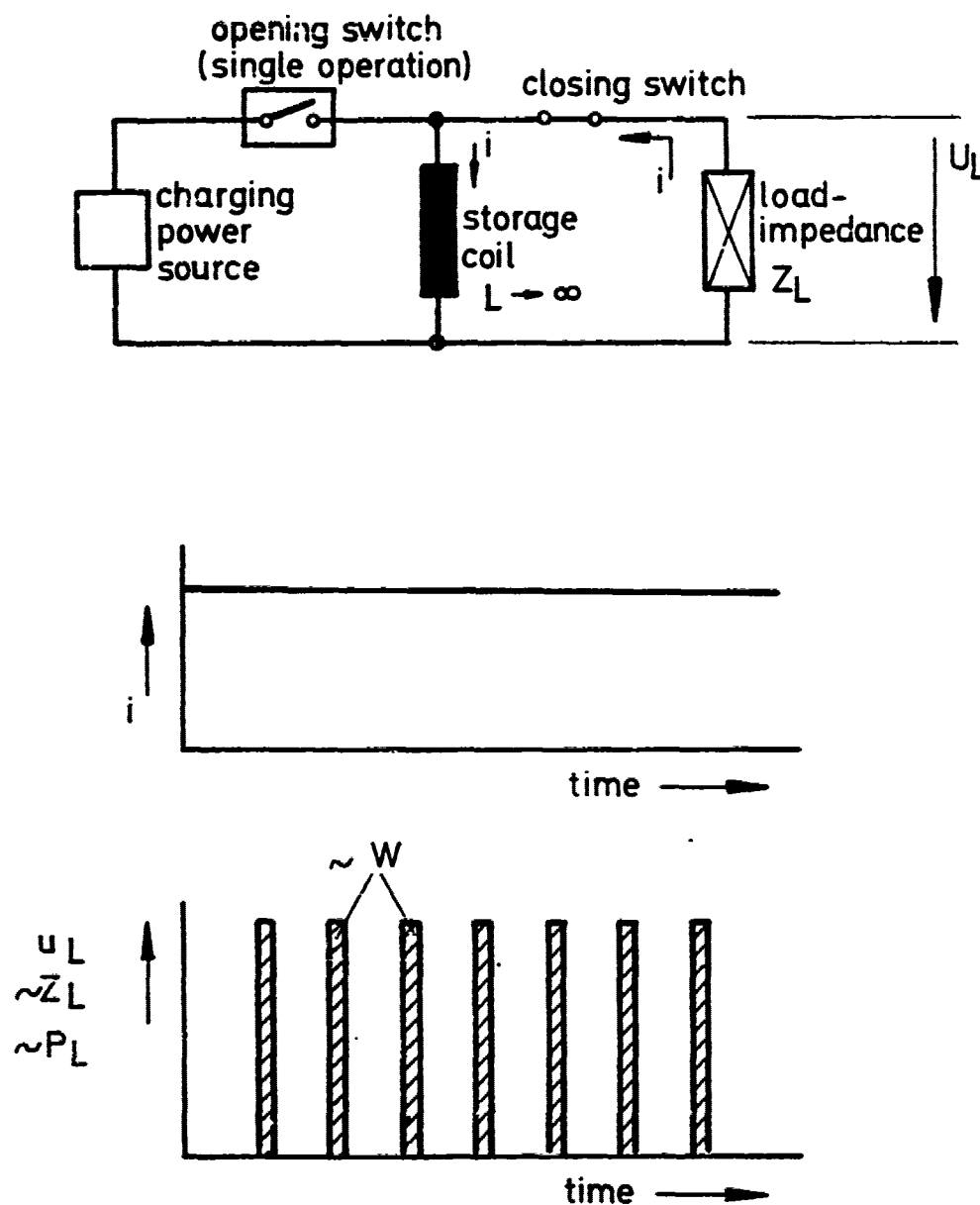


Fig. 1. Repetitive Mode of an Inductive Energy Storage System

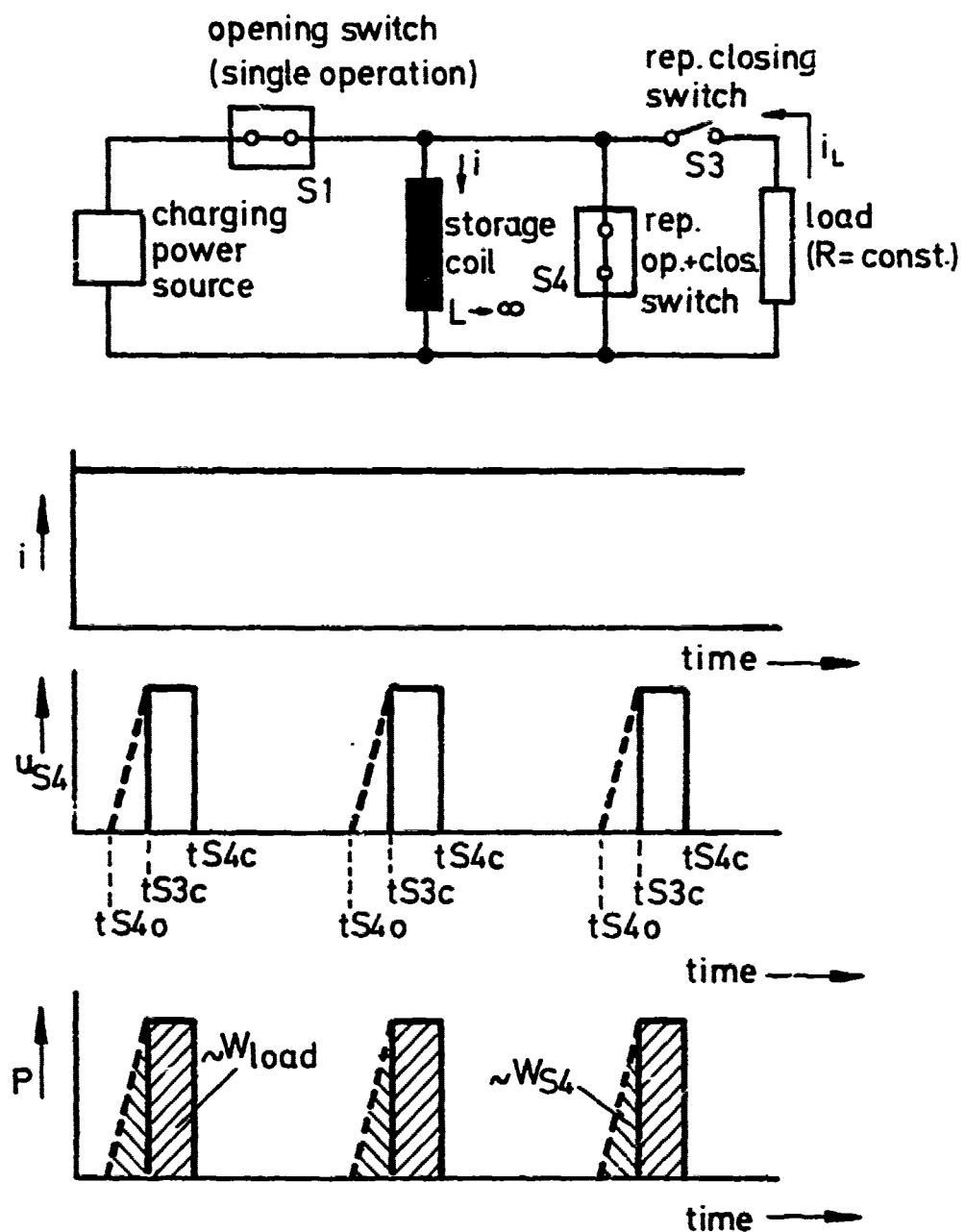


Fig. 2. Repetitive Mode of an Inductive Energy Storage System with Ohmic Load

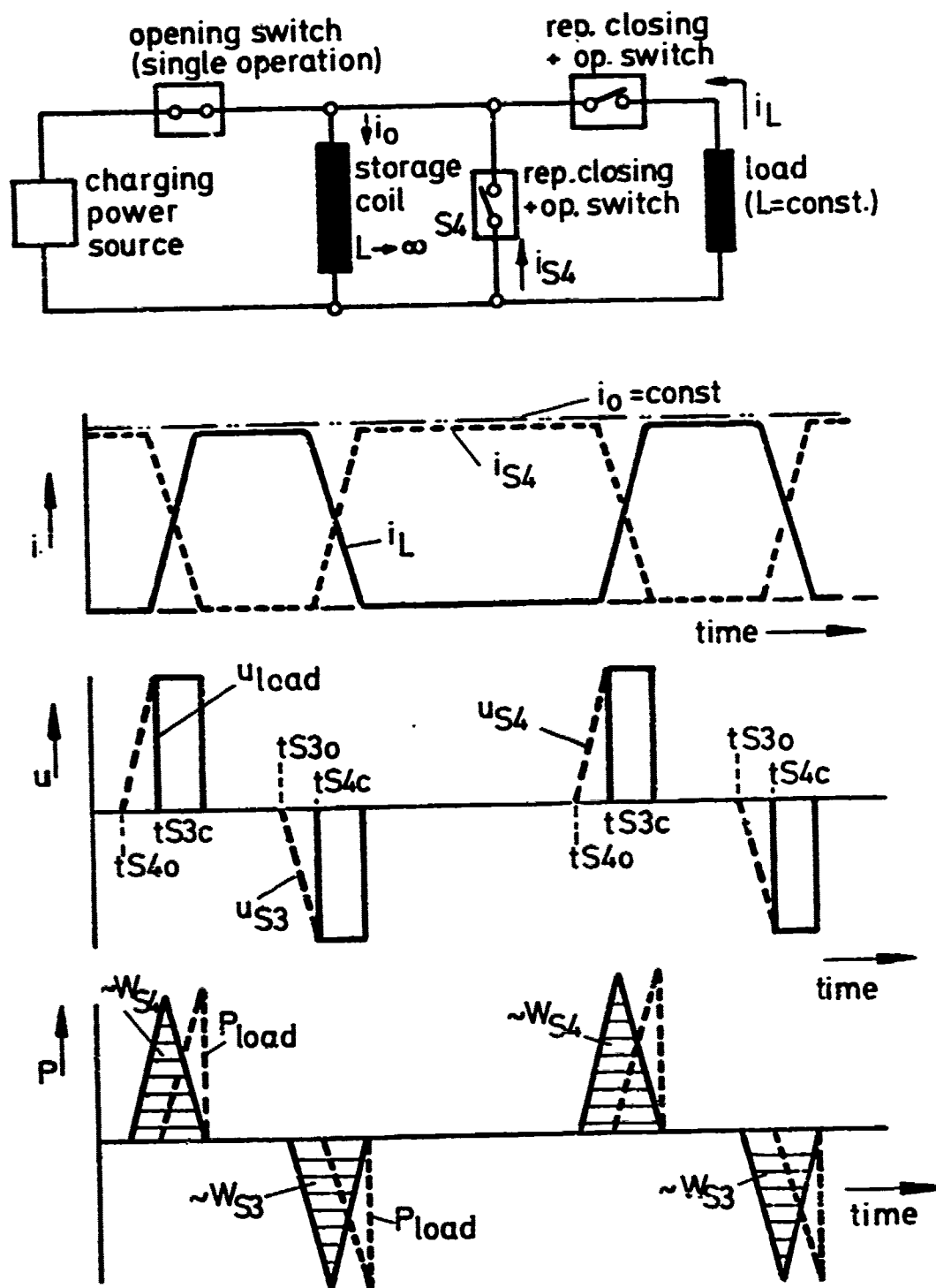


Fig. 3. Repetitive Mode of an Inductive Energy Storage System with Inductive Load

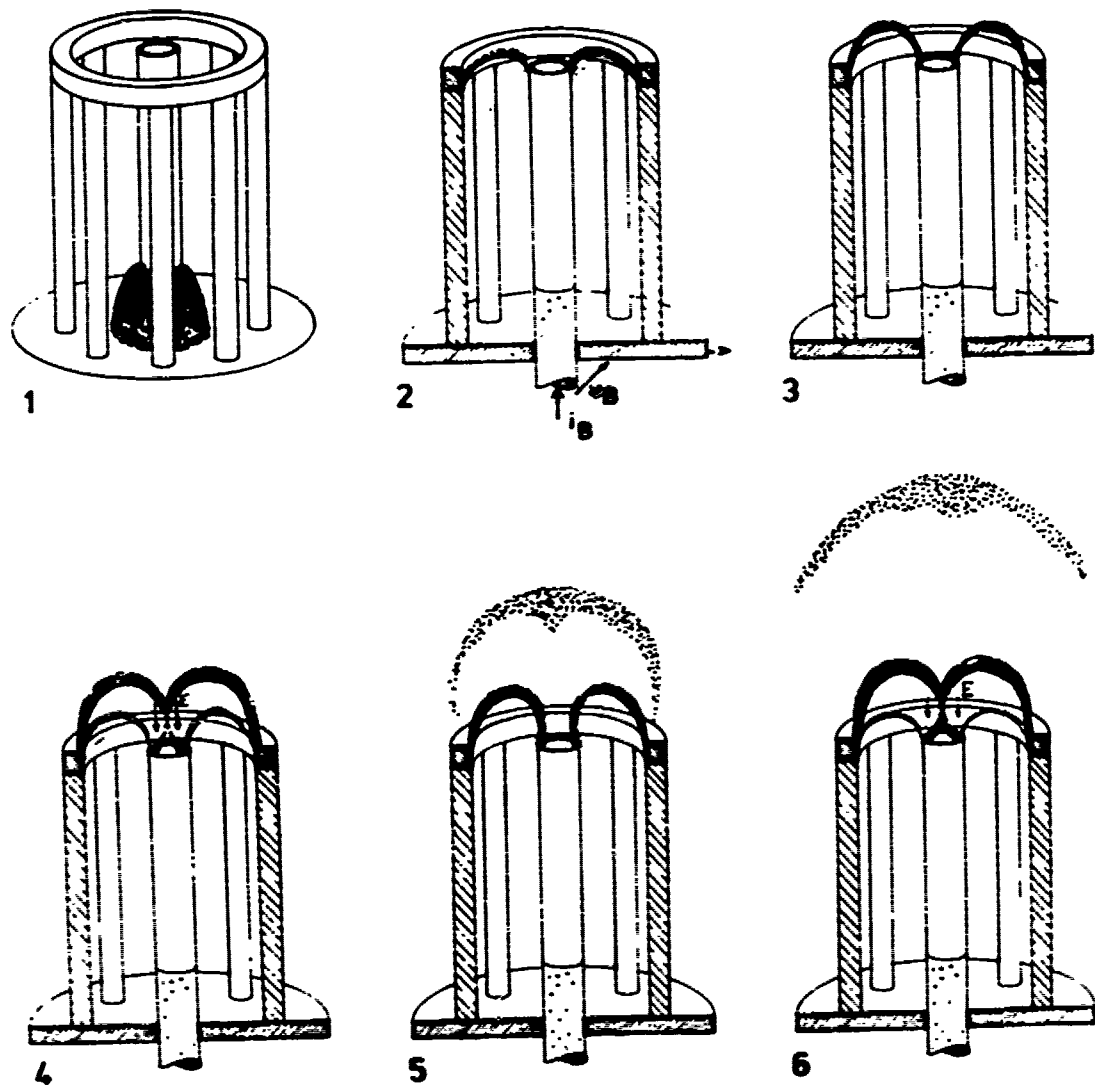


Fig. 4. Repetitive Operation of a Dense Plasmafocus

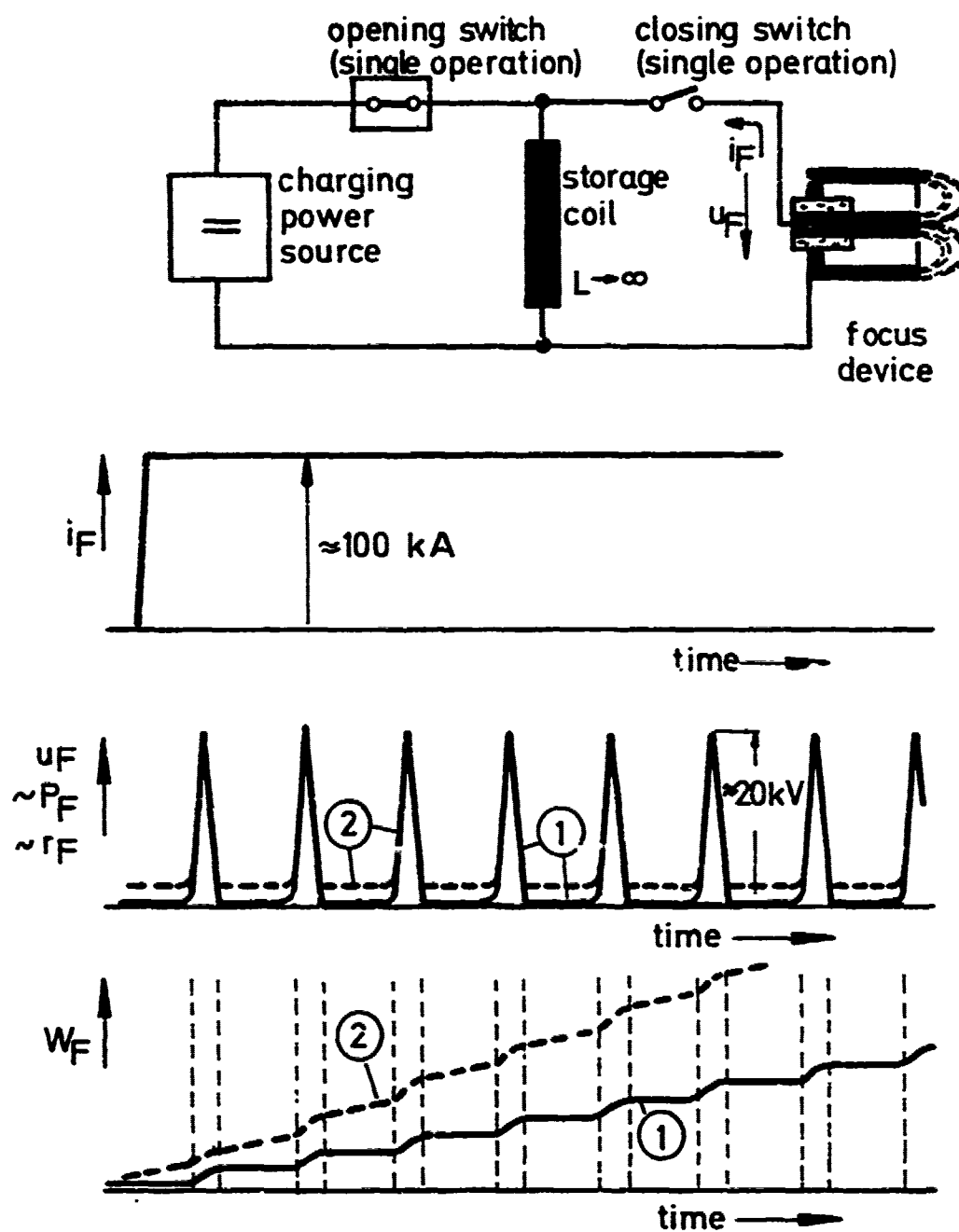


Fig. 5. Ideal Operation of a Repetitive Plasmafocus Device

- ① Losses between 2 Focus-Events = 0
- ② Losses between 2 Focus-Events = finite

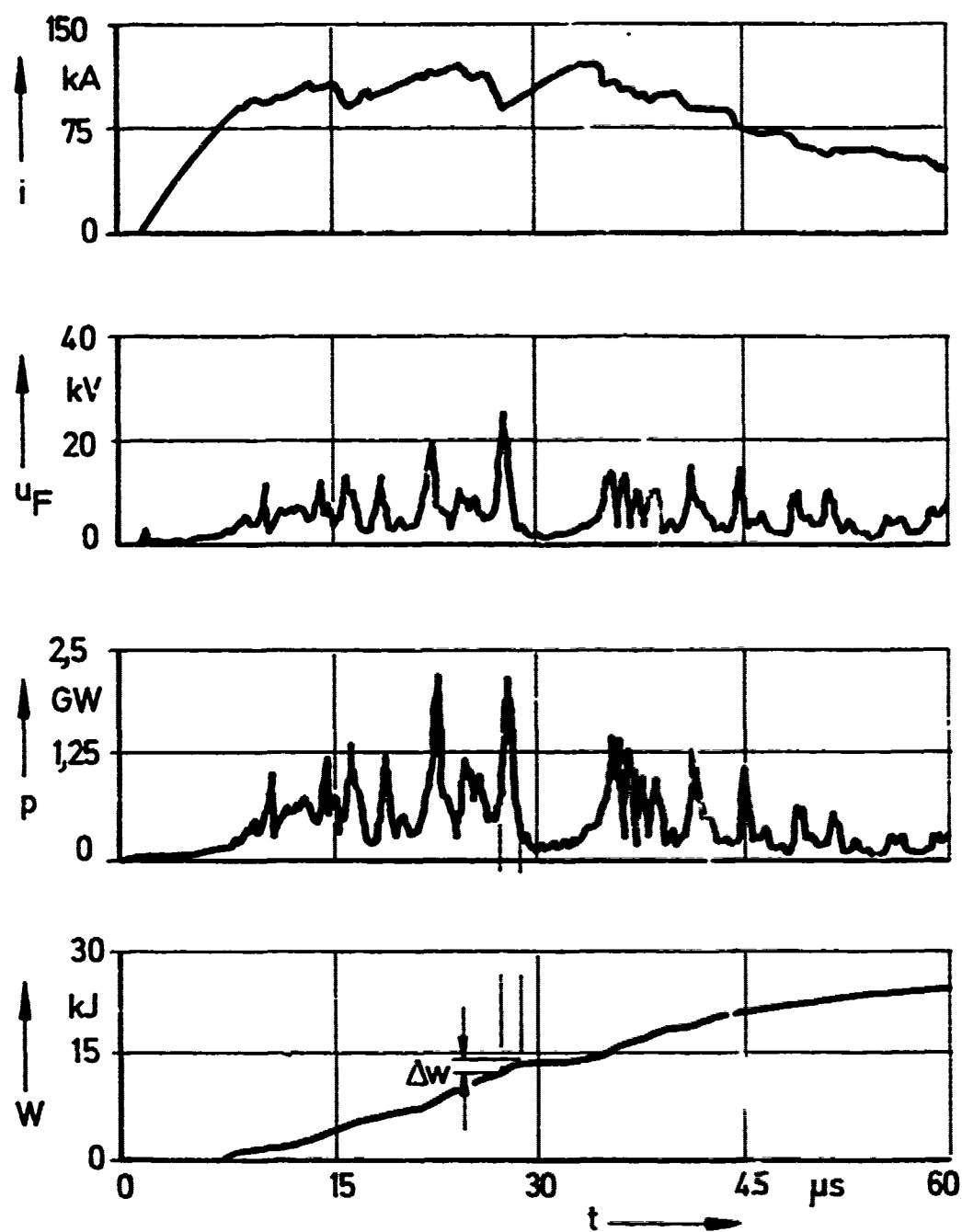


Fig. 6. Current i , Voltage u_F , Power P , and Energy W Versus Time during a Repetitive Operation of a Plasmafocus
Gas: Deuterium, $p = 1$ mbar

OPENING SWITCHES FOR VACUUM INDUCTIVE STORAGE

V. Bailey, J. Creedon, L. Demeter, and
D. Sloan

Physics International Company
San Leandro, California 94577

ABSTRACT

Two opening switches for vacuum inductive stores are described. Both switches eliminate the basic limitation on power flow per unit area caused by insulator breakdown in conventional pulsed power technology.

The staged implosion plasma switch is a $\vec{J} \times \vec{B}$ or \vec{L} switch. The experimental operation of this plasma switch and its voltage multiplying and plasma heating characteristics are described for capacitor bank energies < 180 kJ, currents $\lesssim 3$ MA, and switch opening times of 50-100 ns. An analytical model of the staged implosion is in agreement with the experimental data.

The reflex switch is an ion-enhanced switch in which ions are produced and accelerated within the switch. The ions form a neutralizing background for an electron current that can be orders of magnitude greater than the Langmuir-Child current appropriate for an ordinary diode. Several methods for opening the reflex switch are suggested.

Extrapolation of both switches to multimegajoule bank energies predicts generation of ~ 100 TW pulses delivered in tens of nanoseconds or less. Suggestions for repetitive operation of both switches are discussed.

A. INTRODUCTION

A vacuum inductive storage system with an opening switch offers a very important advantage in addition to its much lighter weight and reduced volume. By performing pulse compression and power amplification in vacuum next to the load, the basic limitation on power flow per unit area (or dI/dt) caused by insulator breakdown^[1] in conventional or mainline pulsed power technology is eliminated. Vacuum magnetic storage allows use of the much higher values of power per unit area that can be achieved with magnetic insulation in vacuum.^[2,3,4] Energy can be transported through an insulator into a vacuum at a relatively low power over a long period of time. This energy is stored as magnetic field energy and is then converted into a short, high-power output pulse when the switch opens.

This paper discusses two opening switches for vacuum inductive stores. Experimental data and scaling laws have been obtained for the first of these switches, the staged implosion plasma (SIP) switch.^[5] Experiments to transfer the vacuum magnetic store to an independent load connected in parallel with the SIP switch have not been attempted, but this transfer appears feasible. The operation of the second, i.e., the reflex switch,^[6,7,8] as an opening switch has never been demonstrated experimentally. However, available theoretical and experimental evidence strongly suggests that it will function as an opening switch.

The SIP switch is a $\vec{J} \times \vec{B}$ or \dot{L} plasma switch that slowly accelerates (small \dot{L}) a heavy foil mass while charging the store, and rapidly accelerates (large \dot{L}) a fraction of this mass during the opening phase. The switching plasma is generated between coaxial electrodes from self-supporting

foils or gas puffs and is not lifted off an insulator. The switch efficiently transfers capacitive energy into magnetic field energy (65- to 70-percent efficiency). The change in impedance between the charging phase and the opening phase is large (≥ 30). The operation of the SIP switch, its voltage multiplying and plasma heating characteristics, have been studied for capacitor bank energies < 100 kJ, currents < 3 MA, and switch opening times as short as 50 to 100 ns. An analytical model that assumes planar motion in the charging phase and collapse of 10 percent of the plasma mass agrees with the experimental data. Extrapolation to multi-megajoule bank energies predicts generation of ~ 60 TW pulses delivered to a load in < 10 ns. Puffed gas streams are suggested as a replacement for the existing thin foils in the switch. If this proves feasible, the switch could, in principle, be repetitively pulsed.

The reflex switch consists of a cathode-anode-virtual cathode configuration in which electrons emitted from the cathode pass back and forth through a thin anode foil where they scatter and lose energy. Ions flow from the anode to the cathode. A magnetic field (orthogonal to the anode) is used to keep electrons from scattering out of the switch. In the closed mode, the total current can be orders of magnitude greater than the Langmuir-Child current for an ordinary diode.^[6,7] The switch operates essentially as a constant voltage device in the closed mode. The switch opens when the virtual cathode is removed and the diode impedance reverts to the ordinary Langmuir-Child bipolar value. The switch opening time is expected to be on the order of an ion transit time, at velocities characteristic of voltage across the switch during the closed mode. Conceptual design studies of a vacuum inductive storage system consisting of a 10-MJ bank and reflex switch predict delivery of ~ 100 TW, 30 to 60 ns pulses to both an imploding plasma and focussed diode load.^[9] For repetitive operation, it may be possible

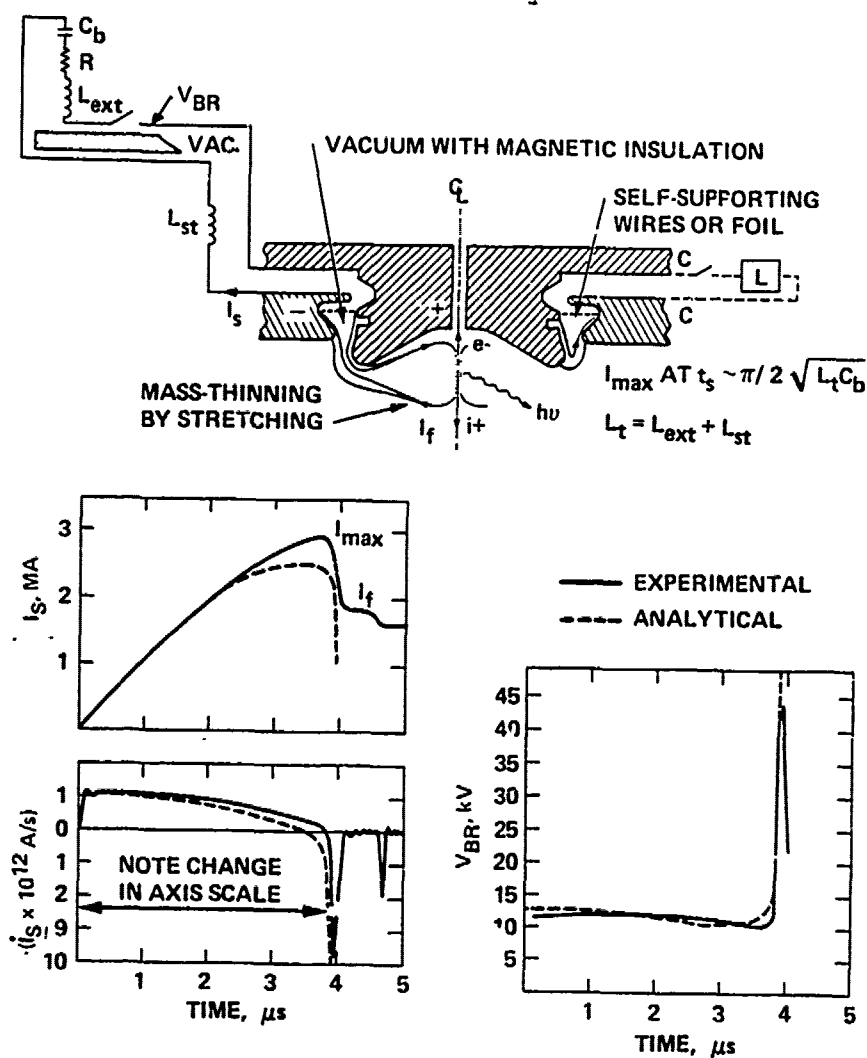
to replace the anode foil with a high-pressure jet (as used in aerodynamic windows) or a puffed gas jet. We have examined several potential opening techniques for the reflex switch. All appear to be compatible with repetitive operation.

B. STAGED IMPLOSION PLASMA SWITCH

1. Switch Operation.

The design of a plasma switch for vacuum magnetic energy stores is shown in Figure 1. The switching plasma is generated between coaxial electrodes from thin wires or foils, which connect a storage inductor, L_{ST} to an external capacitor bank, C_b . During the current rise, the heavy plasma is axially accelerated by $j_r B_\theta$ forces. When maximum current is reached, this plasma is guided to arrive at the tip of the center electrode, where a small fraction of the original mass implodes toward the axis.

Because energy absorption by the slow-moving plasma (i.e., $\int_0^t \dot{L} I^2 / 2 dt \approx KE$) is low during the current buildup, conversion from capacitive to magnetic energy is very efficient. Conversely, the rapid, radial collapse phase is associated with very high \dot{L} and \ddot{L} values. Since the current carrying, fast-stretching plasma sheaths cannot be replenished from the vacuum environment, "density thinning" occurs, which further enhances the rate of implosion.[10] The staged dynamics of the plasma motion, with its sudden jump in \dot{L} , makes this plasma device a useful opening switch for magnetic energy storage systems. In its switching stage it produces a short-lived, dense plasma column at the axis with large $\vec{v}_r \times \vec{B}_\theta$ axial electric fields. The resultant voltage spike is distributed along the inductance of the circuit and can be used to drive high currents into a nearby



81-2414

Figure 1 Design and electrical parameters of the plasma switch at $E_b \approx 140$ kJ.

low-impedance vacuum load connected to carefully chosen taps on the magnetic energy store ("C" in Figure 1).

2. Experimental Results and Scaling.

Operation of the plasma switch and its voltage multiplying and plasma heating characteristics have been studied at up to 180-kJ bank energy. For energies between 50 and 180 kJ the aluminum foils used in the switch had a thickness of 0.5 μm . These foils were mounted between concentric electrodes with diameters of 12 cm and 7.5 cm. Below 50 kJ, fine wires were employed. The experimental findings are described briefly below.

1. Within 300 ns after switching the capacitor bank energy to the inductive circuit, the foil became vaporized and ionized. With increasing current, the magnetic forces accelerated the plasma in the axial channel, leaving magnetically insulated electrodes and unspoiled vacuum conditions behind. The shape and size of the electrodes were adjusted to match the charging time to the quarter period of the switch circuit, $\tau_S \sim (\pi/2) [L_T C_b]^{1/2}$.
2. Depending on store inductance, ($L_{ST} \sim 7\text{--}22$ nH), the plasma sheath reached the end of the center electrode (2.0 to 2.5 cm long) within 4 to 6 μs , with maximum current of 2.5 to 3.0 MA and axial velocity of 3 to 5 cm/ μs . Peak currents corresponded to as high as 80 to 85 percent of the short circuit value calculated for a stationary foil, making the plasma switch an efficient (65 to 70 percent) capacitive-to-inductive energy converter.
3. At the tip of the center electrode, the curving inner edge of the plasma sheath was subjected to a

rapidly increasing radial force, $\vec{j}_z (1/r) \times \vec{B}_\theta$ ($1/r$), and imploded toward the axis. This sudden radial collapse involved only a small fraction (< 10 percent) of the original foil mass, the bulk of which was still slowly moving in the axial direction. In the stretching plasma loops, the areal density decreased and radial velocities of 15 to 20 cm/ μ s were attained. These velocities produced a 20- to 30-fold increase in \dot{L} impedance ($\dot{L}_{\max} \approx 0.15 \Omega$). The fast inductance change choked the current at a rate of 10^{13} A/s to a final value of ~ 60 percent of the maximum.

4. The voltage spikes (V_s) measured at accessible points on the magnetic store were as high as nine times the bank voltage (V_b). The voltage-multiplying capability (V_s/V_b) scaled with bank energy (E_b) as $\sim E_b^{0.75}$. The observed scaling is shown in Figure 2.
5. The pulsewidths of the voltage spikes scaled with bank energy as $\sim E_b^{-0.75}$ (see Figure 2). Typical pulse durations of 50 to 70 ns were measured for the 180-kJ switch.
6. Judged from radiation images on the wall of the vacuum chamber and X-ray pinhole photographs, the pinched plasma was ~ 0.4 cm in diameter and 2 to 3 cm long.

3. Analytical Model.

The switch plasma has been modeled to be a highly conducting plasma sheet accelerated by $\vec{j} \times \vec{B}$. During the charging phase while the plasma is moving between the fixed electrodes, the dynamics have been modeled both as a motion

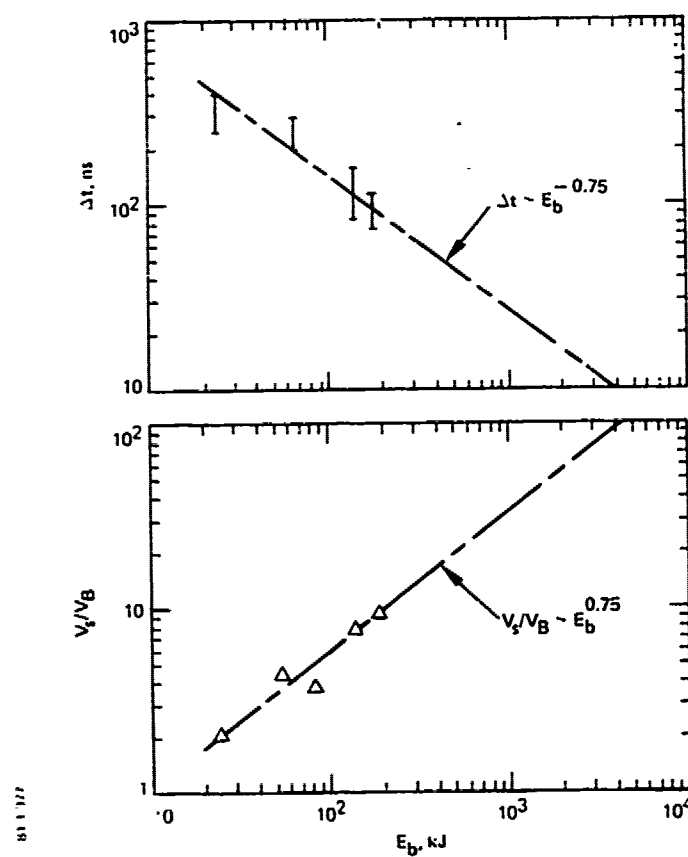


Figure 2 Scaling of voltage multiplication and pulse width as a function of capacitor bank energy.

to reflect the $1/r^2$ variation of magnetic field pressure, and as a uniform (i.e., independent of r) axial motion. In the switching phase, most of the plasma mass continues to move axially, while a small portion, m^* , implodes toward the axis. The analytic model assumes that the axial length of the collapsing sheet varies as $1/r^2$. Since the mass per unit area of plasma changes as r and the magnetic pressure as $1/r^2$, the radial collapse accelerates as $1/r^3$.

Models for the dynamics of the plasma sheet were coupled to the electrical circuitry (Figure 1) of the capacitor bank and inductive store. Results of the numerical code were compared with experimental data for an initial bank energy of 97 kJ to select the proper model and determine m^* . A model in which the plasma sheet moves independently of r during the charging phase and m^* equals 10 percent of the original foil mass, agreed the best.

Predictions by this model for a bank energy of 142 kJ are shown in Figure 1. The model provides a reasonable description of experimental results up until the end of the implosion, when thermal pressure of the pinch formation on axis (neglected in the model) becomes important. The measured maximum switch voltage and $|dI/dt|$ correspond closely to those predicted by the code, when the calculated stagnation pressure becomes equal to the magnetic pressure. The calculated radius of the collapsing plasma when this occurs is 1.2 cm. The model predicts a collapse velocity of 13 cm/ μ s, which agrees with the experimentally measured value of ≈ 15 cm/ μ s. It also concurrently calculates an inductance of $L_{SC} = 4.5$ nH and $\dot{L}_{SC} = 0.11$ ohm for the imploding portion of the switch and 6 nH and 0.005 ohm for that portion of the plasma sheet not participating in the collapse. Therefore, although their inductances are comparable, the rates of change of the switch inductance and voltage multiplication are dominated by the collapsing plasma.

The fastest portion of the plasma sheath near the axis produces the highest voltage ($\dot{I}_{SC} I_S$). This voltage was computed to be 230 kV, which is ~ 1.5 times larger than that measured at the initial foil mounts.

4. Extrapolation to Larger Magnetic Energy Systems.

The voltage producing property of the plasma switch will be affected by connecting an external load to the magnetic store. The impedance of the plasma switch should decrease since part of the current from the magnetic energy store will be diverted through the load in parallel with the switch. The reduced current through the switch will lead to a smaller radial collapse velocity and a proportionately smaller \dot{I}_S . Consequently, lower switch voltages and wider pulse widths can be expected.

Figure 3 shows a preliminary design of crossover electrodes for connecting the magnetic energy store to an external load in parallel with the SIP switch. The load circuit includes a closing switch to hold voltage off the load during the charging phase of the inductive store.

To investigate the effect of connecting the load, the code described above was upgraded to include a load in parallel with the switch. The code was then used to extrapolate the switch behavior to larger magnetic energy systems. Calculations were made for a 10-MJ bank with a SIP switch, driving a vacuum load with a fixed impedance of 0.1Ω . The electrical parameters of the system are shown in Figure 4.

As expected, the pulsewidth of the switch widened by an approximate factor of two when the load was included in the calculation. The results are shown in Table 1. The first column summarizes the results for the standard switch configuration already described. The second column summarizes

81-1-370

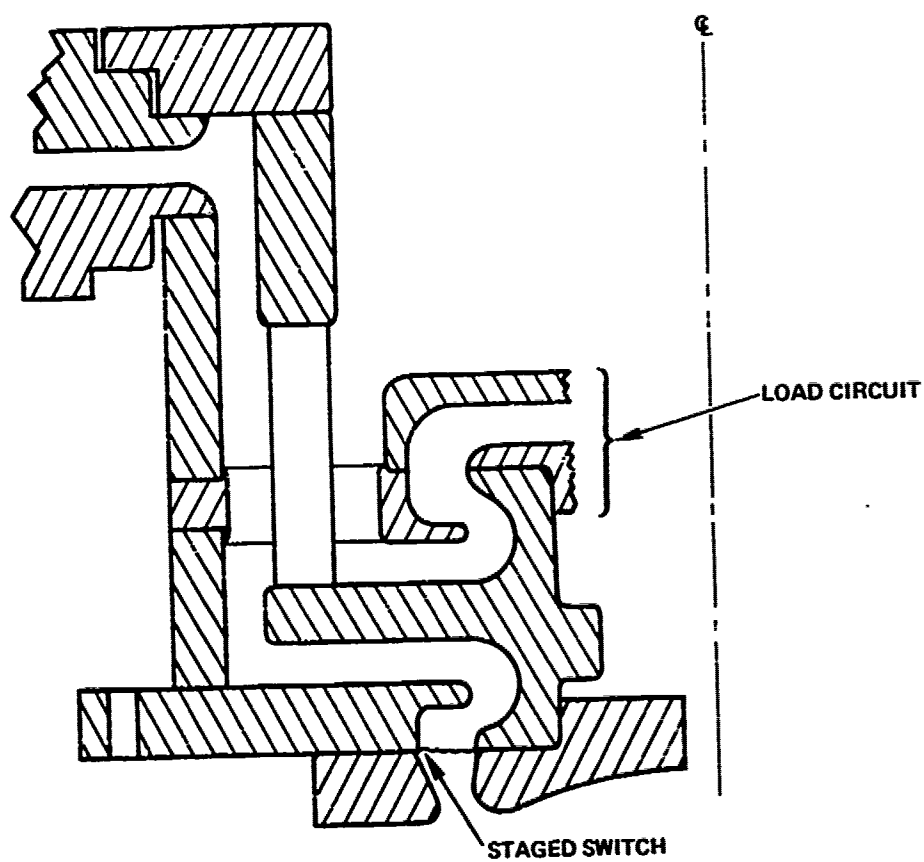


Figure 3 Connection of magnetic energy store to external load circuit.

81-136S

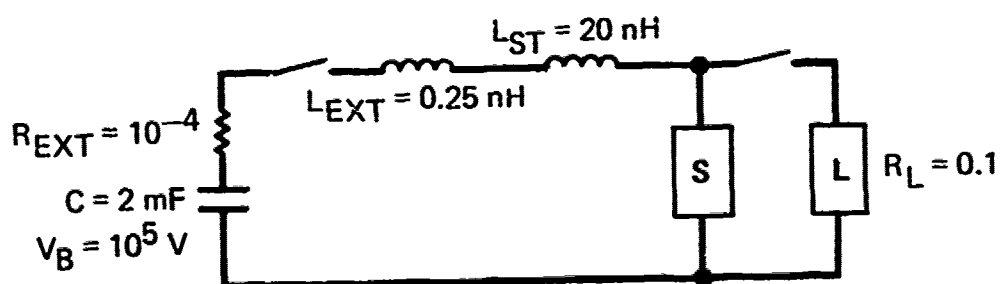


Figure 4 Electrical parameters for 10 MJ system.

Table 1 Summary of calculations for a 10-MJ capacitor bank and staged implosion plasma switch driving a 0.1- Ω load.

	<u>No Screen</u>	<u>Screen</u>	<u>Resistive Phase with Screen</u>
Charging Time	9.4 μ s	9.5 μ s	9.4 μ s
FWHM of Power to Load	115 ns	7.5 ns	7 ns
Maximum Power	14.2 TW	33.3 TW	58 TW
Current at Peak Power	11.8 MA	12.7 MA	19.2 MA
Energy Delivered to Load	1.2 MJ	250 kJ	414 kJ

the power pulse delivered to the load when an inductance-reducing screen (placed beneath the center electrode of the SIP switch) is included in the calculation. The screen clearly shortens the pulse and increases the power to the load at the expense of delivered energy.

It has long been observed in DPFs that the pinched plasma on axis passes through a phase where effective plasma column resistance is anomalously high. When a model for such resistance is included in the calculation, the power delivered to the load and the efficiency of energy transfer increase. The results are summarized in column 3 of Table 1.

The SIP switch is also appropriate for driving imploding plasma loads. In this application, the small fraction of original foil mass imploded toward the axis becomes the load. In our experiments, 35 percent of the initial bank energy was coupled to the imploding plasma load. The scaling of such an application to large capacitor bank energies is shown in Table 2. For a 10-MJ system, five megajoules of energy can be coupled to the imploding plasma at a power level of ~ 90 TW. The efficiencies, power levels, and currents of this system make it an attractive alternative to the more conventional superterawatt generator method for driving imploding plasma loads.^[11]

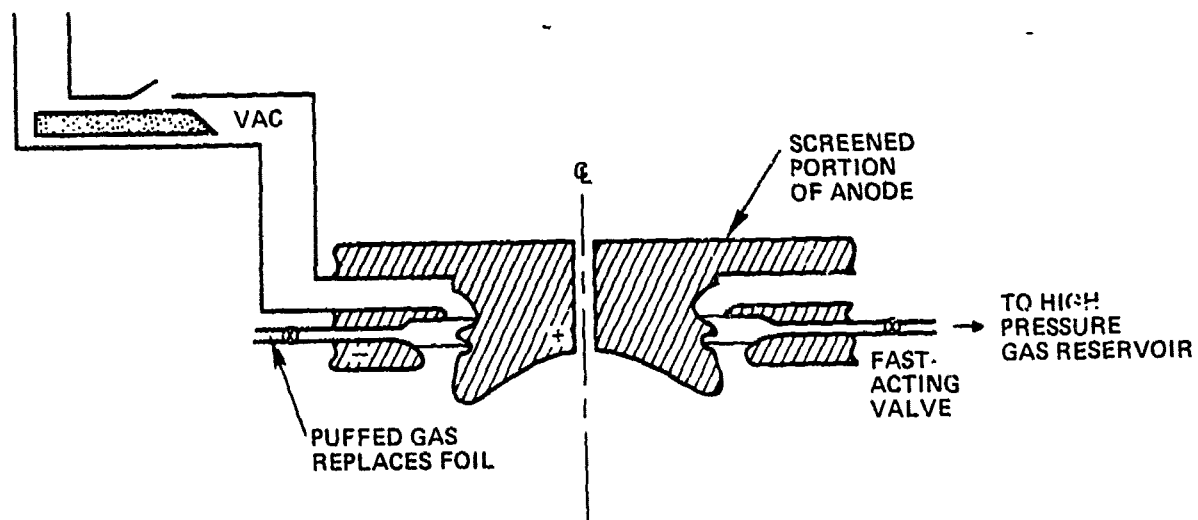
5. Repetitive Operation.

For repetitive operation of the SIP switch a puffed gas would replace the existing foil. A conceptual sketch of such a system is shown in Figure 5. Further analysis and experiments would be required to determine whether it is more appropriate to puff the gas in from the inner or outer electrode.

Table 2 Scaling of SIP switch as imploding plasma load.

<u>Bank Energy</u>	<u>180 kJ*</u>	<u>1.44 MJ</u>	<u>10 MJ</u>
Peak Current in Imploding Plasma	3 MA	14.3 MA	38.2 MA
Percent of Bank Energy Coupled to Imploding Plasma	35%	50%	50%
Peak Power Delivered to Imploding Plasma	0.7 TW	40 TW	90 TW
Power Amplification	22	60	50

*Existing experimental results.



81-1316

Figure 5 Conceptual design of repetitive staged implosion plasma switch.

There would be a continuous gas input during the charging phase of the vacuum inductor as the current increases to a peak value. It is doubtful that a single puff activated prior to current initiation could provide enough mass to keep the switch closed in the charging phase without contaminating the vacuum store.

During the closed phase, the arc acts as a $\vec{J} \times \vec{B}$ plasma accelerator. The arc cannot move downward because gas is continuously being injected. A downward motion would cause an $(\dot{L} I)$ voltage between the electrodes and restrike would occur in the gas being injected behind the arc. The switch opens when the fast-acting valve is closed. Since there would no longer be any gas input, restrike could not occur, and the plasma would accelerate downward, leaving magnetically insulated electrodes and unspoiled vacuum conditions behind. The subsequent implosion would then open the switch.

Two types of repetitive switch operation can be envisioned. The first, and most assuredly the slowest, is to recycle the switch between each cycle. The SIP switch does facilitate this by accelerating most of the mass downward where there is a large volume available for pumping.

Another repetitive mode of operation, the burst mode, may also be possible. This mode would use a large inductive store, and continuous gas input would occur during the charging phase. The first switch opening would occur when the fast-acting valve is closed. For a large inductive store and proper load conditions, only a fraction of the energy in the store would be diverted to the load when the switch opens. After it has opened for the first time, much of the energy would still reside in the inductive store. A small amount of gas would then be puffed between the

electrodes, shorting the switch again. This gas would then be ionized, accelerated downward and imploded, producing the second voltage pulse. The current in the store would be further reduced and energy transferred to the load. The puffing, downward motion, and implosion of the plasma could be repeated until energy in the inductive store is depleted. The current in the inductive store is brought down in steps. Conceptual time sequencing of such a system is shown in Figure 6.

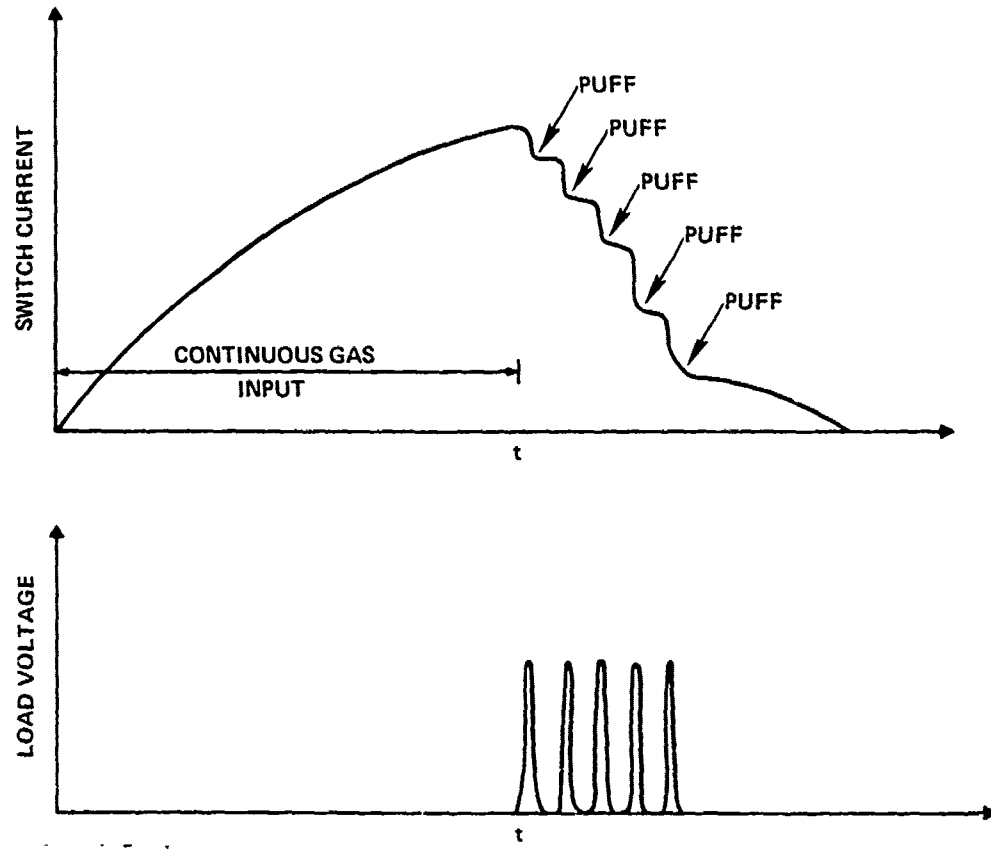
The SIP switch has the potential for repetitive operation. However, more experimental and theoretical investigation is required before a meaningful assessment can be made.

C. REFLEX SWITCH

1. Switch Operation and Related Experimentation.

Operation of a reflex triode as an opening switch has never been demonstrated experimentally. However, theoretical and experimental evidence that is available strongly suggests that this device will function as an opening switch.

Figure 7 shows the basic configuration, in which a cathode-anode-virtual cathode arrangement reflects electrons through the anode foil where they scatter and lose energy. An applied magnetic field orthogonal to the anode is used to keep electrons from scattering out of the triode. Positive ions are then accelerated from the anode to the cathode. This arrangement forms the closed mode. The total current can be orders of magnitude higher than the Langmuir-Child current for the same anode-cathode spacing.^[6,7] In this mode, the switch operates essentially as a constant voltage



81-1-367

Figure 6 Conceptual time sequencing of SIF switch operating in theburst mode.

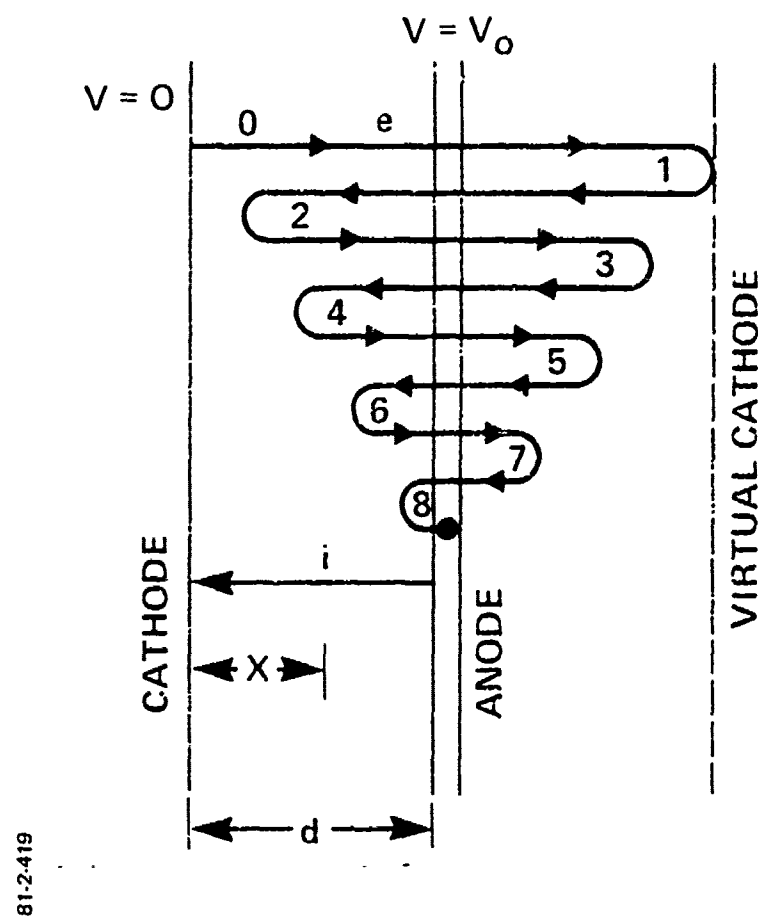


Figure 7 The basic reflex triode configuration.

device. Use of the reflex triode as a switch has been described by Creedon, et al.[8,9]

Experiments by Prono,[7][12-14] using the reflex triode as an ion source, have demonstrated several of the unique properties this device has in the closed mode. Reflex triodes in these experiments have operated with current densities of up to 50 kA/cm^2 , voltages of 60-100 kV, and anode-cathode spacings as large as 6 cm. The observed current density was $> 10^4$ times the bipolar Langmuir-Child value. Experimentally, the switch functioned as a constant voltage device, with the voltage being determined by the areal density of the anode (lower areal densities produce lower voltages). Impedance was found to be independent of gap spacing and only a weak function of cathode area. Recent theory and data by Prono suggest the feasibility of charging times in the microsecond range.

When opening the switch, the virtual cathode is eliminated, thereby stopping reflexing, and the device reverts to the ordinary bipolar flow mode. A large voltage increase accompanies the transition to the "open" switch mode. This transition in operating conditions was observed by Prono, et al.[7] when a voltage increase of $> 800 \text{ kV}$ occurred at a current level of $\sim 300 \text{ kA}$. Calculations have predicted changes in switch impedance of $\sim 10^2$ - 10^3 between the closed and open modes.

A schematic of the reflex switch in the open and closed modes is shown in Figure 8a and 8b.

2. Inductive Storage Systems with a Reflex Switch.

Computational studies have suggested that inductive storage systems using the reflex switch are capable of efficiently driving a wide variety of loads. A few of these

81-2-413

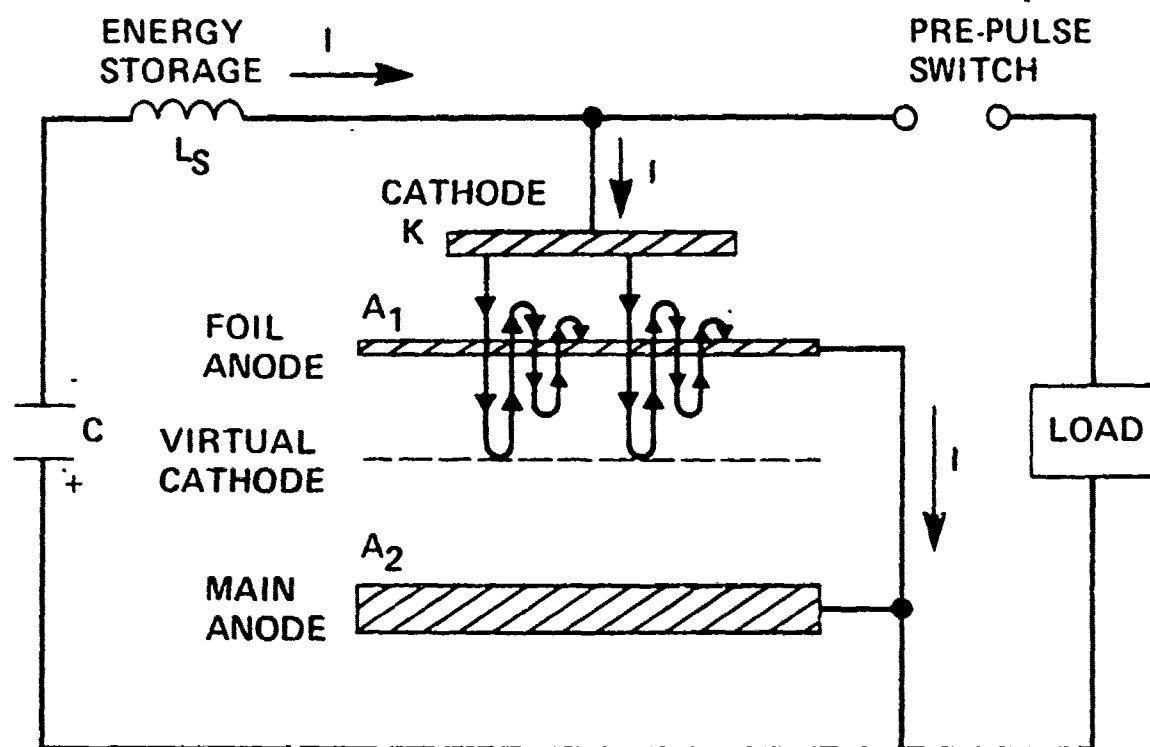


Figure 8a The reflex switch in the "closed" mode.

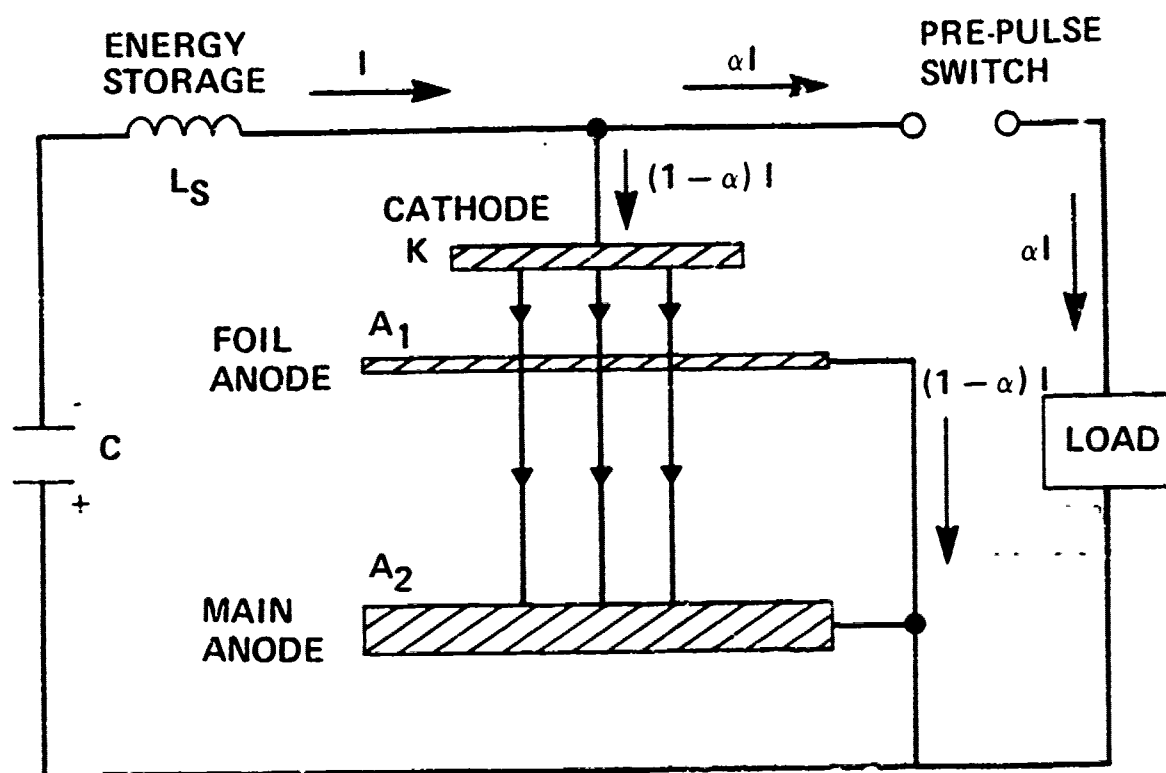


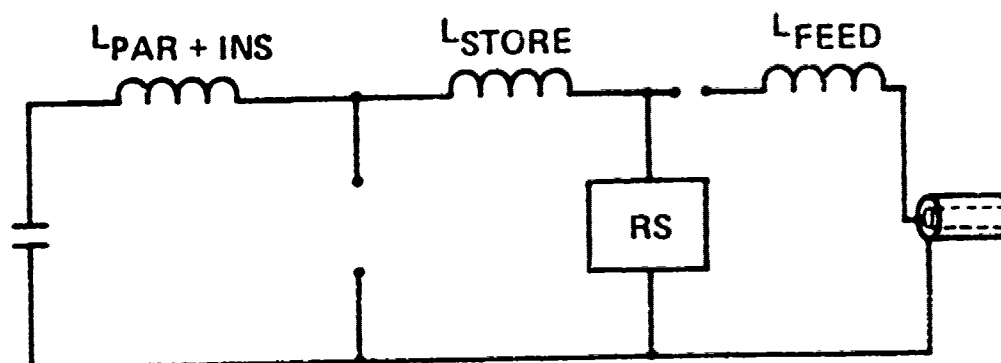
Figure 8b The reflex switch in the "open" mode.

are: 1) imploding plasma loads, 2) focussed diode loads, and 3) high-voltage diodes with flat voltage pulses for application to free electron lasers.

We have designed realistic, self-consistent inductive store systems using the reflex switch to drive imploding plasma loads. Figure 9 shows the equivalent circuit, which has been analyzed numerically. $L_{\text{par} + \text{ins}}$ represents the inductance of the capacitor bank and the insulator separating the dielectric region from the vacuum region. Insulator flashover can be included in the calculation. Energy is stored in L_{store} and switched by the reflex switch, RS. The opening time of the reflex switch has been modeled by assuming movement of an ion sheath from the anode back to the cathode at velocities determined by the voltage across the switch. The inductance of the vacuum feed between the switch and the load is represented by L_{FEED} . Load inductance is included in the model for the imploding plasma.

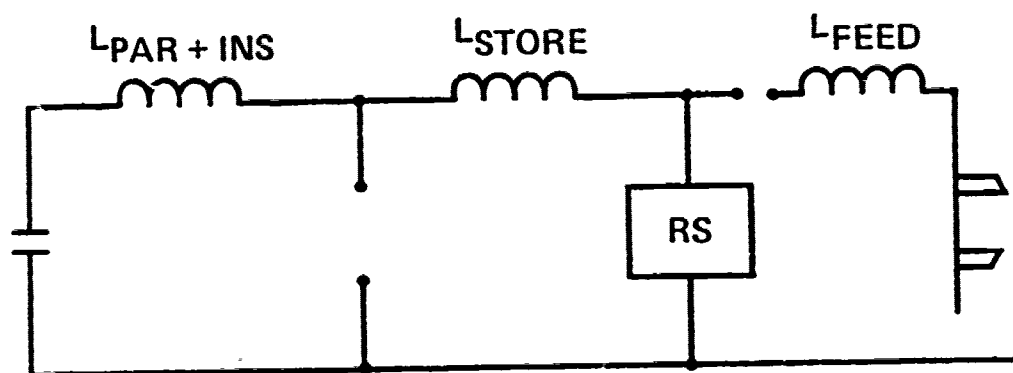
Figure 9 gives the parameters achievable for two low-voltage capacitor banks (120 kV). Magnetic insulation is always maintained in both cases; the radius of the vacuum insulator is ~ 27 cm for the 1.44-MJ bank and 35 cm for the 10-MJ case. Plasma parameters for the load are on the order of hundreds of kJ/cm of kinetic energy attained at implosion. Radii of high-voltage vacuum insulators with conventional pulsed power generators would be several meters by comparison. Small vacuum gaps would be required to minimize the feed inductance. They may, however, cause loss of magnetic insulation.

Self-consistent designs have also been obtained for focussed diode loads. In this case, analytical expressions for the relationship between voltage and current in the diode are used in the numerical calculations. Figure 10 summarizes the parameters achievable for the same two low-



BANK ENERGY	<u>1.44 MJ</u>	<u>10 MJ</u>
MAXIMUM CURRENT IN IMPLoding PLASMA	9.7 MA	24.1 MA
PERCENT OF BANK ENERGY COUPLED TO K. E. OF IMPLoding PLASMA	22%	26%
PERCENT OF BANK ENERGY COUPLED TO LOAD	30%	34%
MAXIMUM POWER DELIVERED TO LOAD	23 TW	106 TW
POWER AMPLIFICATION	27	47

Figure 9 Reflex switch driving imploding plasma loads.



BANK ENERGY	<u>1.44 MJ</u>	<u>10 MJ</u>
MAXIMUM CURRENT IN FOCUSED DIODE	9.5 MA	33.4 MA
PEAK POWER OF FOCUSED DIODE	26 TW	85 TW
IMPEDANCE AT PEAK POWER	0.29 Ω	0.076 Ω
PERCENT OF BANK ENERGY DELIVERED TO DIODE	36%	32%
PULSE WIDTH	43 ns	60 ns
POWER AMPLIFICATION	29	32

Figure 10 Reflex switch driving focused diode loads.

voltage capacitor banks. Once again, magnetic insulation is always maintained in each. When diode impedance is doubled to 0.15Ω for the 10-MJ bank, peak power is ~ 170 TW and peak voltage, ~ 5 MV. These parameters would be of definite interest for ion-beam-pellet irradiation experiments.

The efficiency of the system was limited by anode foil technology in both the imploding plasma load and focussed diode systems. If a plasma anode can be substituted for the foil anode, the efficiencies quoted in Figures 9 and 10 would increase dramatically. Gas puff experiments at PI make this possibility appear feasible.

These previous examples point out the potential and the utility of the reflex switch.

3. Repetitive Reflex Switch Operation.

To operate the reflex switch repetitively, a gaseous anode would replace the anode foil used with the reflex triode in present experiments. The gaseous anode could be provided either by a puffed gas or high-pressure continuous gas jet (Figure 11). Similar types of technical problems are being faced by LLNL for ATA and the laser community in designing an aerodynamic window for high-pressure lasers. As mentioned previously, experiments at PI suggest that the puffed gas anode may also be feasible.

The potential for repetitive reflex switch operation depends on which of the several proposed opening schemes proves most appropriate. Several of these schemes are shown schematically in Figure 12.

In Scheme 1 (Figure 12), no virtual cathode is formed. Initially, the electrons are emitted from cathode C, pass through anode A, and are deposited in structure C'. Struc-

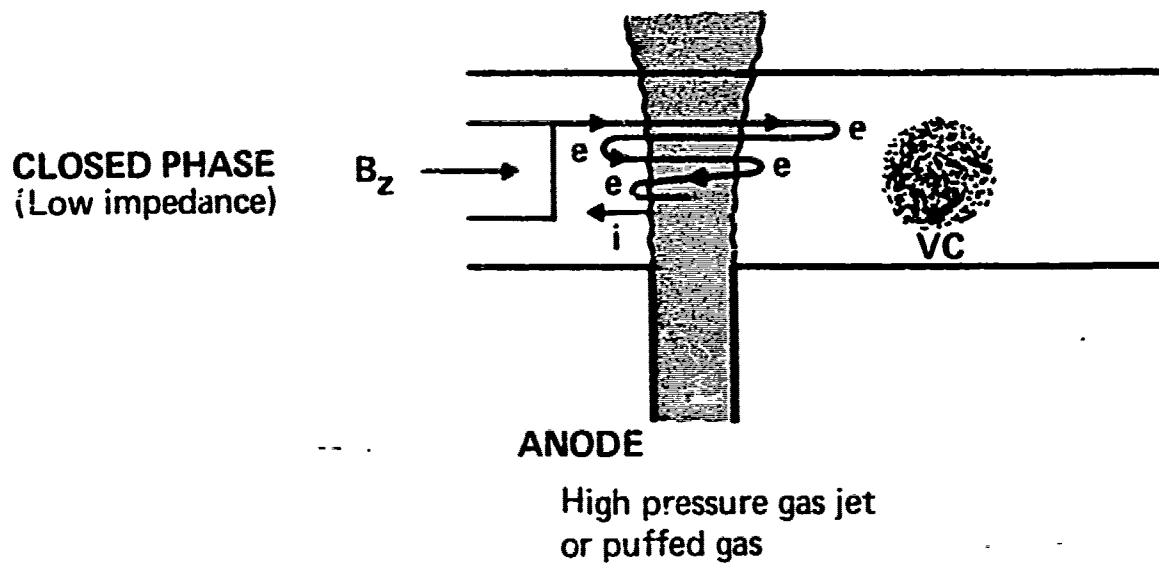


Figure 11 Gaseous anode for reflex switch.

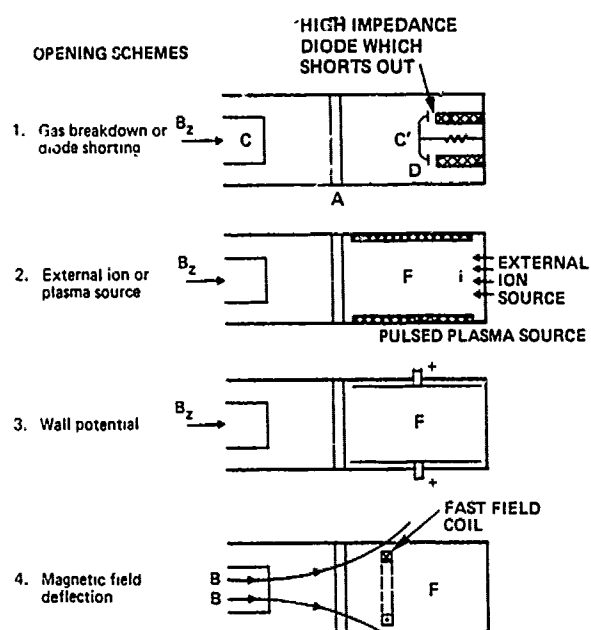


Figure 12 Several possible opening schemes for the reflex switch.

ture C' is connected to ground through a high-impedance resistor and vacuum diode. As charge is deposited in C', voltage builds up to approximately that of cathode C. The build-up of voltage on C' causes the electrons to reflect back through the anode foil. Positive ions are accelerated from the anode to the cathode, and the switch functions in the normal closed mode.

The voltage build-up on C' causes electrons to be emitted from C' and to flow across vacuum gap D. The impedance of this diode is chosen so that only a small amount of charge is drained off C'. The switch opens when plasma motion shorts out vacuum gap D. The structure C' is then connected directly to ground through D. Electron reflexing stops and switch impedance increases to the value given by bipolar Langmuir-Child flow between cathode C and anode A.

The reflex switch in Scheme 1 will remain closed until vacuum gap D is shorted by plasma motion. The amount of time the switch remains closed is adjusted by changing gap spacing D. Larger gap spacings will produce longer operation in the closed mode. Repetitive reflex switch operation for Scheme 1 (Figure 12) will then be limited by the recovery time of vacuum gap D.

In the second scheme, the virtual cathode is destroyed by either of two techniques. The first possibility is to inject ions from an external source into chamber F to destroy the virtual cathode. Since the ion current density within the reflex switch itself is very large, it is doubtful that a sufficiently efficient and intense ion source could be provided. The second technique creates a pulsed plasma at the surface of chamber F to open the switch. The virtual cathode within chamber F causes a radial electric field. When the high-density plasma is produced at the edge of the chamber, the electric field accelerates the plasma

ions inward, and the virtual cathode is eliminated by the neutralizing ions. The repetitive switch operation in Scheme 2 Figure 12) will then be determined by the time required to evacuate the cavity after pulsing the plasma source.

In opening Scheme 3, the virtual cathode is eliminated by adjusting the potential in the chamber. During the closed phase of the switch, the electrodes shown in the sketch are held at ground potential, the same potential as the anode. A small amount of current flows from the virtual cathode to the end of chamber F. The leakage current is given approximately by Bogdankevich and Rukhadze's formula^[15] for space charge limited flow in a strong B_z field. This limiting current can be increased by adjusting the potential of the wall, increasing the beam voltage, or decreasing the gap between a grounded wall and the beam. In Scheme 3, the switch is opened by pulsing the electrodes positive. This can significantly increase the leakage current and may eliminate the virtual cathode by depleting the charge. This scheme has the potential for a high repetition rate.

The final scheme suggested for eliminating the virtual cathode is use of a fast magnetic field coil. During the closed phase, the coil is inactive. The switch is opened by activating the fast magnetic coil, which bucks the initial B_z field. This causes the field passing through the anode to diverge radially outward and intersect the wall shown in Figure 12, opening Scheme 4. Electrons emitted from the cathode then follow the magnetic field line outward and intersect the wall, thus, eliminating the virtual cathode. Repetitive operation of this proposed opening scheme will then be limited by the cycle time of the fast magnetic field coil.

D. CONCLUSIONS

The staged implosion plasma switch and the reflex switch are promising candidates for use with vacuum inductive stores. Both switches have a large change in impedance and are capable of transferring large amounts of power to a variety of loads. Repetitive operation of both switches also appears feasible. Most importantly, both require more experimental and theoretical investigation before their full potential can be realistically assessed.

REFERENCES

- [1] L. I. Rudakov, "Transport of a relativistic electron beam to a fusion target," *Sov. J. Plasma Phys.* 4 (1), 40, Jan-Feb 1978.
- [2] J. M. Creedon, "Magnetic cutoff in high-current diodes," *J. Appl. Phys.* 48, 1070 (1977).
- [3] M. S. DiCapua, D. Pellinen, P. D. Champney, "Magnetic insulation in triplate vacuum transmission lines," Proceedings of the 2nd International Topical Conference on High-Power Electron and Ion Beam Research and Technology, (Cornell University, Ithaca, N.Y.), Oct 3-5, 1977, p. 781.
- [4] D. H. McDaniel, J. W. Poukey, K. D. Bergeron, J. P. Van Devender, D. L. Johnson, "Power flow studies of magnetically insulated lines," *Ibid.*, p. 819.
- [5] L. J. Demeter and V. L. Bailey, Proceedings of the 2nd International Conference on Energy Storage, Compression and Switching, Venice, Italy, Dec 5-8, 1978. (To be published.)
- [6] J. M. Creedon, I. D. Smith, D. S. Prono, "Method of generating very high intense positive-ion beams," *Phys. Rev. Letters* 35, 91 (1975).
- [7] D. S. Prono, J. M. Creedon, I. Smith, N. Bergstrom, "Multiple reflections of electrons and the possibility of intense positive-ion flow in high v/α diodes," *J. Appl. Phys.* 46, 3310 (1975).

- [8] J. M. Creedon, S. D. Putnam, J. D. Smith, "Plasma Reflex Discharge Device," U.S. Patent No. 4080549 (1978).
- [9] J. M. Creedon, B. A. Lippmann, V. L. Bailey, "The reflex switch - An opening switch for use with magnetic energy storage," Proceedings of the 2nd International Conference on Energy Storage Compression and Switching, Venice, Italy, Dec 5-8, 1978. (To be published.)
- [10] V. Bailey, L. Demeter, J. Benford, A. Noeth, and D. Sloan, Physics International Final Report, DNA 3680F-2 (1975).
- [11] S. Putnam, C. Stallings, K. Childers, R. Schneider, I. Roth, J. Creedon, V. Bailey, T. S. T. Young, "Recent developments in fast Z-pinch plasma production using superterawatt generators," Proceedings of the 3rd International Topical Conference on High-Power Electron and Ion Beam Research and Technology. Novosibirsk, U.S.S.R, July 3-6, 1979.
- [12] D. S. Prono, H. Ishizuka, B. Stallard, W. C. Turner, "LLL's long pulse reflex diode ion source (IPINS)." Bull. Amer. Phys. Soc. 23, 903, Sep. 1978.
- [13] D. S. Prono, H. Ishizuka, B. W. Stallard, W. C. Turner, "Charge-Exchange Neutral Atom Filling of Ion Diodes: Its Effect on Diode Performance and A-K Shorting," Lawrence Livermore Laboratory, Report No. UCRL-84438, July, 1980.
- [14] D. S. Prono, J. W. Shearer, R. J. Briggs, "Pulsed ion diode experiments," Phys. Rev. Letters 37, 21 (1976).

VACUUM INTERRUPTERS AND THYRATRONS
AS OPENING SWITCHES*

E. M. Honig
Los Alamos National Laboratory
University of California
P. O. Box 1663
Los Alamos, NM 87545

ABSTRACT

The clear advantages of inductive storage for large scale energy storage applications are creating an increasing interest in the research and development of the opening switches required. Opening switches for single-shot inductive transfers have received considerable attention and are fairly well advanced. The problem addressed by this workshop of high power opening switches for high repetition rate applications is much more severe, however, and may well require a major research and development effort.

This paper will discuss two candidates for such an opening switch: the triggered vacuum interrupter and the magnetically quenched thyatron. By electrically retriggering the discharge in the vacuum interrupter between pulses, the dependence on mechanical motion is eliminated. This should enable repetition rate operation at 10-15 kHz while still maintaining the vacuum interrupter's proven interrupting performance of tens of kiloamps at tens of kilovolts.

The magnetically quenched thyatron, on the other hand, uses a cross magnetic field to raise the switch impedance by decreasing the electron mobility and driving the discharge into an arc chute wall where it is quenched. Successful interruptions of 1 kA at 15 kV and 100 A at 50 kV after conduction for 10 μ s have been demonstrated by previous researchers. Work at Los Alamos is directed toward understanding the basic mechanisms involved and increasing the switch ratings, particularly the conduction time.

*Work performed under the auspices of the US Department of Energy.

INTRODUCTION

Utilization of inductively-stored energy almost always requires the interruption of a dc current with an opening switch. The various types of opening switches may be divided into two general classes, depending upon their operation. In the direct interruption class, the impedance of the opening switch is rapidly increased to cause the current to transfer to a lower impedance load. In the counterpulse class, the switch current is temporarily counterpulsed to zero with an auxiliary circuit to allow the switch to return naturally to its off state. The capacitor inserted by the auxiliary circuit then recharges to force the current transfer to the load. While the counterpulse technique can be used with almost any type of closing switch, it works best with switches that recover rapidly.

A switch from each of these classes is proposed for high-power, high rep-rate applications. In the counterpulse class, the addition of a trigger system to the high-power vacuum interrupter should enable high rep-rate operation. In the direct interruption class, the addition of an arc chute to a high rep-rate thyatron enables the current to be interrupted by the application of a cross magnetic field.

Triggered Vacuum Interrupter

For high power opening switch applications, the mechanically-actuated vacuum interrupter is a leading candidate [1,2]. The vacuum interrupter, which is used extensively in utility distribution systems, consists of two electrodes (1 stationary and 1 movable) inside a vacuum envelope, as shown in Fig. 1. A bellows maintains the vacuum around the movable electrode while the shield prevents the ceramic wall from being coated with a metal film which would eventually short out the switch. The switch is closed when the electrodes are in contact. The contact resistance of 10-35 $\mu\Omega$ gives very low conduction losses. Interruption is achieved by opening the contacts to form a vacuum arc and then forcing the arc current to zero with a counterpulse [3,4]. The electrode gap recovers if the current zero is held long enough to allow plasma deionization (3-15 μs). The current zero time is usually extended with a series saturable reactor. Highly reliable (>90%) operation of single vacuum interrupters has been demonstrated to levels above 40 kA and 30 kV (simultaneously) [5,6], while 60 Hz operation has been reported at 200 kA rms [7] and at 115 kV peak [8]. An axial magnetic field is necessary to operate above about 25 kA [9-11].

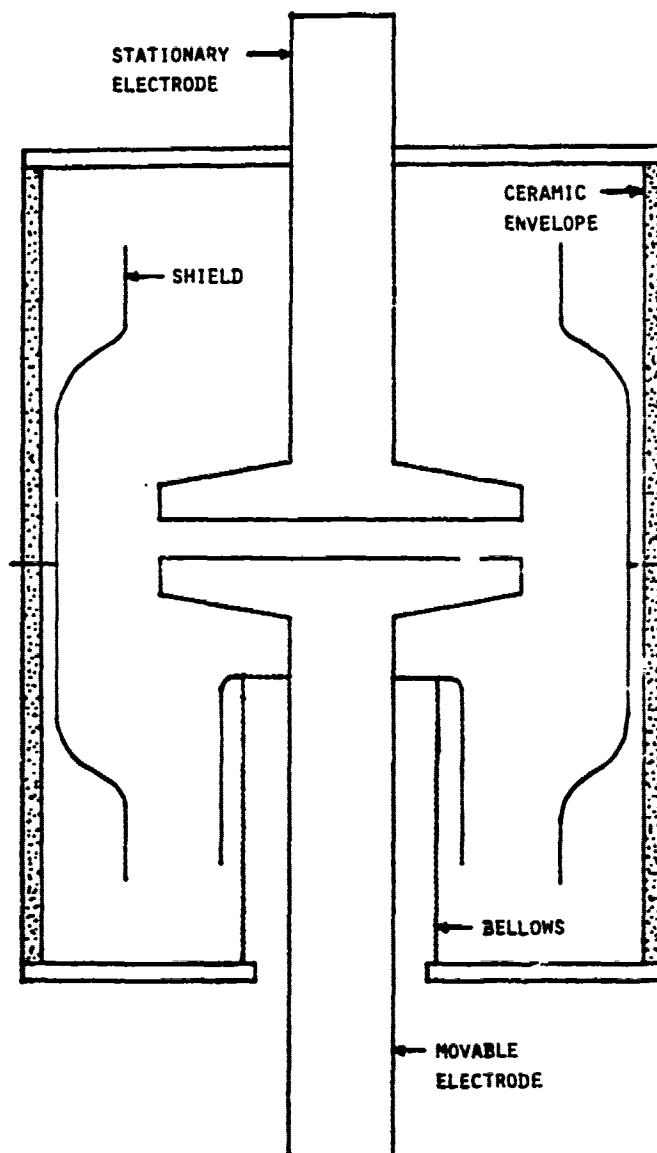


Fig. 1. Standard vacuum interrupter.

For repetitive duty, the standard vacuum interrupter is limited to about 50 Hz because the electrodes must be moved mechanically for each opening and closing operation. To achieve higher repetition rates, a triggered vacuum interrupter is proposed. The triggered vacuum interrupter would be operated exactly like a standard one during the coil charging period and the first output pulse. Between pulses, however, it would be closed electrically by retriggering the arc rather than mechanically closing the contacts. The low arc drop of 25-40 V is still less than the conduction drop of most other types of switches. After the last output pulse, the contacts are closed mechanically to give a very low resistance path for coil recharging. This operational sequence is shown in Fig. 2.

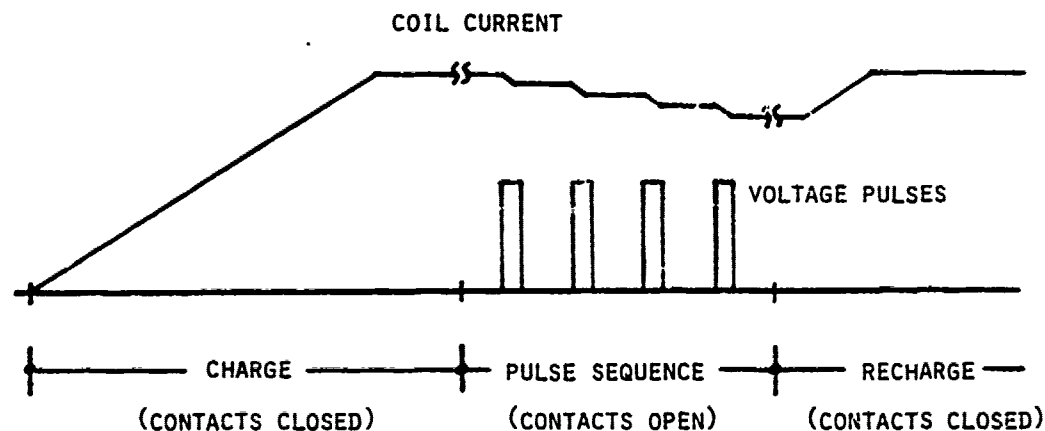


Fig. 2. Voltage and current waveforms typical of rep-rate transfers from inductive storage.

The triggering method developed for the vacuum arc switch [12-14] and for the triggered vacuum gap switch [15-18] appears to be well suited for the vacuum interrupter also. The method depends upon surface flash-over across an insulator to create a plasma to break down the gap. In the vacuum arc switch (Fig. 3) an insulator separating the cathode and a trigger electrode are coated with a thin metal film from the vacuum arc. A high voltage pulse applied to the trigger electrode vaporizes the metal film and generates sufficient plasma to break down the gap.

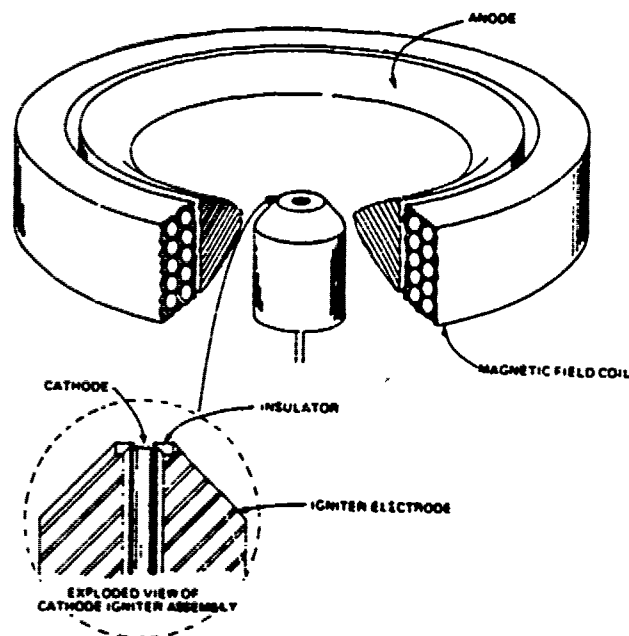


Fig. 3. Vacuum arc switch triggered by the surface flashover mechanism [13].

The surface flashover trigger can be incorporated into the structure of a vacuum interrupter in several ways. One method is to install an insulating ring and trigger electrode around the stationary electrode (Fig. 4) or in a hole at the center of the electrode as is done in triggered vacuum gaps. Plasma generated from an insulator surface in this location would be able to rapidly enter the electrode gap region and cause breakdown. This location for the insulator, however, subjects it to the same mechanical shock and heat stress seen by the main electrodes and could lead to premature failure of the trigger system.

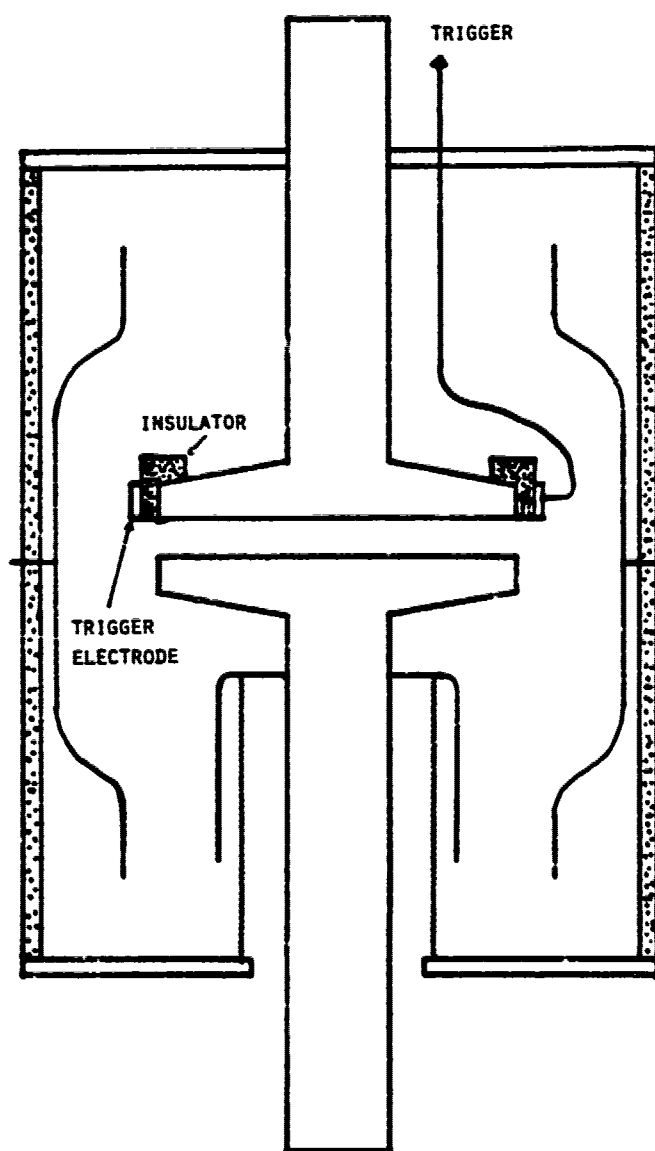


Fig. 4. Vacuum interrupter with trigger system on main electrode.

A triggering system which would be relatively immune to these problems is possible by incorporating the insulator into the shield structure (Fig. 5). The two halves of the shield are separated by an insulator but are electrically shorted through an external resistor to keep them at equal potentials except during the trigger pulse. While the second method would probably result in somewhat longer trigger delays because of the greater distance to the main electrode gap, it is expected that both methods could provide triggering of a vacuum interrupter with delays on the order of a μ s or less.

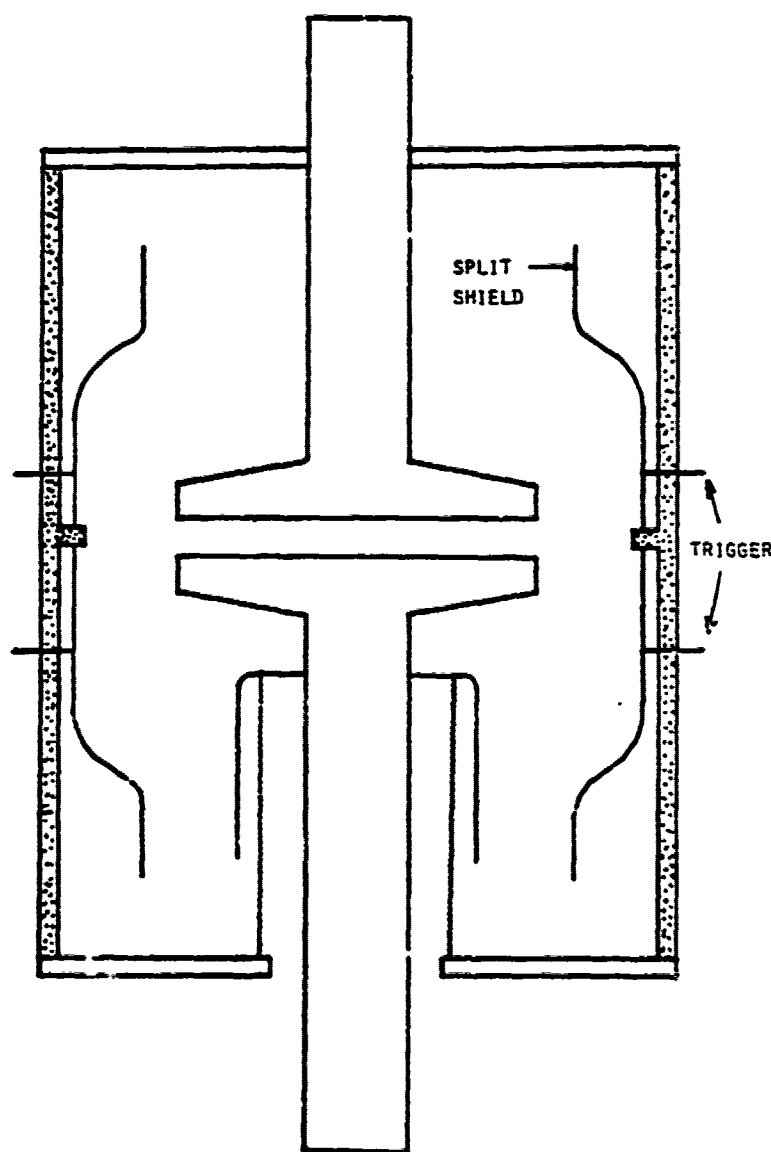


Fig. 5. Vacuum interrupter with trigger system in shield.

The repetition rate of the triggered vacuum interrupter is limited by the minimum counterpulse delay time, that is, the total time required to counterpulse the switch current and recharge the counterpulse capacitor (Fig. 6). The counterpulse delay time, therefore, is given by

$$T_{\text{delay}} = T_{\text{fall}} + T_{\text{hold}} + T_{\text{rise}} \quad (1)$$

where

T_{fall} = fall time of switch current after counterpulse applied,

T_{hold} = hold time of current zero (switch deionization time), and

T_{rise} = recharge time of counterpulse capacitor.

For a system where the load is isolated during the counterpulse recharge (to provide a fast-rising output pulse), the counterpulse voltage risetime is related to the current fall and hold times (from charge considerations) by the relation

$$T_{\text{rise}} = T_{\text{hold}} + 0.5 T_{\text{fall}} \quad (2)$$

Substituting Eq. (2) into Eq. (1) gives

$$T_{\text{delay}} = 2 T_{\text{hold}} + 1.5 T_{\text{fall}} \quad (3)$$

As an example, if one assumes that

$$T_{\text{hold}} = T_{\text{fall}} = 20 \mu\text{s} \quad (4)$$

(typical of vacuum interrupters in single-shot transfer systems), then the total counterpulse delay time is 70 μs and the repetition rate cannot exceed 14 kHz.

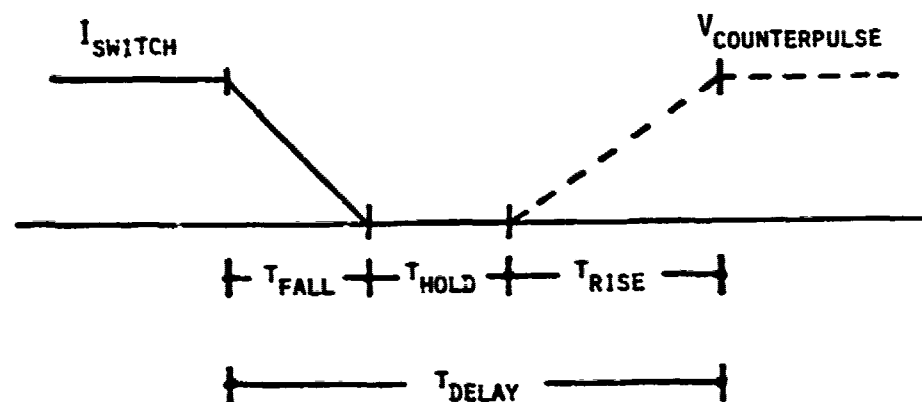


Fig. 6. Switch current and recovery voltage waveforms during counterpulse.

From these equations it can be seen that the minimum counterpulse time (and therefore, the maximum repetition rate) depends almost equally on the deionization time (a switch problem) and on the counterpulse current fall time (a circuit problem). If it is assumed that the fall time can be made much less than the hold time by proper circuit design, then the required switch deionization time becomes the limiting factor for rep-rate operation. With its rapid recovery time (3-15 μ s), the vacuum interrupter is an ideal candidate for high rep-rate operation with the counterpulse technique, assuming that the triggering problem can be solved.

Magnetically Quenched Thyatron

Another opening switch which may prove itself for high power, high rep-rate duty is the magnetically-controlled, surface-quenched, current-interrupting thyatron. The magnetically quenched thyatron behaves much like a standard thyatron on closing but can be opened by applying a cross magnetic field to decrease the electron mobility and drive the discharge into a ceramic arc chute located between the grid and cathode. Contact with the arc chute cools and deionizes the plasma, increasing its impedance and producing the high voltage required for transfer and commutation. If the strength and duration of the magnetic field are sufficient, the discharge can be quenched and the current interrupted. Interruption is permanent if the tube holdoff section has recovered before the magnetic field is removed or has fallen below a minimum level. Figure 7 shows a schematic of a typical current interrupting thyatron. The ceramic arc chute has been inserted between the anode-grid and cathode assemblies of a standard thyatron. The magnetic field is applied perpendicular to the page.

Most of the previous work on current interrupting thyatrons was done under contracts to the US Army Electronics Command from 1964 to 1978 [19-21]. Many of the advances occurred under the Repetitive Series Interrupter II contract with EG&G [22] from 1976 through 1978. From their investigation, some general statements can be made about the magnetically quenched thyatron. The best location for the arc chute (interaction channel) is between the grid and the cathode (due to triggering requirements). The best arc interaction channel consists of a smooth wall and an opposing wall that has chutes into which the plasma is driven to cause the interruption. Short chutes on this wall are better than either deep

chutes or a smooth wall. Performance improves as the number of chutes per inch is increased. Decreasing the magnetic field risetime improves the performance, especially at high recovery voltages. Finally, the recovery voltage is the dominant parameter affecting performance.

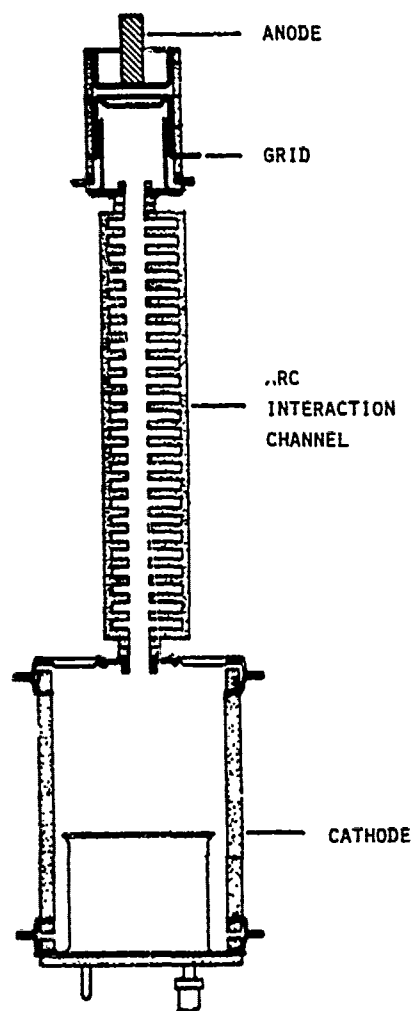


Fig. 7. Current interrupting thyatron with arc interaction channel (EG&G RSI 10A) [23].

The EG&G program demonstrated interruptions of 100 A at 50 kV, 300 A at 32 kV, 600 A at 20 kV, and 1 kA at 15 kV after 10 μ s conduction times. Opening times ranged from 1-10 μ s, depending primarily on the magnetic field risetime. A deionization time of <100 μ s indicated that a repetition rate of 1-10 kHz might be feasible. The research effort was discontinued, however, because the Army no longer had a program need for a 1-kA, 50-kV series fault protector.

Los Alamos became interested in the magnetically quenched thyatron in 1979 as a possible switching solution for inductive storage applications. A research and development program was established in mid-1980 to investigate the concept of the current-interrupting thyatron and the feasibility of extending its performance characteristics. The study will be made with two thyatrons designed and built by EG&G, based on their previous work. These tubes have a performance goal of 2 kA, 25 kV, and 10 ms conduction time. The long conduction time goal requires significantly larger anode, grid, and cathode structures than those used for the previous studies.

Initial testing will determine the self-interruption current level as a function of conduction time. Ion starvation and plasma instabilities are believed to be the mechanisms that limit the current that can be carried in a pulse longer than 0.5 μ s. After finding the self quenching limits, the remaining bench-mark data will be established by determining the cross magnetic field required for interruption (at a given reliability level) as a function of the current, recovery voltage, and conduction time. Determining the effect of conduction time is particularly important to inductive storage applications since the current being interrupted must be carried during the full on time (as opposed to a short pulse in series fault protection applications). The program will also determine whether or not the magnetic pressure mechanism of very fast-rising magnetic fields can improve the opening performance and whether or not axial magnetic fields can help stabilize the discharge to prevent self-quenching and reduce the conduction drop. The results of this program will be used to determine the scaling laws for larger devices and to propose design changes for improved performance. This program is funded for FY81 by Los Alamos National Laboratory supporting research funds.

CONCLUSIONS

Two fundamentally different switches are proposed as candidates for a high power, high rep-rate opening switch. Both types should be able to operate at 1-10 kHz. The triggered vacuum interrupter would be able to handle significantly higher power than the magnetically quenched thyatron (40 kA at 30 kV vs 2 kA at 25 kV) and have considerably lower conduction voltage (25-40 V vs 400-600 V). The thyatron has the advantage

of being totally electronic and totally isolated from the interruption-causing circuit, the cross magnetic field.

Because switches are such key elements of pulse power systems, advances in switching technology will have a significant impact on the feasibility, design, and cost of future pulse power systems. Switching research and development, therefore, should have a large payback potential. The advantages of inductive energy storage make this particularly true for opening switches. Both of the switches being proposed appear to have a good potential for high power, high rep-rate opening duty and should be investigated to determine their feasibility and operating limits and the areas where research is needed to extend the state of the art.

ACKNOWLEDGMENTS

The author gratefully acknowledges the assistance of Jim Sarjeant, who developed the thyatron research proposal. Discussions with Bill Nunnally and Dave Turnquist have also been helpful.

REFERENCES

- [1] C. H. Flurscheim, Editor, Power Circuit Breaker Theory and Design, Peter Peregrinus Ltd., Stevenage, England, pp. 320-352 (1975).
- [2] T. H. Lee, Physics and Engineering of High Power Switching Devices, The MIT Press, Cambridge, Mass., pp. 382-396 (1975).
- [3] A. N. Greenwood and T. H. Lee, "Theory and Application of the Commutation Principle for HVDC Circuit Breakers," *IEEE Trans. Power App. Syst.*, Vol. 91, No. 4, pp. 1570-1574 (1972).
- [4] A. N. Greenwood, P. Barkan, and W. C. Kracht, "HVDC Vacuum Circuit Breakers," *IEEE Trans. Power App. Syst.*, Vol. 91, No. 4, pp. 1575-1588 (1972).
- [5] R. W. Warren and E. M. Honig, "The Use of Vacuum Interrupters at Very High Currents," *Proc. 13th Pulse Power Modulator Symposium*, Buffalo, NY, June 20-22, 1978, IEEE Pub. No. 78CH1371-4ED, pp. 189-193 (1978).

- [6] W. M. Parsons, R. W. Warren, E. M. Honig, J. D. C. Lindsay, P. Bellamo, and R. L. Cassel, "Interrupter and Hybrid-Switch Testing for Fusion Devices," Proc. 8th Symp. Engr. Prob. Fusion Research, San Francisco, CA, Nov. 13-16, 1979, IEEE Pub. No. 79CH1441-5NPS, pp. 689-692 (1979).
- [7] S. Yanabu, E. Kaneko, H. Okumura, and T. Aiyoshi, "Novel Electrode Structure of Vacuum Interrupter and Its Practical Application," Proc. IEEE PES Summer Mtg., Minneapolis, MN, July 13-18, 1980, IEEE No. 80SM700-5.
- [8] D. R. Kurtz, J. C. Sofianek, D. W. Crouch, "Vacuum Interrupters for High Voltage Transmission Circuit Breakers," IEEE PES Winter Mtg., New York, NY, Jan. 26-31, 1975, IEEE No. C75054-2.
- [9] C. W. Kimblin, "The Effect of Axial Magnetic Fields on Vacuum Arcs," Proc. 10th Intl. Conf. Phenom. Ionized Gases, Oxford, England, p. 215 (1971).
- [10] C. W. Kimblin and R. E. Voshall, "Interruption Ability of Vacuum Interrupters Subjected to Axial Magnetic Fields," Proc. IEE, Vol. 119, No. 12, p. 1754 (1972).
- [11] O. Morimiya, S. Sohma, T. Sugawara, and H. Mizutani, "High Current Vacuum Arcs Stabilized by Axial Magnetic Fields," IEEE Trans. Power App. Syst., Vol. 92, No. 5, P. 1723 (1973).
- [12] A. S. Gilmour, Jr., R. F. Hope III, and R. N. Miller, "10 kHz Vacuum Arc Switch Ignition," Proc. 14th Pulse Power Modulator Symp., Orlando, FL, June 3-5, 1980, IEEE Pub. No. 80CH1573-5ED, pp. 80-84 (1980).
- [13] A. S. Gilmour, Jr. and D. L. Lockwood, "The Interruption of Vacuum Arcs at High DC Voltages," IEEE Trans. Electron Devices, Vol. ED-22, No. 4, pp. 173-180 (1975).
- [14] A. S. Gilmour, Jr. and D. L. Lockwood, "Pulsed Metallic-Plasma Generators," Proc. IEEE, Vol. 60, No. 8, pp. 977-991 (1972).
- [15] J. E. Thompson, R. G. Fellers, T. S. Sudarshan, and F. T. Warren, Jr., "Design of a Triggered Vacuum Gap for Crowbar Operation," Proc. 14th Pulse Power Modulator Symp., Orlando, FL, June 3-5, 1980, IEEE Pub. No. 80CH1573-5ED, pp. 85-91 (1980).
- [16] R. L. Boxman, "Triggering Mechanisms in Triggered Vacuum Gaps," IEEE Trans. Electron Devices, Vol. ED-24, No. 2, pp. 122-128 (1977).

- [17] G. A. Farrall, "Vacuum Arcs and Switching," Proc. IEEE, Vol. 61, No. 8, pp. 1113-1136 (1973).
- [18] J. M. Lafferty, "Triggered Vacuum Gaps," Proc. IEEE, Vol. 54, No. 1, pp. 23-32 (1966).
- [19] J. Thomas, H. Vanden Brink, and D. Turnquist, "New Switching Concepts (Final Report)," Technical Report ECOM-00123-F (1967).
- [20] C. L. Shackelford, "Repetitive Series Interrupter (Final Report)," Technical Report ECOM-73-0320-F (1974).
- [21] R. F. Caristi and D. V. Turnquist, "Repetitive Series Interrupter II (Final Report)," Technical Report DELET-TR-76-1301-F (1979).
- [22] EG&G, Inc., Salem, MA, 01970.
- [23] D. V. Turnquist and R. Simon, "Repetitive Series Interrupter II (6th Interim Report)," Technical Report ECOM-76-1301-6 (1978).

A COMPARISON BETWEEN AN SCR AND A VACUUM INTERRUPTER SYSTEM
FOR REPETITIVE OPENING*

W. M. Parsons
Los Alamos National Laboratory
University of California
P. O. Box 1663
Los Alamos, NM 87545

ABSTRACT

Two conceptual systems are analyzed for repetitive interruption of current from an inductive energy storage source. The interruption level for both systems is 25 kA at 25 kV. Factors such as interruption frequency, power dissipation, reliability, maintenance, developmental time, and cost are compared.

The vacuum interrupter system is considered feasible for an interruption frequency of 25 Hz and a 10-20% duty cycle. Five millisecond output pulses deliver 78 MW to a one ohm load with a voltage rise time of less than one microsecond. Hardware costs are less than \$100,000 for the system, and development time is one year.

The SCR system is considered feasible for an interruption frequency of up to 10 kHz. A series spark gap connected to the load limits the otherwise continuous duty factor. Fifteen microsecond output pulses deliver 94 MW to a one ohm load with a voltage rise time of less than one microsecond. Hardware costs for the system exceed \$1,000,000 and development time is 2 to 3 years.

INTRODUCTION

Interruption of direct current from an inductive store can be accomplished by either of two methods. One method involves creating an arc voltage which is greater than the product of the current and the load impedance. Fuses, explosive interrupters, and conventional dc circuit

*Work performed under the auspices of the U.S. Department of Energy.

breakers operate on this principle. The second method involves creating an artificial current zero by injecting an equal but opposite current through the interrupter. This process is known as commutation and is used in the two conceptual systems described here.

Both of the systems utilize a similar interruption circuit, the primary difference being the interrupters. In one case this interrupter is a series-parallel array of 1260 fast switching SCRS, and in the other case the interrupter is a series array of two, seven-inch vacuum interrupters. For sake of comparison, both interrupters are designed for use at 25 kA and 25 kV, although either system could be designed for higher or lower currents or voltages. This paper will examine potential differences in operating frequency, cost, reliability, lifetime, power dissipation, and development time.

1. Background

The Los Alamos National Laboratory has been involved in switchgear development for fusion experiments since 1974.[1] At that time one interrupter test facility rated at 10 kA continuous current, 25 kA pulsed current, and 60 kV recovery voltage was constructed to test switches for inductive energy storage systems. Presently three test facilities are operative, the largest rated at 100 kA steady-state current, 280 kA pulsed current, and 120 kV recovery voltage.[2]

In addition to basic research, Los Alamos has been actively involved in switch testing and development for the national fusion community. During 1978, a system was developed using Westinghouse interrupters for use in the Tokamak Fusion Test Reactor at Princeton.[3] Over 1000 consecutive interruptions were performed at 25 kA and 25 kV. A system designed by Toshiba was also tested over 1000 times for the same application.[3] An experimental General Electric interrupter was tested up to 112 kA using a Los Alamos designed and constructed actuator. In 1979, a 25 kA steady-state interrupting system was designed by Los Alamos and Oak Ridge for use in the Large Coil Project.[4] This system is now being tested and will be used to interrupt current in six superconducting magnets which store as much as 200 MJ each. A 50 kA steady-state interrupting system is presently being designed for interrupting current

in a superconducting magnetic energy system at Los Alamos for the Tokamak Poloidal Field System program.

2. Basic Interrupting Circuit Using Commutation

A schematic of a repetitive interrupting circuit using commutation is shown in Fig. 1. The circuit breaker represents an array of either SCRs or vacuum interrupters and the load will be considered to be a one ohm resistor. The following initial conditions are assumed.

1. The circuit breaker and bypass switch are closed and the power supply has charged the storage inductor to 25 kA.
2. The commutation capacitor is precharged to 25 kV with the polarity shown.
3. The energy stored in the inductor is much greater than the energy delivered to the load.

To begin the sequence, the bypass switch opens transferring all the current into the closed circuit breaker. If the circuit breaker is a vacuum interrupter, its contacts then open. The commutation SCRs labeled "A" are now triggered. This discharges the commutation capacitor through the circuit breaker in a direction opposite to the inductor current. When a net current zero is created in the circuit breaker, interruption occurs. The inductor current now flows through the still conducting

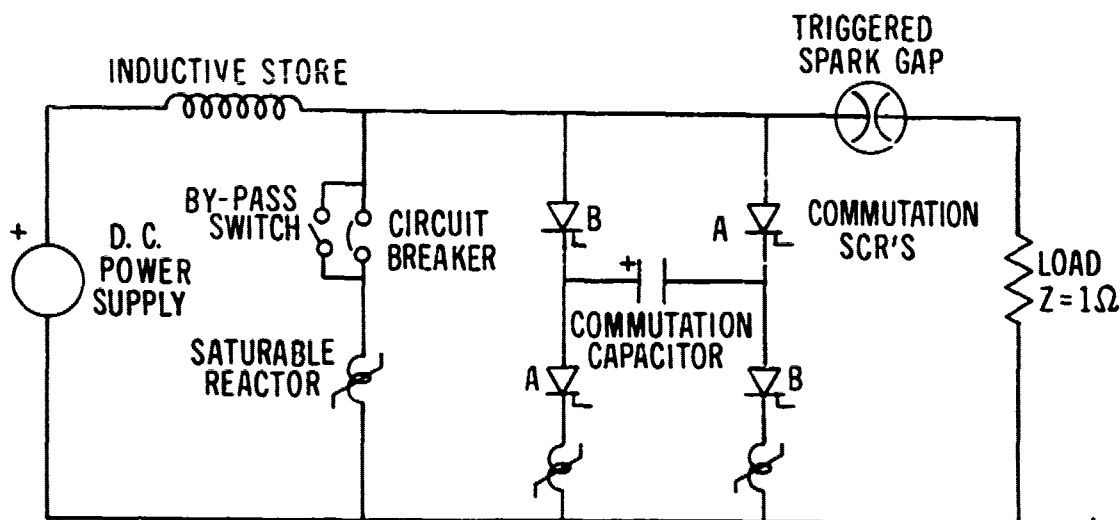


Fig. 1. Repetitive switching circuit.

commutation SCRs, "A", and begins to recharge the commutation capacitor in the opposite direction. When this capacitor voltage reaches slightly over 25 kV, the triggered spark gap closes. This produces a high rate of voltage rise on the load. The full inductor current now flows into the load creating a maximum voltage of 25 kV. Because the commutation capacitor was charged to slightly over 25 kV, a reverse voltage appears across the commutation SCRs, and allows them to recover. To begin a new cycle, the circuit breaker recloses, and the triggered spark gap recovers. The sequence is now repeated except that commutation SCRs, "B", are used this time due to the reverse charge on the commutation capacitor. On the third sequence, SCRs, "A", will be used because the capacitor will be forward charged after the second sequence. Thus, SCRs, "A", are used on odd numbered interruptions and SCRs, "B", are used on even numbered interruptions.

The primary difference in the interrupting circuit when using vacuum interrupters or SCRs is the commutation capacitor. Because the SCRs have a longer turn-off time than the vacuum interrupters, a larger capacitor is required to hold the recovery voltage negative after current zero. The commutation SCRs for the SCR interrupter circuit must also be larger, but this is a result of the higher operating frequency rather than differences in the nature of the circuit breaker used. These details will be examined below.

3. The Vacuum Interrupter as a Circuit Breaker

Figure 2 is a schematic of the vacuum interrupter assembly used as a circuit breaker in the interrupting circuit of Fig. 1. The breaker consists of two Westinghouse WL-33552 commercial interrupters connected in series. The axial field coils maintain a diffuse discharge during arcing in the interelectrode gap and increase the interruption ratings significantly. Similar interrupters have been tested at Los Alamos with currents in excess of 40 kA and voltages in excess of 30 kV simultaneously on a single interrupter.[5] Toshiba has developed a vacuum interrupter which can interrupt 100 kA at 12 kV.[6] The use of two interrupters in series provides a conservative design for high reliability as demonstrated on two similar systems tested for use in

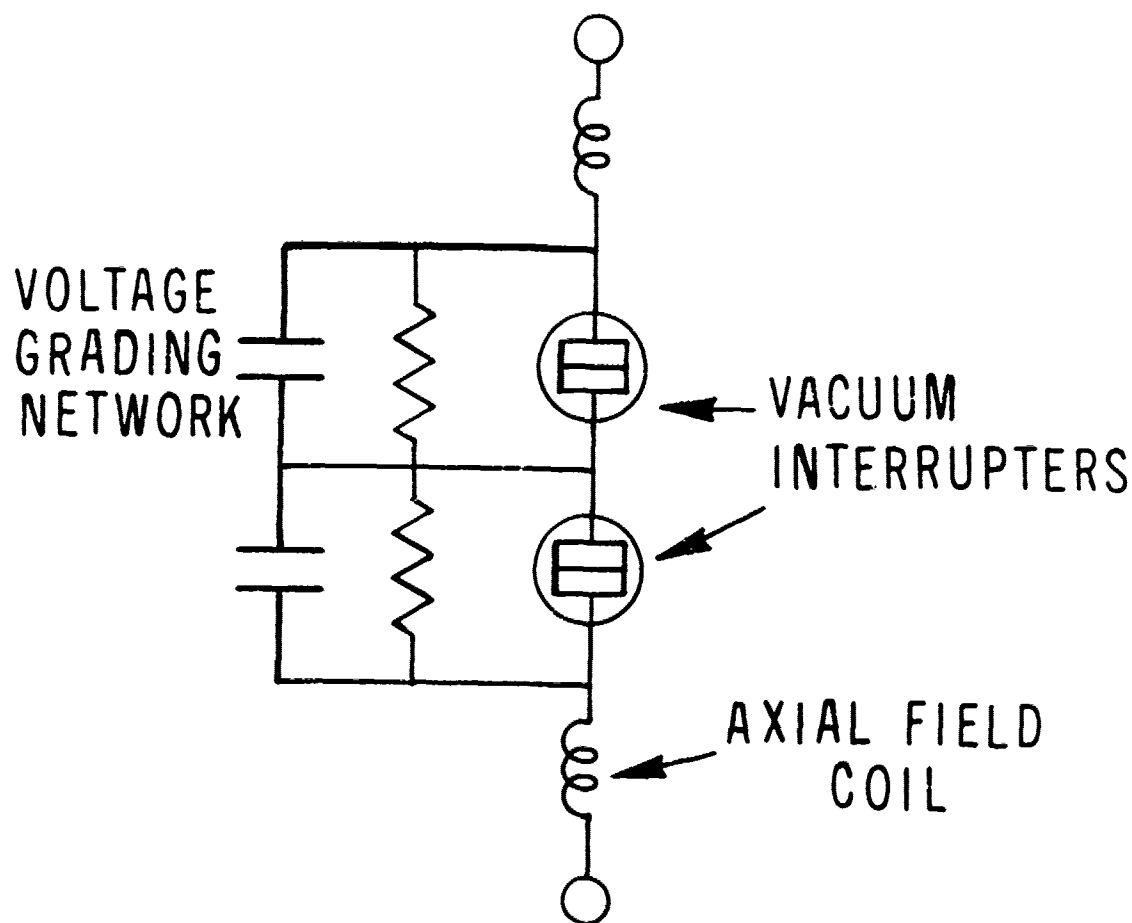


Fig. 2. 25 kA 25 kV vacuum circuit breaker.

TFTR.[3] Estimated contact lifetime for these interrupters is 5000 to 10,000 operations at 25 kA.

The normal steady-state current rating for these interrupters is 2 kA. Los Alamos and Westinghouse have been jointly developing an interrupter with water-cooled stems and contacts over the past several years. The first prototype conducted 10 kA on a continuous basis. A second prototype with an improved electrode-stem design and a special actuator designed at Los Alamos is being prepared for testing. It is designed to carry 25 kA on a continuous basis and would eliminate the need for the external bypass switch shown in Fig. 1. Both options, however, will be discussed in this section.

3.1 Operating Frequency

Commercial actuators for vacuum interrupters are not designed to operate at high repetition rates. Typical mechanical opening times range from 5 to 10 ms and reclosing times vary from 40 to 1000 ms. A special actuator for use at high frequencies would have to be developed. Figure 3 details a conceptual 25 Hz actuator with a motor driven camshaft to operate the linkage of a vacuum interrupter. Table I lists some technical information on design parameters for this device. Besides the

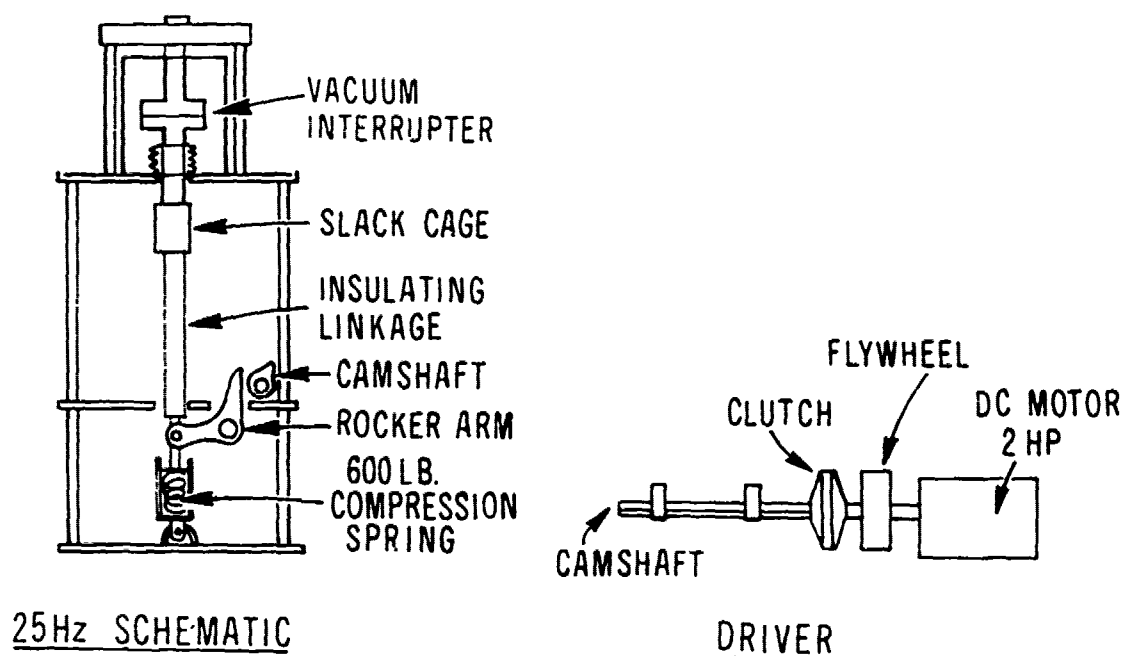


Fig. 3. 25 Hz Actuator.

TABLE I

25 Hz ACTUATOR DETAILS

Operating frequency, Hz	25
Opening time, ms	5
Reclosing time, ms	5
Time in closed position, ms/cycle	30
Mechanical power at 25 Hz, HP/interrupter	0.86
Motor speed, rpm	1500

inherent synchronization in this type of design, the array is easily expandable to include more series or parallel interrupters.

Typical waveforms showing the circuit breaker current, I_{CB} , the commutation capacitor voltage, V_{CC} , and the voltage on a one ohm load are pictured in Fig. 4. The load voltage duration could be extended to as long as 35 ms by camshaft design or shortened to as little as 2 to 3 ms by increasing the force of the return spring. Transient current and voltage stresses on the interrupter during this sequence are discussed in Section 3.3.

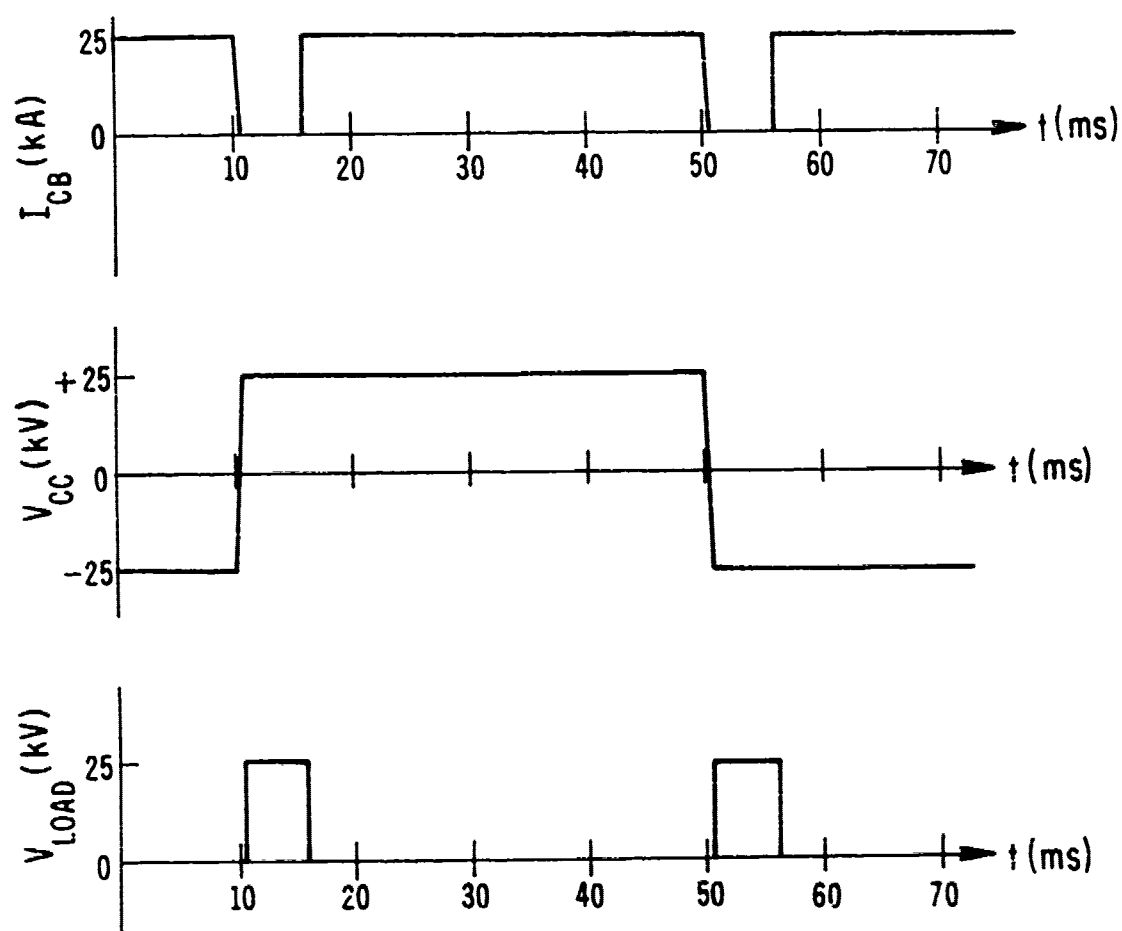


Fig. 4. Current and voltage waveforms for vacuum interrupter system.

3.2 Power Dissipation

Slightly over 3 kJ are generated by the vacuum arc prior to each interruption resulting in a total of 78 kW power consumption at 25 Hz. This energy must be removed from the device. Commercial interrupters are designed to dissipate an average power of only 30 to 60 W during normal conduction at 2 kA. However, their inherent thermal mass is sufficient to absorb the power generated by 25 Hz interruption for about 2 s. The interrupter must be allowed to cool for 30 to 60 min before the sequence could be repeated. The latest water cooled interrupter is designed to remove a maximum of about 20 kW heat loading from the contact region. It would only have to cool for 10 to 20 s between interruption sequences. Either the water-cooled interrupter system or the combined bypass switch and commercial interrupter system generate less than 10 kW dissipation during conduction in the closed state.

The triggered spark gap envisioned for the 25 Hz system is a General Electric rod-array vacuum spark gap. These gaps have been very successful in laboratory testing[7] and have an extremely low voltage drop during conduction. The estimated lifetime at 25 Hz and 25 kA is over 10^5 operations. The 25 Hz power dissipation of the spark gap is also about 80 kW and limits its continuous operation. The inherent thermal mass would allow about 5 to 10 s of continuous duty before cooling becomes necessary. A water-cooled spark gap for a higher duty factor would be recommended if used in conjunction with a water-cooled interrupter.

The SCR commutation switches used in the 25 Hz vacuum interrupter system dissipate a negligible amount of energy. Thus, the total dissipation of the system at a 25 Hz interruption rate is 0.16 MW. The power delivered to the load during this same sequence is 78 MW.

3.3 Interrupter Stresses

The electrical stresses on the individual vacuum interrupters are conservative enough to insure a reliability of greater than 99%. In power systems, these interrupters face peak voltages of 22 kV with a rate of rise of recovery voltage (RRRV) in excess of 25 kV/ μ s. In the 25 Hz system, the peak interrupter voltage is 12.5 kV with an RRRV of only 700 V/ μ s. Due to these unusually low voltage stresses, a commutation

rate of $1 \text{ kA}/\mu\text{s}$ can be utilized while still maintaining a high degree of reliability.

4. The SCR as a Circuit Breaker

Figure 5 is a schematic of the SCR circuit used as a breaker in the interrupting circuit of Fig. 1. The breaker consists of 30 parallel connected arrays of 42 SCRs in series.[8] This circuit has a continuous current rating of 30 kA at a maximum voltage of 50 kV. The 10 kHz switching rate used in this analysis dissipates more energy than a steady-state current of 25 kA. As a result, the 30 kA continuous system must be derated to 25 kA at 10 kHz. Peak voltage ratings that are a

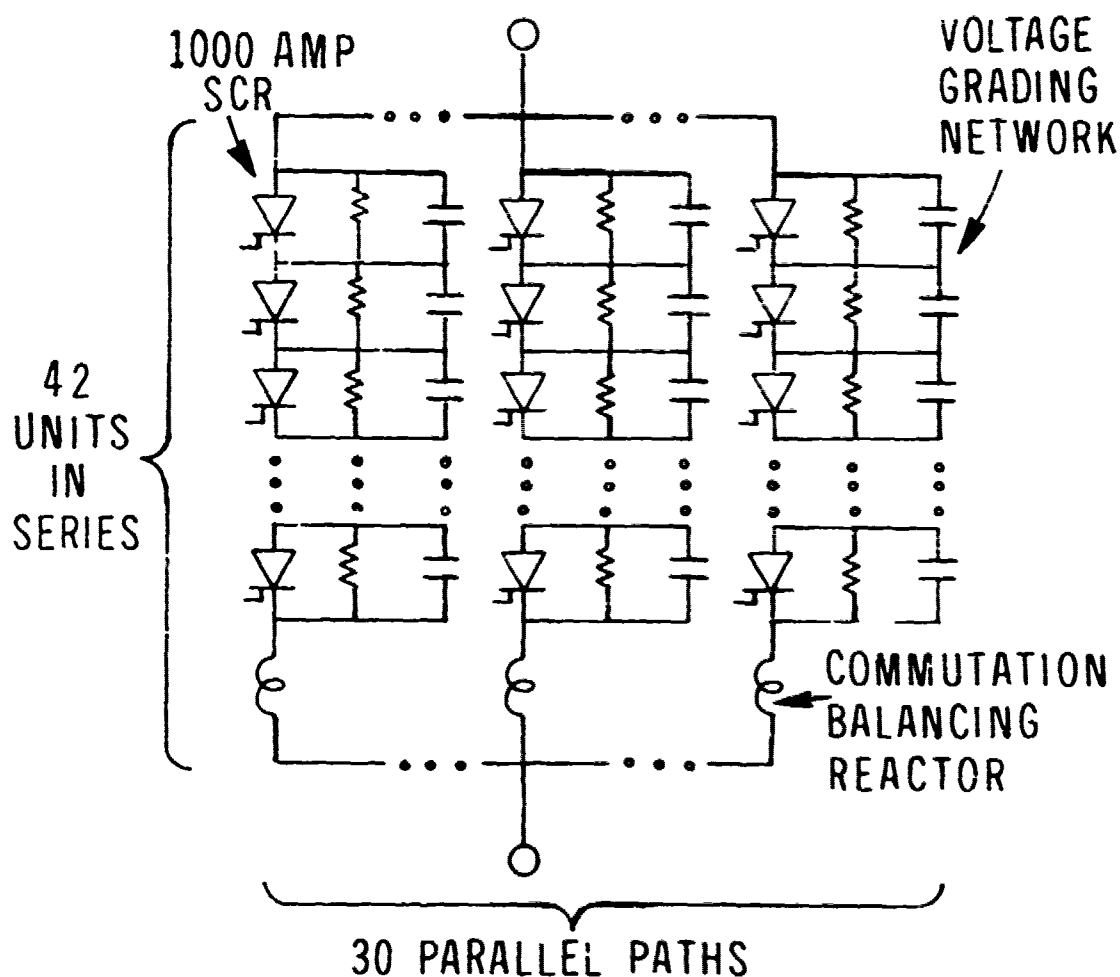


Fig. 5. 25 kA 25 kV SCR circuit breaker.

factor of two above normal operating voltages are quite common in semiconductor systems.

4.1 Operating Frequency

The operating frequency selected for this analysis was chosen as half the maximum operating frequency for the particular SCR used. The SCR was selected on the basis of highest current and voltage ratings for a 20 μ s turn-off device. The fast turn-off time is necessary to minimize the size and weight of the commutation capacitor.

Typical waveforms showing the circuit breaker current, I_{CB} , the commutation capacitor voltage, V_{CC} , and the voltage on a one ohm load are pictured in Fig. 6. The load voltage duration could be extended to as long as 35 μ s by decreasing the conduction time of the interrupter array

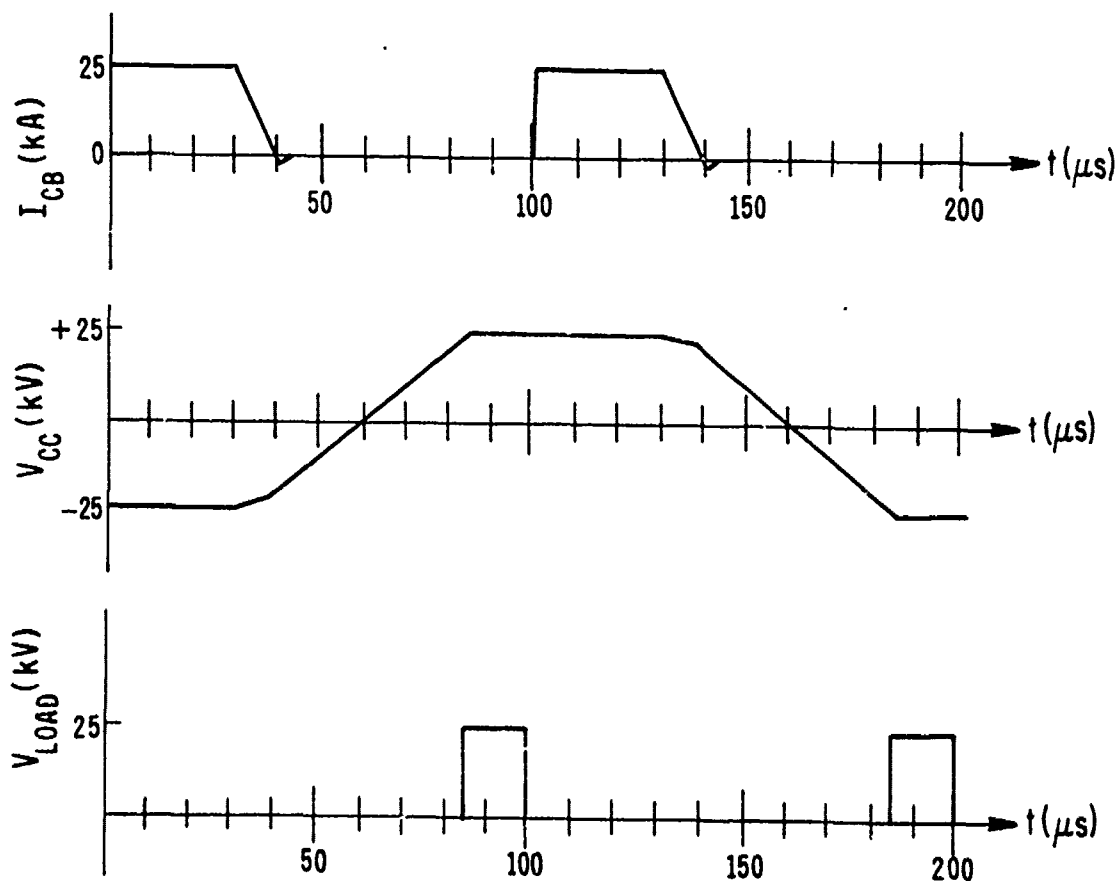


Fig. 6. Current and voltage waveforms for SCR interrupter system.

and shortened indefinitely by increasing the conduction time. Switching stresses are discussed in Section 4.3.

4.2 Power Dissipation

According to published data,[9] power consumption of the SCR array conducting 35 μ s wide pulses at 10 kHz is 1.9 MW. Steady-state conduction losses amount to 1.6 MW. Obviously, a parallel bypass switch would be necessary during inductor charging or when no interruption sequence is required. The commutation SCRs consume even more energy than the primary interrupter. Approximately 2.5 MW are consumed by the commutation SCRs at 10 kHz. If the same spark gap used with the vacuum interrupter system is used with the SCR system, 0.94 MW would be dissipated. Thus, the total power used by the SCR system at 10 kHz is 5.4 MW. The power delivered to the load during the same time is 94 MW. Everything in this system could be run continuously except the spark gap. Another SCR array could be substituted for the spark gap for continuous operation, but the 1 μ s voltage risetime would require a prohibitively large number of SCRs if the published ratings were followed. Transient overrating tests could be conducted to reduce the size of this array.

4.3 Interruption Stresses

The electrical stresses on the SCR interrupter were chosen within the published ratings to insure a high degree of system reliability. A comparison between the published maximum ratings[9] and the actual operating stresses is shown in Table II.

TABLE II
MAXIMUM RATINGS VERSUS OPERATING STRESSES FOR INDIVIDUAL SCRs

	<u>Maximum Ratings</u>	<u>Operating Stresses</u>
Peak voltage, V	1200	600
Average current, A	1000	833
Peak di/dt, A/ μ s	200	100
Turn-off time, μ s	20	20
Peak dv/dt, V/ μ s	400	24
Maximum frequency, kHz	20	10

The dv/dt stresses are unusually low due to the large parallel commutation capacitor required for the 20 μs turn-off time.

5. Systems Comparison and Conclusions

In general, the SCR interrupter system is capable of high frequencies, short output pulses, and continuous operation. It is also an expensive system and would require 2 to 3 yr to develop fully. The vacuum interrupter system is a low frequency, long output pulse, intermittent duty system. It is comparatively inexpensive and the technology is well developed. The required development time is about one year. Table III compares the two systems in more detail.

Both systems appear to be technically feasible with present state-of-the-art devices. Light triggered thyristor technology is advancing rapidly and would be especially useful in these systems, especially if

TABLE III
COMPARISON BETWEEN THE VACUUM AND SCR INTERRUPTER SYSTEMS
RATED AT 25 kA AND 25 kV

	Vacuum Interrupter	SCR
Operating frequency, Hz	25	10,000
Output pulse width, μs	3,000-35,000	1-35
Maximum duty factor, %	10-20	100 ^a
Commutation capacitor, μF	17.5	24.2
Power dissipation during interruption, MW	0.16	5.4
Power delivered to load, MW	78	94
Cost for interrupter alone, \$(10) ³	25	500 ^b
Cost for commutation network, \$(10) ³	45 ^b	500 ^b
Reliability, %	> 99	> 99
Number of interruptions between maintenance, (10) ³	5-10	> 100 ^c

^aContinuous duty spark gap/SCR is utilized.

^bSCR cost at \$200 each plus \$200/SCR for gate circuitry, grading networks, and mounting assemblies.

^cSCR array is used instead of spark gap.

turn-off times could be reduced. Actuator development for the vacuum interrupter system is believed to be minimal at the 25 Hz level described.

REFERENCES

- [1] C. E. Swannack, R. A. Haarman, J. D. G. Lindsay, and D. M. Weldon, "HVDC Interrupter Experiments for Large Magnetic Energy Transfer and Storage (METS) Systems," Proc. 6th Symp. Eng. Problems of Fusion Res., San Diego, CA, Nov. 18-21, 1975; IEEE Pub. No. 75CH 1097-5 NPS, 662, (1976).
- [2] W. M. Parsons, E. M. Honig, and R. W. Warren, "A 33-GVA Interrupter Test Facility," Proc. 2nd IEEE International Pulsed Power Conference, Lubbock, TX, June 12-14, 1979.
- [3] R. W. Warren, W. M. Parsons, E. M. Honig, and J. D. G. Lindsay, "Tests of Vacuum Interrupters for the Tokamak Fusion Test Reactor," Informal report LA-7759-MS, April 1979.
- [4] W. M. Parsons and R. J. Wood, "Protection Circuits for Superconducting Magnets," Proc. 4th ANS Topical meeting on Tech. of Controlled Nuc. Fusion, King of Prussia, PA, Oct. 14-17, 1980.
- [5] R. W. Warren and E. M. Honig, "The Use of Vacuum Interrupters at Very High Currents," Proc. 13th Pulse Power Modulator Sym., Buffalo, NY, June 20-22, 1978.
- [6] S. Yanabu, E. Kaneko, H. Okumura, and T. Aiyoshi, "Novel Electrode Structure of Vacuum Interrupter and Its Practical Application," Proc. IEF PES Summer Mts., Minneapolis, MN, July 13-18, 1980, IEEE No. 80SM700-5.
- [7] C. P. Goudy, General Electric Research and Development Center, personal communication.
- [8] Westinghouse Model T9GH121062DH
- [9] J. F. Donlon and W. H. Karstaedt, Westinghouse Fast Switching SCR Data Book, Westinghouse Electric Corp., 1978.

Fuse Switches for High Current
Inductive Pulse Compression Systems

R. E. Reinovsky

D. L. Smith

Air Force Weapons Laboratory

Kirtland Air Force Base, New 87117

ABSTRACT

Fuse opening switches for inductive pulse compression systems have been explored and their use has resulted in the routine operation of an inductive store/opening switch power conditioning system for a 1.9 MJ capacitor bank. With the power conditioning system in operation the bank delivers an 8 MA/190 ns risetime current pulse to a 5 nH load.

INTRODUCTION

For several years, the Air Force Weapons Laboratory has been pursuing the development of electrically exploded conductor opening switches (fuses) for near term applications in inductive store/opening switch pulse power systems. Power systems capable of delivering multimegamp pulses with a few hundred nanosecond risetime are needed as drivers for a variety of plasma physics experiments, including imploding plasma loads. This work has led to the operation of fuses on a variety of dc charged capacitor banks with energies from 100 kJ to about 2 MJ. These experiments have both provided scaling data and have demonstrated the successful performance of the fuses as the interrupt voltages and currents increased. Recent work has resulted in the routine operation of a 1.9 MJ capacitor bank in a reliable inductive store pulse power system.

AFWL opening switch requirements as initially envisioned are listed in Table I:

Table I

Interrupt Current	15-20 MA
Interrupt Voltage	300-500 kA
Opening Time	200 ns

In addition, engineering designs were required which were low in inductance, because the first application was the low impedance inductor to inductor transfer requirement of an imploding plasma load. Furthermore, the switch needed to be simple in order to permit its

routine use by operations personnel and economical to minimize the hardware investment. Lastly, a timely solution was required which could be implemented using present technology.

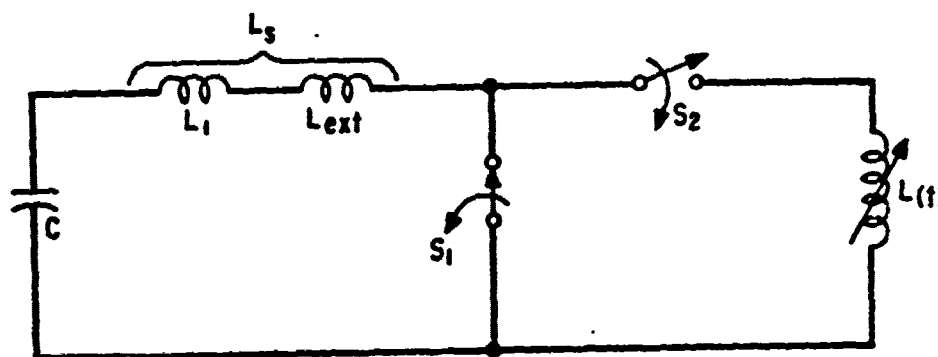


FIGURE 1 Inductive Compression Circuit

The circuit which was employed was the simple, shunt switch arrangement shown in Figure 1. By shunting the load with a low inductance switch and taking the output across the switch, the internal inductance of the primary energy store (a capacitor bank in this case) can be used as part of the inductive store making energy that would otherwise be lost, available to the load.

MODEL EXPERIMENTS

A variety of capacitor banks have been employed in the testing of fuse technology at the AFWL. Results of work done on a 100 kJ/100 kV and on a 200 kJ/50 kV system have previously been reported (1). Within the last year, the 100 kJ system has been upgraded to store more than 500 kJ at 120 kV and fuses have successfully operated on the upgraded system with encouraging results. The mechanical arrangement

of the fuse package is shown in Figure 2. The primary insulation for the output voltage is a 0.125" polycarbonate sheet overlayed with 4 layers of .005" mylar. The fuse material is a .001" thick aluminum foil whose width is adjusted according to scaling principles outlined by Maisonnier in 1966 (2). The quench material surrounding the hairpin folded fuse is quartz sand (glass beads) of nominally 60-100 μm diameter. The entire fuse is assembled in place on the machines and confined by approximately 1" of moderate density foam rubber to compress the package, absorb shock and confine the beads. The entire assembly is situated between the output transmission lines of the system in a volume which also serves as the inductive store.

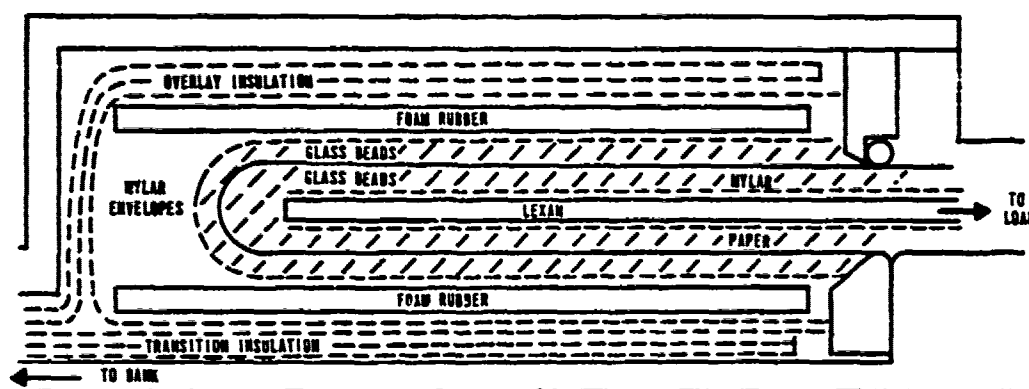


FIGURE 2 Fuse Construction

Open circuit experiments in which no energy was transferred to a load, and therefore all the capacitive stored energy was dissipated in the fuse, were conducted at energies up to 300 kJ resulting in output voltages across the fuse of about 1/2 MV and interrupted currents of 2-3 MA. Voltage and current data are shown in Figure 3 for a .001" aluminum fuse, 70 cm long and 44 cm wide.

The inductively corrected voltage (Fig 4) and current data were

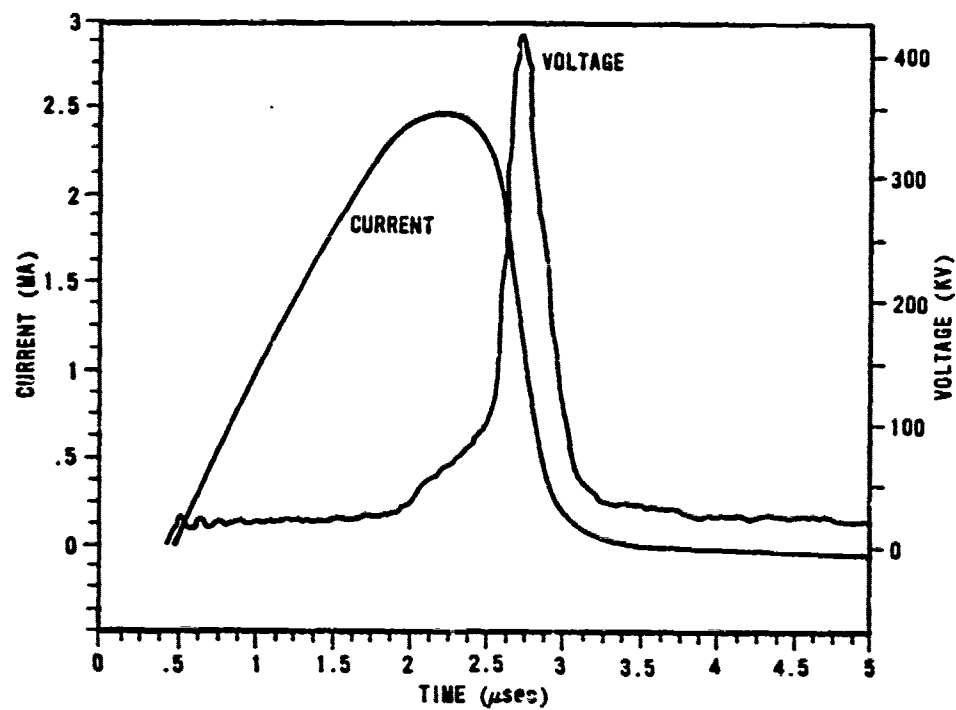


FIGURE 3 Data from 300 KJ experiment.

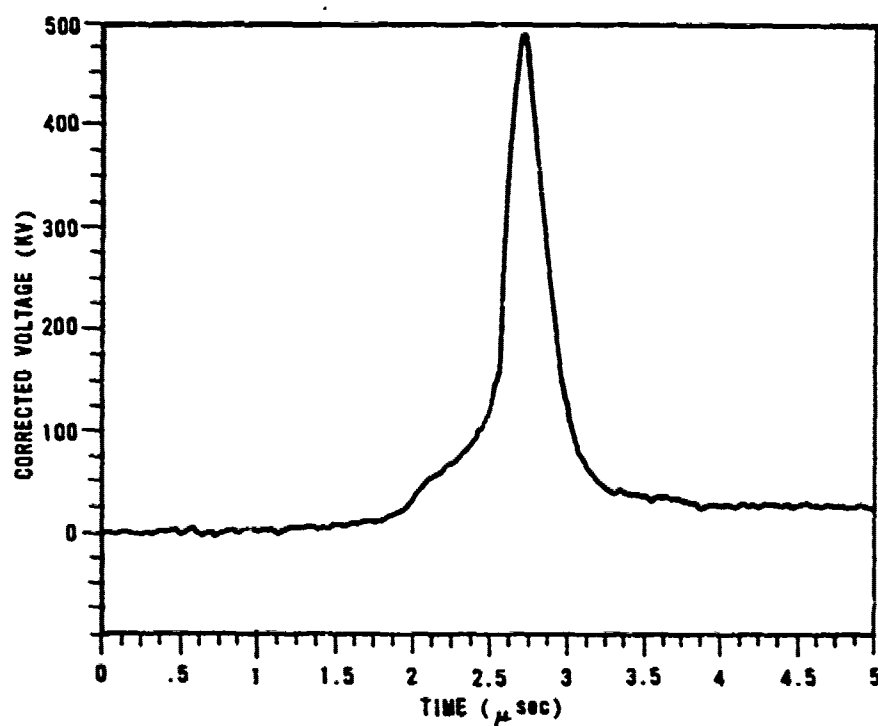


FIGURE 4 Inductively Corrected Voltage

analyzed to yield the resistivity information in Figure 5 where resistivity is based on measured resistance and the initial cross section (pre-vaporization cross section) and the specific internal energy is determined by the $j^2\rho$ heating rate. Also plotted on the figure are some data from exploding bridge wire experiments conducted by Tucker and Toth (3) at much lower total energies. Experiments at

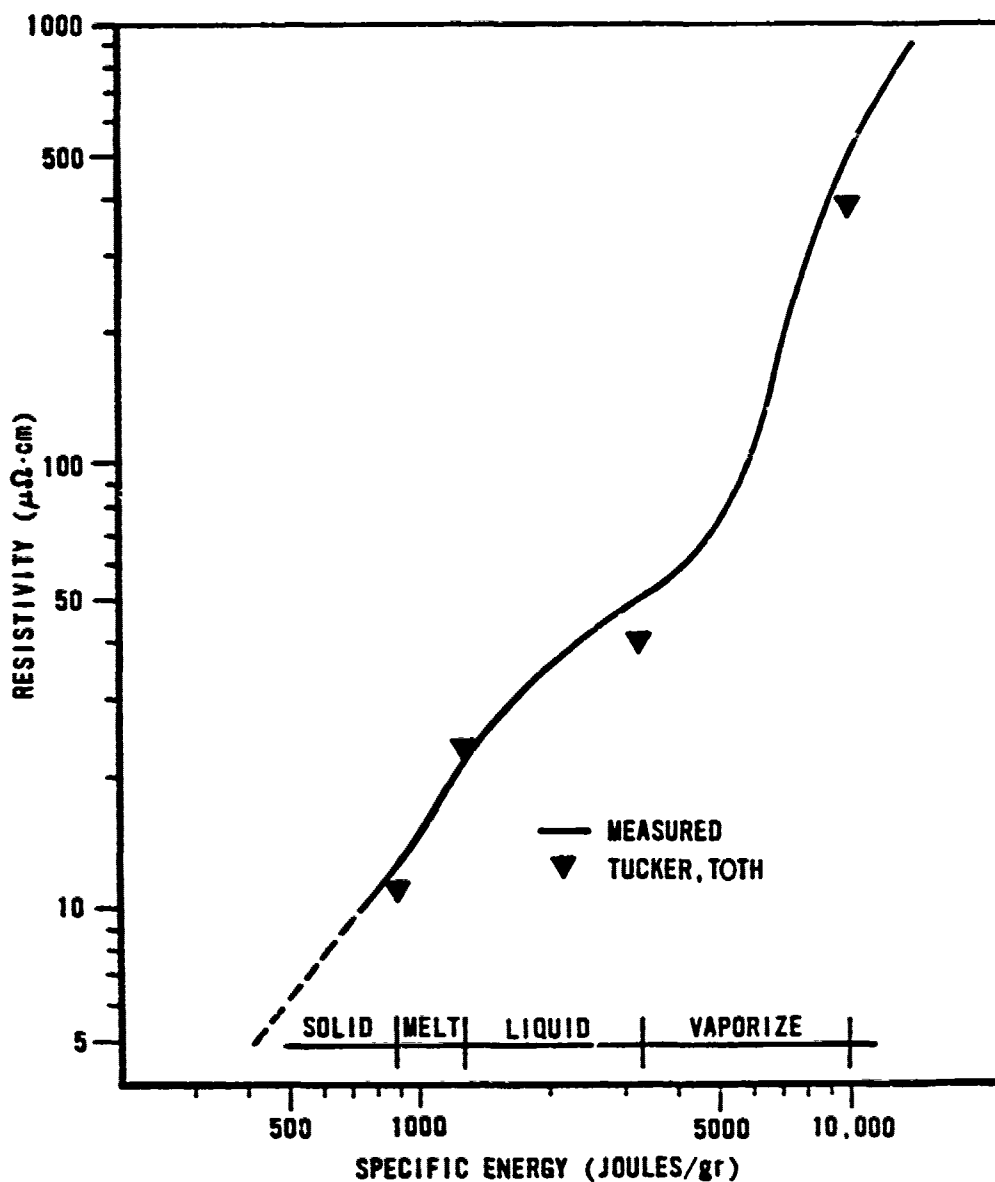


FIGURE 5 Aluminum Fuse Resistivity

energies of over 300 kJ resulted in even higher voltage but difficulties in handling MV level voltage in air made conclusive measurements impossible.

Experiments have also been conducted in which energy was transferred into an external load of approximately 9 nH. Figure 6 shows the results of such experiments where about 4 MA of current were interrupted and almost 2 MA transferred to the load. Because the low

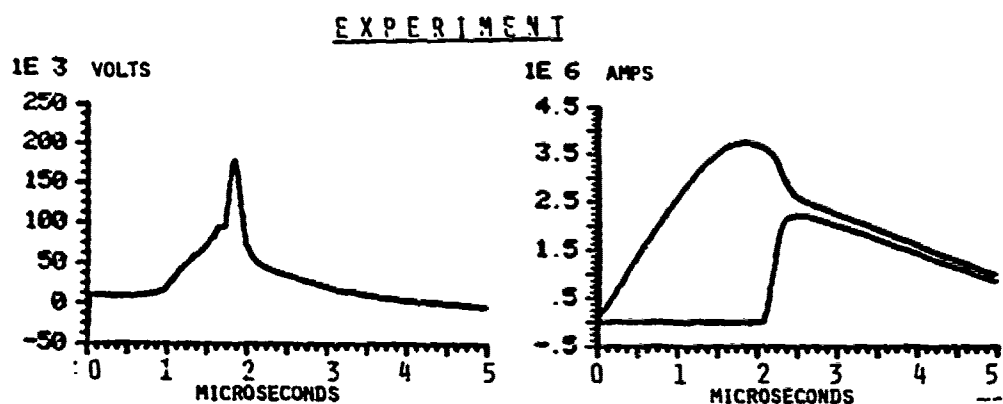


FIGURE 6 Current Transfer to a Dummy Load

impedance load is connected in parallel with the switch during opening time, the peak voltage observed in the transfer case is only 200 kV as compared to the 500 kV in the open circuit case. Figure 7 shows the results of a simple circuit model calculation employing resistivity

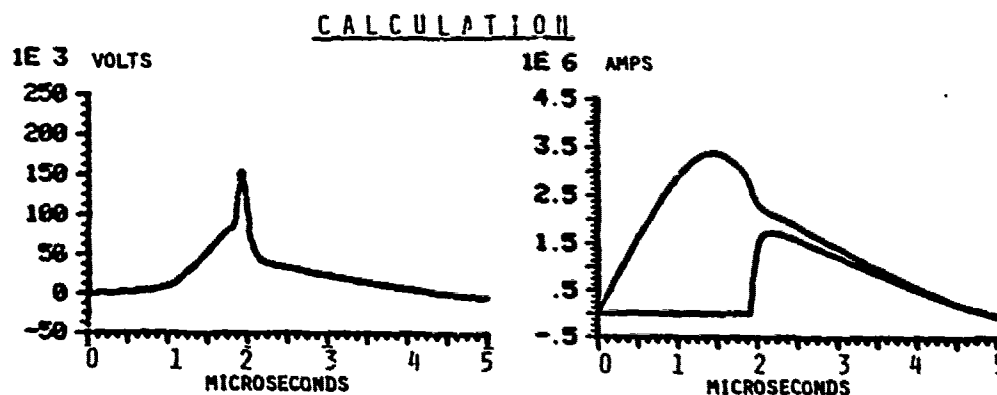


FIGURE 7 Model of experiment in Fig 6

data similar to that gathered for open circuit cases and adequately predicts the performance of the circuits in energy transfer operations.

Results of scale model experiments are summarized in Table II:

TABLE II

Peak Interrupt Current	4 MA
Peak Voltage	500 kV
Peak E Field	10 kV/cm
Peak Resistivity	500 $\mu\Omega$ cm

FULL SCALE EXPERIMENTS

Fuse opening switches have been implemented on the AFWL 1.9 MJ high energy capacitor bank in order to decrease the rise time of current into a load. With a capacitance of 260 μF and bank inductance of 3 nH, the bank current risetime into an initially 5 nH load is about 1.5 μsec (10% to 90%). By using fuses in geometries similar to that shown in Figure 2 and a stabbed solid dielectric output switch between fuse and load, current measurements shown in Figure 8 were obtained with the bank operating at its full 120 kV rated voltage. The current risetime into the 5 nH load is 190 ns (10% - 90%). Thus, the inductive compression system results in about an order of magnitude decrease in risetime at a cost of a reduction of about 1/2 in the peak current.

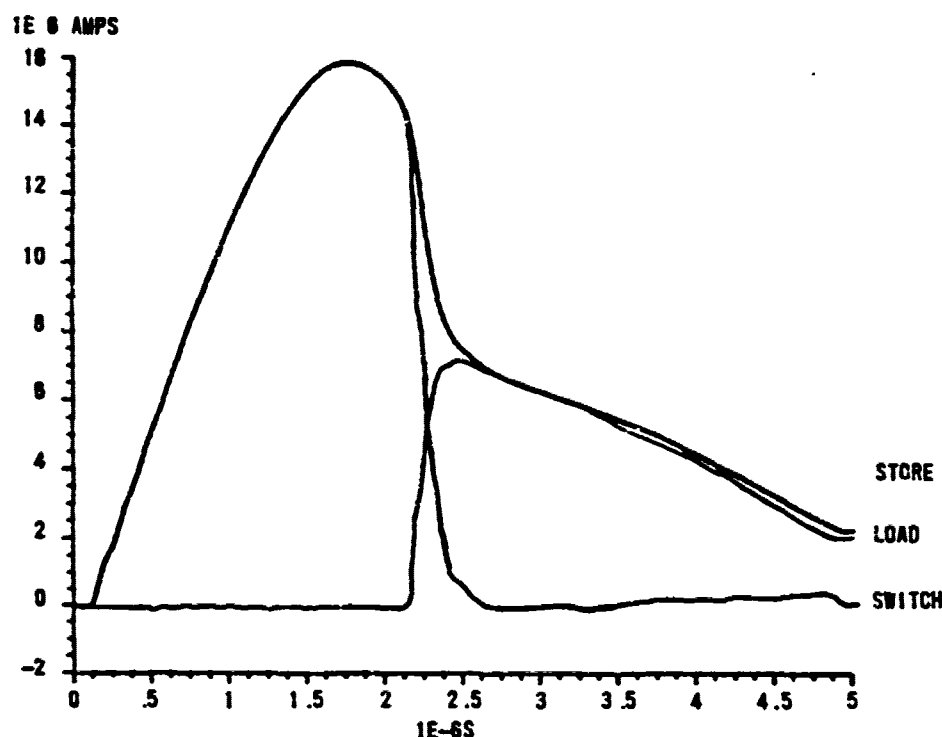


FIGURE 8 Experimental Data from 1.9 MJ Fuse

CONCLUSION

Fuse switching for inductive pulse compression systems have been demonstrated as a viable technique for energy levels up to 2MJ. Using such techniques, a variety of power conditioning configurations can be envisioned for operating higher energy, short pulse time systems, including the use of multiple staged store/switch combinations.

REFERENCES

- (1) Henderson, et al, "Preliminary Inductive Energy Transfer Experiments," Proceedings of Second IEEE International Pulse Power Conf. Lubbock, Tx (1979) .
- (2) Maisonnier, et al, "Rapid Transfer of Magnetic Energy by Means of

Exploding Foil," Rev. Sci. Instr. 34, #10 , 1966.

(3) Tucker, et al, "EBW1: A Computer code for the Prediction of the Behavior of Electrical Circuits Containing Exploding Wire Elements," Sandia National Labs Report 75-0041, (1975).

FUSES AND REPETITIVE CURRENT INTERRUPTION

Ihor M. Vitkovitsky
Naval Research Laboratory
Washington, D.C. 20375

ABSTRACT

Two characteristics of exploding wire and foil fuses have been studied as part of the development of pulse-train generator with high peak power and small pulse-to-pulse separation. These characteristics, the induced voltage resulting from current interruption in an inductive storage system and the subsequent recovery, have been studied for fuses in vacuum, air and water. The results can be used for design of the pulse-train generators as well as to indicate some of the problems that can be expected in the development of future opening switches with repetitive capability.

A. INTRODUCTION

Metal fuses are rather simple devices with a capability to perform demanding functions associated with inductive storage systems for generating single pulse output. They are employed in megajoule level systems,^{1,2,3} where opening times of about a microsecond are achieved. In smaller pulser systems much faster (~ 100 nsec) output voltage risetime has also been obtained.^{4,5} To extend their usefulness, staging of fuses has been employed to provide multiplication of the power flow from the storage to the load.^{2,6} Because staging requires that the voltage generated by the succeeding switches appear across fuses that have previously exploded, the rate at which the dielectric strength is restored determines the duration of current flow

in the succeeding stage (and, thus, indirectly affects system efficiency and power multiplication). In repetitively operated closing and opening switches, as well as in cascade pulse-burst generators,⁷ dielectric strength recovery plays a similar role in determining the minimum pulse-to-pulse separation. Recent studies of the fuse recovery phenomena in water⁵ and in air and vacuum⁸ have established a base of data on recovery rates for design of pulse-burst generators and for comparison of rates, as well as other switch characteristics, with those of repetitive opening switches employing other principles of operation.

Comparative data discussed below suggests that operational repetitively opening switches for low power or low frequency regime will be based on switching techniques other than fusing. For very high power operation or for very high repetition frequency, the fuse cascade switches⁷ will remain for some time the only practical devices capable of performing in that regime.

B. SWITCH RECOVERY CHARACTERISTICS

One of the more important aspects of repetitive current interruption is the understanding of the conditions in the opening switch in the time interval between pulses generated by the opening action. Data, probing the conditions that vary rapidly in time, has been collected in studies of recovery rates for fuses^{5,8} and for high pressure^{9,10} and vacuum¹¹ arcs. Both types of interrupters conduct at high current density (typically, in the range of 10^4 to 10^6 A/cm²) at the time of interruption. Their recovery fields are below 25 kV/cm. The highest recovery fields (~ 100 kV/cm) and rates ($\sim 10^{11}$ V/cm-sec) are expected to be those associated with the electron beam controlled switch,^{12,13} with low current density (~ 10 A/cm²). On the other hand, the electron

beam controlled switch has at least 10^6 times lower conductivity, compared to fully ionized gas*. Its conduction time is also limited by the duration of the injected beam, typically to 1 μ sec period. Because of limitations arising from gas heating,¹³ e-beam switches are limited to burst mode, analogously to the limitations imposed on fuses.

In selecting the approaches to switching for burst output pulser systems (with high repetition frequency, ≥ 10 kHz, and high peak power output) behavior of recovery rates, rates of change of resistance, current density and other properties must be known in considerable detail. Expected performance of the electron beam controlled switch has been discussed previously.¹³ Also less detailed suggestions were made¹⁴ that indicate significant switching performance can be obtained using high power lasers for turning "on" and "off" selected gases, in a manner similar to control achieved by the electron beam. Recently obtained data for recovery rates of fuses is compared with that of expected performance of e-beam controlled switch in Table I. More detailed behavior of the fuse recovery is shown in Figures 1 and 2.

1. Atmospheric Air.

In Fig. 1 dielectric strength of the fuse exploded in air is shown as a function of time delay before the succeeding voltage pulse is reapplied, as discussed in Ref. 8. For delay times of more than 50 μ sec Borisov et.al.¹⁵ have obtained recovery level, E_r , similar to that shown at 10 μ sec in Fig. 1. In their work, E_r begins to increase after about 50 μ sec from 2-3 kV/cm

*The conductivity of the e-beam controlled gas is given by Fernsler et.al.¹³ to be about 10^{-3} mho/cm.

TABLE I

Medium	Max. Induced Field (kV/cm)	Max. Recovery Field (kV/cm)	Reference
<u>a. Fuse Switches</u>			
Water	6	24	2,8
Air	20	20	8
Vacuum*	10	0	8
<u>b. Externally Ionized Gas Switch</u>			
High pressure with e-beam control.	100	100	13

*Walls of the vacuum container at more than 15 cm from the fuse.

and reaches steady state conditions, with $E_r \approx 20$ kV/cm after a millisecond period. The factors that determine the recovery field, E_r , of the fuse exploded in air, are pressure and temperature distributions of the expanding fuse and of the heated air that surrounds the fuse. Because of the rapid change of these distributions, E_r is expected to depend on the delay between the vaporization (that leads to current interruption and subsequent commutation) and the reapplication of the voltage. This dependence on the delay is seen in Fig. 1. For small Δt , the recovery field $E_r(t + \Delta t)$ is approximately equal to the restrike field, $E(t)$, shown in Fig. 2. At large t , the recovery field of Fig. 1 is much lower, due to substantial expansion of the fuse channel.

The late time characteristics of the expansion of the air, resulting from the deposition of energy into the fuse, can also be obtained from electrical discharges in air as studied by Greig et.al.¹⁶ Fig. 3 shows Schlieren photographs of the expansion in air at atmospheric pressure, p_0 , (and density ρ_0) induced by the discharge

initially guided by an intense laser breakdown. Approximately 300 J/m are deposited in the first 5 μ sec. Resulting density depression is 0.05 ρ_0 at 40 μ sec. As the density diagram (Fig. 4) as well as qualitative photography (Fig. 3.) show the relaxation to initial conditions is slow. In addition to the data of Fig. 2 and Fig. 3, conductivity measurements (Fig. 3 of Ref. 16) show that the channel conditions are approaching undisturbed air conditions at about 10 msec. This coincides with the observation of Borisov et.al.¹⁵ that the channel recovery field E_r is again increasing with time to the level associated with undisturbed air (for $\Delta t \leq 1 \mu$ sec). These results suggest that fuses operated in air can be used for pulse bursts with pulse repetition of 100 Hz. Future work is planned to determine the repetition rates for channels with deposited energy density in the 10 kJ/m range.

2. Water.

If higher specific density medium is used for containment of the expanding fuse channel, higher recovery fields can be maintained over the times of interest in repetitive or burst pulser applications. For example, water surrounding the foil fuse provides enough containment to maintain large recovery fields for at least 10 μ sec as shown in Fig. 5. Similar pressure-history dependent phenomena is also observed for fuses exploded in water. Initial data obtained using foils and wires shows that much lower recovery fields are obtainable with wires, due to higher energy density and pressure associated with cylindrical geometry.

3. Vacuum.

The recovery characteristics of fuses exploded in vacuum are more complex, because from the time of on-set of vaporization substantial ionization of the channel is

generated simultaneously with vaporization, in contrast to wires exploded in air. Such ionization results from the thermionic emission of electrons and ions (and their acceleration in the Ohmic potential drop across the fuse) during the heating and vaporization phase as suggested in References 17 and 18. The resistance of the vapor is lowered by ionization, relative to fuses in air.⁸ These measurements were obtained in a geometry with the walls sufficiently far away to prevent quenching of the experiment time scale. The on-set of ionization was indicated in References 17 and 18. This is also supported by resistivity measurements, during and after vaporization, which are consistent with presence of free electrons⁸. The resistance is of Spitzer type, i.e., the resistivity (for T_e in $^{\circ}\text{K}$), valid for $n_e/n_0 \approx 10^{-2}$, is

$$\eta = 3.8 \cdot 10^3 \frac{Z \ln \Lambda}{T^{3/2}} \text{ (Ohm-cm)}$$

and does not depend significantly on the electron density, n_e . The resistance per unit length, $r = \eta/A$, scales inversely with the cross section area, A , of the expanding channel. At vaporization time (for charging time of 3.5 μsec) Bennet¹⁹ shows that typical fuse channel diameter (in air) is 0.2 cm at the time of current cut-off, so that for T_e of 1 to 2 eV and effective $Z \approx 1$, the value of r is 0.2 Ohm/cm. Observed values of r were in the same range. Such behavior of the fuse in vacuum makes it difficult to achieve total current interruption in the fuse. As the current commutation is attempted, residual current continues through the fuse. The voltage of a subsequent pulse applied across the fuse indicates that fuse resistance, drops slowly⁸ with increasing Δt . This drop can be explained by the scaling $r = \eta / A$,

with A increasing with radial velocity of about 5×10^5 cm/s for current driven channels.²⁰ As can be noted from Fig. 2, the fuse resistance reflected through the measurement of the induced voltage approaches that of the fuses exploded in air, as the charging time becomes very short. Such behaviour of the fuses in vacuum indicates that this approach is not suitable for burst-pulse generation.

References

- (1) V.I. Bogdanova, V.A. Burtsev, I.V. Kalinin, O.L. Kamorov, V.N. Litunovsky, Preprint K-0410, Efremov Institute (NIIIEFA), Leningrad USSR, (1978).
- (2) D. Conte, R.D. Ford, W.H. Lupton, I.M. Vitkovitsky, Digest of Technical Papers of the 2nd IEEE Intern'l Pulse Power Conference in Lubbock, Texas, IEEE Catalog #79CHI505-7, p. 276, (1979).
- (3) D.L. Smith, R.P. Henderson, R.E. Reinovskii, Digest of Technical Papers of the 2nd IEEE Intern'l Pulse Power Conference in Lubbock, Texas, IEEE Catalog #79CHI505-7, p. 287, (1979).
- (4) U.A. Kotov, B.M. Kovalchuk, N.G. Kolganov, G.A. Mesyats, V.S. Sedoi, A.L. Ipatov, Sov. Tech. Phys. Lett. 3, 359, (1977).
- (5) D. Conte, R.D. Ford, W.H. Lupton, I.M. Vitkovitsky, Proceedings of the 7th Symposium on Engineering Problems of Fusion Research, Vol. II, IEEE No. 77CHI267-4-NPS.
- (6) V.A. Zheltov, A.V. Ivlev, A.V. Kibardin, A.S. Komin, A.V. Kuchinsky, Yu.A. Morozov, Preprint K-0297, Efremov Institute (NIIIEFA), Leningrad, USSR (1976).
- (7) R.D. Ford, I.M. Vitkovitsky, IEEE Trans. on Electron Devices, Vol. ED-26, 1527, (1979).
- (8) I.M. Vitkovitsky, V.E. Scherrer, to be published in the March 1981 issue of J. Appl. Phys. Also part of this work is published by I.M. Vitkovitsky and V.E. Scherrer, NRL Memo Report 4416, 26 Dec 1980.
- (9) G. Frind, "Current Interruption in High Voltage Network", ed. K. Rogaller, p. 67-94, Plenum Press, New York (1978).
- (10) T.H. Lee, "Physics and Engineering of High Power Switching Devices", The MIT Press, Cambridge, Mass. (1975).

- (11) R. Dethlefsen, J. Mylinus, IEEE Trans. on Electron Devices ED-26, 1491 (1979).
- (12) B.M. Kovalchuk, G.A. Mesyats, Sov. Tech. Phys. Lett. Vol. 2, No. 7, (1976).
- (13) R. Fernsler, D. Conte, I.M. Vitkovitsky, IEEE Trans. on Plasma Science PS-8, 176 (1980).
- (14) A. Guenther, Proceedings of the Repetitive Opening Switch Workshop, Durango, Colorado, Jan 1981.
- (15) R.K. Borisov, V.L. Budovich, I.P. Kuzhekin, Sov. Tech. Phys. Lett. 3, 516 (1977).
- (16) J.R. Greig, et.al., Proceedings of the AIAA 13th Fluid and Plasma Dynamics Conference, Snowmass, CO, July, 1980.
- (17) B. Stenerhag, S. K. Handle, I. Holmstrom, Z. F. Physik, 198, 172 (1967).
- (18) B. Stenerhag, S. K. Handle, B. Gohle, J. Appl. Phys. 42, 1876, (1971).
- (19) F. D. Bennett, G. D. Kahl, Ref. 9, Vol. IV, p.1.
- (20) D. C. Chern, T. Korneff, "Exploding Wires", Vol. IV, p. 173, Plenum Press, NY (1968).

Figure Captions

- Fig. 1. Recovery field, E_r , of fuses exploded in air. The field is determined by converging the breakdown and no-breakdown data (by adjusting the fuse length) to a minimum difference.
- Fig. 2. Inductively generated electric field, E , at restrike, shown as a function of t for fuses exploded in vacuum and at atmospheric pressure.
- Fig. 3. Schlieren photographs of air expansion induced by an electrical discharge. Time between frames is shown in seconds.
- Fig. 4. Density distribution following a discharge in air as determined by an interferometric measurement.^{16A}
- Fig. 5. Dependence of the dielectric strength, E_r , of Al foil fuses in water. Higher values of E_r are obtained in the fuse which also is associated with a higher inductive voltage shown as a parameter for each curve.

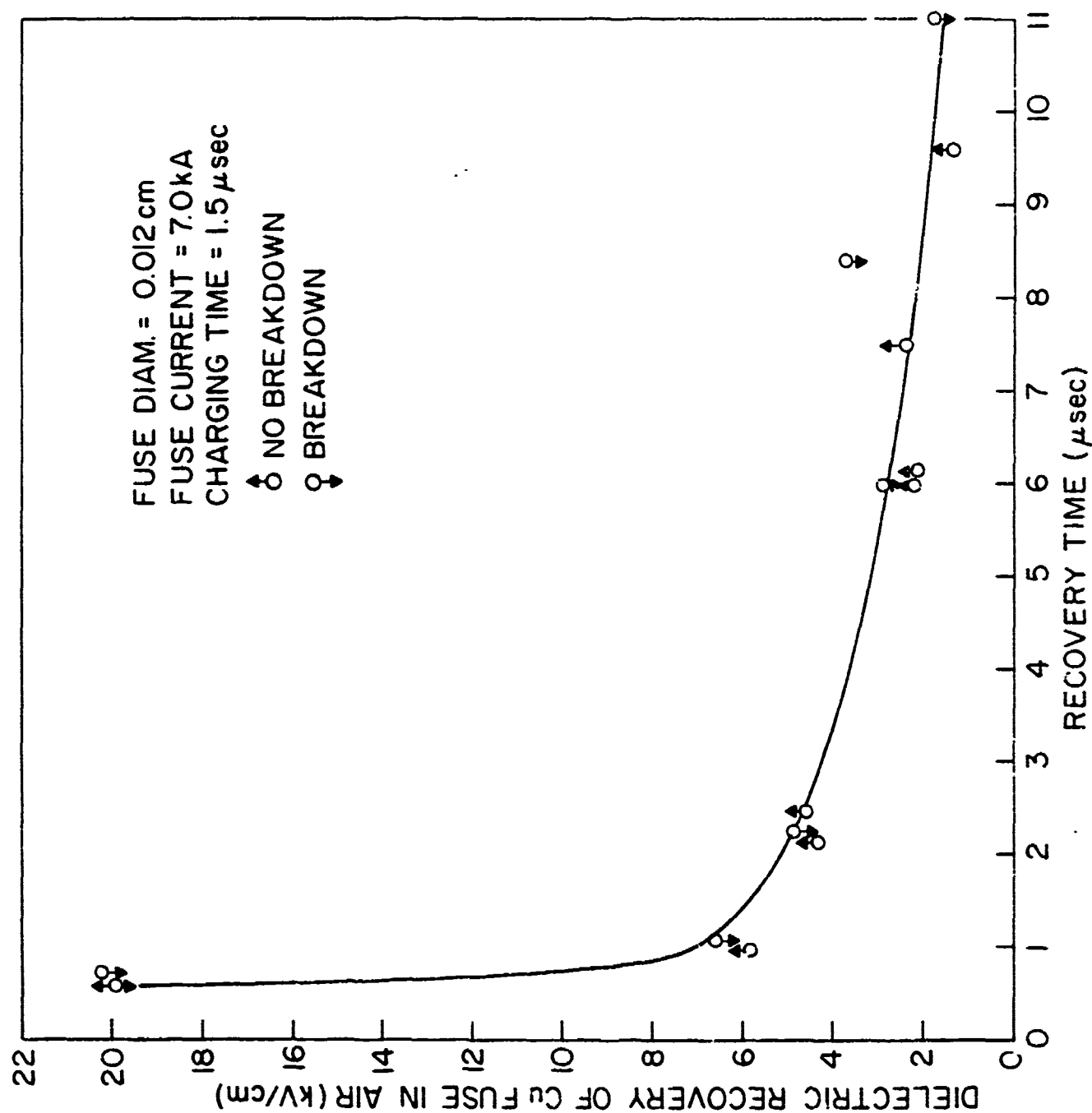


Fig. 1 Recovery field, E_r , of fuses exploded in air. The field is determined by covering the breakdown and no-breakdown data (by adjusting the fuse length) to a minimum difference.

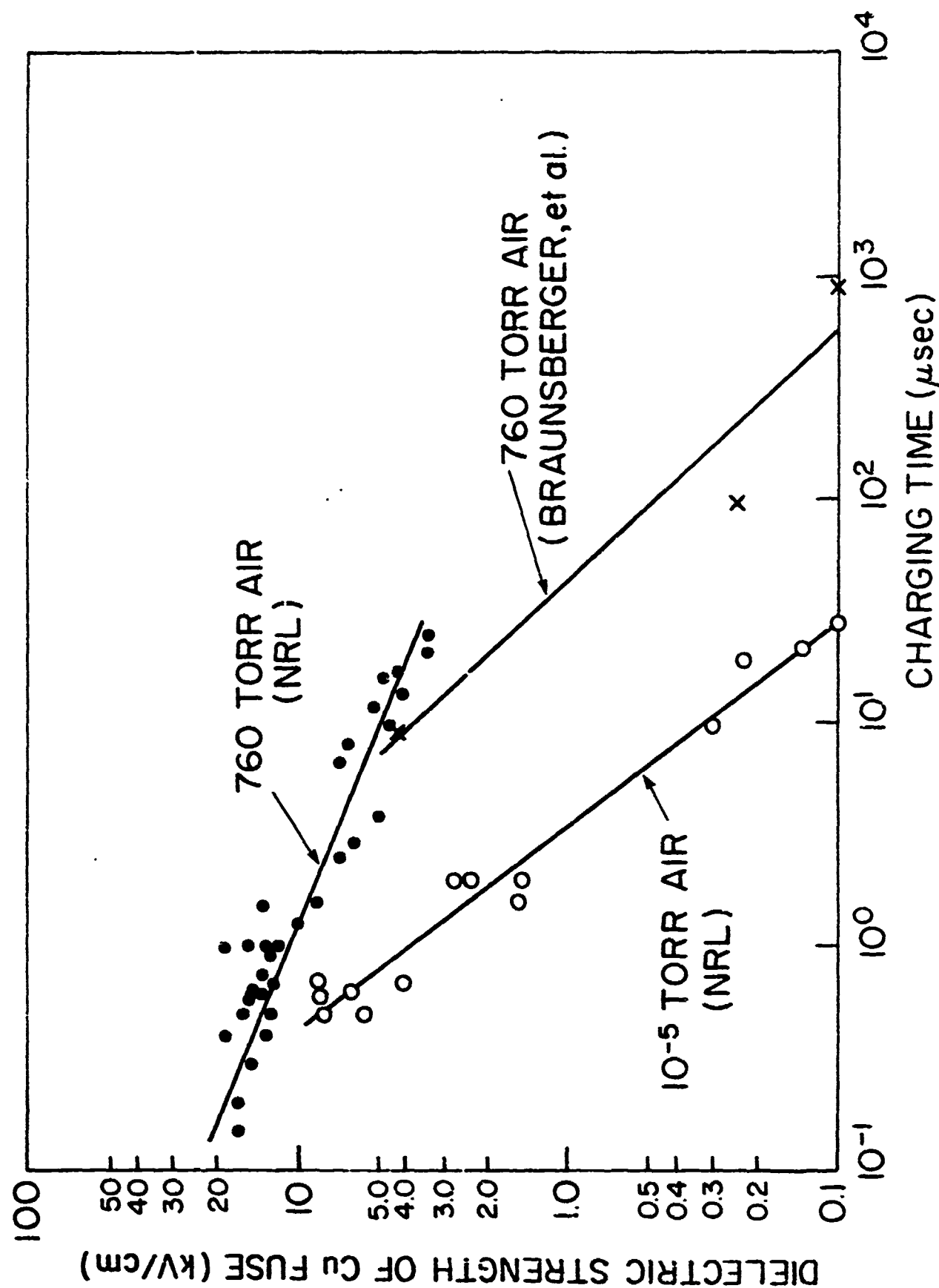


Fig. 2 Inductively generated electric field, E , at restrike, shown as a function of t for fuses exploded in vacuum and at atmospheric pressure.

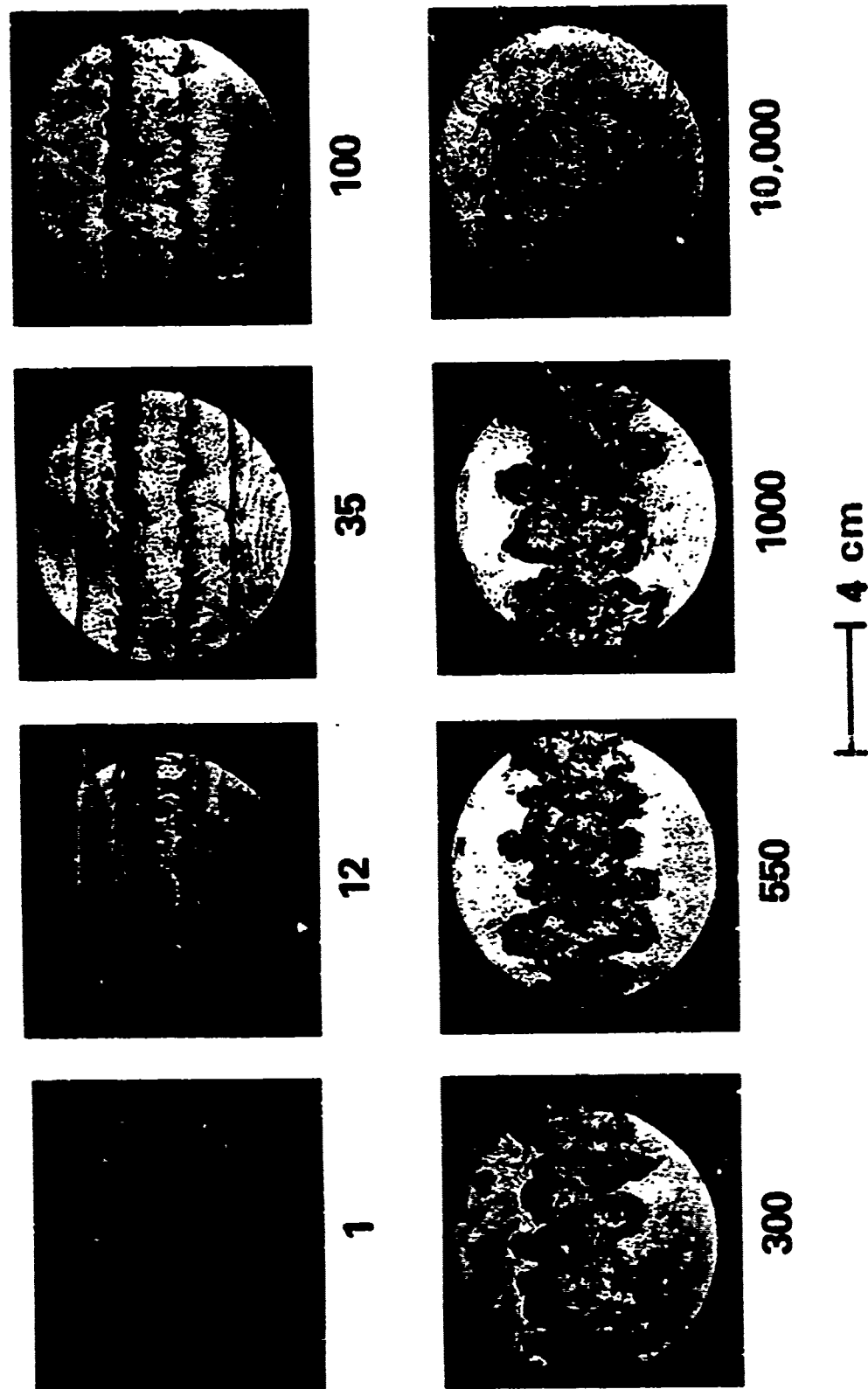


Fig. 3 Schlieren photographs of air expansion induced by an electrical discharge
Time between frames is shown in seconds.

CHANNEL DENSITY vs RADIUS

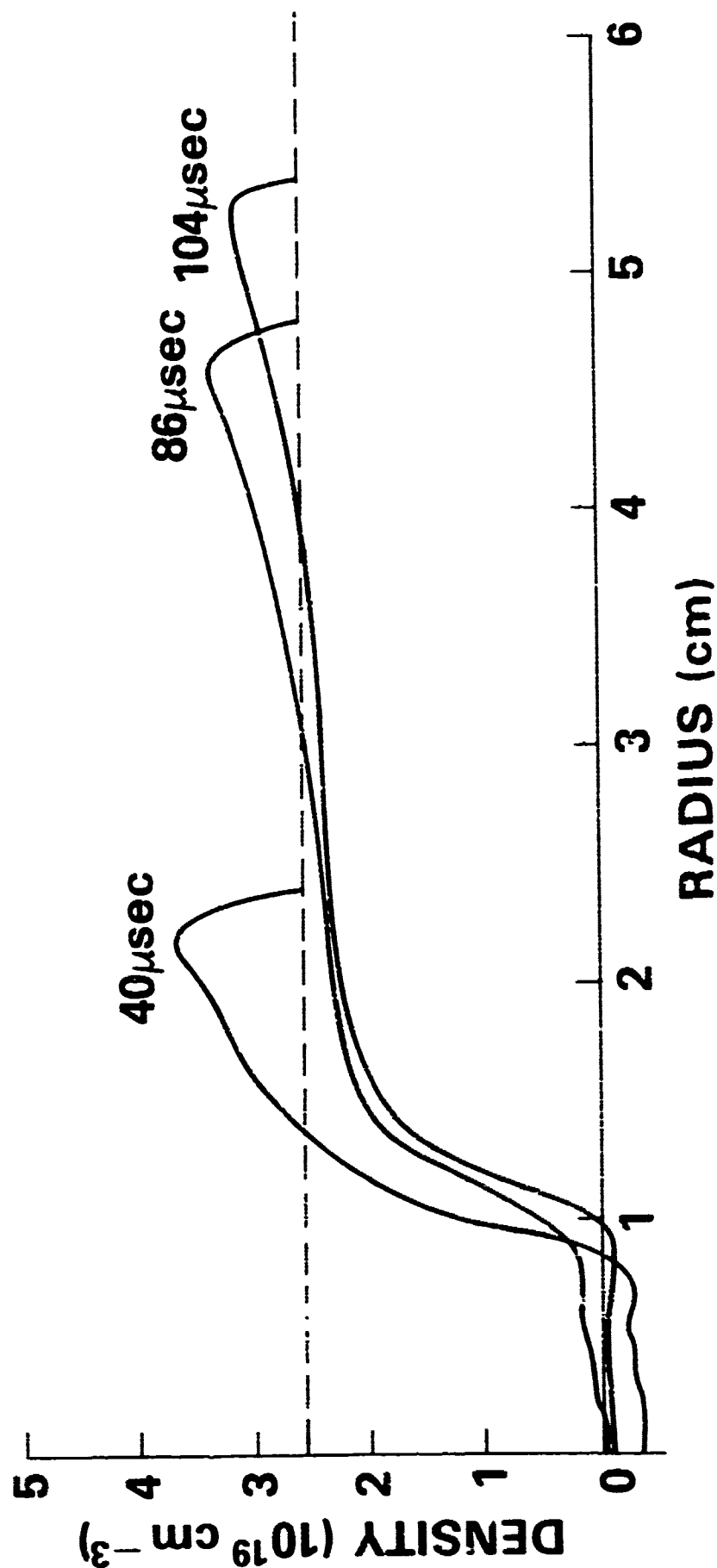


Fig. 4 Density distribution following a discharge in air as determined by an interferometric measurement. 16A

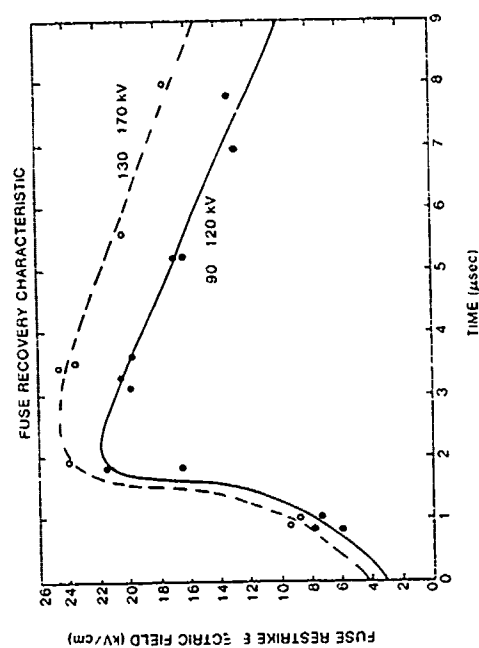


Fig. 5 Dependence of the dielectric strength, E_r , of Al foil fuses in water. Higher values of E_r are obtained in the fuse which also is associated with a higher inductive voltage shown as a parameter for each curve.

EXPERIMENTS WITH AN EXPLOSIVELY OPENED PLASMA SWITCH*

B. N. Turman and T. J. Tucker
Sandia National Laboratories
Albuquerque, New Mexico 87185

ABSTRACT

Scaling experiments have been performed on an explosively activated plasma opening switch. Current density and choice of explosive apparently are the most important variables in determining switch performance. Granular nitroguanadine, Octol, and Comp B3 explosives provide the fastest switching times. Granular nitroguanadine, when used to quench a planar plasma channel, gave a switch time of 0.3 μ s at a current density of 60 kA/cm (90 kA current). Detasheet explosive was used to quench a cylindrical plasma channel, with submicrosecond switching time of megampere currents.

A. INTRODUCTION

Pavlovskii [1,2] showed that multi-megampere currents can be switched on a time-scale shorter than one microsecond with the use of an explosively-compressed plasma channel. He reported an experiment in which a 7 MA current was diverted to a 30 nH load with a current risetime of 0.5 μ s and a voltage gradient of 25 kV/cm. Baker [3] suggested that the observed resistance increase of the switch is due to Rayleigh-Taylor mixing of low-conductivity explosive products into the plasma channel. His model predicts that the resistance rise-time is influenced by the following parameters: foil mass per unit area (m), channel width (d_0), channel pressure at explosive breakout (P_0), and explosive pressure (P_e). The resistance rise time in nanoseconds, τ_R , is given by:

*This work was supported by the U.S. Dept. of Energy, under Contract DE-AC04-76-DP00789 and U.S. Air Force Weapons Laboratory, under Project Order 80-109.

$$\tau_R = 13 (md_o)^{1/2} p_o^2 p_e^{-5/2}$$

with all parameters in c.g.s. units. On the basis of this model, Baker [3] predicted that switching time on the order of 100 ns should be achievable.

This concept appears to be useful for large current, single pulse applications, and we are now investigating the physical characteristics and operational limitations of the device. In its present configuration, this switch certainly cannot be operated repetitively, but the basic physics of plasma quenching may have future application for repetitive switching.

B. DESCRIPTION OF EXPERIMENTS

Two parallel experiments have been conducted to survey the parameters which are most important in establishing the resistance risetime and peak resistance of the plasma switch. The first experiment has a cylindrical plasma channel, in much the same configuration as Pavlovskii's switch. The second experiment uses a planar plasma channel, which facilitates testing of different explosives.

1. Cylindrical Switch

Figure 1 is a schematic drawing of the cylindrical switch. The plasma switching element is located coaxially around a cylinder of high explosive material. The plasma is initiated with a thin aluminum foil, typically a seamless paralene film with about 350 Å aluminum coating. The diameter of the foil is 4.5 cm and its length is 3 cm. About 10% of the inductively stored energy is dissipated in the plasma, which is heated to a blackbody temperature of about 2 eV. Detasheet was chosen as the explosive for these tests, based on results from an early feasibility study [4]. The switch is activated by detonating the cylindrical explosive at the axis with a long, exploding bridgewire detonator. A cylindrical detonation wave moves through the explosive, and the

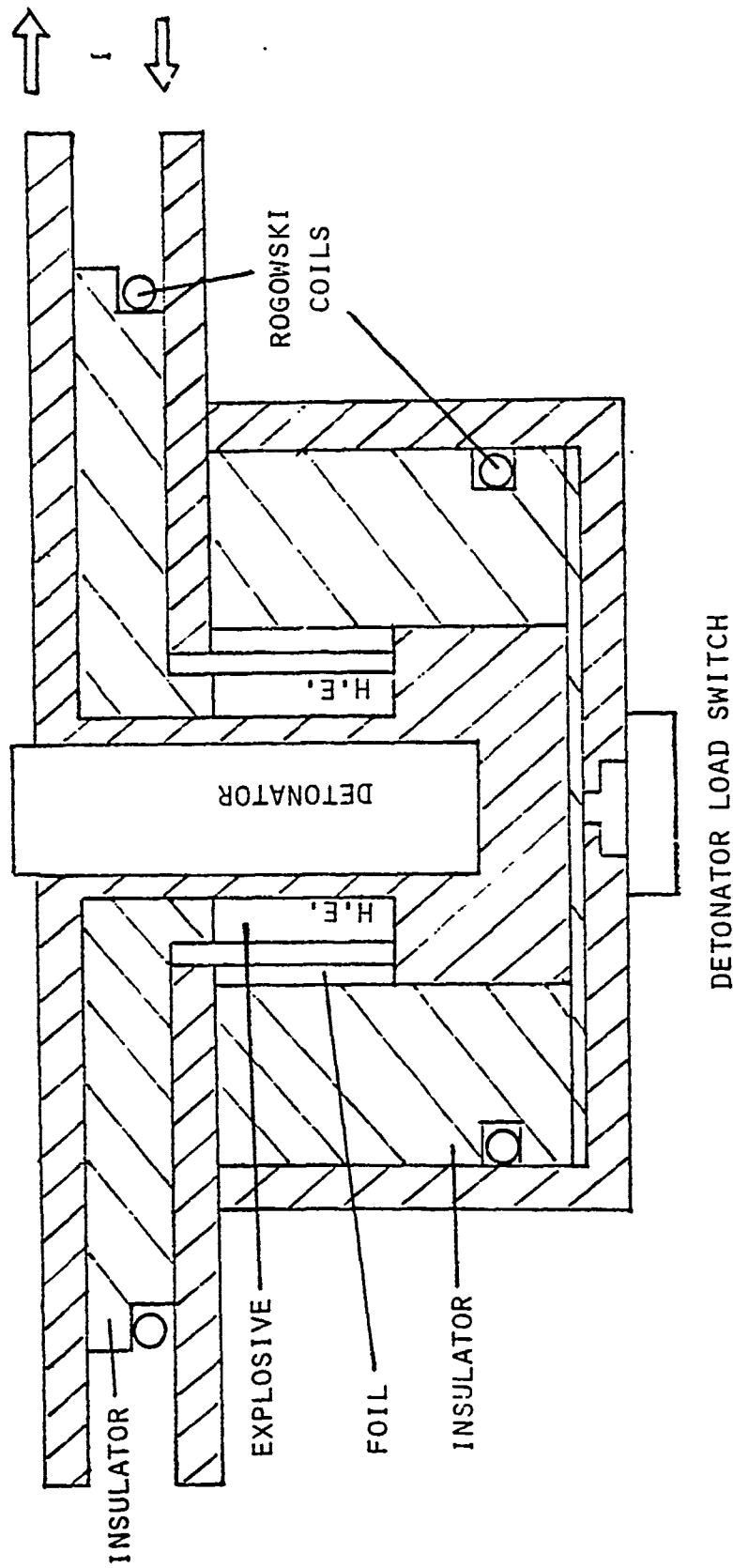


Figure 1. Schematic diagram (not to scale) of cylindrical plasma switch used for high current tests.

plasma channel is compressed as this wave emerges from the surface of the explosive. The interface between the plasma and the explosive gases is Rayleigh-Taylor unstable, so that spikes of low conductivity gas presumably mix quickly into the plasma. The plasma resistance increases from about 1 milliohm to a value of 20-400 milliohm within a microsecond or less.

Figure 2 shows the circuit diagram and a typical set of primary and load current profiles, from test #3. A dummy load of 10 nH is switched across the plasma about one microsecond before it opens. This closing switch (a detonator switch) is also explosively operated. The initial increase in load current in Figure 2 from 29-30 μ s, comes from the closure of the load switch; the large increase in load current, starting at 30 μ s, is the result of opening the plasma switch. Switch resistance for this test is plotted in Figure 3.

2. Planar Switch

Figure 4 shows the layout for the planar experiment for explosives characterization. This device features easy access to the explosive, allowing us to determine explosive shock front position concurrently with voltage and current waveform data. Different explosives can be introduced easily in this geometry. Operation of this experiment is similar to that for the cylindrical switch, with the exception that this switch was opened across a line inductance of 60 nH.

C. EXPERIMENTAL RESULTS

1. Cylindrical Test Results

Seven cylindrical switch tests have been completed to date. In these tests we were interested in identifying the experimental parameters which influenced switch performance. The following parameters were changed: current, foil mass, channel width, and initial plasma channel pressure (and

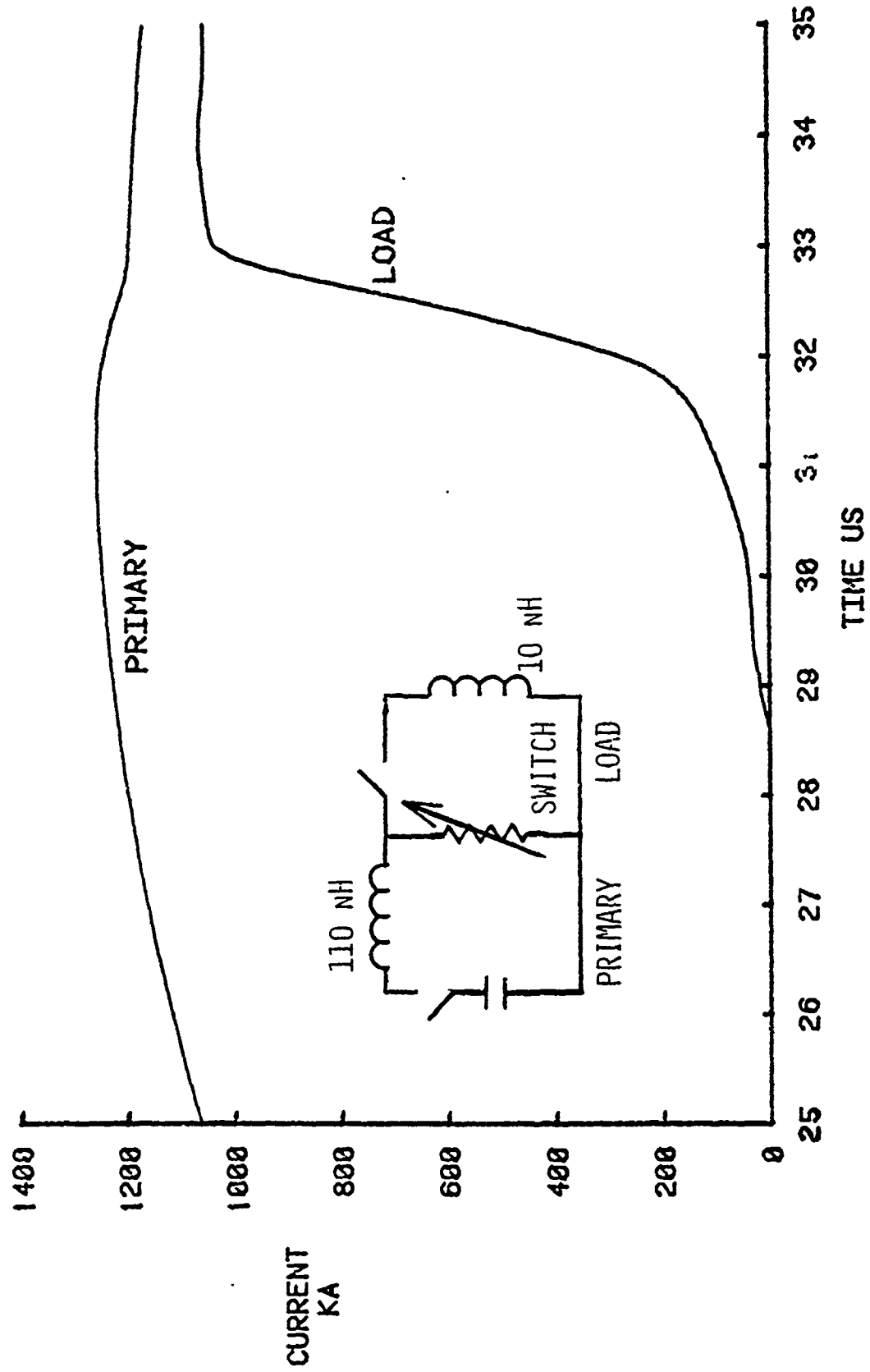


Figure 2. Test circuit and typical primary and load current profiles.
Load switch closed at 29 μ s; plasma switch opened at 30.5 μ s.

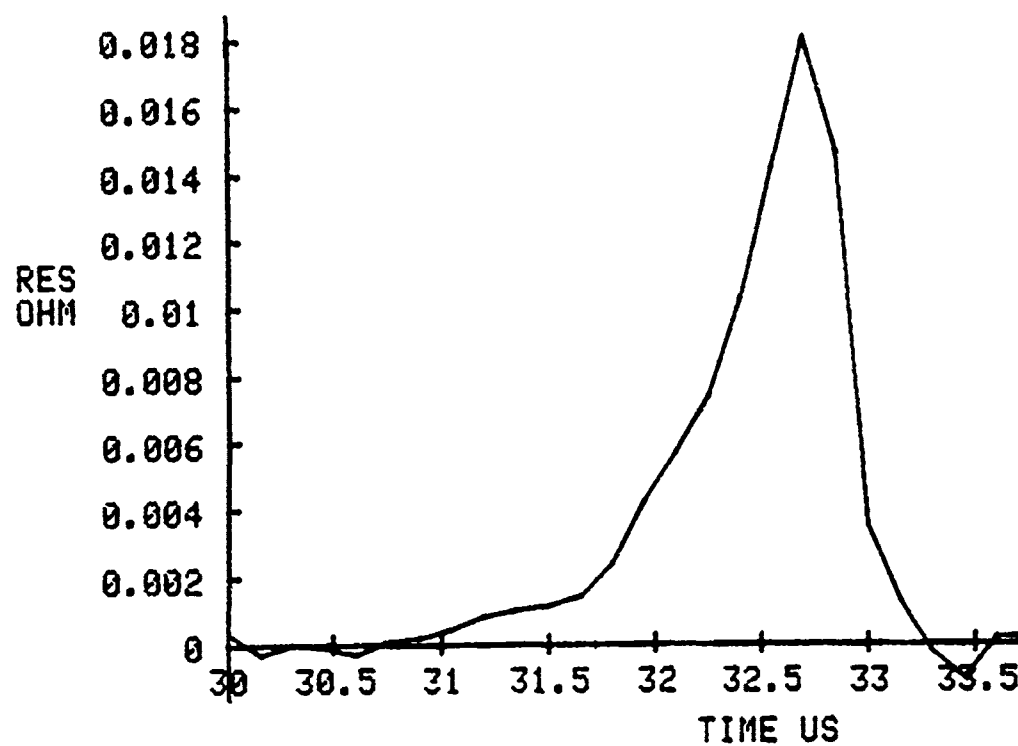


Figure 3. Plasma switch resistance which produced the current profiles of Figure 2.

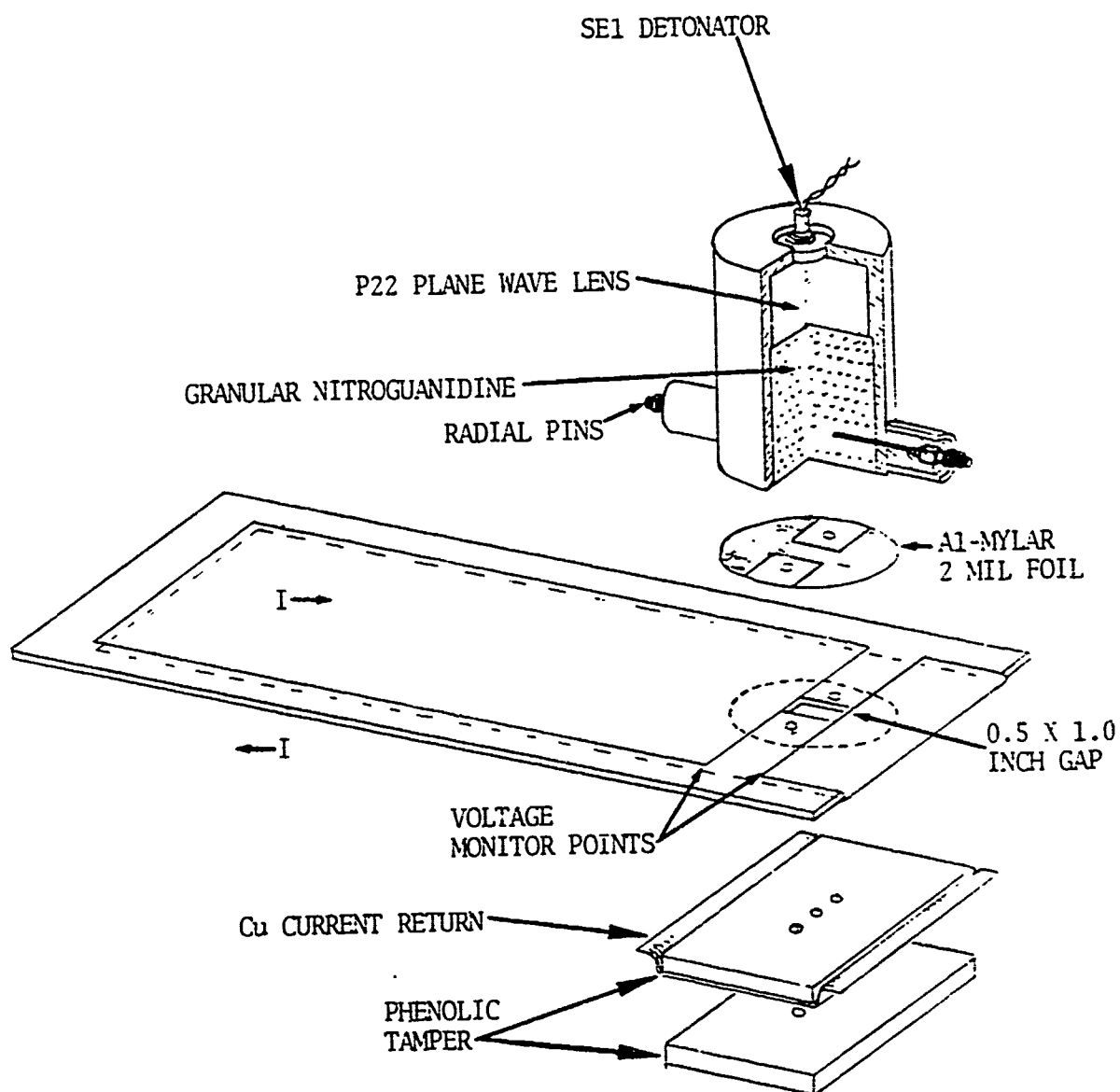


Figure 4. Experimental arrangement for explosive characterization with planar plasma switch.

therefore plasma density). Test results are summarized in Table 1. It appears that current is the most important variable for this series of tests with Detasheet explosive. Resistance risetime shows a strong correlation (about 96% correlation coefficient) with the square of the current, as plotted in Figure 5. Least squares fit to the data is shown by the straight line. The y-intercept for this line is $0.3 \mu s$, the same value that was independently measured for total asymmetry in break-out time of the detonation wave. Thus the minimum switching time for this device seems to be determined mainly by asymmetry in the detonation. Dependence of switching time on the square of the current may be the result of magnetic pressure or resistive heating of the plasma. Further tests and computer modeling will help resolve this issue.

Is the operation of this switch reproducible from one test to the next? If we assume that foil mass and initial plasma pressure have small effects on switch operation, we can consider tests #1 and #4 (current at 0.9 MA), and also tests #3 and #5 (current at 1.3 MA) as reproducibility experiments. Resistance risetime is reproduced within 10%, and peak resistance is reproduced within 30%.

In the first six tests the load switch was closed about a microsecond before the opening switch was activated. The result is that load current risetime is about the same as resistance risetime. Circuit modeling shows that load current rise can be sharpened dramatically, by a factor of 2 or more, by closing the load switch during resistance rise of the opening switch. This effect is illustrated vividly in test #7; the load switch closed at the mid-point of the resistance rise of the plasma switch, giving a load current rise which was a factor of 2 faster than resistance rise. To exploit this effect, we plan to incorporate a dielectric breakdown switch (which is more precisely controllable than the detonator switch) in future tests.

Table 1
Cylindrical Foil Test Results

Shot Parameters	#1	#2	#3	#4	#5	#6	#7
Channel Width (cm)	0.8	0.8	0.8	0.5	0.8	0.8	0.8
Foil Mass (gm/cm ²)	5x10 ⁻⁴	5x10 ⁻⁴	5x10 ⁻⁴	5x10 ⁻⁴	1.2x10 ⁻³	5x10 ⁻⁴	5x10 ⁻⁴
Fill Pressure (atm)	0.1	1	1	1	1	1	1
Switch Current (MA)	0.85	0.45	1.25	0.96	1.28	2.10	2.63
Current Density (MA/cm)	0.060	0.032	0.088	0.068	0.091	0.149	0.186
Peak E field (kV/cm)	3.1	4.3	2.8	3.8	7.1	4.4	4.3
10-90% Current Risettime (μs)	0.80	0.50	1.20	0.75	-	1.65	1.75
10-90% Resistance Risettime (μs)	0.63	0.66	0.93	0.62	1.0	1.60	3.60
Initial Resistance (mΩ)	1.6	1.0	0.5	1.0	0.8	1.6	1.0
Peak Resistance (mΩ)	67	400	18	40	18	30	12

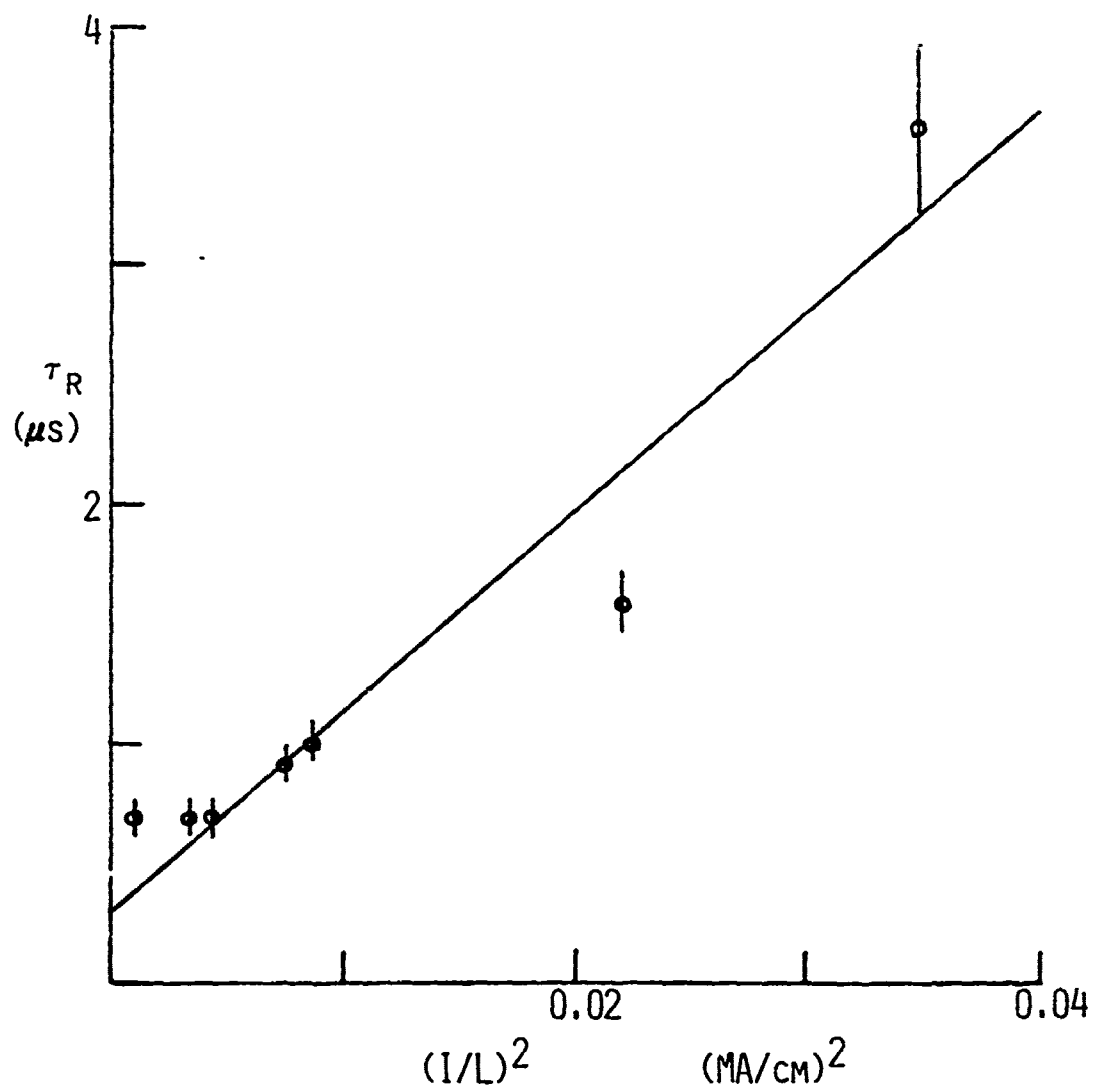


Figure 5. Current scaling of resistance risetime for cylindrical plasma switch.

Table 2
Explosive Characterization Results

<u>Explosive</u>	<u>P_O⁺ (Kbar)</u>	<u>Peak Current Density (kA/cm)</u>	<u>Peak E-Field (kV/cm)</u>	<u>Current Switch Time (μs)</u>
Nitroguanadine (Test #1)	75	58	> 7	0.30
Nitroguanadine (Test #4)	75	54	8	0.25
Octol	342	47	-	0.4
Comp B3	280	69	5	1.1
Detasheet	184	69	1	1.7
Baratol	140	47	-	1.8
TNT	190	47	-	2.0
PBX-9404	375	46	No switching observed	

+ Chapman-Jouquet pressure

2. The Choice of Explosive

Planar switch tests have shown that the choice of explosive has a crucial influence on switch operation. Test results are summarized in Table 2. Chapman-Jouguet explosive pressure gives no clear order to the switching times that have been observed. It does appear, however, that granular explosive (nitroguanadine) or mixtures of explosive (Octol and Comp B3) give the fastest switching. Enhanced turbulence in these explosives may decrease the effective conductivity in the explosive reaction zone through stronger Rayleigh-Taylor mixing. We plan to study this phenomenon in more detail in later tests.

D. CONCLUSIONS

These experiments suggest that the explosive is the most important variable in determining switch performance. Current density (per unit width) also appears to be important, while foil mass, channel width and initial plasma pressure introduce small effects or none at all. The fastest current switching time measured in these experiments was $0.3 \mu\text{s}$ at a current density of 60 kA/cm , with nitroguanadine in the planar configuration. Peak electric field across the plasma was 8 kV/cm , with no indication of breakdown of the switch at this stress. The cylindrical switch has been tested at high current, up to 2.6 MA . The Detasheet explosive used in these tests is not the optimal choice for this device, but we have none-the-less switched megampere currents in $1 \mu\text{s}$ or less. We intend to use more suitable explosives in the cylindrical switch in the next test series.

E. REFERENCES

- [1] A. I. Pavlovskii, V. A. Vasyukov and A. S. Russkov, "Magnetoimplosive Generators for Rapid-Risetime Megampere Pulses", Soviet Tech. Phys. Lett. 3, 320-321, 1977.

- [2] A. I. Pavlovskii, R. Z. Lyudaev, A. S. Kravchenko, V. A. Vasyukov, L. N. Pljashkevich, A. M. Shuvalov, A. S. Russkov, Y. Ye. Gurin, B. A. Boyko and V. A. Zolotov, "Formation and Transmission of Magnetic Cumulation Generators Electromagnetic Energy Pulses", Megagauss Physics and Technology, Peter J. Turchi, Editor, Plenum Press, New York, pp. 595-609, 1980.
- [3] L. Baker, "Theoretical Model for Plasma Opening Switch", Sandia National Laboratories Report SAND80-1178, July 1980.
- [4] G. L. Sauve and B. W. Duggin, "Intrepid--An Explosively Driven Plasma as a Fast Opening Switch", Particle Beam Fusion Report - January 1980 through June 1980, Sandia National Laboratories Report SAND80-2500.

PULSES OF ENERGY FROM AN INDUCTIVE STORE*

by

Gordon K. Simcox

1. Introduction.

The purpose of this Workshop is to examine reasonable approaches to the design of a repetitive opening switch, operating with an inductive energy store.

The required switching parameters are:

Peak voltage	>10 kV
Peak current	>10 kA
Voltage rise-time	$\leq 1 \mu\text{sec}$
Repetition rate	>10 Hz

The applications have not been defined and therefore one can speculate that the power source can be applied to:

- o Drive a load directly
- o Charge a capacitive energy store which is probably water insulated

If the latter is intended or seen to be a frequent requirement, then a case must be made for broadening the interest to slower rates of energy extraction from the sources.

There is a growing realization that reliable, repetitive, pulsed power systems require the simplest circuit arrangements. Critical switching and dielectric functions should therefore be kept to a minimum. In many cases, particularly in the nanosecond pulse regime, the final stage energy switching and transmission problems cannot be avoided but the associated power conditioning, back to the prime energy source, can operate in non-critical modes.

This notion of simplicity is supported by the concept of a Compensated Pulsed Alternator (Compulsator) directly charging a pulse-forming line or network in periods of 50-100 microsecond^[1] Solid dielectrics and cooled water have been advocated as PFL insulants to make this possible^{[2][3]}

* This paper was submitted later and was not presented at the workshop.

In an ideal case, all of the inter-pulse, or inter-burst period should be available for charging the final energy store of a system, after due allowance for circuit recovery. If this is so, then the demands on the prime energy source are at a minimum and if that source is an inductive store, energy may be extracted by the use of conventional circuits and commercial types of switches.

The following is an edited version of a report on a short study performed for the A.F. Foreign Technology Division in 1980. A concept for the repetitive removal of energy packages from an inductive store is examined. The examination is not in depth but intended to expose technology which could be worthy of further development and application.

2. Statement of the Requirement.

There is a pulse generator which must discharge 10^6 joules of capacitively stored energy to a load 20-30 times per second. This capacitive store is to be charged to 10^5 volts for each discharge.

A cooled, 40×10^6 joule, inductive energy store is provided as an energy source for the pulse generator. The preferred inductance value is $4.0 \times 10^{-6} \text{H}$.

The requirement is to devise a switching scheme which has the potential to extract the 10^6 joule energy parcels from the inductive store at the required rate. Figure 2.1 illustrates the requirement in simple outline.

3. Background and Selection of a Concept.

The economic and physical advantages of inductive energy storage have been recognized for the past twenty-five years but the engineering problems associated with current interruption and energy transfer to a load have been difficult to solve.

Concepts which rely on exploding switches, fuses and vacuum circuit-breakers have attained varying degrees of success when coupled with commutation assisting circuits.

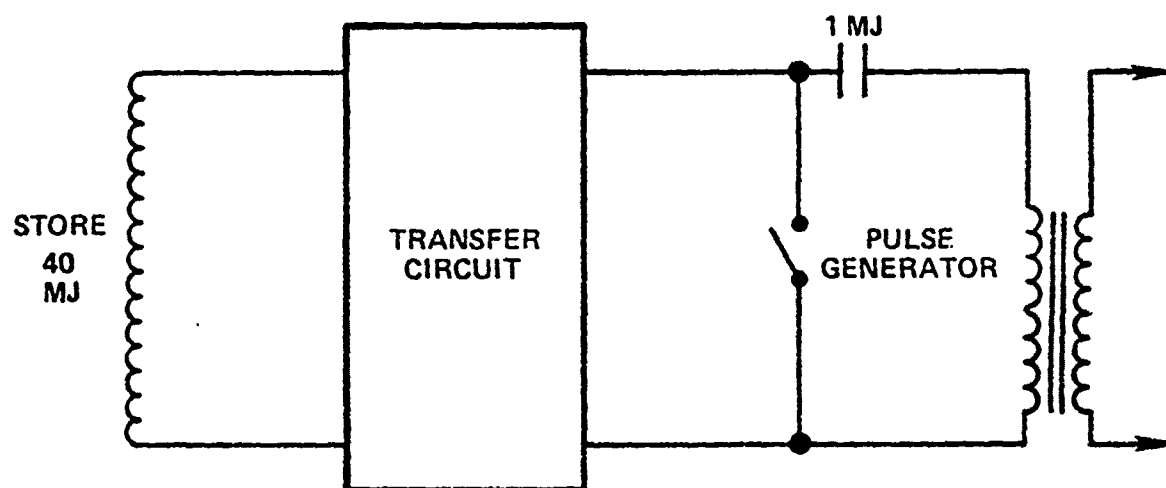


Fig. 2.1 Circuit Outline

The general implication is that if the inductor current is successfully interrupted then all the stored energy will be released to the load with an acceptable commutation efficiency. If, as required in this problem, the energy release must be in discrete quantities spaced over periods in order of 1 second, then the switching issues are even more difficult. Such a requirement is likely to assume more importance with the emergence of new charged particle accelerators.

In the 1960's and 70's the electrical requirements for the field coils of Magnetic Confinement Fusion reactors became a major issue. The stored energy levels needed

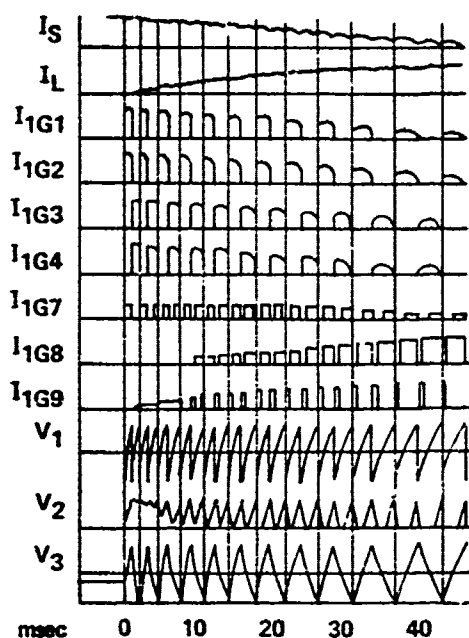
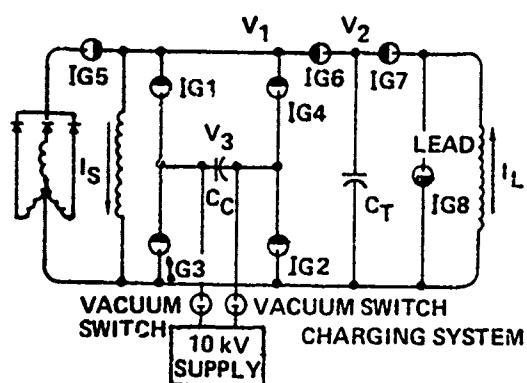
were in the 10^8 - 10^{10} joule range and eventual repetitive operation had to be considered.

Mechanical and chemical storage has been used but the ultimate use of superconducting, magnetic storage was recognized. To utilize this technology a satisfactory method of transferring the stored energy to the load coils was required. The interrupting switch technology was not attractive for a complex, high cost facility of a fusion test reactor - a more conventional and controlled technique was wanted.

Early efforts to solve this energy transfer problem were made at the Princeton Plasma Physics Lab during the planning phases of TFTR. SIMON & BRONNER[4] proposed a scheme for inverting the direct current of an inductive store to an alternating current of triangular waveform at a 500 Hz rate. This alternating current could then be switched and rectified to produce a direct current in the load. An outline of this circuit with energy transfer waveforms is given in Figure 3.1. This scheme has been experimentally verified for both inductive and resistive loads, using ignitron and SCR switches and claims for >90% energy transfer efficiency are made.

The problem has also been addressed in Germany, DICK and DUSTMANN[5] have reported using a "Flying Capacitor" between the super-conducting store and inductive load. This capacitor is alternately charged from the inductive store and discharged to the load via an SCR switching arrangement. This scheme, with waveforms is shown in Figure 3.2. It is not immediately obvious how this method could apply to resistive or capacitive loads but the principle of energy transference is confirmed.

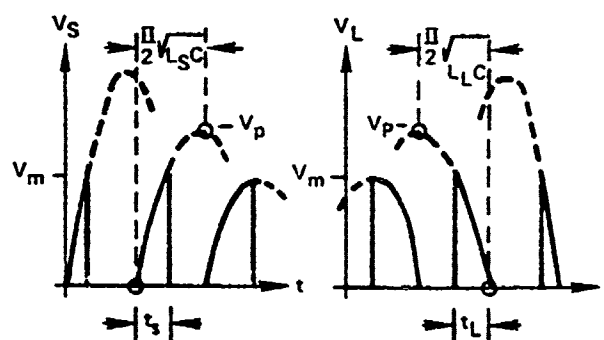
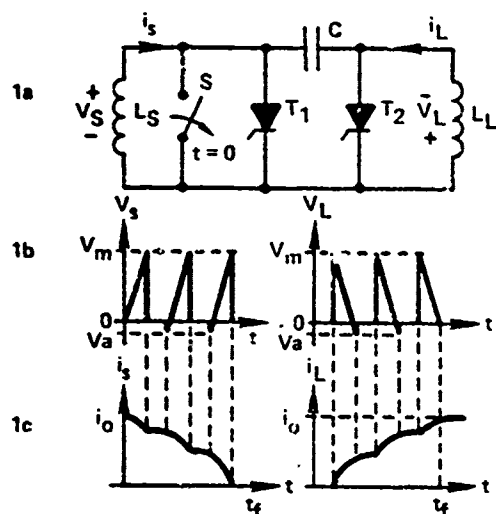
Workers at the University of Wisconsin Tokamak, UW MAK-I have evaluated methods of reducing the peak load requirements on the three-phase prime power supply through the use



Separate Charging System

Current and Voltage Waveforms

Fig. 3.1



Flying Capacitor Transfer

Variable Step Time

Fig. 3.2

of a coupled super-conductive store. PETERSON, et al, [6] have reported in detail on a scheme in which a large super-conducting store is charged from a three-phase supply via a power source inverter. Energy can then be commutated to the inductive load via further inverter controls -or- energy can be returned to the source inductive store from the load.

In this arrangement, a number of loads may be supplied from the inductive store by programmed operation of inverter systems. Figure 3.3 shows a block schematic and the circuit of an inverter arrangement.

From the foregoing, it is evident that there are candidate technologies for extracting parcels of energy from inductive stores. It remains to evaluate the potential for supplying the capacitive loads of particle accelerators rather than the inductive loads of fusion reactors, etc.

Because there should be little need for component development, the inverter switching schemes are attractive and, in particular the scheme of SIMON & BRONNER seems worthy of a first inspection. This will be done without prejudice to the other schemes, which could prove more effective in the last analysis.

4. Evaluation of USSR Literature.

It is of prime interest to this limited study that any technique(s) examined should not lie outside the range of Soviet concept evaluations and possible developments. In a review paper on inductive energy storage, GLUKHIKH, GUSEV et al [7] present a table of main switching methods for "tapping" energy from inductive stores.

The principle methods include:

- o Arc Switching (b)
- o Explosive Foils (c)
- o Arcless Switching (d)
- o Changing Inductance (e)

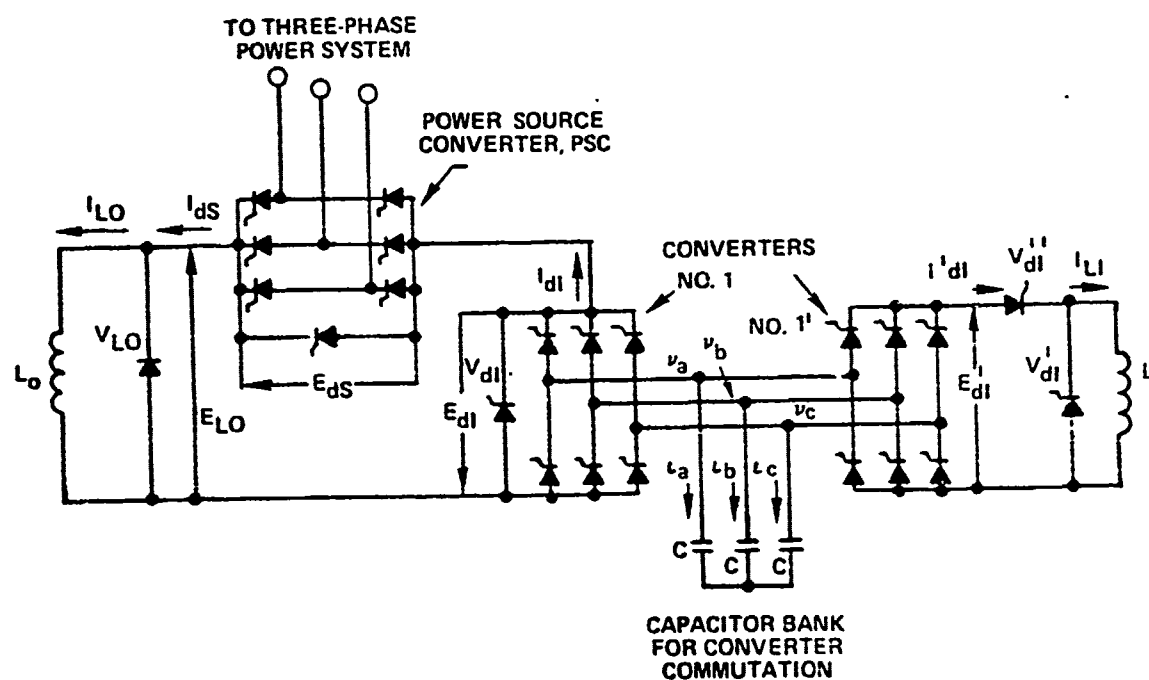
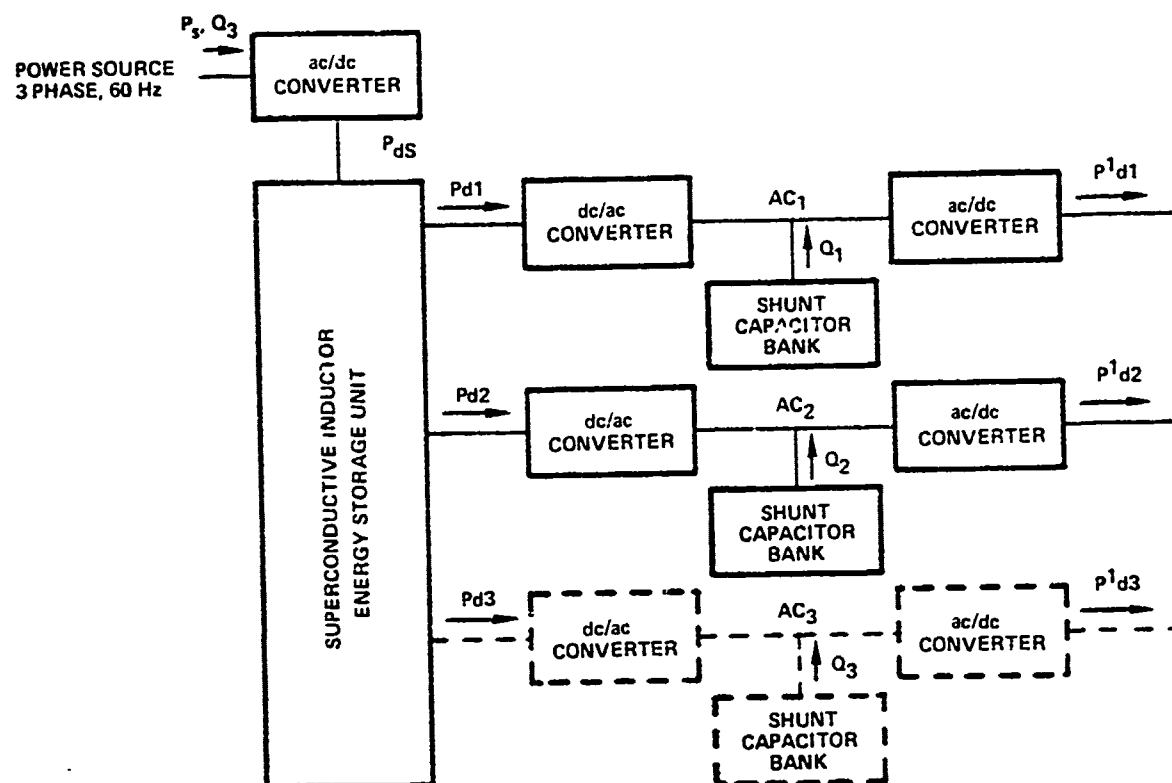


Fig. 3.3 Basic Arrangement to Supply Pulsed Power Using Three Phase Intermediate Conversion

A branch in the arcless switching is denoted by:

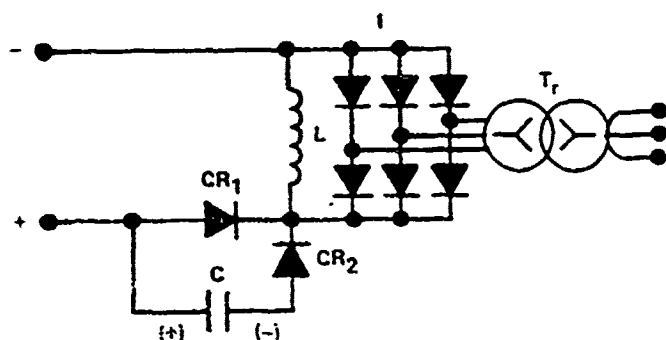
"Semiconductor of Controllable Valve"

This is tentatively related to an item in another branch:

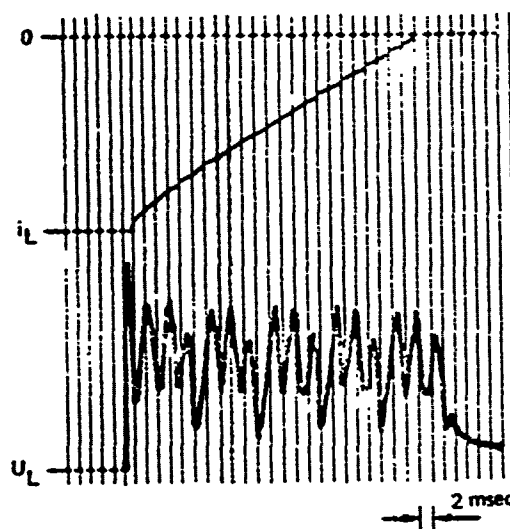
"Circuits for Lowering the Energy of Auxiliary Battery"

There is no supporting information on these in the paper but it is possible that schemes such as those in References [4], [5] and [6] fall into these classes.

From the literature reviewed the most apt paper was originated at the Institute for High Temperatures by V. V. ANDRIANOV et al (8 authors). [8] This paper deals directly with the extraction of energy from super-conducting stores via an inverter/transformer. The schematic for the technique is shown in Figure 4.1. The first two paragraphs of this paper are generally interesting reading.



Schematic Diagram of the Experimental Apparatus. See text for explanation.



Oscillogram of the Voltage (U_L) across the Superconductor Solenoid and of the Current (i_L) through the Solenoid

Fig. 4.1

The evidence is not overwhelming but, based on the above, it is reasonable to postulate that the potentials of the technology are recognized in the USSR.

5. Application of the SIMON & BRONNER Concept.

Firstly, for any scheme which extracts energy from an inductive store in an incremental manner, the inductance of the store must be high enough such that the energy stored in the stray inductances of the switching circuit is less than the energy parcel to be delivered.

For the inverter type of circuit, it would be difficult to obtain switching circuit inductance $< 1 \mu\text{H}$. This is not compatible with a $4 \mu\text{H}$ energy store and it has been agreed to change the store inductance to 1 mH .

For this case, the concept has three parts:

- o An inverter circuit which can satisfy the current flow requirements of the energy store.
- o A transfer capacitor which will extract parcels of energy from the store.
- o An energy transformation circuit which can charge the pulse generator capacitive store to 100 kV .

5.1 Inverter Circuit (Figure 5.1).

For 40 MJ stored the current will be 283 kA . This current is too high for single module inverter switching and therefore the inverter should have a number of parallel modules which is suitable for the type of switch chosen.

In this case, let it be assumed that SCR's will be used. This implies that in the order of 100 modules will be necessary and this can still be relatively compact.

The commutating capacitor (C_c) should now be sized. It is recommended that no more than 1 percent of the stored energy should be transferred to the commutating capacitor. That is $< 400 \text{ kJ}$ total or $< 4 \text{ kJ/module}$. If we allow the peak voltage of the commutating capacitor to reach 15 kV , the

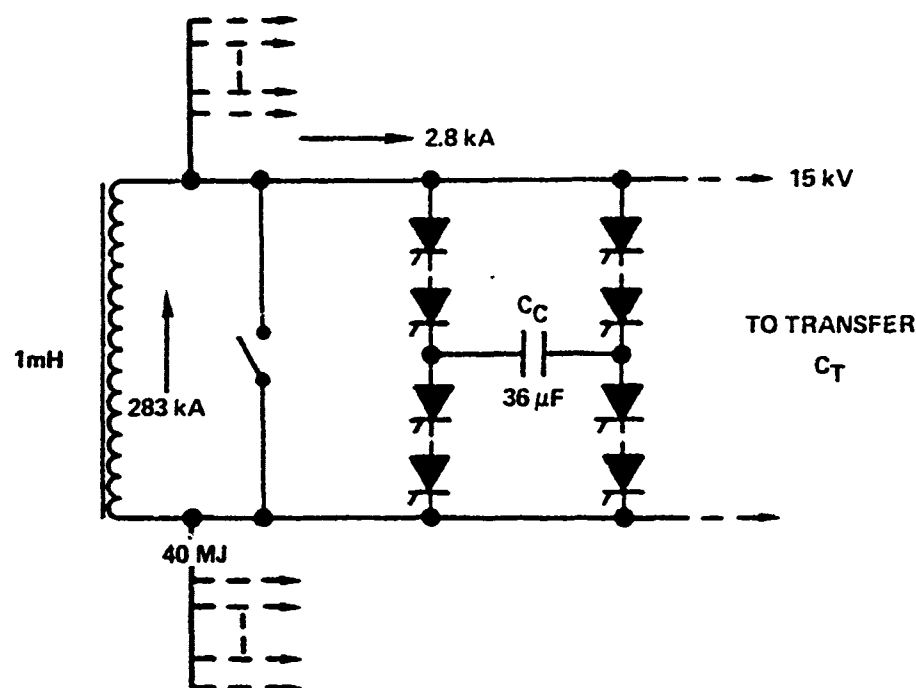


Fig. 5.1 Inverter Circuit

module capacity will be $\sim 36 \mu\text{f}$ and the time to full charge from a 2.8 kA constant current source will be $\sim 200 \mu\text{sec}$. Given that some of the current will be diverted to the transfer capacitor, the frequency of the inverter will be in the range 1.5-2.0 kHz - but this is not critical.

5.2 Transfer and Transformation Circuits.

Energy can now be fed to a transfer capacitor - as in the SIMON & BRONNER scheme - at an inverter voltage of 15 kV. This voltage has been chosen as a practical level for the arduous inverter switching. The problem now is to transfer the energy to the pulse generator capacity at 100 kV.

Two candidate circuits have been chosen for this duty:

- o A DC-DC converter (self-commutating) [9]
- o A Cockroft-Walton Multiplier

The converter scheme is probably the more flexible and will be treated first.

This type of converter will be operated at a frequency about an order of magnitude higher than the inverter that handles the inductive store current. In principle, relatively small packages of energy are transferred at a high rate from the transfer capacitor, C_t , to the pulse generator energy store via a step-up transformer.

If 20 pulses/sec are required of the 1 MJ pulse generator, then the maximum charge time to 1 MJ is 50 msec. Allow 40 msec, then if the converter is operating at 15 kHz there will be 750 charging pulses at 1.33 kJ/pulse. If the main inverter is operating at 1.5 kHz the transfer capacitor, C_t , will be recharged every 0.66 msec and between these recharges 10 pulses of 1.33 kJ, or 13.3 kJ will be removed by the 15 kHz converter. To a first order, C_t should store ten times this, or ~133 kJ.

The action of the converter is controlled by monitoring the pulse generator store voltage and using a voltage comparator to stop the SCR triggering action at 100 kV. The complete circuit is shown in Figure 5.2.

The degree to which C_t and the converter should be modularized will not be discussed here but the converter will certainly have far fewer than 100 modules.

An alternate method of voltage transformation and energy storage charging has been suggested by Mr. Donald Bingley, Section Manager of Power Conditioning at Raytheon, Bedford. This method, shown in Figure 5.3, uses the alternating voltage of the transfer capacitor C_t to drive a Cockroft-Walton network. The series connected capacitor units would represent the pulse generator

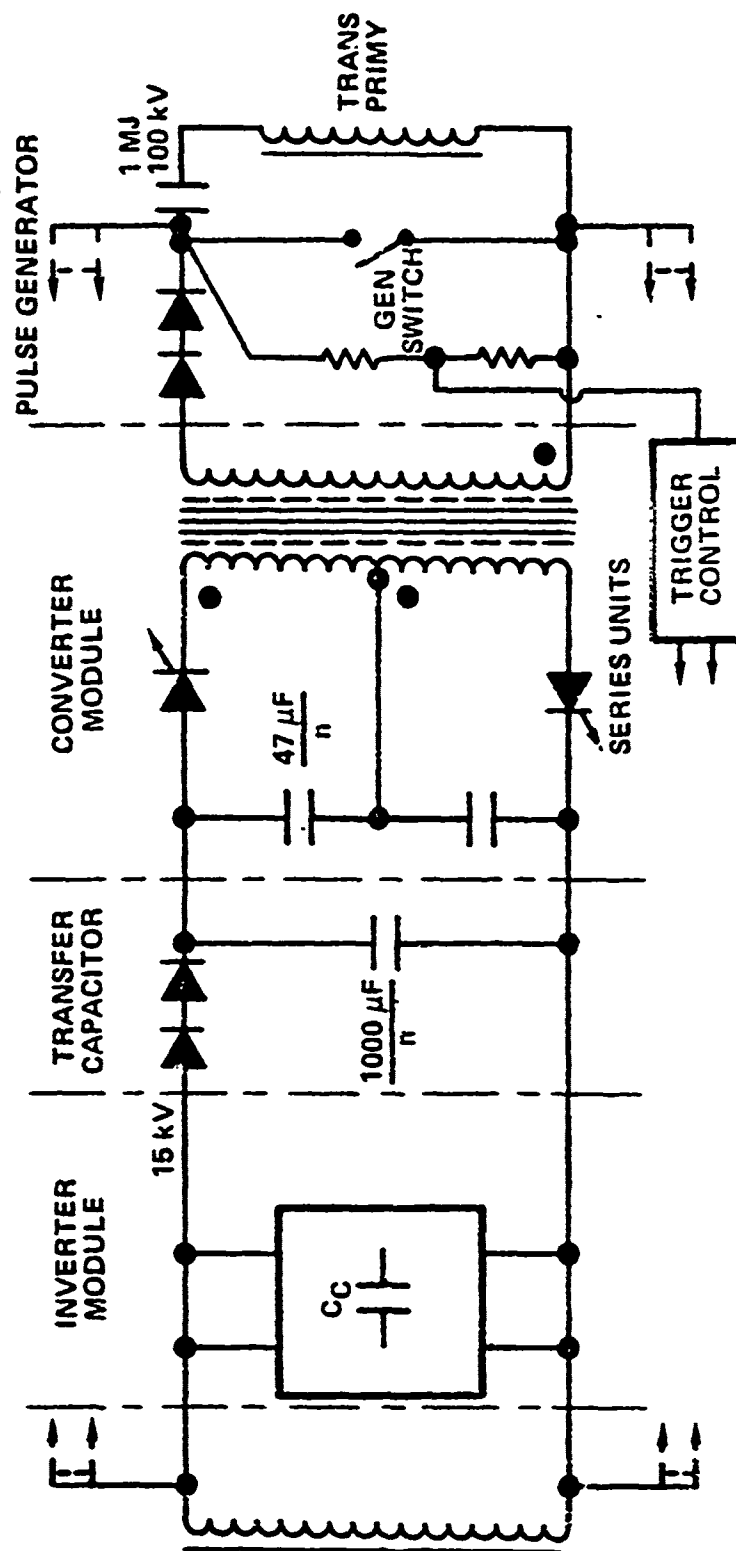


Figure 5.2 Pulses of Energy from an Inductive Store

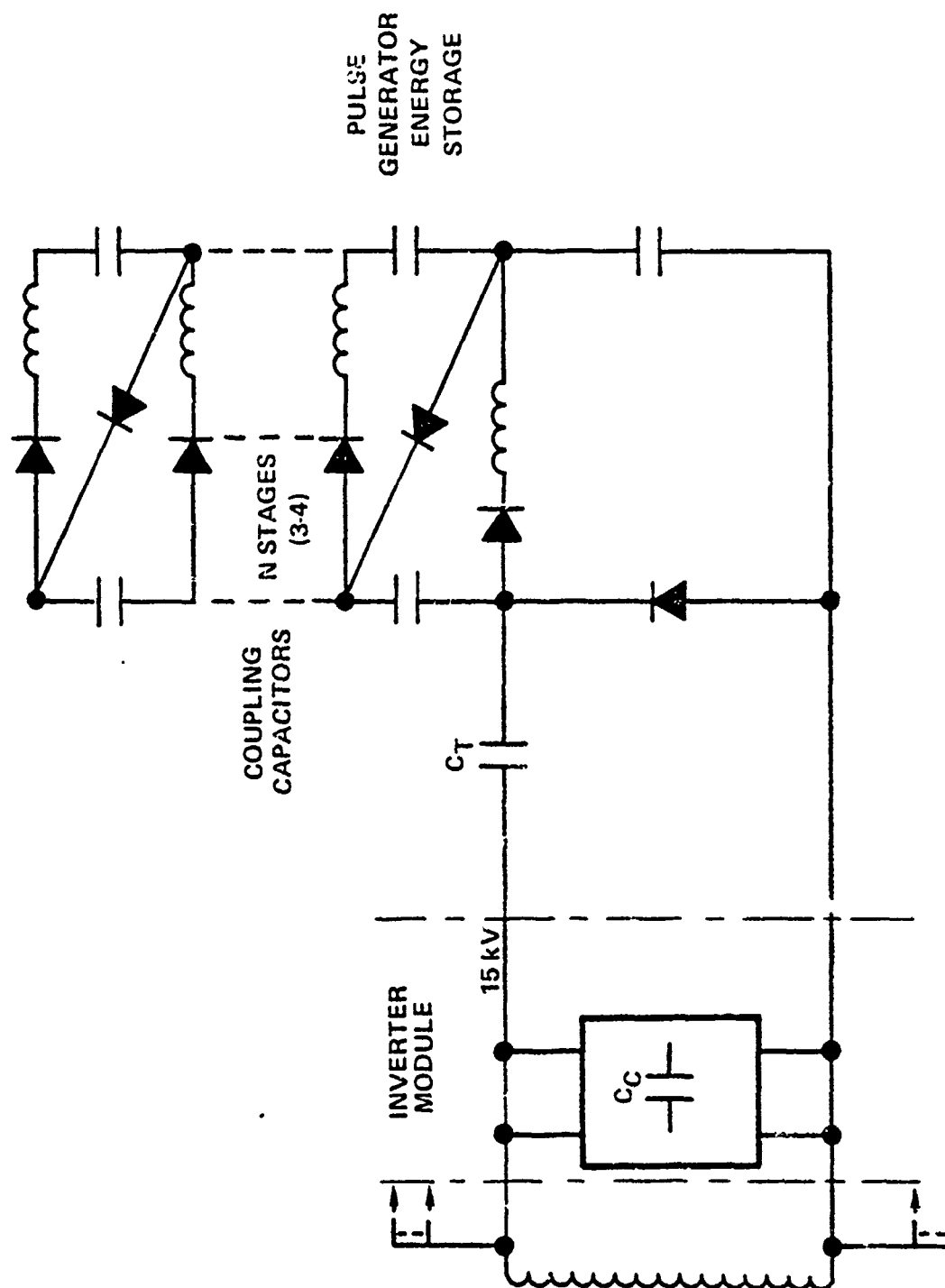


Fig. 5.3 Cockroft-Walton Version

energy storage and this assembly could be placed in low inductance configurations remote from the coupling capacitor/rectifier branch(s) of the C-W generator.

This is an unusual adaptation of the generator form when only the capacitor charging characteristics are of interest. Under these conditions the normal sizing of the C-W coupling capacitors does not apply - they could be relatively small compared with the energy storage branch, thus reducing unwanted energy storage.

6. Issues to be Resolved.

Detailed design concepts cannot be completed within the resources of this study and only preliminary estimates of practicability have been made. In spite of this the available technology looks a lot more promising here than it does for other areas of pulsed power and the techniques are worthy of more in-depth treatment.

The issues to be resolved would include the following:

- o Coupling parameters from the prime generator
- o Optimum switch type and circuit parameters
- o Modularity
- o System energy loss analysis

These issues would apply to any variants of this type of circuit and future work need not be limited to the SIMON & BRONNER concept.

REFERENCES

- [1] J. Bendford, et al, "A Unified Pulsed Power Development Plan for Inertial Confinement Fusion", Physics International Final Report Sandia Document No. 06-9262, 1979
- [2] D. B. Fenneman; R. J. Gripshover, "The Electrical Performance of Water Under Long Duration Stress", IEEE Conf. Rec. 14th Pulse Power Modulator Symposium, 1980, p. 150
- [3] D. Brower, et al, "Study of Development of Key Elements of a High Repetition Rate, High Energy Pulse System", DASG-60-78-C-0085 Final Report; FPCR No. 201 U-of-Texas at Austin; Fusion Research Center, August 1979
- [4] E. Simon & G. Bronner, "An Inductive Energy Storage System Using Ignitron Switching", IEEE Transaction on Nuclear Science, October 1967, pp 33-40
- [5] E. P. Dick & C. H. Dustmann, "Inductive Energy Transfer Using a Flying Capacitor", "Energy Storage, Compression and Switching", Editors, Bostick, Nardi & Zucker, 1979, Plenum Press, pp 485-489
- [6] H. A. Peterson, et al, "Superconductive Inductor-Converter Units for Pulsed Power Loads", Energy Storage, Compression and Switching, Editors, Bostick, Nardi & Zucker, Plenum Press, pp 309-317
- [7] V. A. Glukhikh, O. A. Gusev, et al, "Pulse Power Sources on Inductive Storage Device Base", FTD-ID (RS) T-1672-79

REFERNCES (Cont.)

- [8] V. V. Andrianov, et al, "Discharge of a Superconductive Storage Device into an Inverter Transformer", DAN 196, 2, pp 320-323, 1971
- [9] P. W. Clarke, "Self-Commutated Thyristor DC-DC Converter", IEEE Transaction on Magnetics, Vol. MAG-6, No. 1, March 1970

APPENDIX A
FUNDAMENTALS OF INDUCTIVE ENERGY STORAGE

M. Kristiansen
Plasma and Switching Laboratory
Department of Electrical Engineering
Texas Tech University
Lubbock, Texas 79409

A. INTRODUCTION

Electrical energy can be stored in both capacitors and inductors. From a circuits viewpoint we have that the capacitive energy stored is

$$E_C = \frac{1}{2} CV^2$$

and that the inductive energy is

$$E_L = \frac{1}{2} LI^2,$$

where C and L are the capacitance and inductance, respectively, and V and I are the capacitor voltage and inductor current, respectively. Energy can, of course, also be stored in other forms, such as chemical (batteries) or inertial (homopolar generators and superflywheels), and then converted to electricity. For fast discharge applications, however, the energy is, at the present time, almost always stored in capacitors of various forms and shapes. The interest in using inductive energy storage is related to the energy storage density. From an electromagnetic fields viewpoint the capacitive energy storage density is

$$W_C = \frac{1}{2} \bar{D} \cdot \bar{E} = \frac{1}{2} \epsilon E^2$$

and the inductive energy storage density is

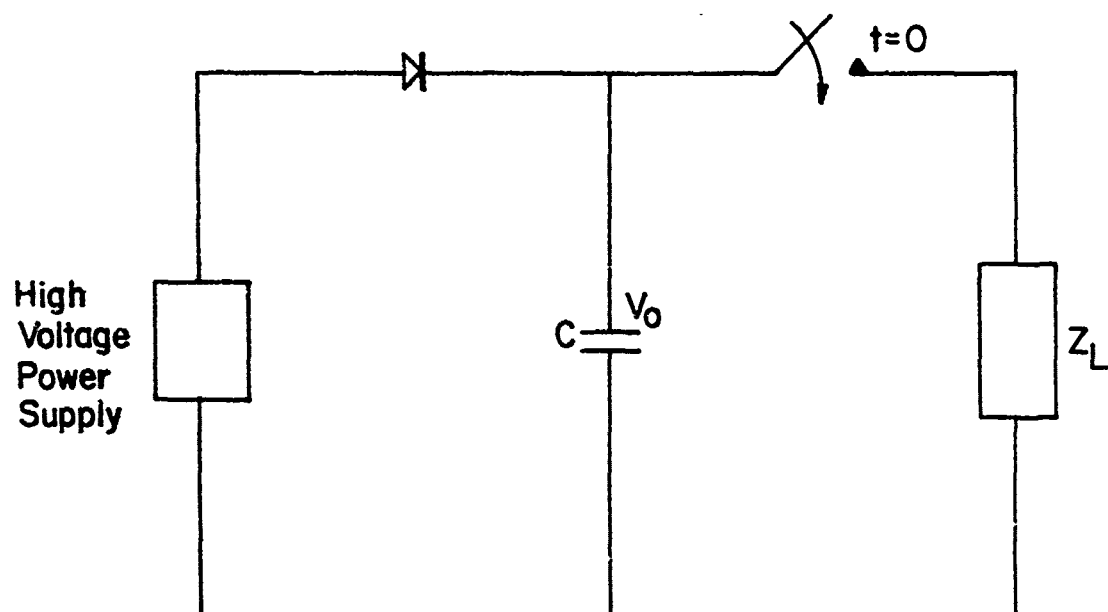
$$W_L = \frac{1}{2} \bar{B} \cdot \bar{H} = \frac{1}{2} \mu H^2,$$

where \vec{D} is the electric flux density vector, \vec{E} is the electric field intensity vector, \vec{B} is the magnetic flux density vector and \vec{H} is the magnetic field intensity vector. The constant ϵ is the electric permittivity, which is the product of the relative permittivity (ϵ_r) and the permittivity of free space (ϵ_0). Likewise μ is the magnetic permeability, which is the product of the relative permeability and the permeability of free space. The constants ϵ_r and μ_r thus describes the effects of the insulating materials and inductor core materials used. For fast discharge applications μ_r will essentially always be $\mu_r=1$ and for most practical insulating materials $\epsilon_r \sim 2.0-4.5$, except for water where $\epsilon_r \approx 80$. Water is, however, not useful for energy storage times in excess of 10's μs . It then turns out that the limiting factor on energy storage density is the electric breakdown field strength for insulating materials and the maximum magnetic field which the inductor can sustain. The maximum magnetic field is essentially limited by the $\vec{I} \times \vec{B}$ forces in the coil and hence the strength of materials. When comparing these two cases one finds, depending upon the exact assumptions of choice of materials, that

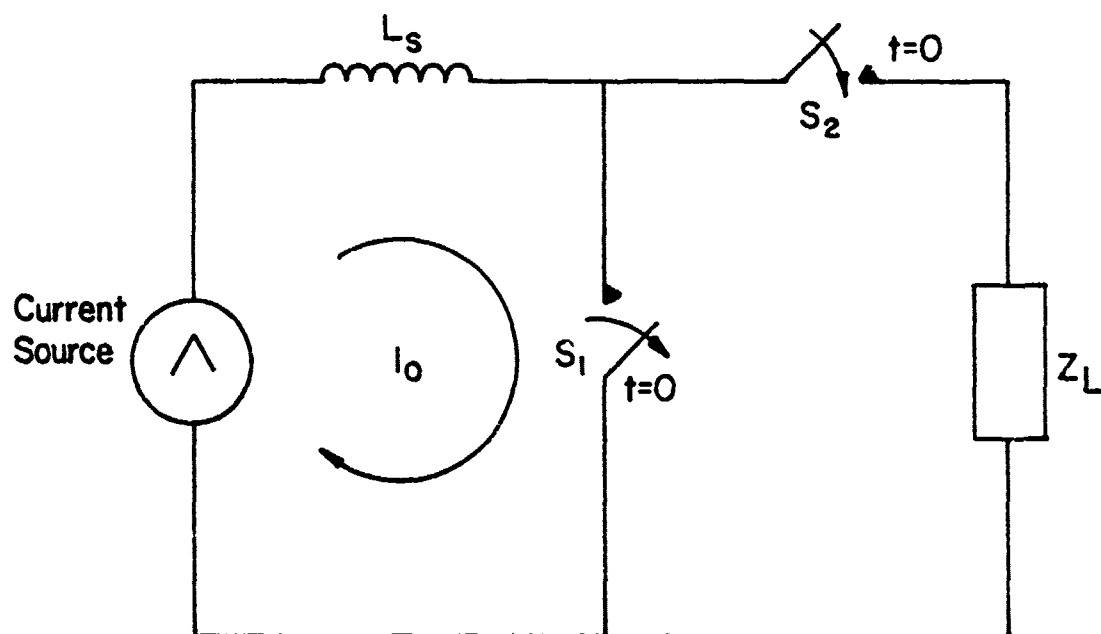
$$W_L \gtrsim 100 W_C$$

When one includes the necessary support systems (power supplies, charging generators, cooling equipment, etc.) it is not clear that the advantage in energy storage density is going to be quite this much in favor of magnetic (or inductive) storage. It is clear, however, that the potential payoff is high.

The basic capacitive and inductive energy discharge circuits are shown for comparison in Fig. 1. In Fig. 1 a) the capacitor is charged to the voltage V_0 . The switch is then closed, discharging the capacitor into the load. In Fig. 1 b) the current source establishes a current I_0 in the storage inductor, whereupon Switch S_1 is opened and Switch S_2 is closed simultaneously so that the current path changes to the



a) Capacitive Energy Discharge Circuit



b) Inductive Energy Discharge Circuit

Fig. 1 Comparison of Basic Capacitive and Inductive Energy Discharge Circuits

load. If the load has a substantial inductive component (i.e. $Z_L = R + jX_L$) then it becomes very difficult to open (interrupt the current) switch S_1 . The problem addressed at this workshop is how to achieve this current interruption at high currents, short opening times, in a repetitive mode. Some of the basic circuit relations and some fundamental limits and considerations for inductive energy storage are given below.

BASIC INDUCTIVE ENERGY STORAGE

Consider first the case in Fig. 1 b) where the load, Z_L , is purely inductive. In this case the principle of conservation of flux can be used to establish the magnitude of the load current I_L . One has that

$$I_O L_S = I_L (L_S + L_L)$$

from which $I_L = I_O L_S / (L_S + L_L)$

The initial stored energy in L_S is

$$W_O = \frac{1}{2} L_S I_O^2$$

The maximum energy transferred to the load inductor is

$$W_L = \frac{1}{2} L_L I_L^2 = \frac{1}{2} L_L \left(\frac{I_O L_S}{L_S + L_L} \right)^2$$

$$W_L = \frac{1}{2} L_S I_O^2 \frac{L_S L_L}{(L_S + L_L)^2}$$

$$W_L = W_O \frac{L_S L_L}{(L_S + L_L)^2}$$

This expression has a maximum when $L_S = L_L$ which gives

$$W_{Lmax} = \frac{1}{4} W_O$$

The implication is that only 25% of the initially stored energy is transferred to the load inductor. Another 25% remains in the storage inductor since I_L flows through both inductors and $L_S = L_L$. The remaining 50% is dissipated in the opening switch resistance (R_S) independent of its size and functional form. The switch resistance $R(t)$ only determines the time it takes to establish I_L . If the load inductance is less than optimum then a relatively larger fraction of the total energy is left in the storage inductor and a lesser fraction is dissipated in the switch but this does, of course never improve the 25% maximum energy transfer efficiency for inductive loads.

If the load is purely resistive then matters are simplified considerably and the energy transfer efficiency can, in principle, approach 100 % if the switch resistance (R_{sw}) during opening is much larger than the load resistance (R_L), i.e. $R_{sw} \gg R_L$. In practice, we never (except for totally superconducting systems) have either purely inductive or purely resistive load. Connecting leads, the switches themselves, etc. introduce "stray" inductances and resistances which may affect the circuit behaviour considerably.

Several methods have been proposed to improve the 25% maximum energy transfer efficiency for an inductive load. The most commonly considered one is the capacitive energy transfer depicted in Fig. 2. A capacitor is then connected in parallel with the opening switch. This forms a dual resonant circuit. Solving the time dependent circuit equations for this case we find again that maximum energy storage occur for $L_L = L_S$. In addition, we find that the maximum transfer efficiency can become 100%. There is, however, a price to pay for this, -- namely that the capacitor in this case ($\eta = 100\%$), must be able to store half of the energy which was stored in the storage inductor. Thus the attractiveness of the inductive energy storage has diminished since we must provide a supplementary capacitor bank with half the energy storage capacity of the storage inductor.

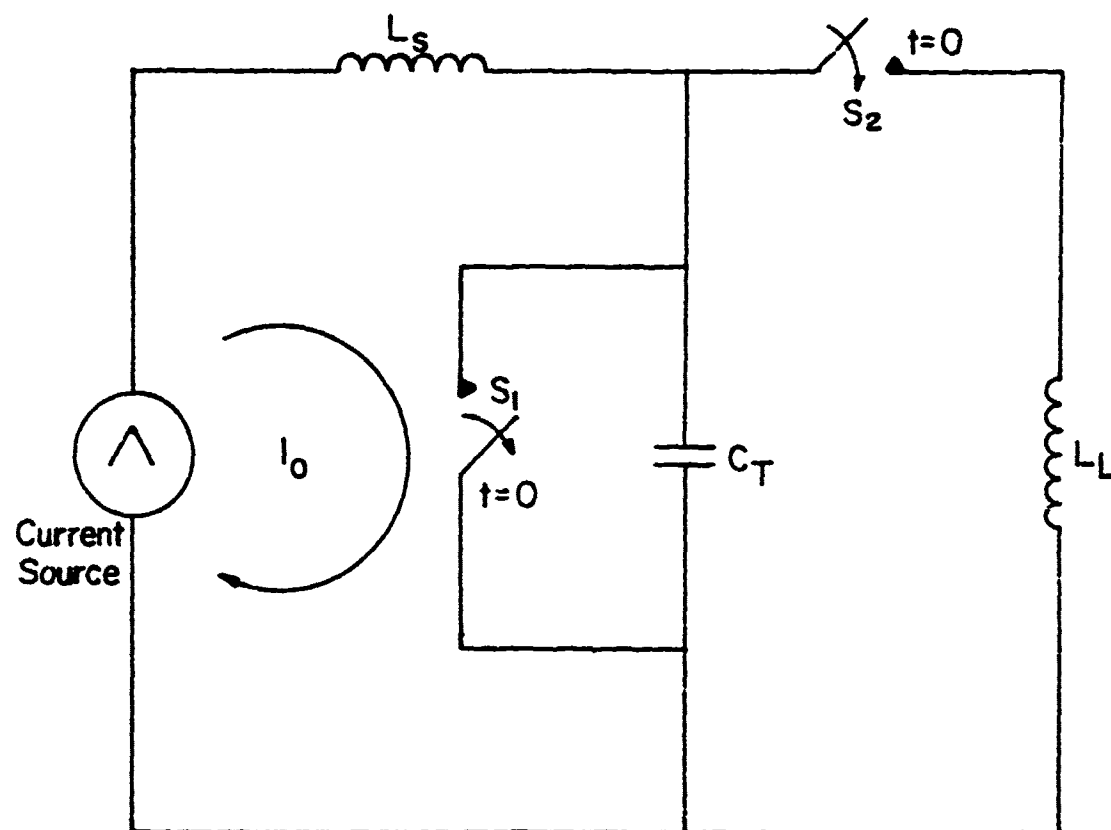


Fig. 2 Capacitive Energy Transfer

The effect of varying the load inductance with respect to storage inductance is summarized* in Fig. 3. The exact circuit behaviour with a resistive-inductive load ($Z_L = R_L + jX_L$) must be analyzed in detail on a case by case basis, -- usually with the help of a circuit analysis computer code. It is, however, extremely important to make sure that the stray inductances in the switch and the connecting leads are properly accounted for since these constitute additional ΔL_S 's and ΔL_L 's which may affect the circuit behaviour profoundly.

Another important application of inductive energy storage is in combination with a capacitive main storage system. The series connected inductive energy storage system then performs the function of a pulse sharpener but still requires an opening switch.

There are essentially two main classes of opening switches, -- "true opening" switches and counterpulsed opening switches. True opening switches, such as vacuum triodes (which has only limited current carrying capability and relatively high internal losses), can interrupt the current without developing an arc or causing other switch damage. Counterpulsed switches use an external energy source, usually a capacitor bank, to force the opening switch current momentarily to zero such that it can open (e.g. physical contact separation) and hold off the resulting high electrode voltage. This capacitor bank is then connected essentially as the transfer capacitor bank shown in Fig. 2, except that it is pre-charged and switched in at time of current interruption so as to establish near zero current through the switch itself. Such an application is discussed in the paper by M. Parsons in this report.

An important consideration for all the various opening switch concepts is the "pulse compression ratio". The inductor is charged from some current source in time T_{ch} . The opening switch is then activated (triggered) and produces an

* Sketch due to J. Marshall, LANL

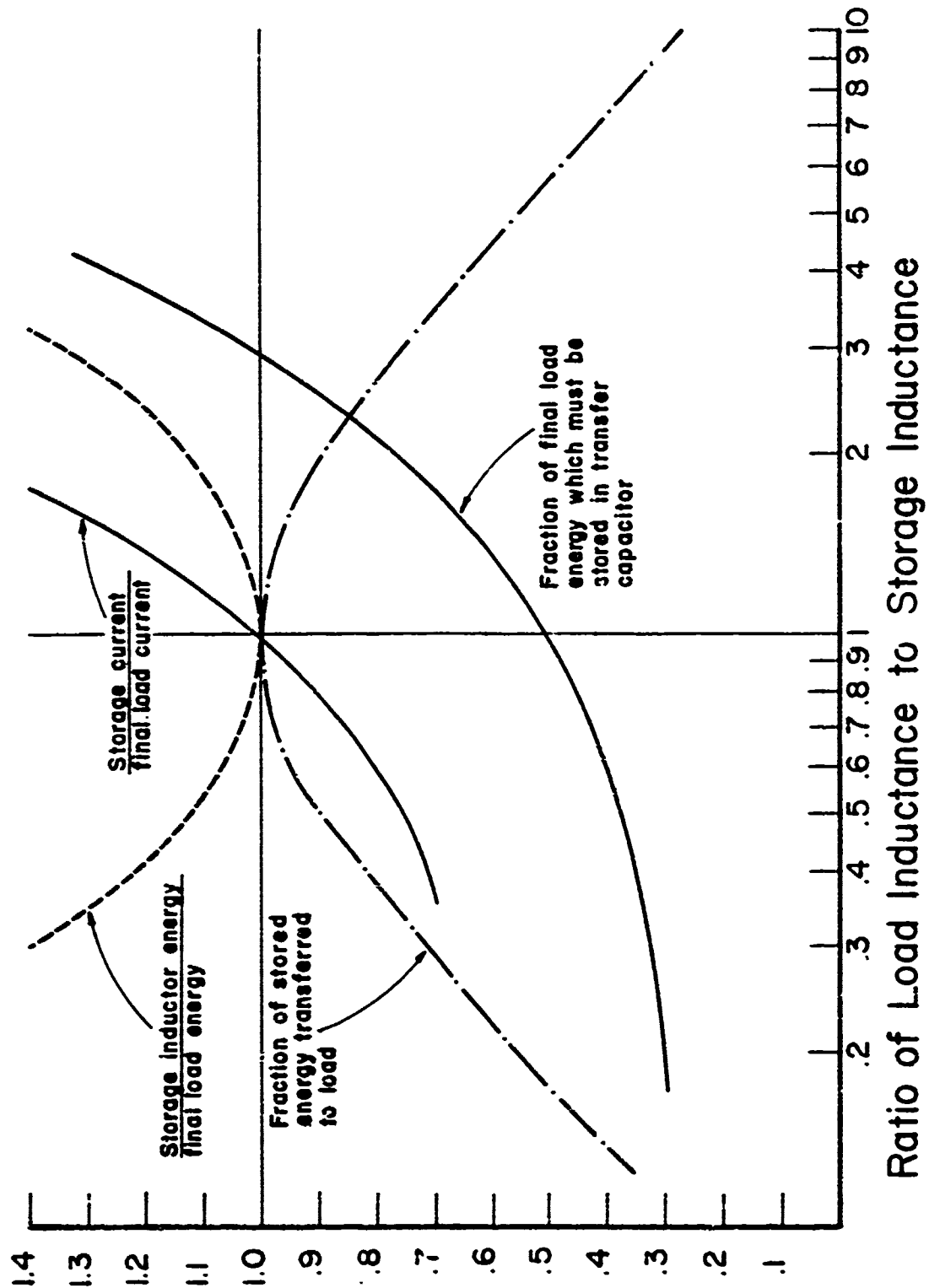


Fig. 3 Effects of varying L_L/L_S in Inductive Energy Storage System (redrawn from original Figure by J. Marshall, LANL)

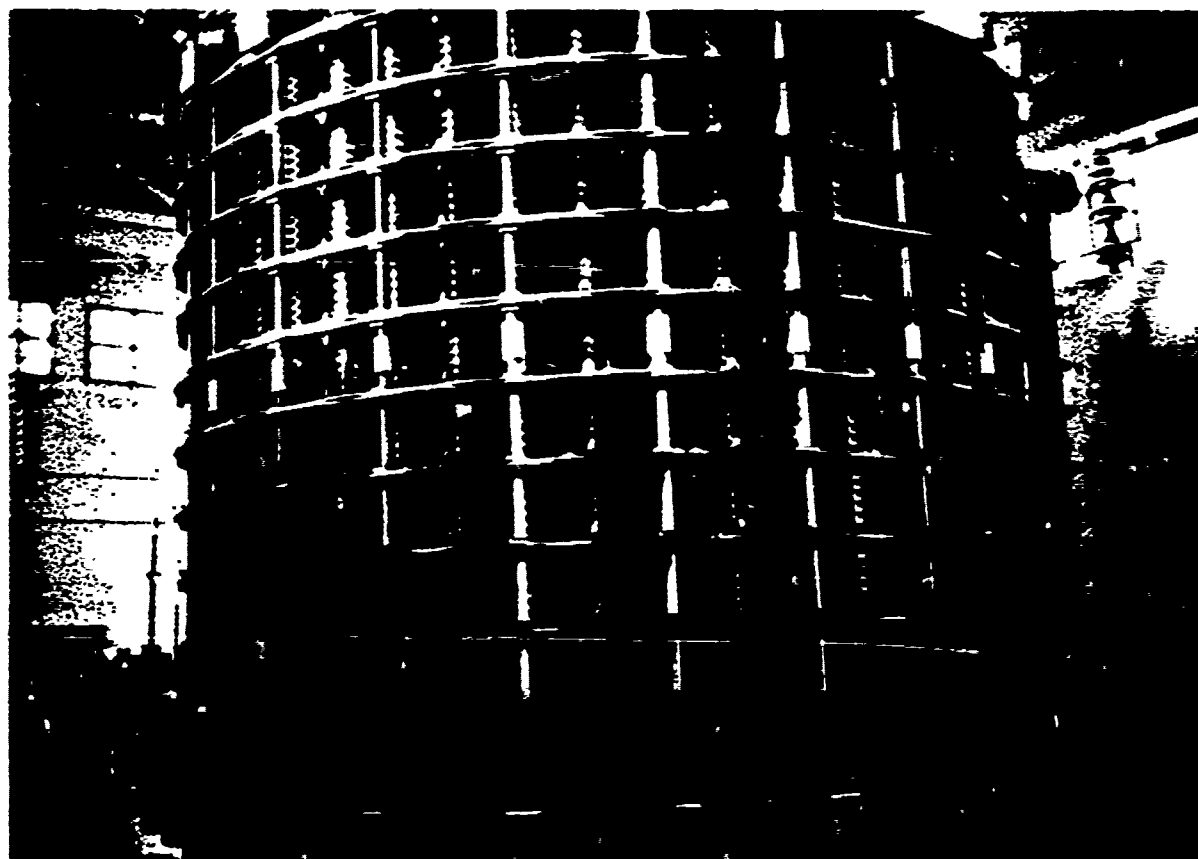
output pulse of duration T_p . Unless the output pulse can be made considerably shorter than the charging time, it is not much purpose in going through the intermediate inductive energy storage system. A practical lower limit on the pulse compression ratio may be $T_{ch}/T_p > 10$. This then imposes a constraint on the opening switch which must be able to sustain the charging current, with low loss, until we activate it. The simultaneous requirements of fast switch action (to get short pulse rise times and long conduction times) often poses a conflicting requirement since the first condition often implies small mass and the second condition usually implies large thermal capacity. This "dilemma" is sometimes handled by using several switches of successively smaller mass and faster action in parallel and then transferring the current from one switch to the other during opening action. This provides large switch mass (heat capacity) for current build-up and low mass for fast opening switch action.

There are many technical problems associated with the various inductive energy storage components, -- charging system, inductor design, switch construction, etc. The most difficult one, by far, appears to be the opening switch, however. What we want is a switch which can conduct large currents (10 kA - 1 MA) for long times ($T_{ch}/T_p > 10$), interrupt the currents in short times ($\leq \mu s$), hold off large electrode voltages (10 kV - 1 MV) during and immediately after the opening process, and then be able to repeat this operation frequently (10 - 10⁵/sec) with long life (10⁶ - 10⁸ pulses).

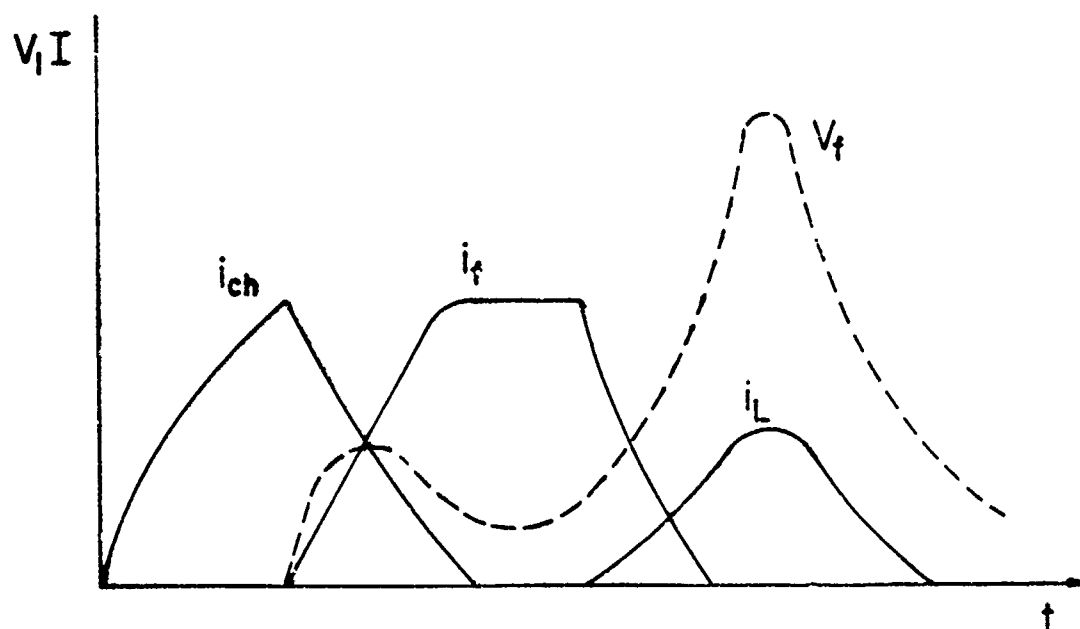
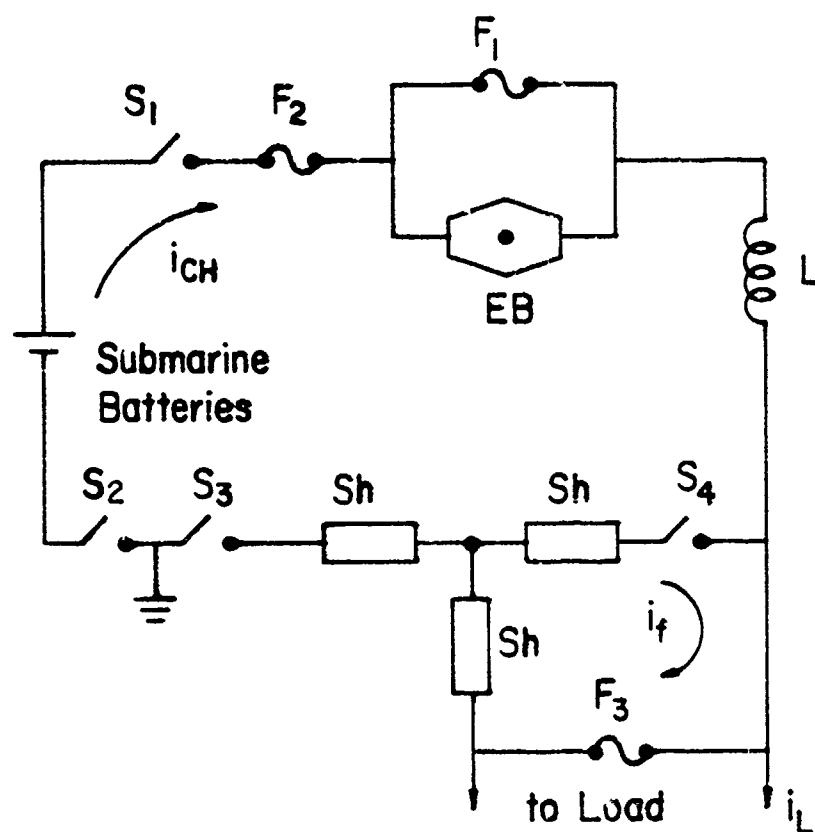
A challenging problem, indeed, and one which was addressed at this workshop.

EXAMPLE OF LARGE, OPERATING, SINGLE SHOT
INDUCTIVE ENERGY STORAGE SYSTEM

Located at the
Heifei Plasma Physics Research Center
of the
Academy of Sciences
Peoples Republic of China
Source of Information: M. Kristiansen



See next two pages for further description



Circuit Diagram and Current-Voltage Waveforms
(see next page for Symbol Definitions and Circuit Parameters)

S_1	- Isolation switch
S_2	- Isolation switch
S_3	- Fast closing switch
S_4	- Main opening switch
F_1	- Primary protection fuse
F_2	- Secondary protection fuse
F_3	- Main exploding fuse (commutating fuse)
EB	- Exploding bridge
Sh	- Current shunt
L	- Storage inductor
i_{ch}	- Charging current
i_f	- Fuse current
i_L	- Load current
V_f	- Fuse voltage

Circuit Parameters

Coil inductance	$L = 26.3 \times 10^{-3} \text{ H}$
Coil resistance	$R = 2.85 \times 10^{-3} \text{ Ohms}$
Time const. for inductor	$\tau = L/R = 9 \text{ sec}$
Maximum voltage	$V = 560 \text{ kV}$
Expected stored energy	$W = 200 \text{ MJ}$
Actual stored energy (limited by present power supply)	$W = 60 \text{ MJ}$
Discharge time	$\tau = 20\text{-}30 \text{ ms}$
Power amplification	$K = (.5\text{-}10) \times 10^3$
No. of coil turns	$N = 100$
Wire cross-section	$S = 12 \times 150 \text{ mm}^2$
Coil height	$H = 6.1 \text{ m}$
Average coil diameter	$D = 4.7 \text{ m}$

APPENDIX B

SUGGESTED SOURCES OF INFORMATION FOR VARIOUS OPENING

SWITCH CONCEPTS

- | | |
|--|--|
| 1) Electron Beam
Controlled: | E. Nolting
NSWC/White Oak
(202) 394-2119 |
| | L. Kline
Westinghouse
(412) 256-7552 |
| 2) Optically Con-
trolled: | K. Schoenbach
Texas Tech University
(806) 742-3595 |
| | A. Guenther
AFWL
(505) 844-9856 |
| 3) Dense Plasma
Focus: | M. Molen
Old Dominion University
(804) 440-3750 |
| | K. Schoenbach
Texas Tech University
(806) 742-3595 |
| 4) Plasma Erosion: | V. Bailey
Physics International Company
(415) 357-4610 |
| | P. Vandevender
SNL
(505) 844-5429 |
| 5) Reflex Discharge: | V. Bailey
Physics International Company
(415) 357-4610 |
| 6) Spoiled Electro-
static Confinement: | I. Alexeff
University of Tennessee
(615) 974-5475 |
| 7) Controlled Plasma
Instability: | K. Schoenbach
Texas Tech University
(806) 742-3595 |

- 8) JxB Thyatron: E. Honig
LANL
(505) 667-1688
- 9) SCR (Counter-
pulsed): M. Parsons
LANL
(505) 667-7872
- 10) Vacuum Int.
(Counterpulsed): M. Parsons
LANL
(505) 667-7872
- 11) Fuse: D. Smith
SNL
(505) 844-7773

I. Vitkovitsky
NRL
(202) 767-2298
- 12) Explosive (Chem-
ical): B. Furman
SNL
(505) 846-0405

I. Vitkovitsky
NRL
(202) 767-2298
- 13) Crossed Field
Tube: R. Harvey
Hughes Research Labs
(213) 456-6411
- 14) Vacuum Arc
Opening: S. Gilmer
SUNY, Buffalo
(716) 831-6405
- 15) Hall Effect: P. Turchi
R&D Associates
(703) 522-5400
- 16) Magneto-plasma-
dynamic: P. Turchi
R&D Associates
(703) 522-5400

LIST OF PARTICIPANTS

Igor Alexeff
Dept. Elec. Engr.
University of Tennessee
Knoxville, TN 37916
615/974-5475

Vern Bailey
Physics International
2700 Merced Street
San Leandro, CA 94577
415/357-4610

Barry Ballard
Foreign Technology Div.
Wright-Patterson AFB
Dayton, OH 45433
513/257-3158

Bruce Carder
L469
Lawrence Livermore National
Laboratories
P.O. Box 808
Livermore, CA 94550
415/422-5936

Edmond Chu
Maxwell Laboratories, Inc.
9244 Balboa Avenue
San Diego, CA 92123
714/279-5100

Laszlo Demeter
Physics International
2700 Merced Street
San Leandro, CA 94577
415/357-4610

Karl Freytag
Lawrence Livermore National
Laboratories
P.O. Box 808
L 469
Livermore, CA 94550
415/422-5418

A.S. Gilmour
Dept. Elec. Engr.
State University of New York
at Buffalo
4232 Ridge Lea Road
Amherst, N.Y. 14226
716/831-3165

A.H. Guenther
AFWL/CA
Kirtland AFB, NM 87117
505/344-9856

Bobby Guenther
U.S. Army Research Office
P.O. Box 12211
Research Triangle Park, NC
919/549-0641 27709

Robin H. Harvey
Hughes Research Labs
3011 Malibu Canyon Road
Malibu, CA 90265
213/456-6411

Emanuel Honig
Los Alamos National Laboratory
Group E-11
MS 429
Los Alamos, NM 87545
505/667-1688

A.K. Hyder
Directorate of Physics
Room C 225
Bolling Air Force Base
Bldg. 410
Washington, D.C. 20332
202/767-4908

Laurence E. Kline
Westinghouse Research Lab
1310 Beulah Road
Pittsburgh, PA 15235
412/256-7552

M. Kristiansen
Elec. Engr. Dept.
Texas Tech University
P.O. Box 4439
Lubbock, TX 79409
806/742-2224

E.E. Kunhardt
Elec. Engr. Dept.
Texas Tech University
P.O. Box 4439
Lubbock, TX 79409
806/742-3545

Donald C. Lorents
SRI International
333 Ravenswood Avenue
Menlo Park, CA 94025
415/326-6200

Robert J. Lontz
U.S. Army Research Office
P.O. Box 12211
Research Triangle Park, NC 27709
919/549-0641

Lawrence H. Luessen
Naval Surface Weapons Center
Code F 12
Dahlgren, VA 22448
703/663-8057

Michael Mando
U.S. MERADCOM
DRDME-EA
Fort Belvoir, VA 22060
703/664-5587

Thomas Martin
Pulsed Power Systems Dept.
Sandia National Laboratories
Albuquerque, NM 87117
505/844-2270

Dick Milton
DRSMI-RMC
Redstone Arsenal
Huntsville, AL 35809
205/876-2151

Marshall Molen
Old Dominion University
Elec. Engr. Dept.
Norfolk, VA 23508
804/440-3750

Eugene F. Nolting
Naval Surface Weapons Center
White Oak Lab
Silver Spring, MD 20910
202/394-2119

Mark Parsons
MS 464
P.O. Box 1663
Los Alamos National Scientific
Laboratory
Los Alamos, NM 87544
505/667-7872

A.V. Phelps
Joint Institute for
Laboratory Astro-Physics
University of Colorado
Boulder, CO 80309
303/492-7850

Robert E. Reinovsky
AFWL/NTYP
Kirtland AFB, NM 87117
505/844-1851

Frank Rose
Naval Surface Weapons Center
F-04
Dahlgren, VA 22448
703/663-8026

Juergen Salge
Inst. fur Hochspannungstechnik
Technische Universitaet
Braunschweig
Postfach 3323
Pockelsstrasse 4
D-3300 Braunschweig
FRG
(0531) 391 2312

K.H. Schoenbach
Elec. Engr. Dept.
Texas Tech University
P.O. Box 4439
Lubbock, TX 79409
806/742-3595

David L. Smith
Sandia National Laboratories
Div. 4253
Albuquerque, NM 87115
505/844-7773

Ian Smith
PSI-Suite 610
1615 Broadway
Oakland, CA 94612
415/521-2142

J.E. Thompson
University of South Carolina
College of Engineering
Columbia, SC 29208
803/777-7304

Peter Turchi
R&D Associates
1401 Wilson Blvd.
Arlington, VA 22209
703/522-5400

Bobby N. Turman
Org. 4252
Sandia National Laboratories
P.O. Box 5800
Albuquerque, NM 87185
505-846-0405

Larry Turner
USA FSTC
220 7th St., N.E.
Charlottesville, VA 22901
804/296-5171

David Turnquist
EG&G
35 Congress Street
Salem, MA 01970
617/745-3200

I.M. Vitkovitsky
Naval Research Lab
Code 6770
Washington, D.C. 20375
202/767-2298

Richard J. Wasneski
NAVAIR-350F
Washington, D.C. 20361
202/692-2523